DASA 2166--3

AD 723412

Approved for public release;
distribution unlimited

TELEDYNE
ISOTOPES

218

DISCLAIMER NOTICE

THIS DOCUMENT IS THE BEST QUALITY AVAILABLE.

COPY FURNISHED CONTAINED A SIGNIFICANT NUMBER OF PAGES WHICH DO NOT REPRODUCE LEGIBLY.

UNCLASS

Security Classification

DOCUMENT CONTROL DATA - R & D

(Security classification of title, body of abstract and indexing annotation must be entered when the overall report is classified)

1. ORIGINATING ACTIVITY (Corporate author) Isotopes, Inc. 50 Van Buren Avenue Westwood, New Jersey 07675	2a. REPORT SECURITY CLASSIFICATION UNCLASS 2b. GROUP

3. REPORT TITLE

FINAL REPORT ON PROJECT STARDUST, VOLUME III

4. DESCRIPTIVE NOTES (Type of report and inclusive dates)

Final Report

5. AUTHOR(S) (First name, middle initial, last name)

Herbert W. Feely, James P. Friend, Harold Seitz, John D. Martin, Woodland E. Erlebach

6. REPORT DATE March 15, 1971	7a. TOTAL NO. OF PAGES 221	7b. NO. OF REFS 117

8a. CONTRACT OR GRANT NO. DA-49-146-XZ-079 b. PROJECT NO. ARPA Order #0172 c. d.	9a. ORIGINATOR'S REPORT NUMBER(S) IWL-0001-143 9b. OTHER REPORT NO(S) (Any other numbers that may be assigned this report) DASA 2166-3

10. DISTRIBUTION STATEMENT

Approved for public release; distribution unlimited.

11. SUPPLEMENTARY NOTES Work sponsored by ARPA, managed and contracted by DNA	12. SPONSORING MILITARY ACTIVITY Director, Advanced Research Projects Agency, 1400 Wilson Blvd., Arlington, Virginia 22209

13. ABSTRACT

In this, the final report of Project STARDUST, a review is given of the results of analyses of filter and gas samples collected during the course of the program, 1961 to 1967, and a summary is given of the conclusions reached on the basis of these results concerning the influence of atmospheric processes on the transfer and fallout of radioactive materials injected into the stratosphere. Reference is made to results obtained during Project HASP also, for in many ways, Project STARDUST was a continuation of that program.

14 KEY WORDS	LINK A		LINK B		LINK C	
	ROLE	WT	ROLE	WT	ROLE	WT
STARDUST						
Atmospheric Transport & Deposition						
Worldwide Fallout						
Atmospheric Radioactivity						
Stratospheric Radioactivity						
High Altitude Sampling, Aircraft						
Upper Atmosphere Meteorology						
Mathematical Fallout Model						
Mathematical Upper Atmosphere Model						
Analysis Fission Products						
Analysis Neutron Activation Products						
Upper Atmosphere Meterology						
SNAP-9A Reentry Burnup						

DASA 2166-3

FINAL REPORT ON PROJECT STARDUST

VOLUME III, Chapters 9 to 13

This work was supported by the
Advanced Research Projects Agency
ARPA Order No. 0172

by

Herbert W. Feely
James P. Friend
Harold Seitz
John D. Martin
Woodland E. Erlebach

March 15, 1971

This research has been sponsored by the
Defense Nuclear Agency under
Contract DA-49-146-XZ-079

Approved for public release;
distribution unlimited.

TELEDYNE ISOTOPES
50 Van Buren Avenue
Westwood, New Jersey 07675

BLANK PAGE

VOLUME III

CONTENTS

CHAPTER 9. THE STRATOSPHERIC TRANSPORT OF PLUTONIUM-238 FROM THE APRIL 1964 SNAP-9A BURNUP

9.1 Injection of SNAP-9A Plutonium-238

Plutonium-238 was injected into the upper stratosphere on 21 April 1964 when a Transit navigational satellite carrying a SNAP-9A power source, which contained 17 kilocuries of plutonium-238, failed to achieve orbit and burned up upon reentry into the atmosphere[52,53,54]. Presumably the debris from the SNAP-9A was distributed initially in the atmospheric layer between 30 and 100 kilometers altitude, and thus had an initial distribution similar to that of debris from the Orange event in the 1962 Hardtack series of nuclear weapons tests[54]. It was of great interest, therefore, to monitor the transfer of the SNAP-9A plutonium-238 from the upper to the lower stratosphere, and from the lower stratosphere to the troposphere and to the surface of the earth. The resulting information is pertinent to studies of fallout rates of debris from nuclear explosions in the upper atmosphere as well as to studies of potential atmospheric contamination resulting from the use of nuclear power sources in space.

9.2 First Detection of Plutonium-238 from the SNAP-9A Burnup

The first detection of SNAP-9A plutonium-238 was in filter samples collected by the USAEC high altitude balloon program[55] at 33 kilometers at 34°S in August 1964, and in January 1965 it was detected in the Northern Hemisphere in samples collected at 32.6 and 33.2 kilometers at 31°N. Results of measurements of subsequent balloon samples permitted the tracing of the gradual descent of the SNAP-9A debris to lower levels. The first definite detection of this debris in STARDUST samples was in samples collected in May 1965 at 19 and

20 kilometers between 38°S and 55°S. The plutonium-238 concentrations in the lower northern polar stratosphere attributable to SNAP-9A debris increased gradually during 1965. By October and November 1965 half of the plutonium-238 in some samples collected in this region could be attributed to the SNAP-9A source. STARDUST sampling was limited in latitudinal coverage during December 1965, but evidently the influx of SNAP-9A debris into the lower stratosphere of the Northern Hemisphere had greatly accelerated by then, for one sample contained twice as much SNAP-9A plutonium-238 as had any previously collected in that region.

9.3 Distribution of SNAP-9A Plutonium-238 from March to December 1965

The plutonium-238 concentrations and the Pu^{238}/Pu^{239} activity ratios measured in samples collected during each month between March and December 1965 are plotted in Figures 83 to 88. In these cross sections a horizontal line is drawn representing the flight track followed during the collection of each sample. The plutonium-238 concentrations, in pCi/100 SCM, are given in the upper halves of the figures, and the Pu^{238}/Pu^{239} ratios are given in the lower halves. A diagrammatic representation of the tropopause is given in each figure for general reference. The data are placed in parentheses when it is suspected that an error has been made in the flight data supplied with the sample or during the analysis of the sample.

It appears that Pu^{238}/Pu^{239} ratios between 0.02 and 0.04 are typical of debris from nuclear weapon tests, for results of nearly all analyses of STARDUST samples collected before May 1965 in the Southern Hemisphere and before September 1965 in the Northern Hemisphere fell within that range. No clear sign of SNAP-9A debris was found in samples collected during March 1965 (Figure 83) or April 1965 (Figure 84).

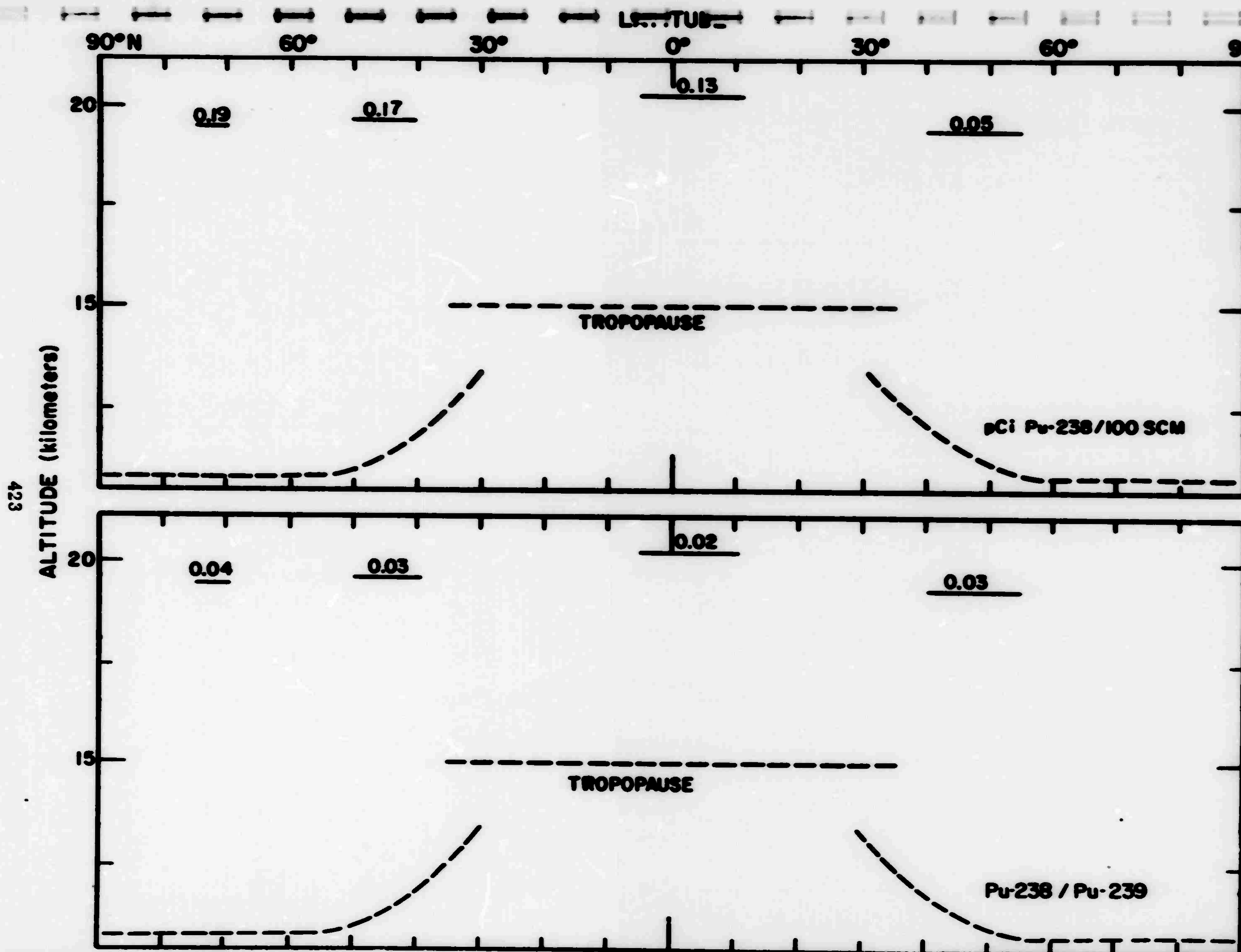

FIGURE 83. DISTRIBUTION OF Pu-238 AND OF THE ACTIVITY RATIO Pu-238/Pu-239 DURING MARCH 1965

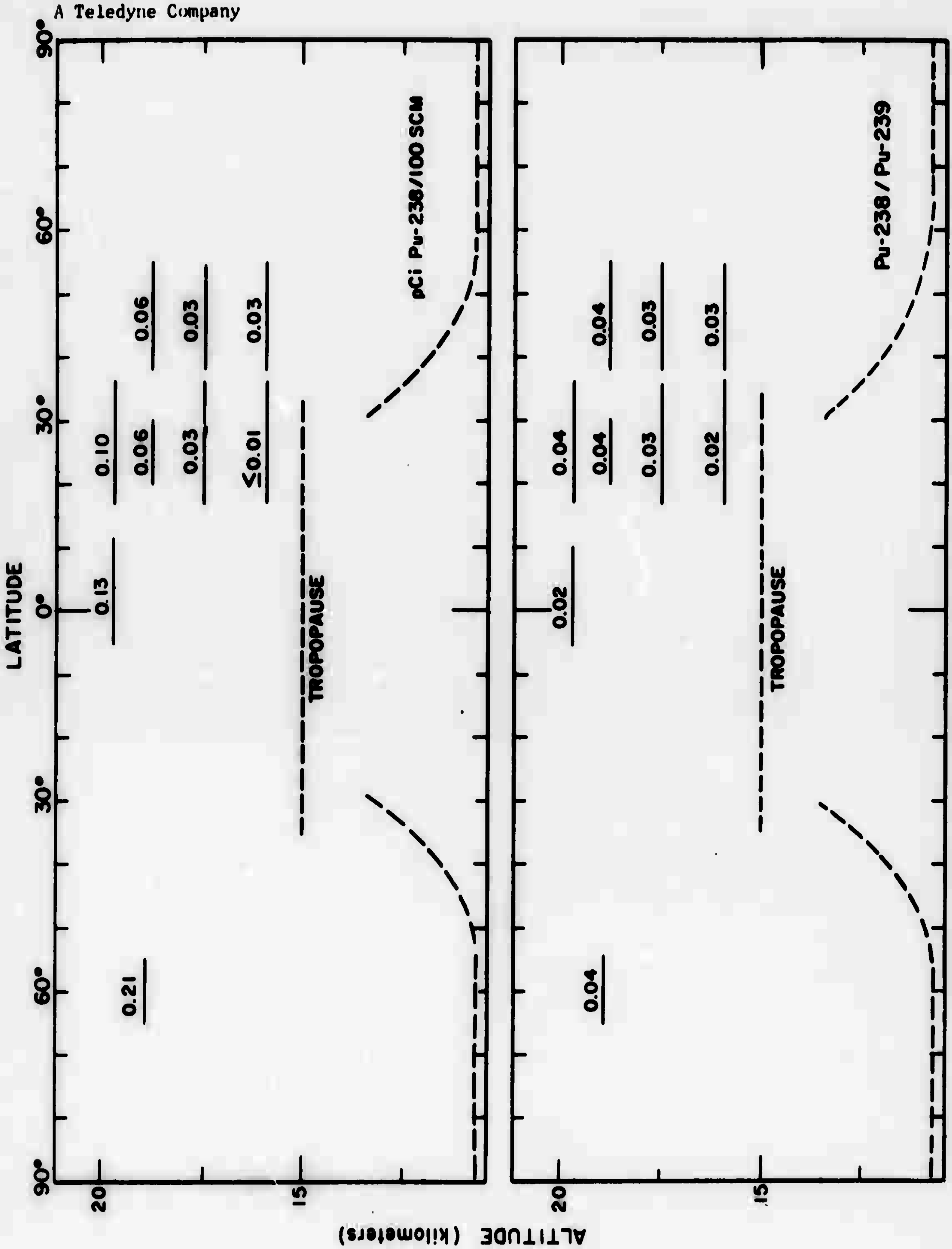

FIGURE 84. DISTRIBUTION OF Pu-238 AND OF THE ACTIVITY RATIO Pu-238/Pu-239 D[illegible]INC [illegible]PR[illegible] 19[illegible]

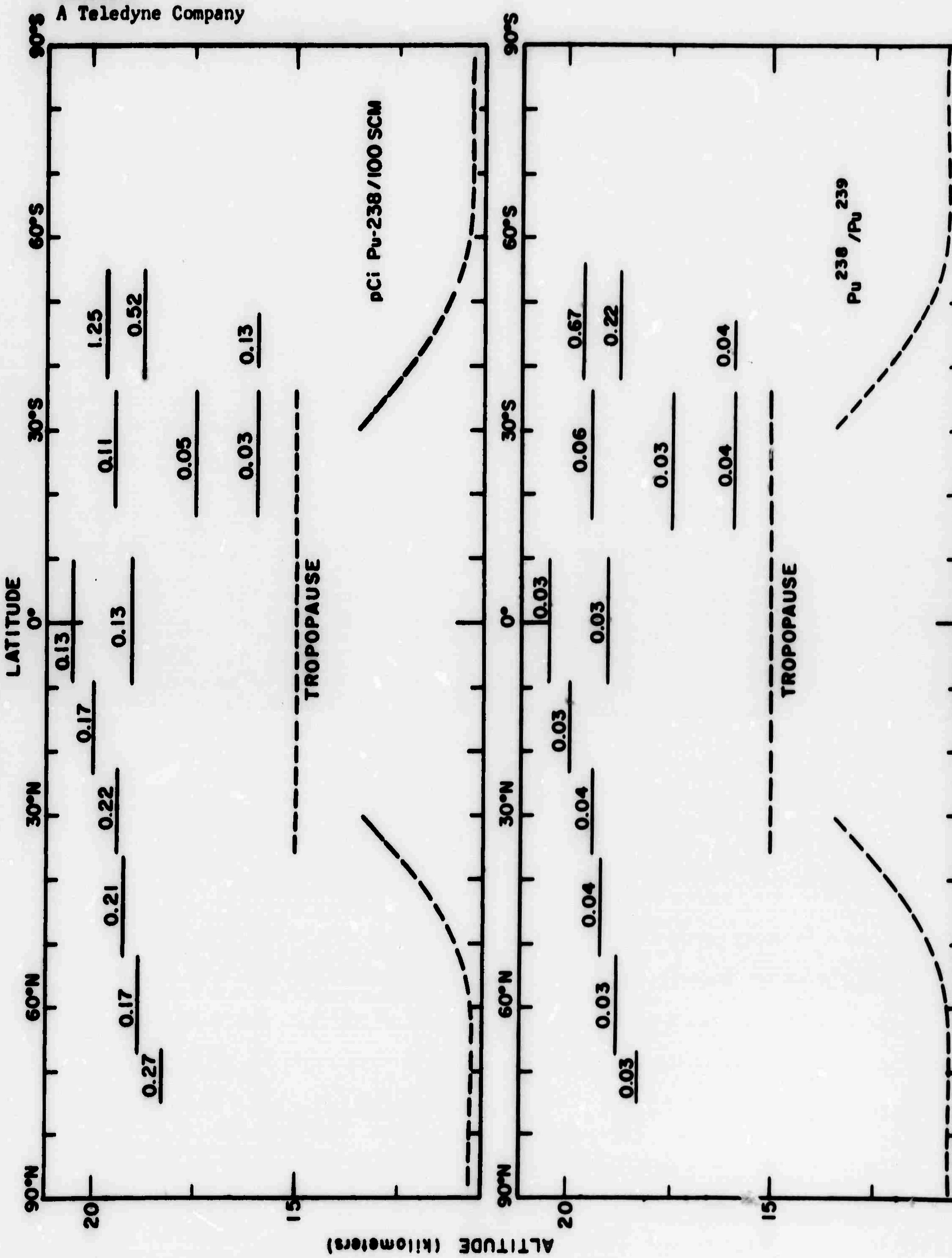

FIGURE 85. DISTRIBUTION OF Pu-238 AND OF THE ACTIVITY RATIO Pu-238/Pu-239 DURING MAY 1965

During May 1965 SNAP-9A debris, identified both by relatively high plutonium-238 concentrations and by relatively high Pu^{238}/Pu^{239} ratios, was found in samples collected at 19 and 20 kilometers at 38° - 55°S (Figure 85). Still higher concentrations of SNAP-9A debris were found in this region during June to August 1965 (Figures 86 to 88). Indeed, the concentrations in the lower southern polar stratosphere generally continued to increase slowly during September to December 1965 (Figures 89 to 92). It is evident from the data in Figures 85 to 92 that the SNAP-9A debris was spreading equatorward and downward within the lower southern stratosphere during the final two thirds of 1965.

Apparently a slow influx of SNAP-9A debris into the lower northern polar stratosphere had begun by mid-1965, for beginning in August Pu^{238}/Pu^{239} ratios greater than 0.04 began to appear in samples in that region. Ratios of 0.05 were measured in samples collected there during August and September 1965 (Figures 88 and 89), and a ratio of 0.06 was found in an October sample (Figure 90), 0.08 in two November samples (Figure 91), and 0.14 in a December sample (F[illegible]ure 92). Evidently the influx of SNAP-9A debris accelerated with the o[illegible] of the winter circulation.

By combining STARDUST data with data from the USAEC high altitude balloon sampling program[49,50,51], one may obtain a picture of the downward movement of the SNAP-9A debris within the stratosphere during 1964 and 1965. Results of plutonium-238 measurements performed during these two programs on samples collected at 35° - 45°S, at 5° - 10°N, at 30° - 40°N, and at 65° - 70°N are plotted in Figures 93, 94, 95 and 96 respectively.

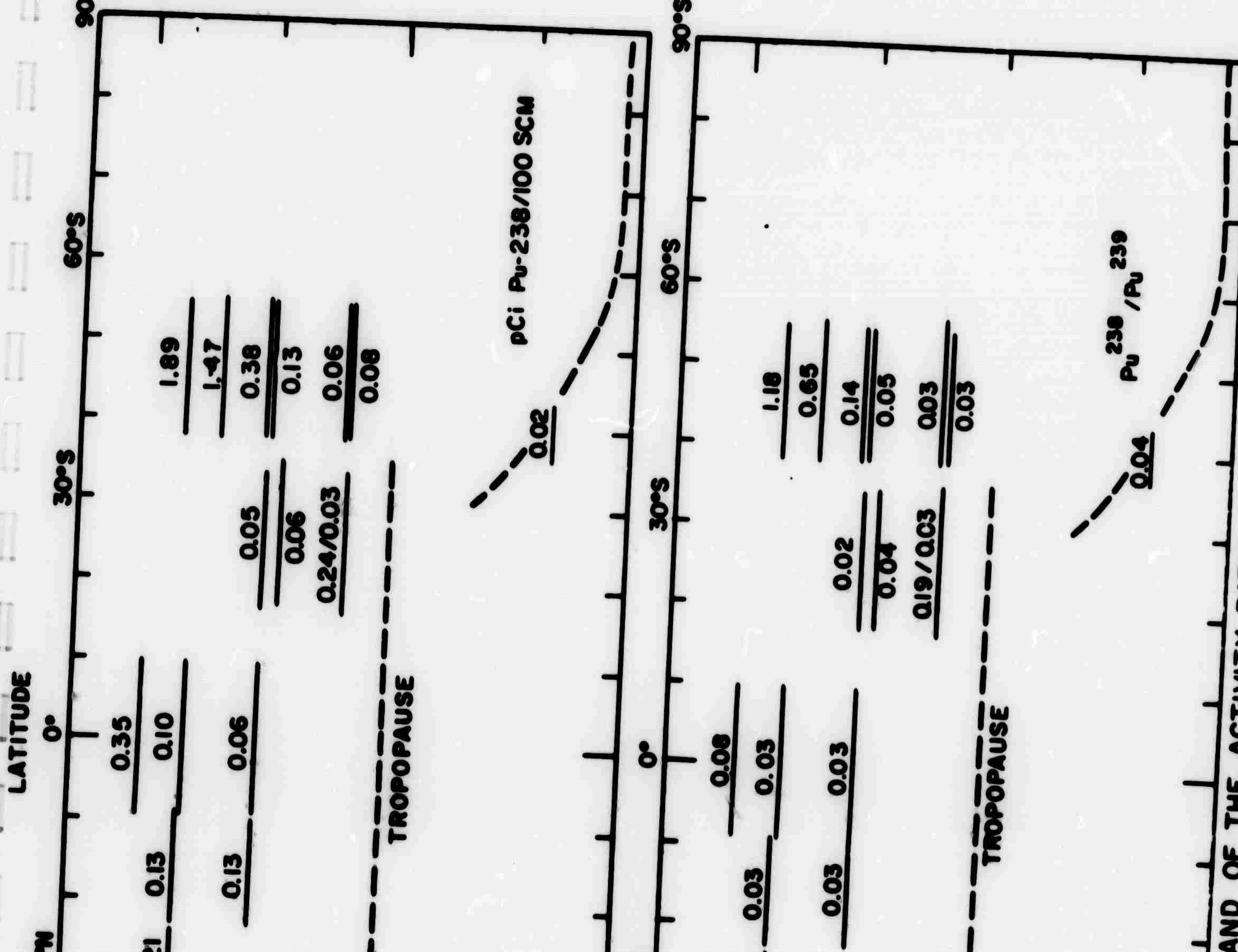

FIGURE 86. DISTRIBUTION OF Pu-238 AND OF THE ACTIVITY RATIO Pu-238/Pu-239 DURING JUNE 1965

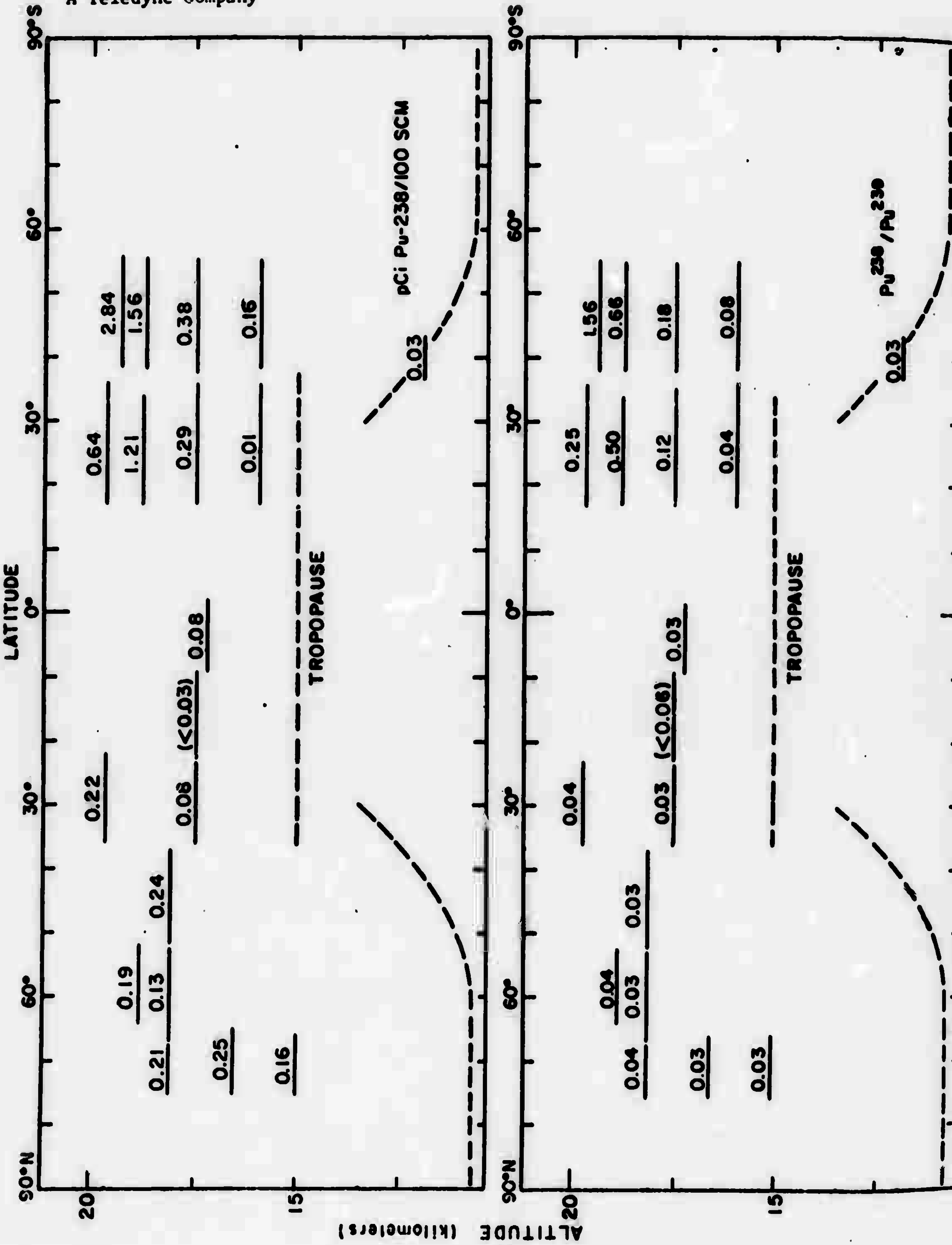

FIGURE 87. DISTRIBUTION OF Pu-238 AND OF THE ACTIVITY RATIO Pu-238/Pu-239 DURING JULY 1965

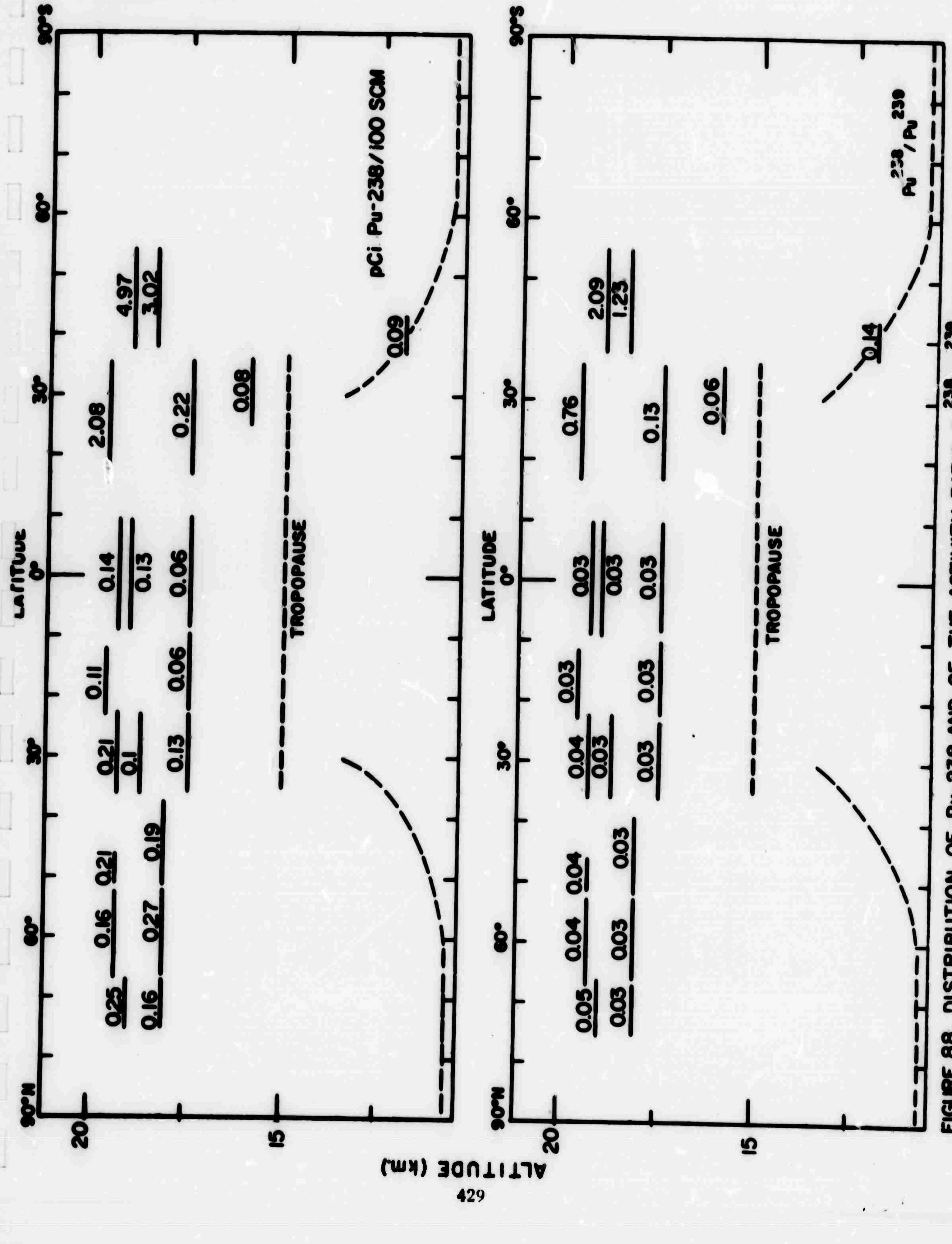

FIGURE 88. DISTRIBUTION OF Pu-238 AND OF THE ACTIVITY RATIO Pu^{238}/Pu^{239} DURING AUGUST 1965

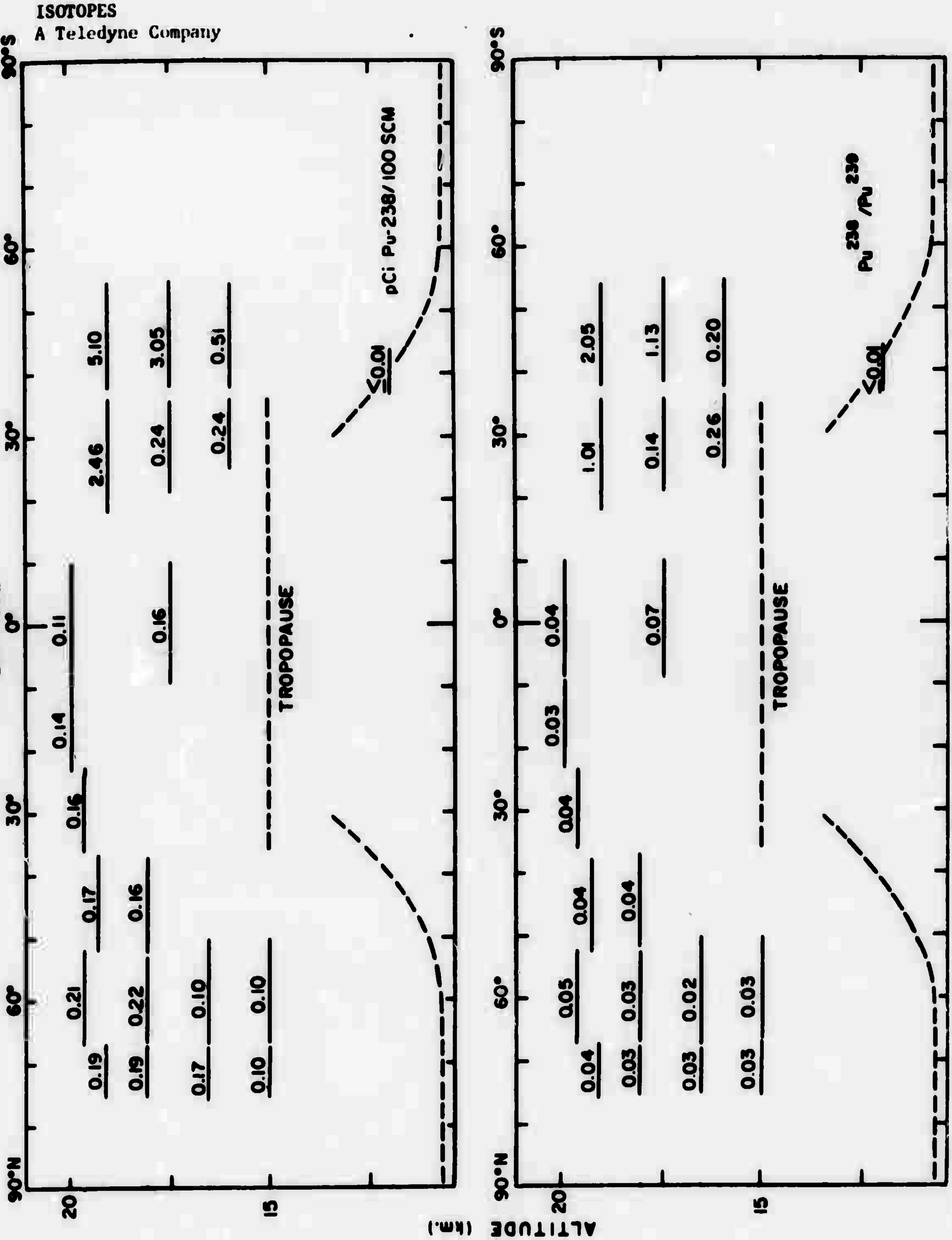

FIG... 8S... STI... JTK... OF ... 238 ... ID ... THE ...TIV... RA... PL... 8/... 39 ...RINC ...EPT. ...65

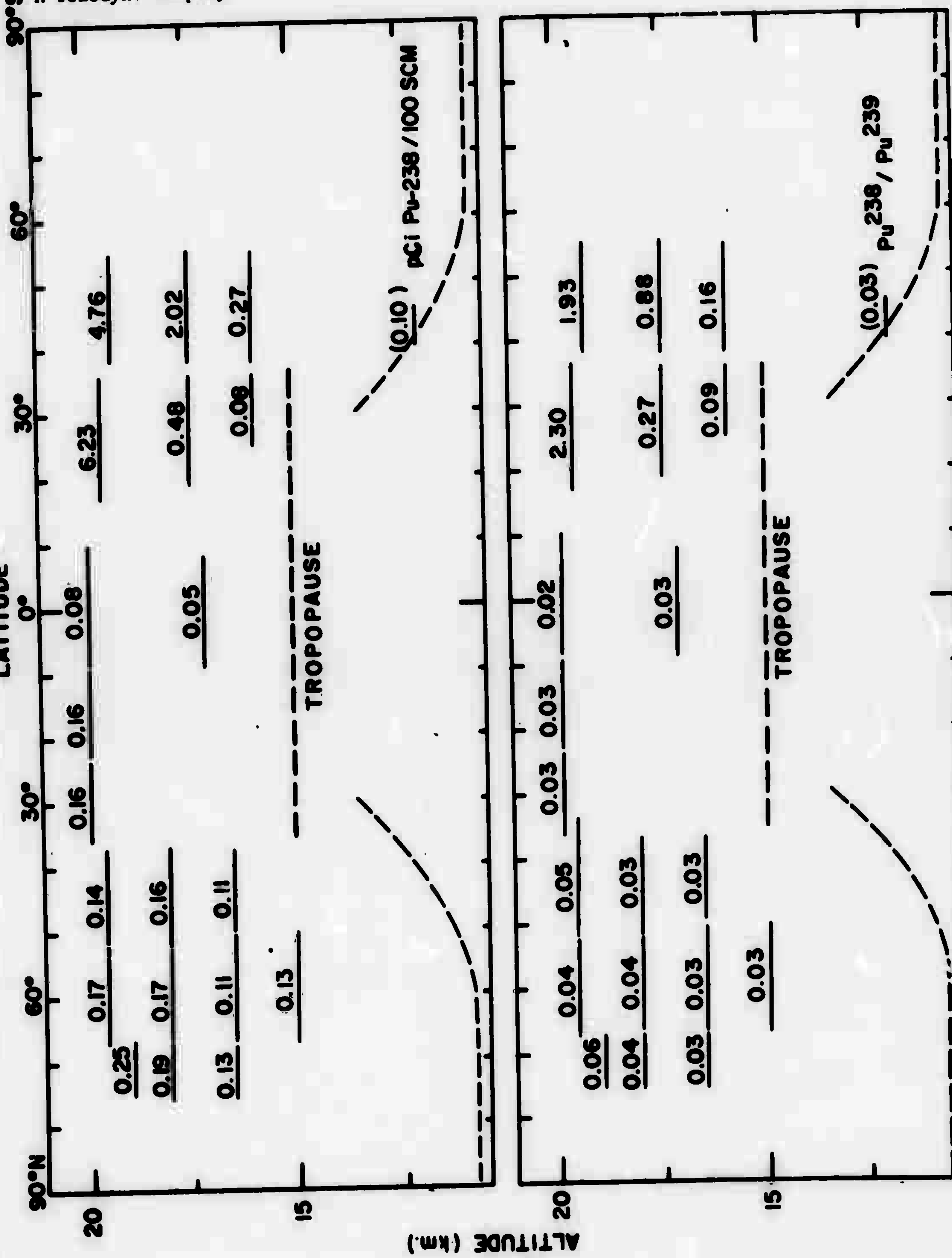

FIGURE 90. DISTRIBUTION OF Pu-238 AND OF THE ACTIVITY RATIO Pu-238/Pu-239 DURING OCT. 1965

ISOTOPES
A Teledyne Company

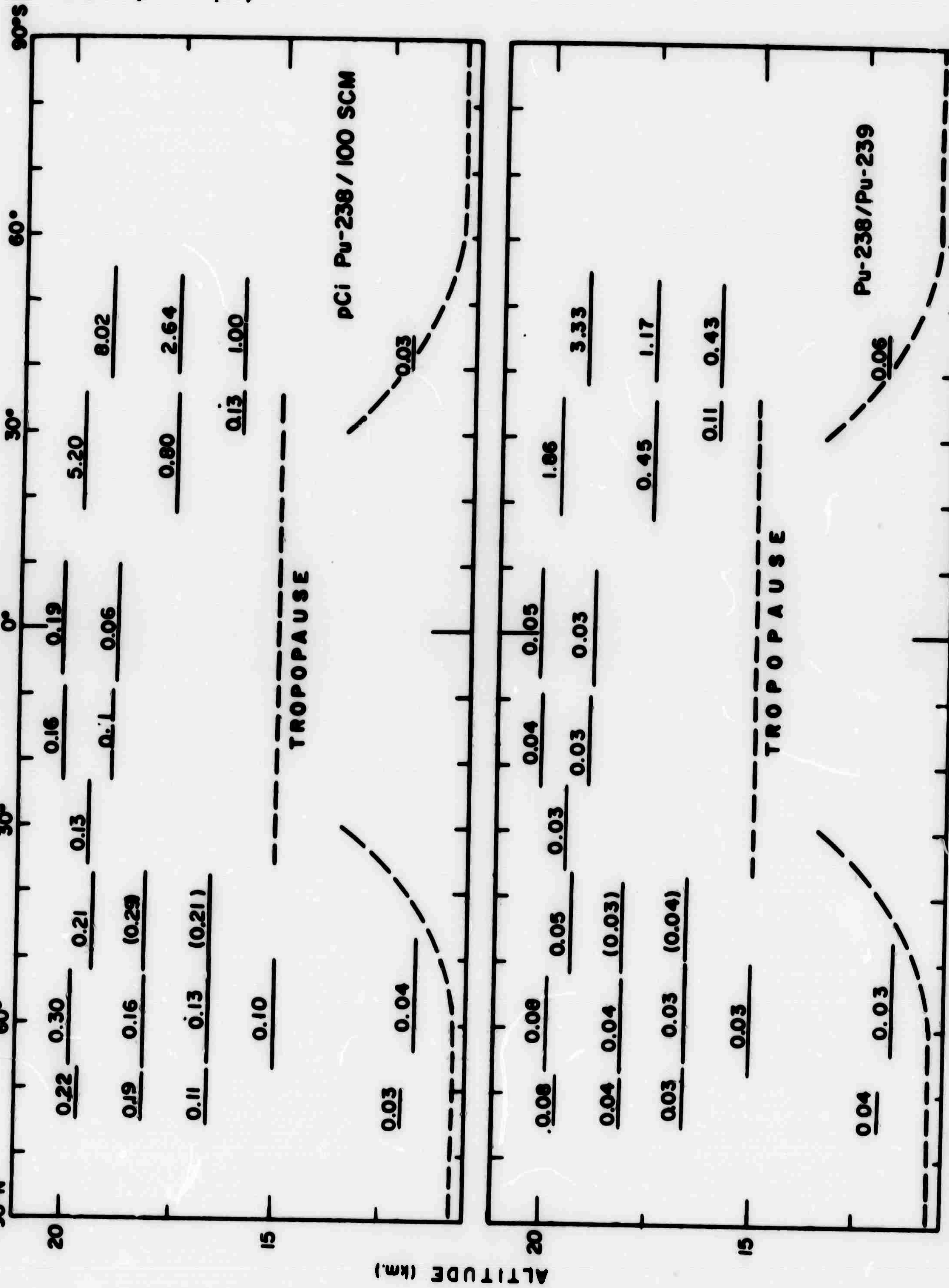

FIGURE 91. DISTRIBUTION OF Pu-238 AND OF THE ACTIVITY RATIO Pu-238/Pu-239 DURING NOVEMBER 1965.

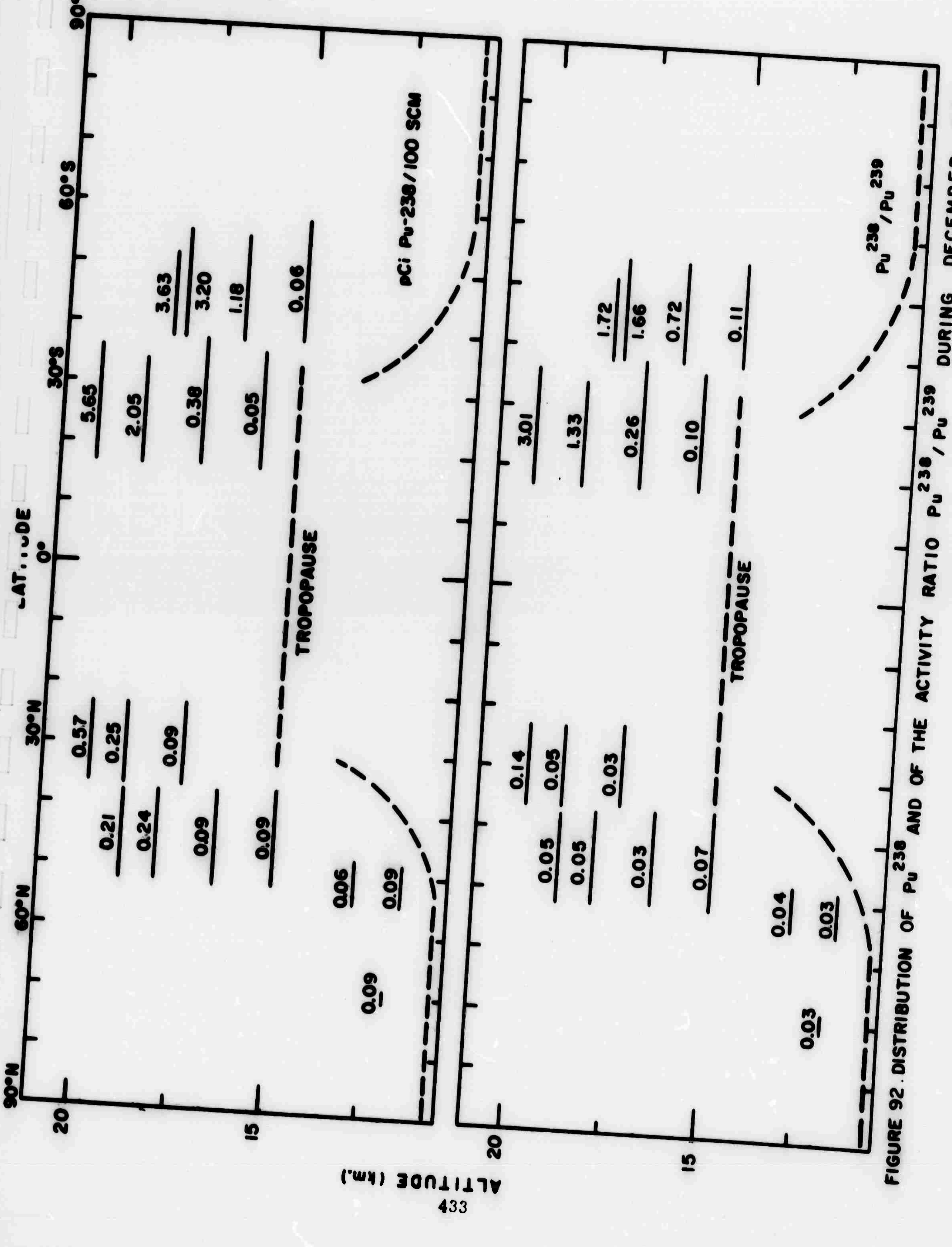

FIGURE 92. DISTRIBUTION OF Pu^{238} AND OF THE ACTIVITY RATIO Pu^{238}/Pu^{239} DURING DECEMBER 1965.

At 35° - 45°S (Figure 93) the plutonium-238 concentrations at 32 and then at 27.5 kilometers increased during the late winter and early spring seasons (August-October) of the Southern Hemisphere during 1964 as SNAP-9A debris moved downward from the higher levels where it had been injected in April 1964 (and perhaps as it moved equatorward from higher latitudes where most of the downward movement may actually have occurred.) Little additional downward movement of the SNAP-9A debris occurred at 35° - 45°S during October 1964 to March 1965 (the summer season of the Southern Hemisphere), but during April to August 1965 (the autumn and the winter seasons) the debris moved downward again, reaching the level of the tropical tropopause in detectable quantities. This downward motion of the debris resulted in about a tenfold decrease in the plutonium-238 concentrations at 32 kilometers. After August 1965 any additional downward movement of the SNAP-9A debris at 35° - 45°S was slow, as the winter circulation gave way to the spring and summer circulation of the stratosphere.

At 5° - 10°N (Figure 94) in the tropical stratosphere SNAP-9A debris was present at 32 kilometers by the beginning of 1965, but had not reached 19.8 kilometers by November 1965.

In the northern polar stratosphere (Figures 95 and 96) SNAP-9A plutonium-238 reached 27 kilometers, coming from the region above 32 kilometers during the winter of 1964-1965, and reached 24 kilometers during the spring and summer of 1965. It was not until December 1965, after the winter circulation of the polar stratosphere had again been established in the Northern Hemisphere, that it reached 19.8 kilometers at 30° - 40°N (and presumably also at 65° - 70°N), where it was sampled by STARDUST aircraft.

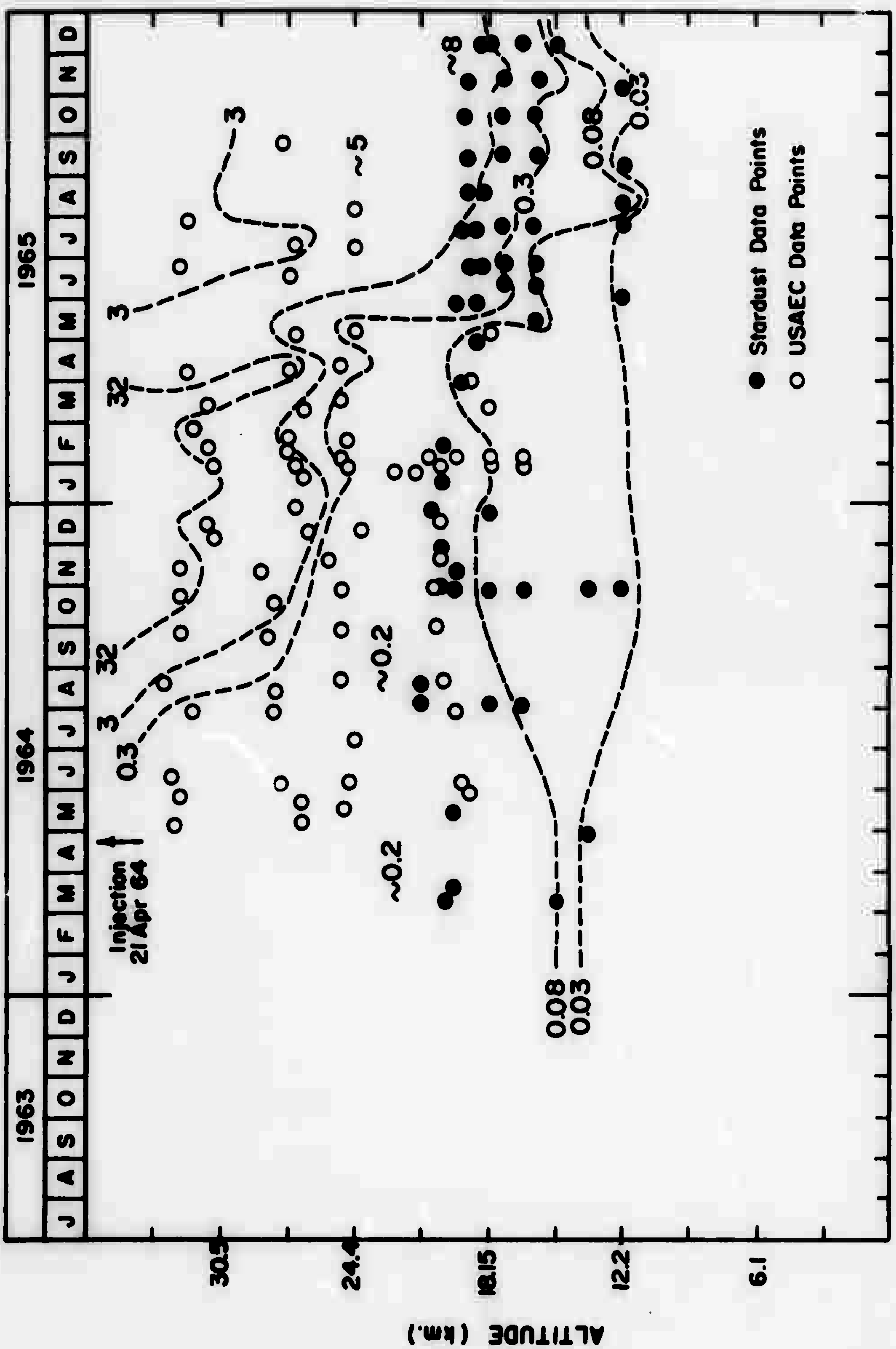

FIGURE 93. PLUTONIUM-238 ACTIVITIES (pCi Pu-238/100 SCM) AT 35°-45°S DURING 1964 - 1965

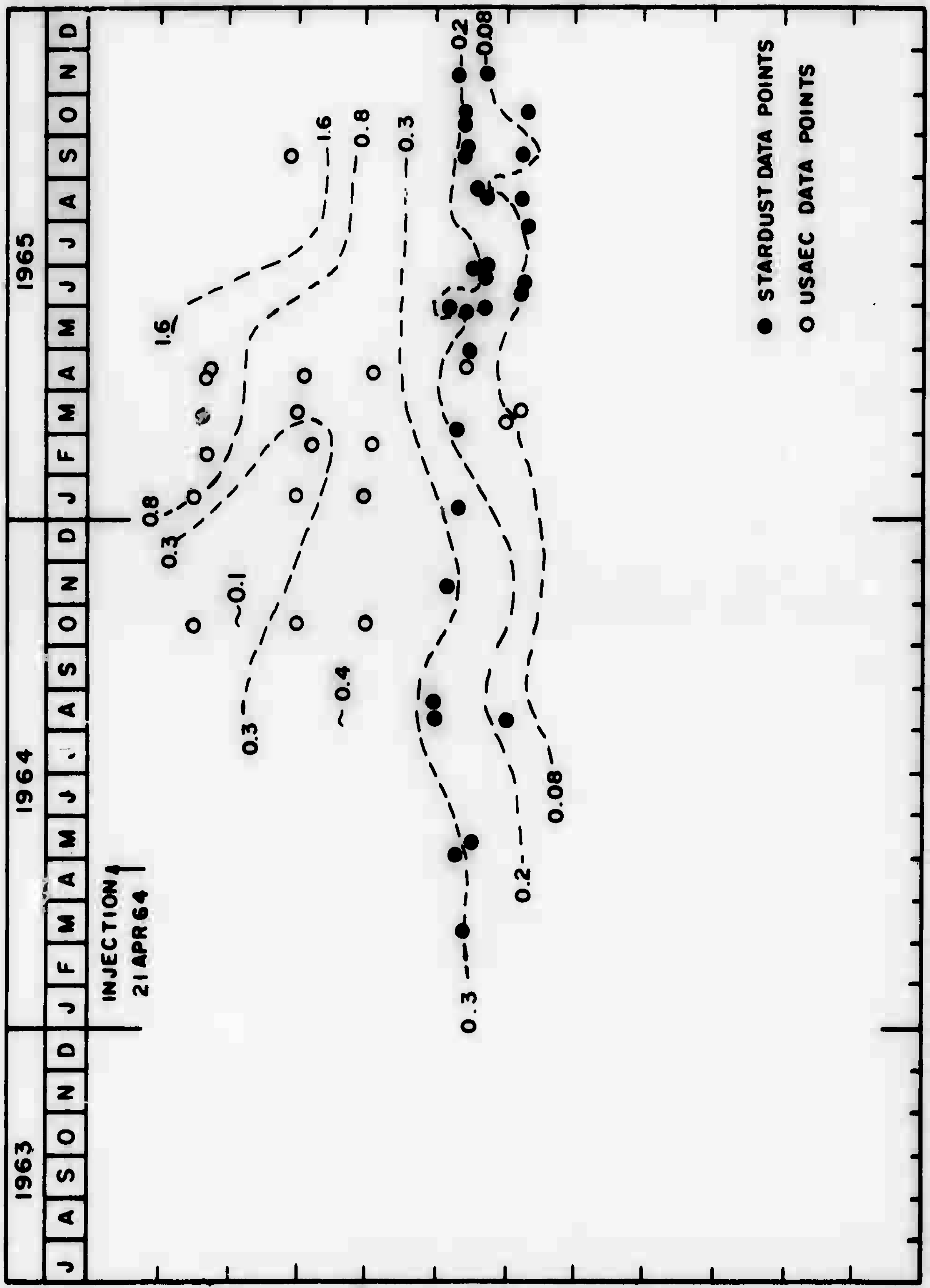

FIGURE 94. PLUTONIUM-238 ACTIVITIES (pCi Pu-238/100 SCM) AT 5°-10°N DURING 1964-1965

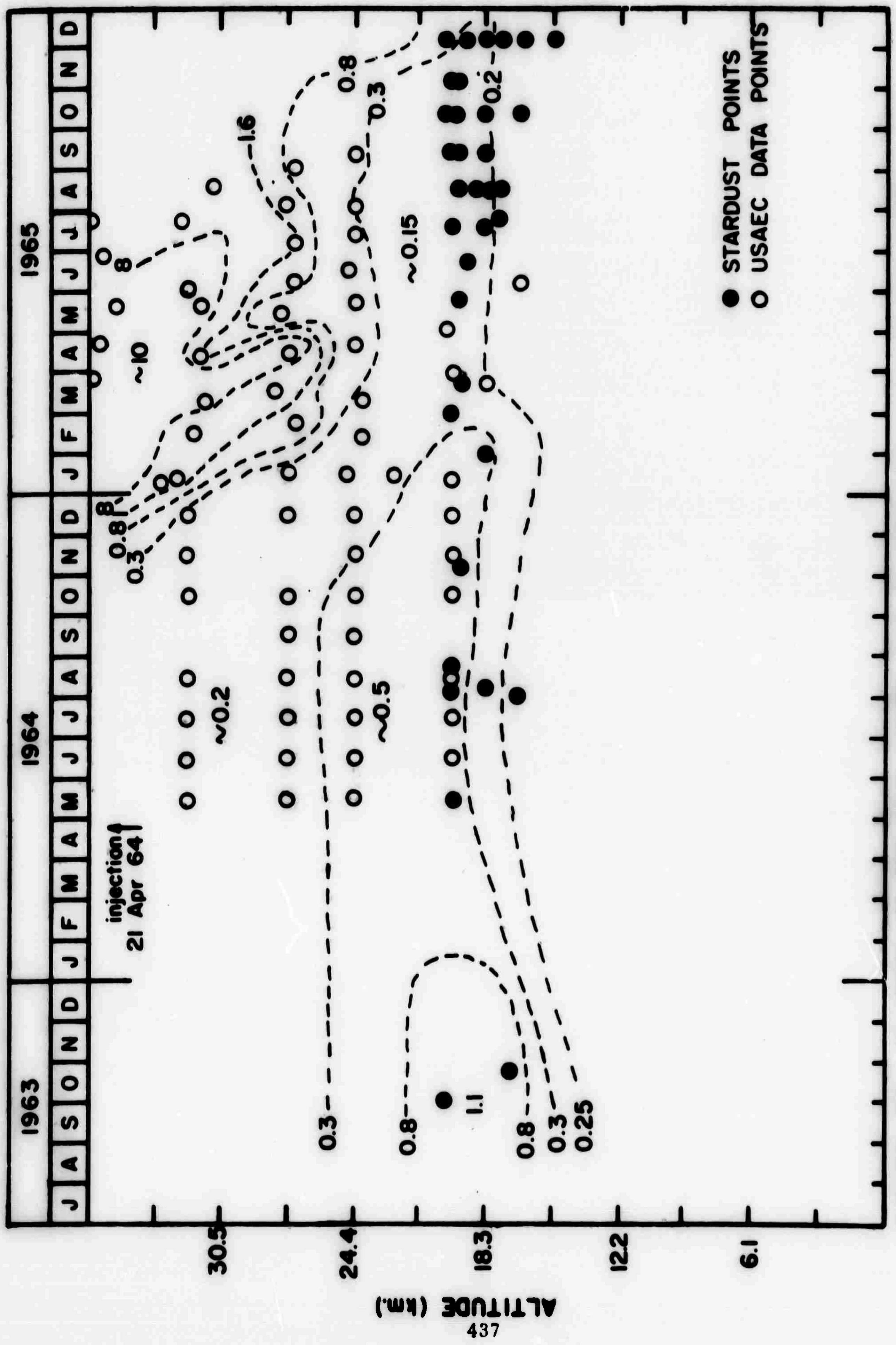

FIGURE 95. PLUTONIUM-238 ACTIVITIES (pCi Pu-238/100 SCM) AT 30°-40°N DURING 1963 - 1965

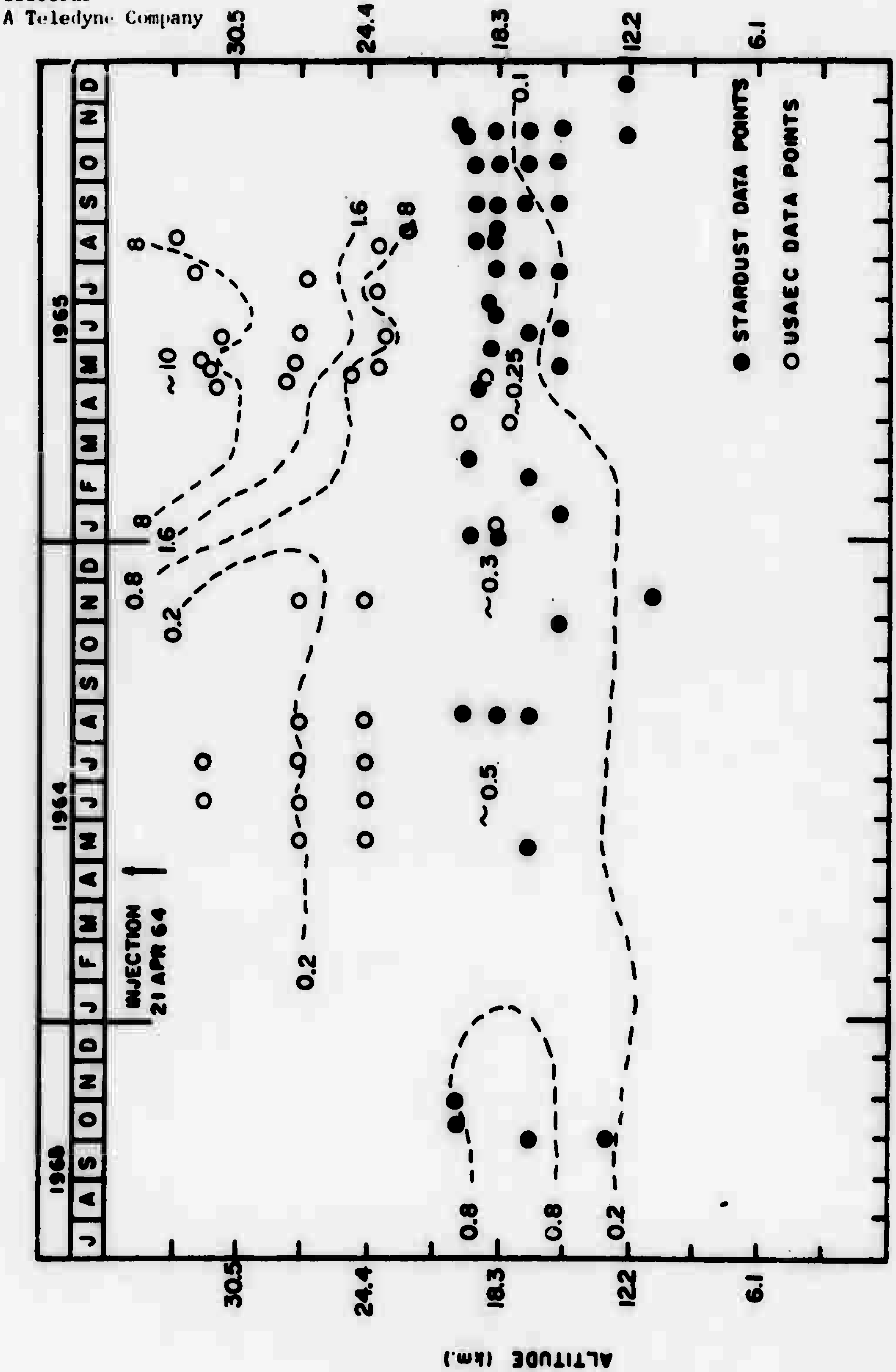

FIGURE 96. PLUTONIUM-238 ACTIVITIES (pCi Pu-238/100 SCM) AT 65°-70° N DURING 1963-1965

ISOTOPES
A Teledyne Company

The value of the Pu^{238}/Pu^{239} activity ratio was approximately 0.03 in STARDUST samples collected in the Southern Hemisphere before May 1965 and in the Northern Hemisphere before November 1965. Using this value, then, as the Pu^{238}/Pu^{239} ratio in debris from nuclear weapon tests, we have calculated the weapons component of plutonium-238 in each STARDUST sample based on the measured plutonium-239 concentration in the sample. We have subtracted this weapons component from the total plutonium-238 concentration of each sample to determine the SNAP-9A component (see Appendix 9-A).

The concentrations of SNAP-9A plutonium-238 in samples collected at 40°S and in samples collected at 25°S have been plotted in time-altitude sections in Figure 97 and concentration isolines have been drawn through the data points. At 40°S SNAP-9A plutonium-238 reached 20 kilometers during May 1965 and reached 14 kilometers in the vicinity of the polar tropopause in August 1965. At 25°S the SNAP-9A plutonium-238 probably reached 20 kilometers during June 1965 and reached 16 kilometers in the vicinity of the tropical tropopause by September 1965. It is evident that the mechanisms of atmospheric transport which cause the movement of radioactive debris from the upper into the lower stratosphere are capable of transferring significant quantities of the debris through virtually the entire thickness of the lower stratosphere over the course of a few months. Such rapid transfer is probably more readily explained in terms of eddy diffusion than in terms of mean advective transport within the stratosphere.

After August 1965 changes in the distribution of SNAP-9A plutonium-238 at 40°S occurred only slowly. Presumably this reflects a decrease in the rate of vertical exchange with the onset of the summer circulation in the southern stratosphere. The decrease in concentrations in the layer between 12 and 17

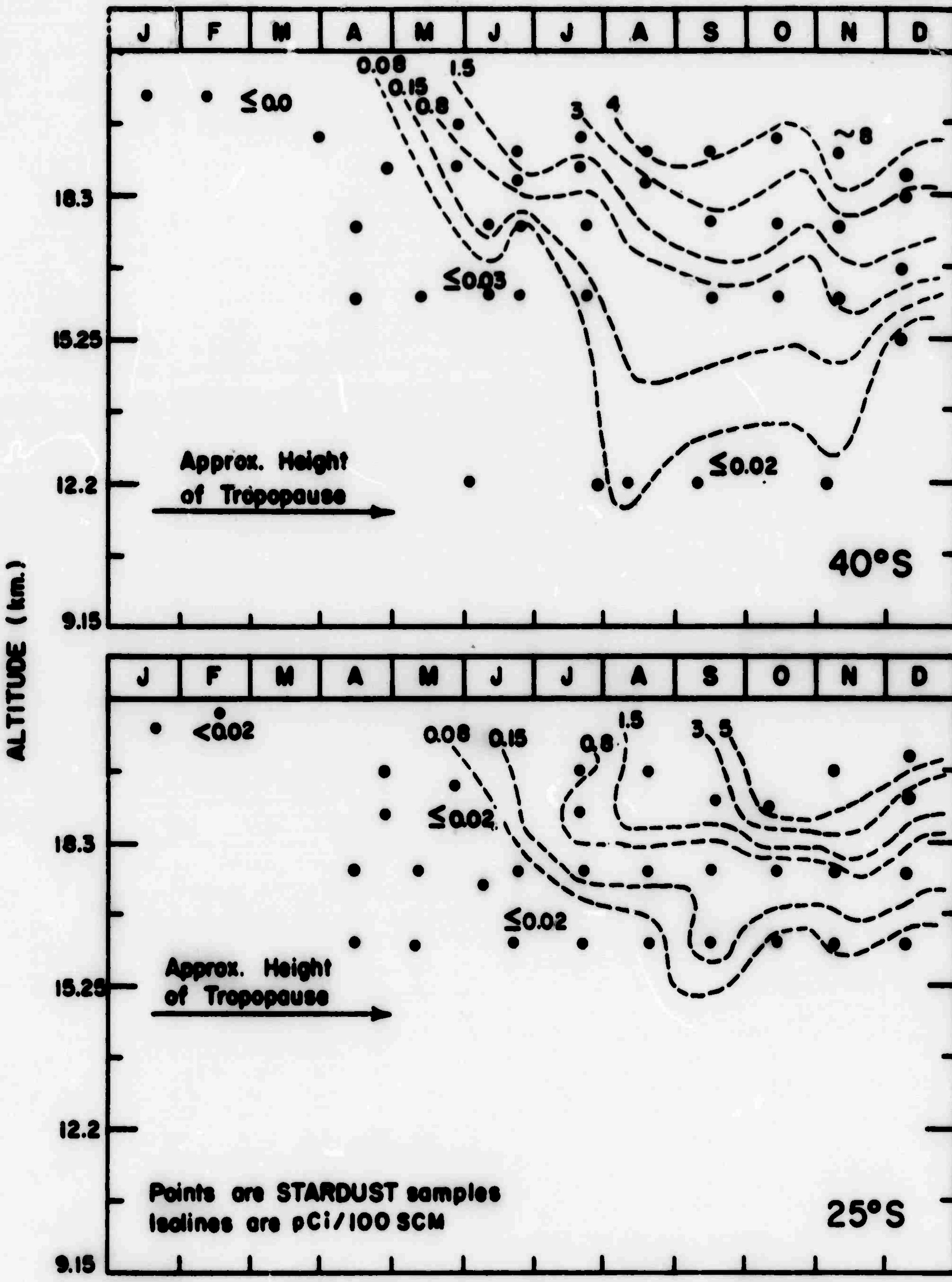

FIGURE 97. TIME-ALTITUDE DISTRIBUTION OF SNAP-9A Pu-238 AT 40°S AND 25°S DURING 1965

kilometers at 40°S after October 1965 probably resulted from the poleward migration of the jet stream to latitudes higher than 40° during the spring months, with the resultant replacement of the low polar tropopause by the high tropical tropopause at 40°S.

9.4 Distribution of SNAP-9A Plutonium-238 from January 1966 to June 1967

The concentrations of SNAP-9A plutonium-238 in samples collected at three latitudes at 19 to 20 km during 1966 and 1967 are included with the 1964 and 1965 data and are plotted in Figure 98. SNAP-9A plutonium-238 reached the 19- to 20-km level at 40°S during the Southern Hemisphere winter season in mid-1965, with concentrations rising rapidly from below 0.05 pCi/100 SCM in April to over 1 pCi/100 SCM in May, and to 5 pCi/100 SCM by August. These dropped back to a value of about 3 pCi/100 SCM and remained fairly steady during the first six months of 1967. At 70°N concentrations increased gradually at 19 to 20 km during the course of 1965, but then rose rapidly during the Northern Hemisphere winter season of 1965-1966. They continued to maintain the peak level of 1.5 to 2 pCi/100 SCM to June 1967. Some SNAP-9A plutonium-238 was intercepted in the equatorial region at 19 to 20 km during June 1965, shortly after it reached the lower southern polar stratosphere. It was not until late 1965, however, when SNAP-9A plutonium-238 also reached the lower northern polar stratosphere, that a sustained upward trend began in the concentrations found at the equator. This trend appeared to have terminated in March 1967.

Plutonium-238 data from the USAEC balloon sampling program[51,56,57] have been combined with data from Project STARDUST to calculate the vertical profiles of SNAP-9A plutonium-238 concentrations shown in Figures 99 and 100.

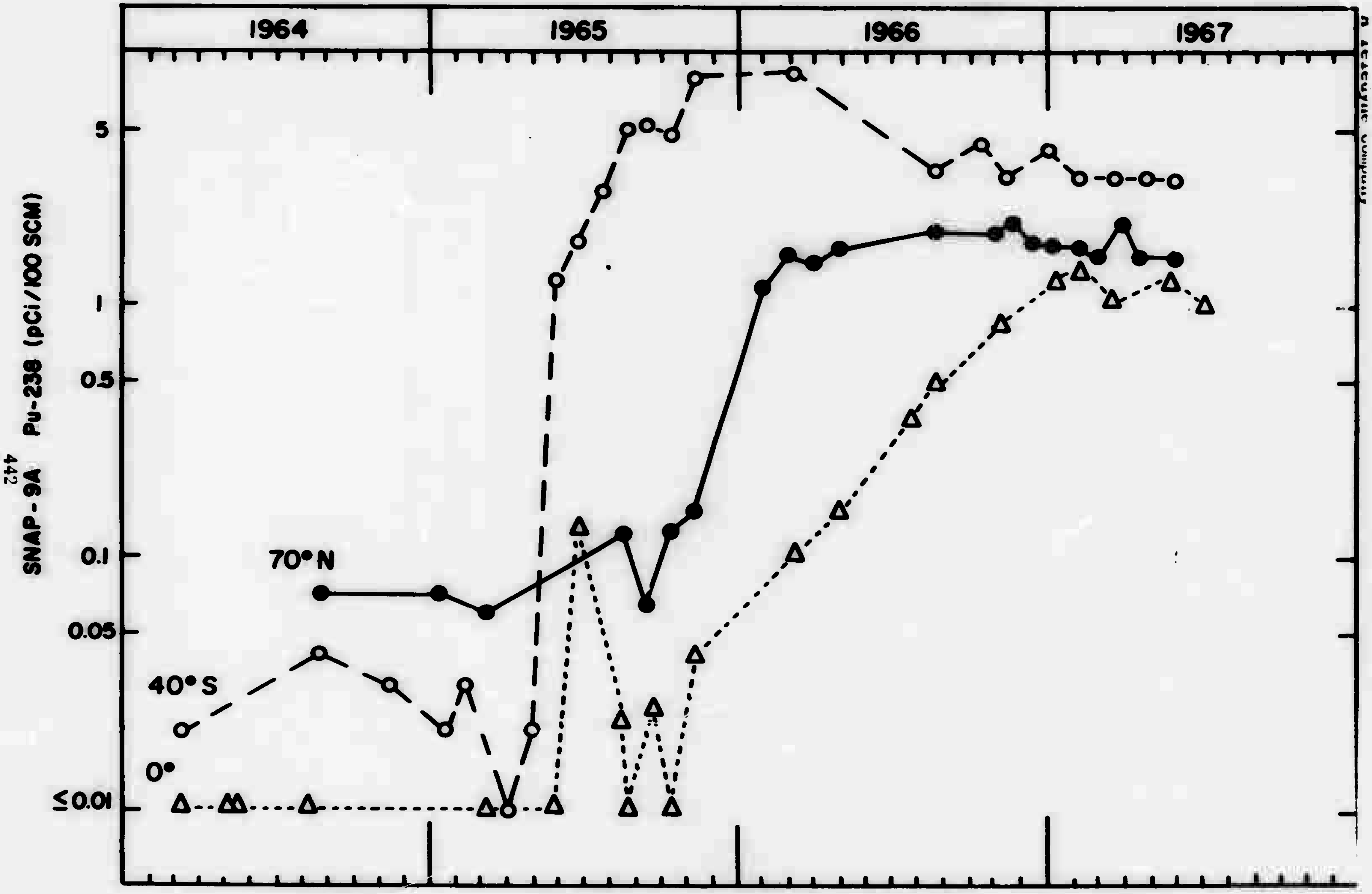

FIG. 98 CONCENTRATIONS OF SNAP-9A PLUTONIUM-238 AT 19-20 km.

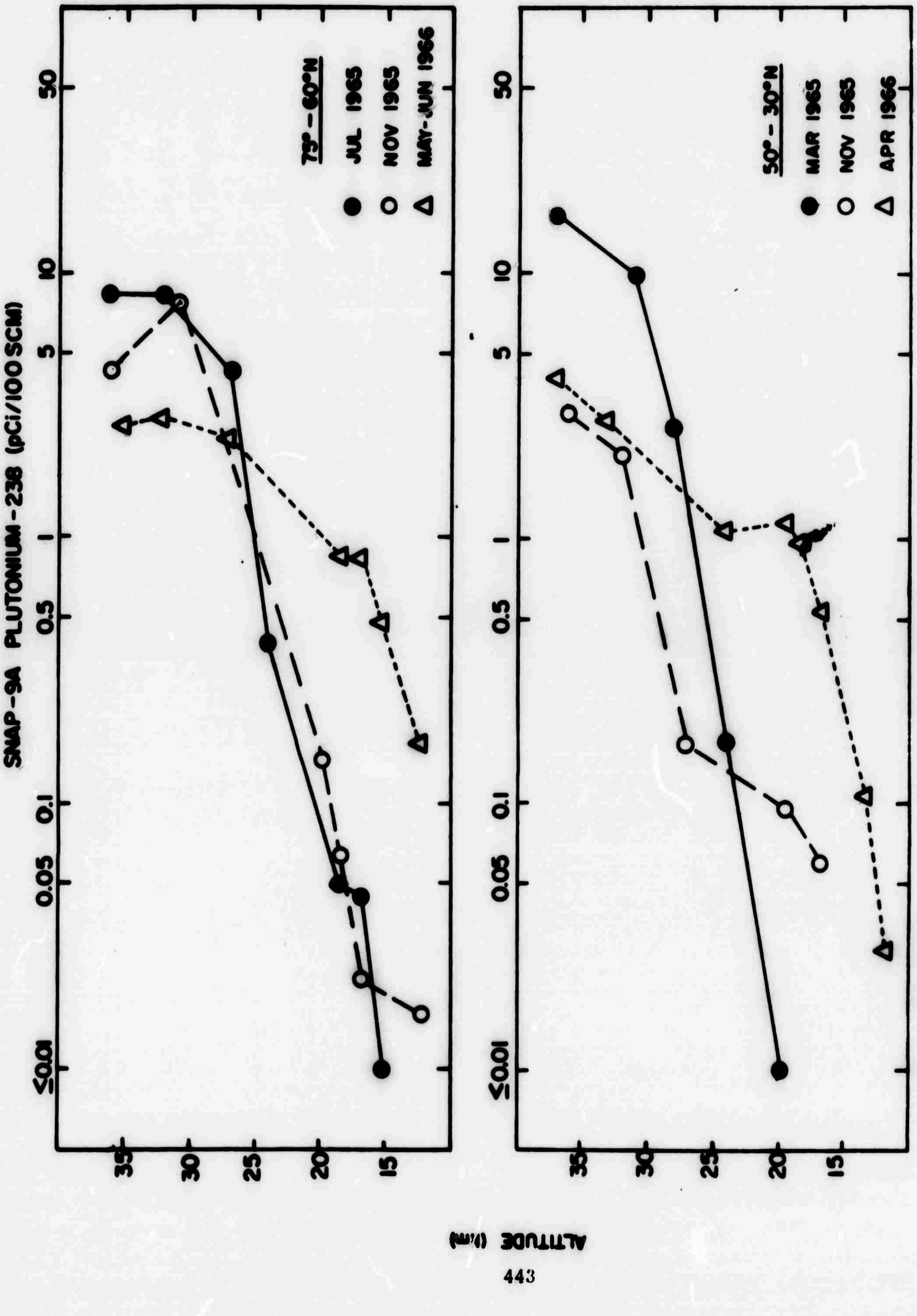

FIG. 99. VERTICAL PROFILES OF SNAP-9A PLUTONIUM-238 IN THE NORTHERN HEMISPHERE STRATOSPHERE

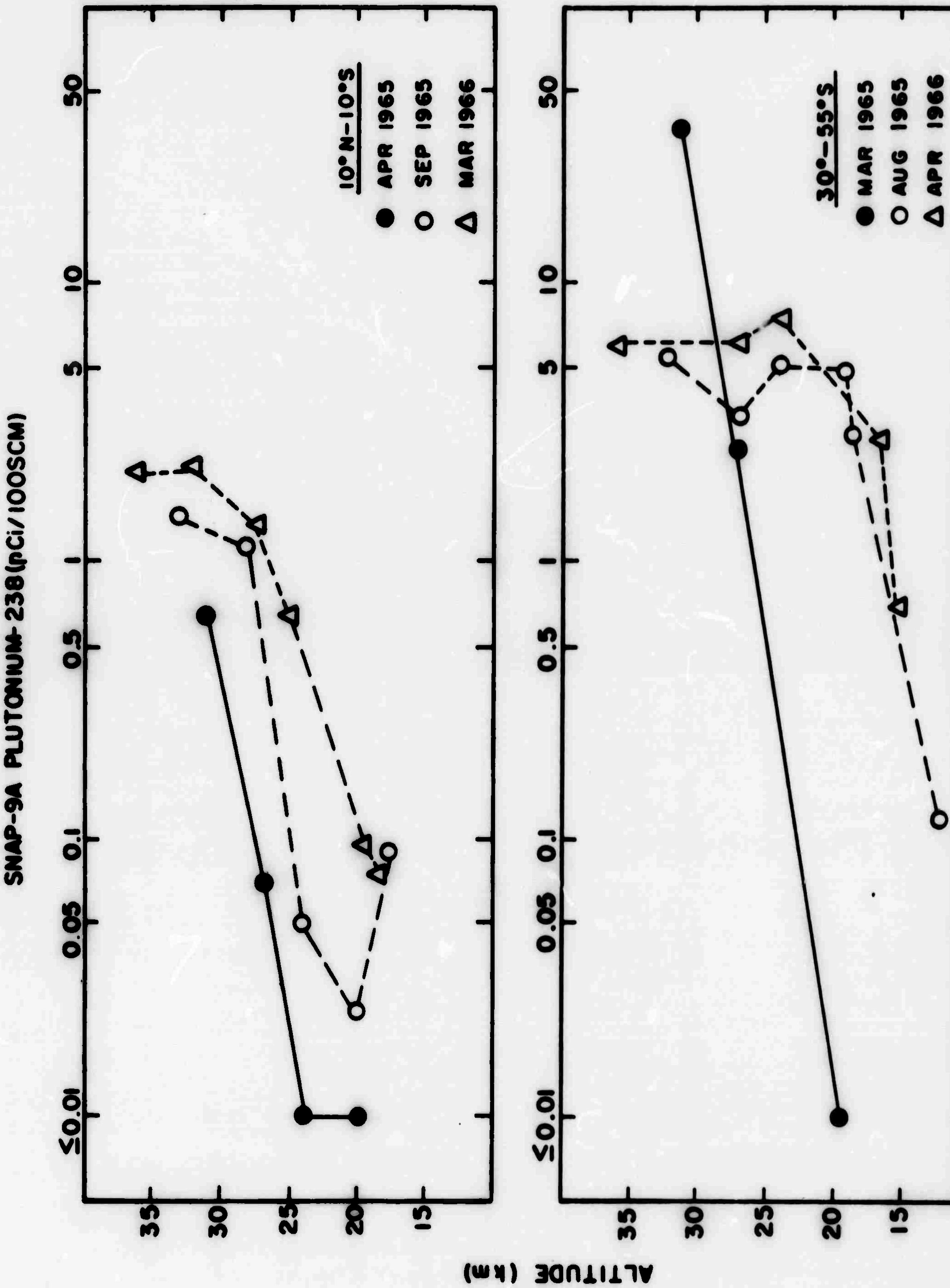

FIG. 100 VERTICAL PROFILES OF SNAP-9A PLUTONIUM-238 IN THE EQUATORIAL AND SOUTHERN HEMISPHERE STRATOSPHERE

In Figure 99 are shown profiles for July 1965, November 1965 and May-June 1966, at 75° - 60°N, and March 1965, November 1965 and April 1966 at 50°- 30°N. It is evident from this figure that in the northern polar stratosphere during 1965 to 1966 the concentrations of SNAP-9A plutonium-238 decreased with time at the higher altitudes and increased at the lower altitudes. Nevertheless, during early 1966 the highest concentrations were still present in the upper stratosphere, and the vertical gradient was still quite steep in the lower northern polar stratosphere. In Figure 100 are shown profiles for April 1965, September 1965 and March 1966 at 10°N - 10°S, and March 1965, August 1965 and April 1966 at 30°- 55°S. In the equatorial region there was a steep vertical concentration gradient during 1965 to 1966, with the highest concentrations at the highest altitudes sampled. The concentrations increased at all altitudes, including the highest sampled, during the course of 1965-1966. Before May 1965 there was a steep vertical concentration gradient at 30° - 55°S, with the highest concentrations at the highest altitudes sampled. By the end of the mid-1965 winter season, however, fairly uniform concentrations were found at all altitudes from 25 km to the highest altitude sampled, about 32 km, and significant concentrations of SNAP-9A plutonium-238 were found at all levels in the lower southern polar stratosphere. By April 1966 the layer of rather uniform concentrations appeared to extend from 26 km or higher down to 19 km. No substantial change below 20 km was found up to February 1967.

The concentrations of SNAP-9A plutonium-238 measured in samples collected at about 20 km have been plotted on a latitude-time diagram in Figure 101, together with the flight tracks of the sampling aircraft, and concentration isolines have been drawn through the data. The rather sudden entrance of SNAP-9A

plutonium-238 into the lower southern polar stratosphere during mid-1965, and its apparent subsequent equatorward migration may be seen in the figure. A steep concentration gradient was established between the southern polar and southern tropical stratosphere at about 20°S during the second half of 1965, and this gradient grew less steep only slowly from then until mid-1966. Between mid-1965 and early 1966 SNAP-9A plutonium-238 entered the lower northern polar stratosphere -- at first slowly, during the late summer and the autumn seasons, and then rather rapidly, during the winter season -- and showed an apparent equatorward movement as it did so. This movement ceased in October 1966. By the second quarter of 1967 the concentrations over all latitudes sampled at 20 km showed about a fourfold variation, from 1.5 pCi/100 SCM in the north to 0.7 at the equator and 3.0 at 45°S.

The concentrations of SNAP-9A plutonium-238 measured in samples collected in a series of latitude bands have been plotted on altitude-time diagrams in Figures 102 to 105, together with points representing sample collections, and concentration isolines have been drawn through the data. Data for 75° - 67°N and 67° - 52°N are plotted in Figure 102, those for 52° - 36°N and 36° - 23°N in Figure 103, those for 23° - 9°N and 9°N - 10°S in Figure 104, and those for 15° - 37°S and 38° - 55°S in Figure 105. The downward movement of plutonium-238 into the lower northern polar stratosphere during the 1965-1966 winter season is evident in Figures 102 and 103. It is noteworthy that by the beginning of the spring season in 1966 the SNAP-9A plutonium-238 had reached the lowest stratospheric levels sampled, in the vicinity of the tropopause. The downward movement of SNAP-9A plutonium-238 into the lower southern polar stratosphere during the mid-1965 winter season is evident in Figure 105. By the

ISOTOPES,
A Teledyne Company

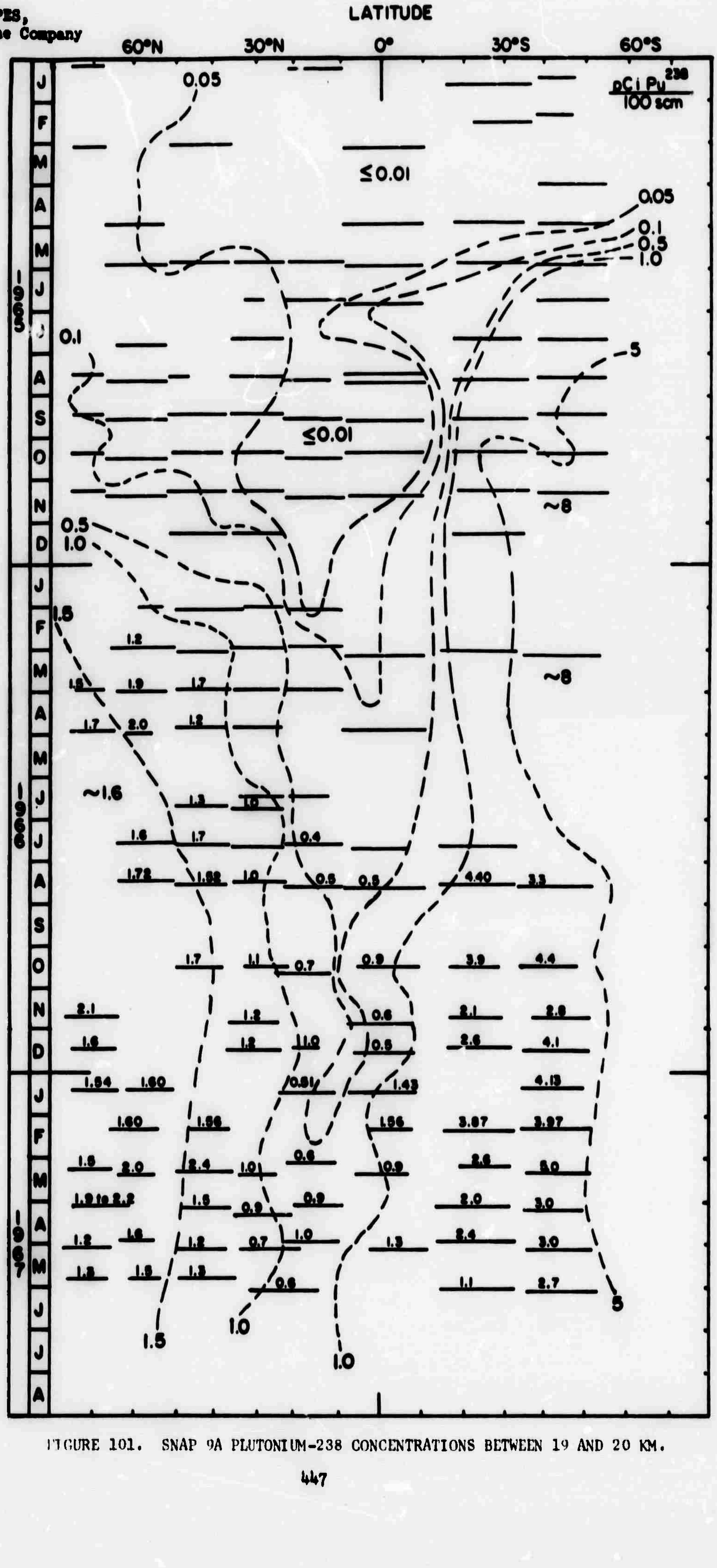

FIGURE 101. SNAP 9A PLUTONIUM-238 CONCENTRATIONS BETWEEN 19 AND 20 KM.

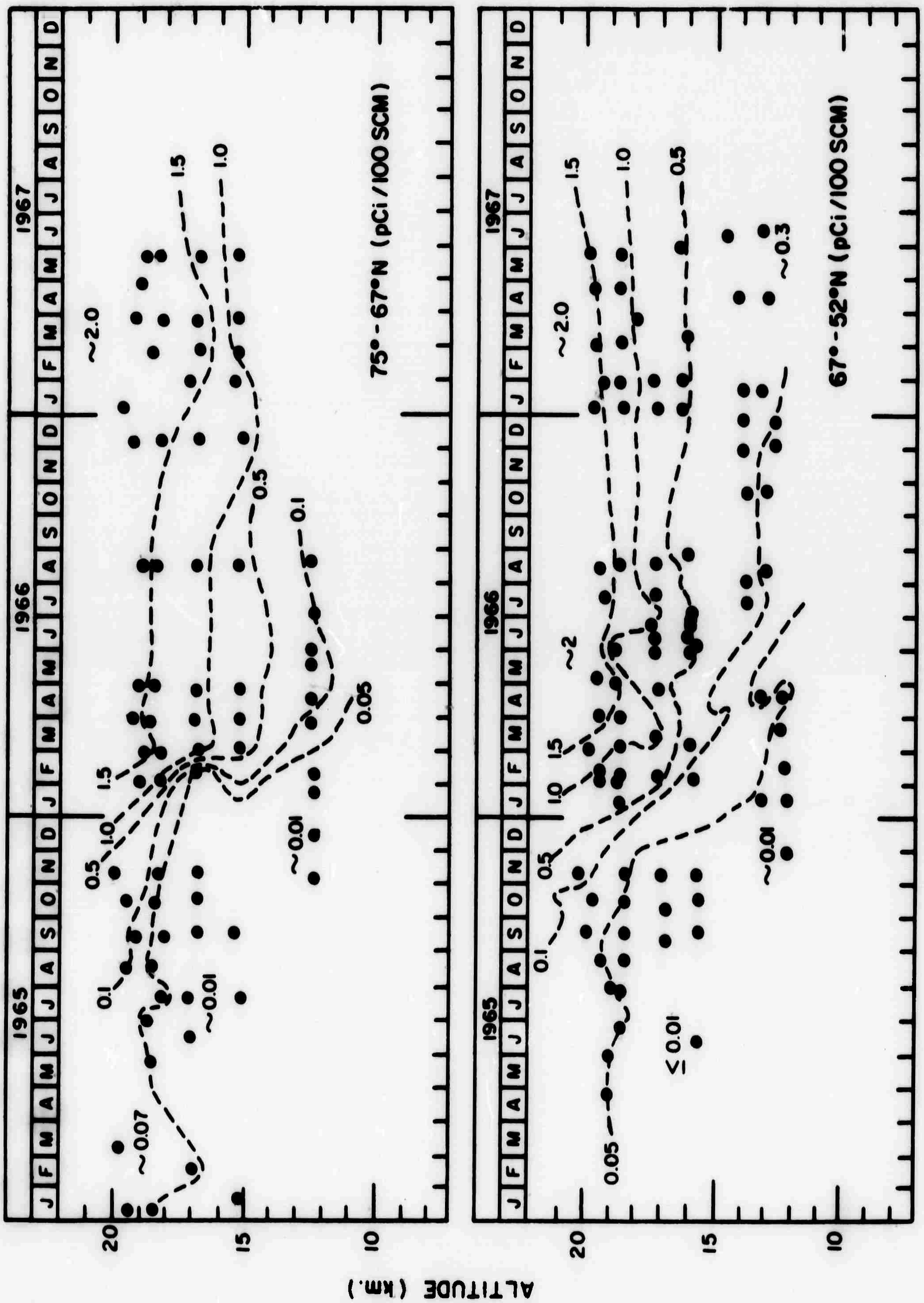

FIG. 102 SNAP-9A PLUTONIUM-238 CONCENTRATIONS AT 75°-67°N AND 67°-52°N

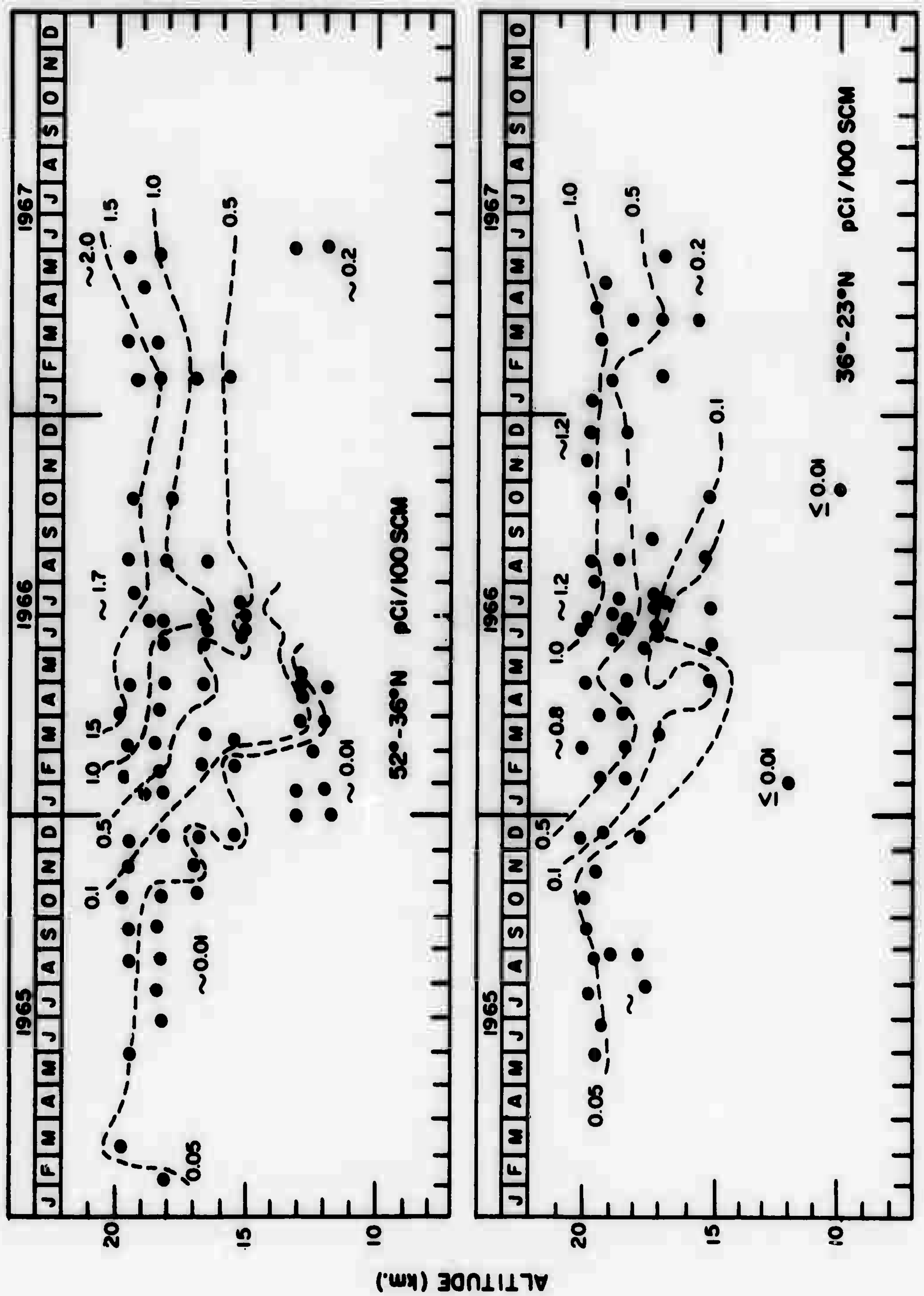

FIG. 103 SNAP-9A PLUTONIUM-238 CONCENTRATIONS AT 52°-36°N AND 36°-23°N

ISOTOPES
A Teledyne Company

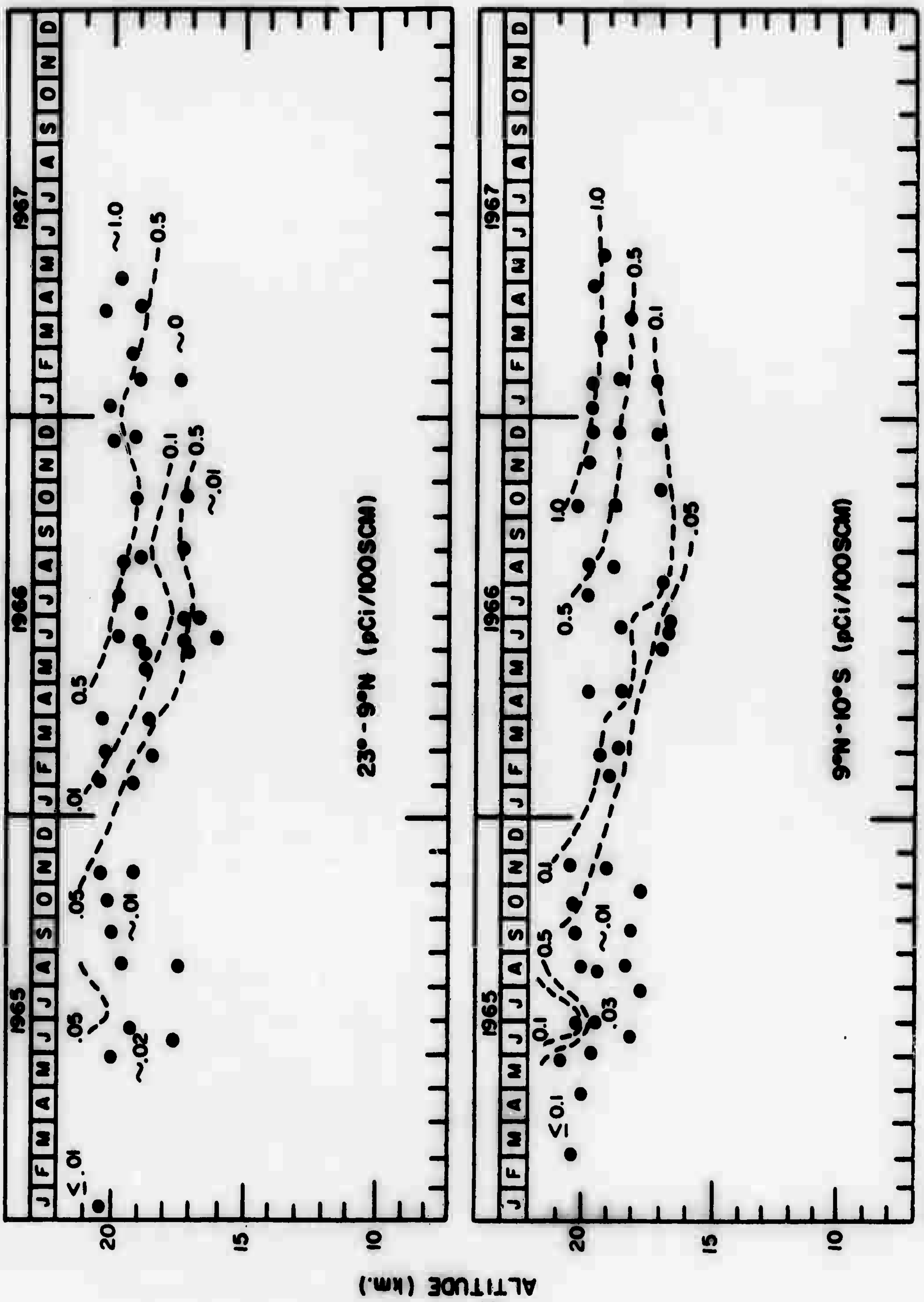

FIG. 104 SNAP-9A PLUTONIUM-238 CONCENTRATIONS AT 23°-9°N AND 9°N-10°S

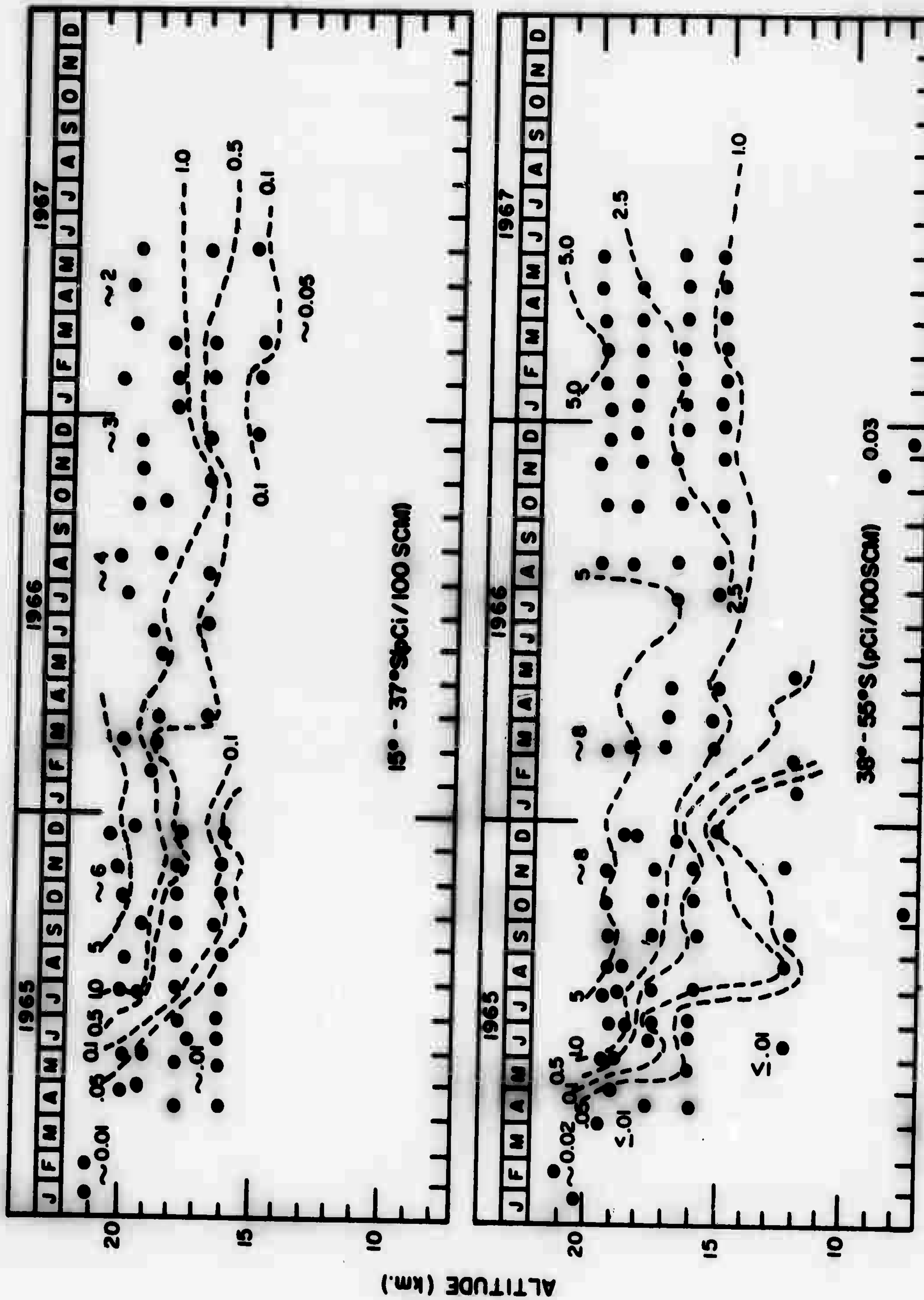

FIG. 105 SNAP-9A PLUTONIUM-238 CONCENTRATIONS AT 15°-37°S AND 38°-55°S

beginning of the spring season in late 1966 plutonium-238 had reached the lowest stratospheric levels sampled, in the vicinity of the tropopause. The movement of plutonium-238 into the tropical stratosphere during late 1965 and early 1966 by downward and/or equatorward migration is evident in Figure 104.

The concentration isopleths of SNAP-9A plutonium-238 in the Northern Hemisphere (Figures 102 and 103) showed little change during the period from mid-1966 to mid-1967. In the equatorial region the concentrations during this period were still slowly increasing at the 19- and 20-kilometer levels. In the region of 38°to 55°S shown in Figure 105 a significant decrease in the concentrations between 16 and 20 km is seen starting in mid-1966.

One could conclude that during late 1966 and early 1967 at 15 to 20 km in the Northern Hemisphere transfer of plutonium-238 to the south or to the troposphere was offset by contributions from the upper stratosphere. This could imply that the supply of plutonium-238 in the upper northern stratosphere was not substantially depleted. Near the equator contributions to the lower stratosphere continued to be greater than the amounts transferred to the troposphere. However, closer to the southern polar region the contribution from the upper stratosphere was less than that lost to the troposphere. Thus the concentrations remaining in the upper stratosphere were too low to offset the effects of fallout. Nevertheless these remaining concentrations are still higher than those in the Northern Hemisphere.

9.5 Conclusions on the Transport Mechanism

Telegadas and List[58] concluded that the observed downward movement in the northern polar stratosphere of rhodium-102, cerium-144 and strontium-90 from the 1958 nuclear weapon tests "suggests that mass movement rather than

vertical diffusion is the dominant mechanism in the polar winter stratosphere between 14 and 20 km." List, et al.[59] believe that observations of the movement of cadmium-109 in the stratosphere are compatible with that conclusion.

It is evident from the STARDUST measurements of SNAP-9A plutonium-238, however, that the mechanism of vertical transport of radioactivity in the polar stratosphere of both hemispheres is capable of moving significant quantities of a tracer nuclide from the region above the 20 km level to below the 12 km level in the course of a single winter season. If this transfer is attributed to mass movement of the air, it is implied that all of the air below the 20 km level in the polar stratosphere is transferred downward into the troposphere during the course of the winter. If this occurred, all of the fission products, activation products and cosmic ray products in the lower polar stratosphere would also enter the troposphere during the winter, and the highest rates of fallout of these nuclides would occur in the winter and not in the spring, as is actually observed. Moreover, the replacement of the 18×10^{16} kg of air between 12 and 20 km in the polar stratosphere (30° - 90° latitude) by air moving down from the upper stratosphere would also require an influx of air from the tropical stratosphere into the upper polar stratosphere, for the latter region contains only 7×10^{16} kg. If the extra 11×10^{16} kg of replacement air came from the tropical stratosphere of the same hemisphere, all of the air above about 17 km would be required.

If this massive movement of air occurred, all of the air in the upper atmosphere -- and all of the tracer nuclide as well -- would be transferred into the lower polar stratosphere within a single year, and this is clearly not true. In fact, more than a year had passed following their injections at high altitude

before any rhodium-102, cadmium-109 or plutonium-238 entered the lower stratosphere, and two years after their injections the concentrations of these nuclides in the upper stratosphere were still high. Furthermore, if virtually all of the air in the tropical stratosphere of each hemisphere were transferred into the polar stratosphere during the winter it would have to be replaced by air from the tropical stratosphere of the other hemisphere or by tropospheric air. If the replacement came from the stratosphere of the other hemisphere one result would be a rapid equalization of concentrations of radioactive debris within the tropical stratosphere of both hemispheres. There was a steep horizontal gradient in strontium-90 concentrations within the lower southern tropical stratosphere (0° - 30°S), however, for at least one year following the 1958 low latitude tests of nuclear weapons, and for two years following the 1962 tests. If the replacement came from the troposphere, the concentrations of radioactive debris in the tropical stratosphere should have become virtually zero within a year following the last injection into that region. Quite the contrary, by 1965 the highest concentrations of strontium-90 were found in the upper tropical stratosphere.

We would conclude, then, that the rapid movement of SNAP-9A plutonium-238 from the upper stratosphere down to the level of the tropopause during the course of only a single winter season can best be attributed to turbulent exchange within the winter polar vortex. This process would produce the observed gentle concentration gradient in the lower stratosphere, whereas downward mass movement would produce in the lower stratosphere the same steep concentration gradient observed in the upper stratosphere during the months which preceded the mass movement. Moreover, vertical turbulent exchange would cause high concentrations

of the tracer nuclides to remain in the upper stratosphere for several years, and this too is observed to occur.

9.6 Calculation of the SNAP-9A Plutonium-238 Stratospheric Burden

As an increasing fraction of the SNAP-9A plutonium-238 has entered the lower stratosphere it has become possible to calculate more accurately the stratospheric burden of this nuclide. The total injection has been reported[52,53] to be 17 kilocuries.

Thus, except for the negligible quantity that may have entered the troposphere by early 1966, the calculated stratospheric burden should be 17 kilocuries. Using the data from Project STARDUST and from the USAEC balloon program, however, we calculated the stratospheric burden of SNAP-9A plutonium-238 during September-December 1965 to be 7.5 kilocuries according to the distribution shown in Figure 105-A. Presumably this low value resulted from our under-estimating concentrations in the upper atmosphere, and perhaps in the lower southern polar stratosphere.

By early 1966 SNAP-9A plutonium-238 had entered the lower northern polar stratosphere. The estimated distribution of this nuclide in the STARDUST sampling corridor during January to April 1966 is shown in Figure 106. We have extrapolated this distribution into the upper atmosphere using data from the USAEC balloon program[57] and have calculated a total stratospheric burden of 12 kilocuries of SNAP-9A plutonium-238. The distribution of this burden and of that calculated for late 1965 are summarized in Table 109. According to our estimate for early 1966 only 6.5 kilocuries had entered the lower stratosphere by April 1966, two years following the injection of the plutonium-238. Presumably the burden in the atmospheric region above 22 km is more nearly 10.5 than

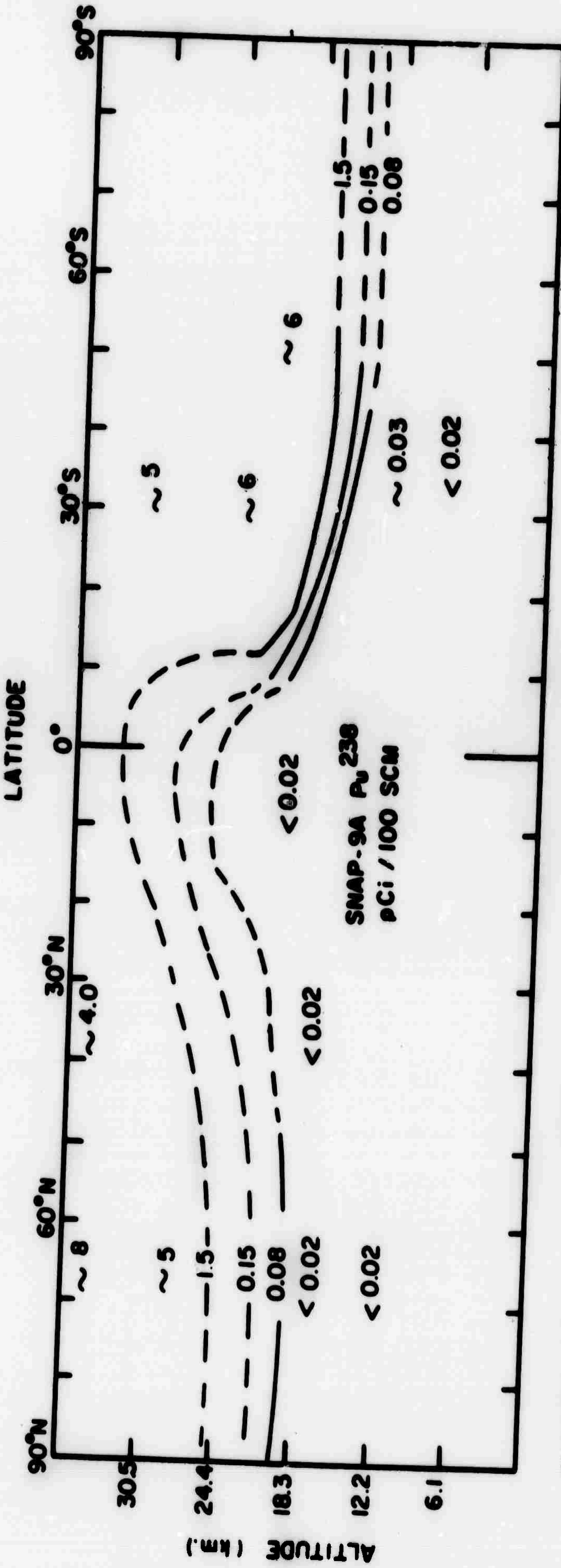

FIGURE 105A. THE STRATOSPHERIC DISTRIBUTION OF SNAP-9A Pu^{238} DURING SEPT-DEC 1965

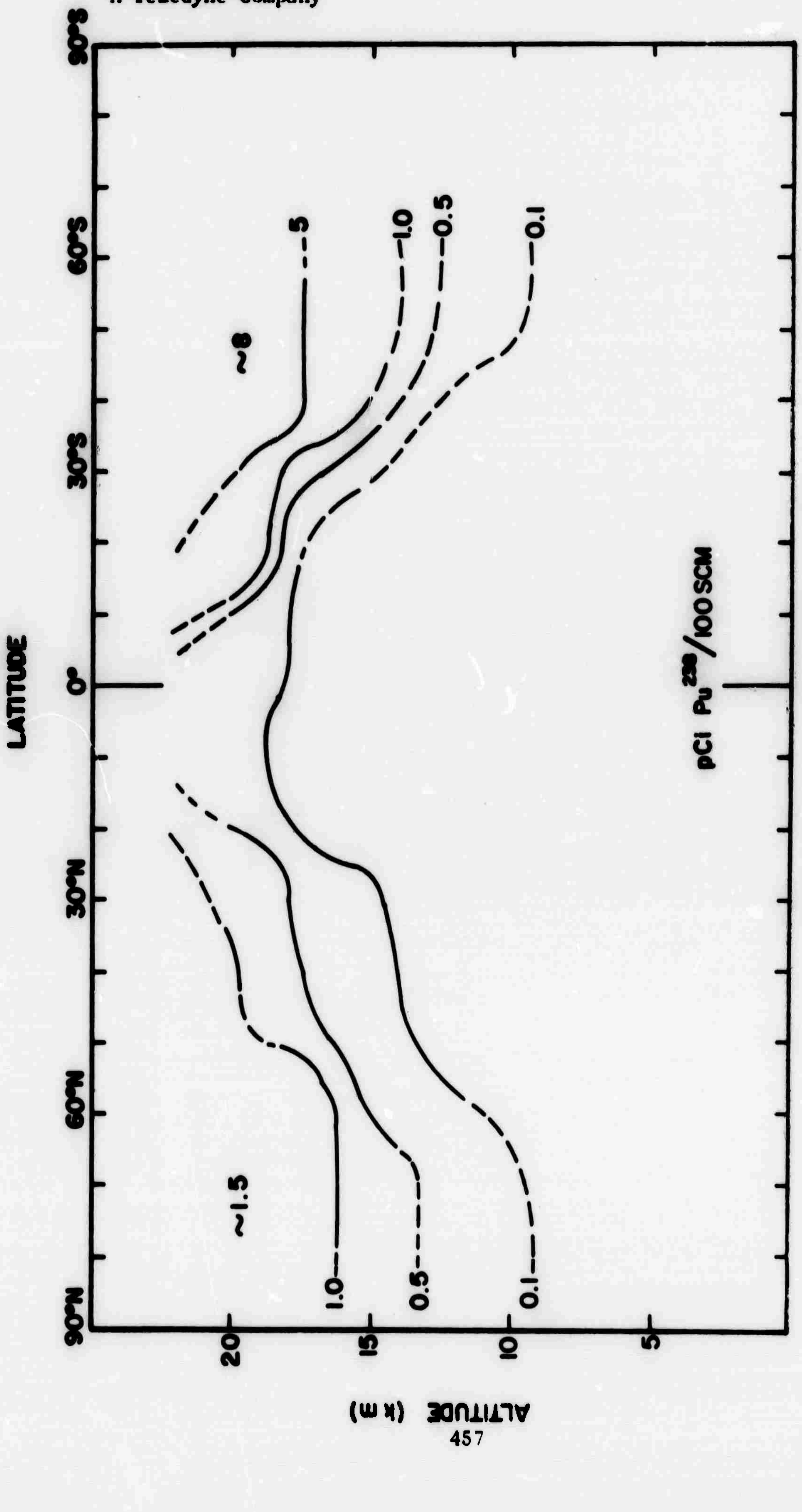

FIG. 106. THE STRATOSPHERIC DISTRIBUTION OF SNAP-9A PLUTONIUM-238, JANUARY-APRIL-1966

TABLE 109. The Distribution of the Stratospheric Burden of SNAP-9A Plutonium-238 (in kilocuries)

Altitude km	Altitude mb	Latitude 90-30°N	30°-0°N	0-30°S	30-90°S	Total
September-December 1965						
60-22	0-40	1.4	0.5	1.2	2.0	5.1
22-15	40-120	0.0	0.0	0.5	1.9	2.4
15-9	120-300	0.0	-	-	0.0	0.0
		1.4	0.5	1.7	3.9	7.5
January-April 1966						
60-22	0-40	1.0	0.7	1.7	2.1	5.5
22-15	40-120	0.8	0.2	0.6	4.0	5.6
15-9	120-300	0.3	0.0	0.0	0.6	0.9
		2.1	0.9	2.3	6.7	12.0

5.5 aci, which could suggest that the collection efficiencies of the balloon samplers are less than 100 percent, or that concentrations measured at 34°S by the balloon program are often not representative of those in the southern polar stratosphere.

Since less than 10 percent of the SNAP-9A plutonium-238 injected was found in the stratospheric regions below 15 km in early 1966, it seems unlikely that a significant amount of this tracer nuclide had entered the troposphere by then.

9.7 Anomalous Measurements - Effect of Particle Size

Two samples collected between 17°S and about 35°S, one during May and one during June 1965, appeared to contain SNAP-9A plutonium-238. These results seem anomalous, however, for samples collected farther south at the same altitude and at higher altitudes at the same latitude did not contain SNAP-9A debris. These two samples, SQ-7251 and SQ-7264, were reanalyzed, as SQ-7565 and SQ-7566 respectively, to confirm these potentially significant results. In the original analyses one half of each filter was used, and in the reanalyses one quarter of each was used. Data from the analyses of these four samples are contained in Table 110. The reanalyses failed to confirm the presence of SNAP-9A plutonium-238 in the samples.

The failure of the reanalyses to find SNAP-9A debris may mean that the original analyses were in error, but there is another possibility. If the SNAP-9A debris which entered the lower stratosphere during the first half of 1965 was carried by particles large enough to contain between 10^8 to 10^9 atoms of plutonium-238, only one or two such particles would have to be included in a sample to give the level of plutonium-238 activity displayed by samples SQ-7251

TABLE 110. Results of Plutonium Analyses of Selected Samples, Including Reanalyses of Two Anomalous Samples

Sample Number	Collection Date	Latitude	Altitude (km)	$\frac{Pu^{238}}{Pu^{239}}$	pCi/100 SCM Total Pu^{239}	pCi/100 SCM Total Pu^{238}	pCi/100 SCM SNAP-9A Pu^{238}
SQ-7564	28 Apr 65	38°-55°S	18.9	0.04	1.72	0.06	< 0.03
SX-7476	9 Nov 65	38°-55°S	19.2	3.34	2.40	8.02	7.94
SQ-7251	11 May 65	17°-36°S	16.2	0.13	0.86	0.11	0.08
SQ-7565	11 May 65	17°-36°S	16.2	0.04	0.92	0.03	< 0.02
SQ-7264	23 Jun 65	17°-34°S	16.2	0.19	1.26	0.24	0.21
SQ-7566	23 Jun 65	17°-34°S	16.2	0.03	1.16	0.03	< 0.03

and SQ-7264. The sizes of the hypothetical spherical particles of $Pu^{238}O_2$ required to contain all of the SNAP-9A plutonium-238 in each of the two samples, SQ-7251 and SQ-7264, have been calculated. The calculation, which is shown in Table 111, indicates radii of 0.15 and 0.12 micron for these hypothetical spherical particles at theoretical density. If the SNAP-9A plutonium-238 were actually present as aggregates of smaller spherical particles, and the aggregates consisted of 50 percent open spaces and 50 percent particles of millimicron size, the radii of the spherical aggregates would be 26 percent larger than is calculated in Table 111.

No evidence is currently available to confirm the possible correctness of the original analyses and of the reanalyses of the two anomalous samples, but the alpha spectra obtained in both sets of analyses appear to be of good quality. Data are included in Table 110 for sample SQ-7564, collected at 38° - 55°S one month before the first definite interception there of SNAP-9A debris, and for sample SX-7476, collected at approximately the same location after comparatively high concentrations of SNAP-9A debris had arrived. The alpha spectra for these two samples are plotted in Figure 107. Peaks are shown which are attributable to plutonium-239, plutonium-238 and plutonium-236 (which is added to the samples before analysis to permit calculation of radiochemical yields). The addition of SNAP-9A plutonium-238 to plutonium from weapons debris causes a readily discernible increase in the ratio of the area under the 5.5 Mev plutonium-238 peak to the area under the 5.1 Mev plutonium-239 peak. Alpha spectra for samples SQ-7251 and SQ-7565 and for samples SQ-7264 and SQ-7566 (all with the 5.8 Mev plutonium-236 peaks deleted) are compared in Figure 108. All spectra are of reasonably good quality, suggesting that perhaps

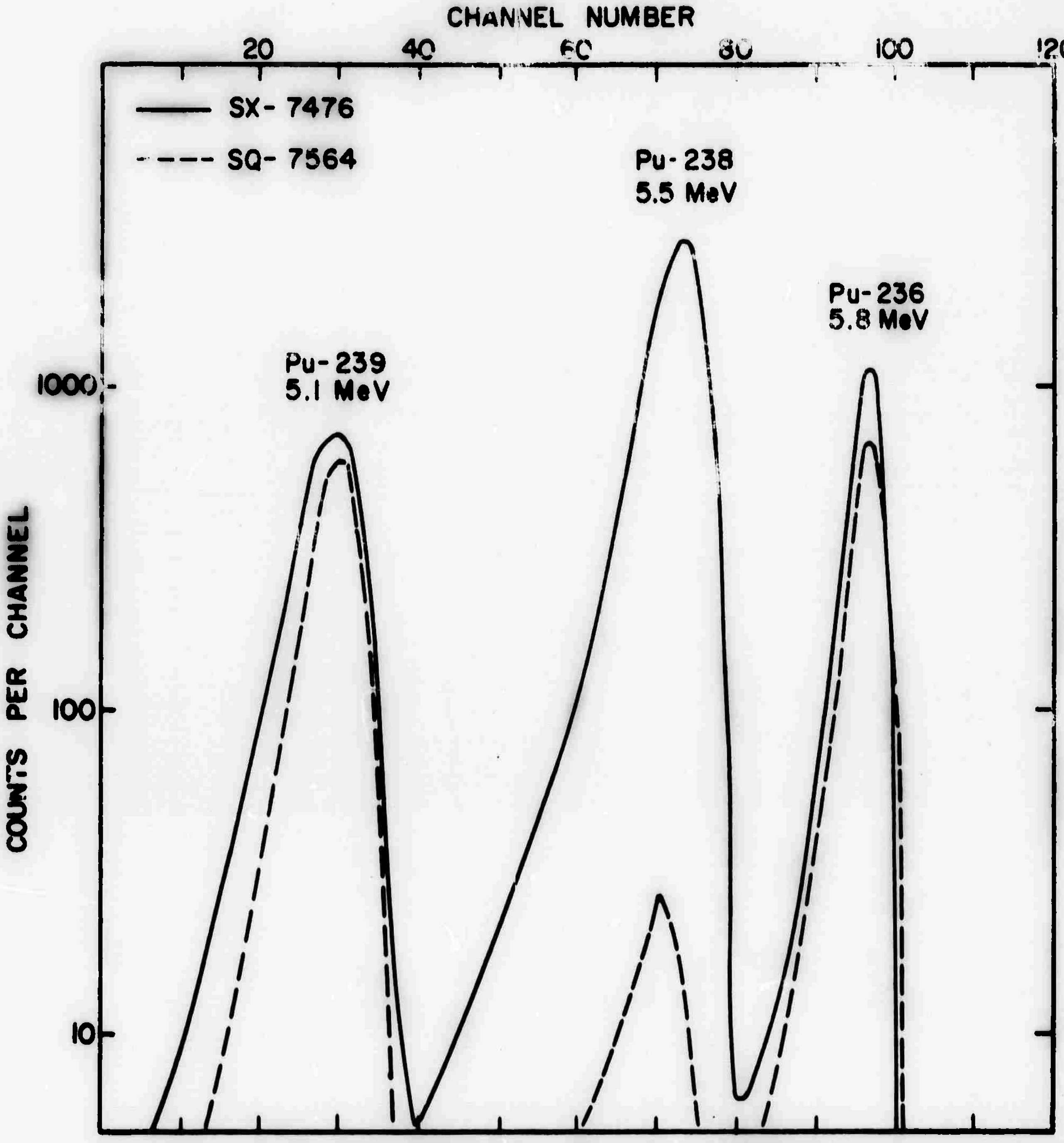

FIGURE 107. ALPHA SPECTRA OF SX-7476 CONTAINING SNAP-9A Pu-238 AND SQ-7564 CONTAINING ONLY WEAPONS Pu-238

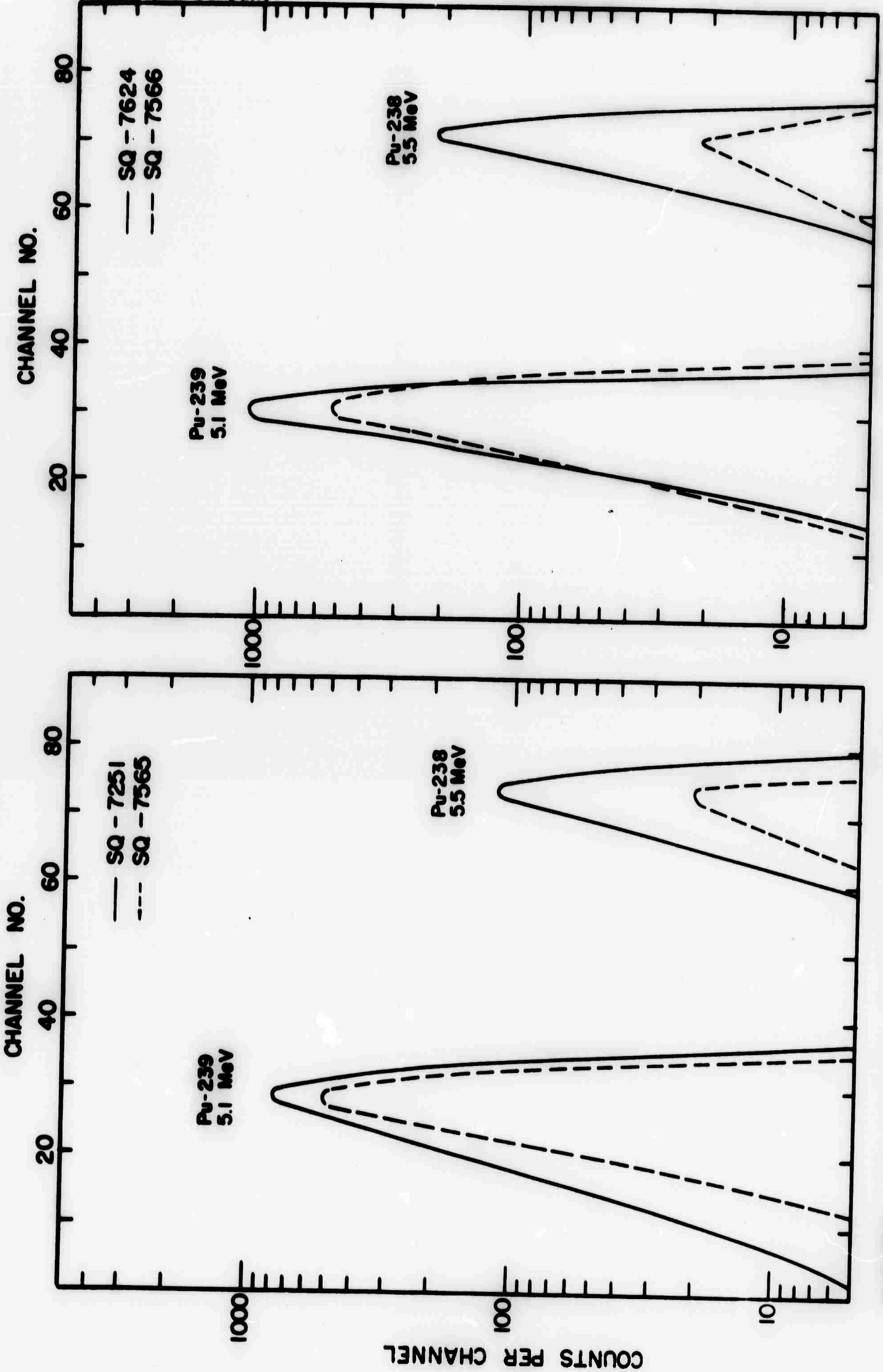

FIGURE 108. ALPHA SPECTRA OF DUPLICATE ANALYSES OF TWO ANOMALOUS SAMPLES

the analyses are indeed correct, and that failure of the plutonium-238 results to agree on duplicate samples results from inhomogeneous distribution of SNAP-9A debris on the filters. This could result if the particles carrying the debris had radii in the range of 0.12 to 0.15 micron.

TABLE 111. Estimates of Sizes of Hypothetical Spherical Particles of PuO_2

(1) $\frac{\Delta N}{\Delta t} = D = \lambda N$,

where $D = \frac{\Delta N}{\Delta t}$ = observed disintegration rate of Pu^{238}, in atoms/min.,

λ = decay constant of Pu^{238}, 1.48×10^{-8} $min.^{-1}$,

N = atoms of Pu^{238} in the sample

(2) $N = A \frac{V \rho}{M}$,

where A = Avogadro's number = 6.02×10^{23} atoms/mole

V = volume of $Pu^{238}O_2$ particle, in cm^3

ρ = density of Pu^{238} = $11.46\ g/cm^3$

M = molecular weight of $Pu^{238}O_2$ = 270 g/mole

(3) $r^3 = \frac{V}{4.189}$

where r = radius of particles, in cm.

(4) $$r^3 = \frac{V}{4.189} = \frac{NM}{4.189\ A\rho} = \frac{DM}{4.189\ \lambda A\rho} = \frac{270\ D}{(4.189)(1.48\times10^{-8})(6.02\times10^{23})(11.46)}$$

$$r^3 = 0.631 \times 10^{-15} D$$

For SQ-7264:

$$D = (4.59\times10^{-3}\ dpm/SCM)(1.29\times10^{3}\ SCM) = 5.9\ dpm.$$

$$r^3 = (0.631 \times 10^{-15})(5.9) = 3.72 \times 10^{-15}$$

$$r = 1.5 \times 10^{-5}\ cm. = 0.15\ \mu$$

For SQ-7251:

$$D = (1.77\times10^{-3}\ dpm/SCM)(1.64\times10^{3}\ SCM) = 2.9\ dpm$$

$$r^3 = (0.631 \times 10^{-15})(2.9) = 1.83 \times 10^{-15}$$

$$r = 1.2 \times 10^{-5}\ cm. = 0.12\ \mu$$

APPENDIX 9-A

TABLE 9A-1. Plutonium Nuclide Concentrations in Stratospheric Samples January 1965 to June 1967.

Sample	Collection Date	Latitude Range	Altitude (km)	Nuclide Concentrations (pCi/100 SCM) Total Sr^{90}	Total Pu^{239}	Total Pu^{238}	Weapon Pu^{238}	SNAP-9A Pu^{238}
SQ-7034	5 Jan 65	75°N-67°N	18.3	633	11.4	0.36	0.31	0.05
SQ-7035	5 Jan 65	75°N-67°N	19.4	461	8.68	0.30	0.23	0.07
SQ-7043	7 Jan 65	22°N-09°N	20.4	625	11.7	0.30	0.32	$\leq$ 0.01
SQ-6982	15 Jan 65	38°S-47°S	20.4	221	3.37	0.11	0.09	0.02
SQ-7038	19 Jan 65	75°N-67°N	15.2	566	11.1	0.32	0.30	0.02
SQ-7047	19 Jan 65	15°S-37°S	20.9	223	3.69	0.11	0.10	0.01
SQ-7056	2 Feb 65	52°N-37°N	18.3	496	10.1	0.33	0.27	0.06
SQ-7061	11 Feb 65	38°S-47°S	20.5	164	1.99	0.08	0.05	0.03
SQ-7052	16 Feb 65	75°N-67°N	16.8	499	8.62	0.31	0.23	0.08
SQ-7065	16 Feb 65	22°S-37°S	21.0	165	2.34	0.06	0.06	$\leq$ 0.01
SQ-7107	2 Mar 65	52°N-36°N	19.8	480	6.14	0.18	0.17	0.01
SQ-7106	3 Mar 65	75°N-67°N	19.7	388	4.67	0.19	0.13	0.06
SQ-7151	4 Mar 65	09°N-10°S	20.4	367	5.63	0.12	0.15	$\leq$ 0.01
SQ-7141	31 Mar 65	38°S-55°S	19.6	134	1.52	0.04	0.04	$\leq$ 0.01
SQ-7558	13 Apr 65	17°S-36°S	16.2	32	0.45	0.01	0.01	$\leq$ 0.01
SQ-7559	13 Apr 65	17°S-36°S	17.7	44	0.73	0.02	0.02	$\leq$ 0.01
SQ-7561	14 Apr 65	38°S-55°S	16.2	58	0.83	0.02	0.02	$\leq$ 0.01
SQ-7562	14 Apr 65	38°S-55°S	17.7	74	0.87	0.02	0.02	$\leq$ 0.01
SQ-7143	27 Apr 65	17°S-34°S	19.0	151	2.07	0.07	0.06	0.01
SQ-7563	27 Apr 65	17°S-36°S	19.9	136	2.07	0.09	0.06	0.03
SQ-7142	28 Apr 65	67°N-53°N	19.1	416	6.04	0.21	0.16	0.05
SQ-7152	28 Apr 65	09°N-10°S	19.9	339	5.68	0.13	0.15	$\leq$ 0.01
SQ-7564	28 Apr 65	38°S-55°S	19.0	129	1.72	0.07	0.05	0.02
SQ-7251	11 May 65	17°S-36°S	16.2	46	0.86	(0.11)	0.02	(0.09)
SQ-7565	11 May 65	17°S-36°S	16.2	65	0.92	0.03	0.02	0.01
SQ-7739	11 May 65	17°S-36°S	16.2	51	0.79	0.03	0.02	0.01
SQ-7252	11 May 65	17°S-36°S	17.7	80	1.57	0.05	0.04	0.01
SQ-7741	11 May 65	17°S-36°S	17.7	77	1.15	0.03	0.03	$\leq$ 0.01

TABLE 9A-1. (continued)

Sample	Collection Date	Latitude Range	Altitude (km)	Nuclide Concentrations (pCi/100 SCM) Total Sr^{90}	Total Pu^{239}	Total Pu^{238}	Weapon Pu^{238}	SNAP-9A Pu^{238}
SQ-7253	12 May 65	39°S-47S°	16.2	160	3.05	0.13	0.08	0.05
SX-7237	25 May 65	75°N-67°N	18.5	334	8.28	0.27	0.22	0.05
SQ-7160	25 May 65	52°N-37°N	19.5	302	5.68	0.20	0.15	0.05
SQ-7161	25 May 65	36°N-23°N	19.6	315	5.95	0.22	0.16	0.06
SX-7175	25 May 65	23°N-09°N	20.1	(181)	5.99	0.18	0.16	0.02
SQ-7742	26 May 65	19°S-34°S	18.9	149	2.07	0.06	0.06	≤ 0.01
SQ-7162	26 May 65	18°S-36°S	19.6	197	2.00	0.11	0.05	0.06
SQ-7743	26 May 65	18°S-36°S	19.6	155	1.81	0.13	0.05	0.08
SQ-7159	27 May 65	67°N-52°N	19.0	296	5.30	0.18	0.14	0.04
SQ-7164	27 May 65	38°S-55°S	18.9	127	2.34	0.52	0.06	0.46
SQ-7163	27 May 65	38°S-55°S	19.8	97	1.88	1.26	0.05	1.21
SX-7238	28 May 65	9°N-10°S	19.2	180	4.42	0.13	0.12	0.01
SX-7176	28 May 65	9°N-10°S	20.7	235	5.02	0.13	0.14	≤ 0.01
SQ-7397	1 Jun 65	40°S	12.2	42	0.70	0.02	0.02	≤ 0.01
SQ-7254	8 Jun 65	75°N-67°N	16.8	423	8.63	0.24	0.23	0.01
SQ-7255	8 Jun 65	9°N-10°S	17.7	88	1.84	0.05	0.05	≤ 0.01
SQ-7744	8 Jun 65	17°S-35°S	16.2	24	0.35	0.01	0.01	≤ 0.01
SQ-7256	8 Jun 65	17°S-35°S	17.4	88	1.50	0.06	0.04	0.02
SQ-7745	8 Jun 65	17°S-35°S	17.4	96	1.53	0.07	0.04	0.03
SQ-7257	10 Jun 65	67°N-50°N	15.2	223	4.78	0.13	0.13	≤ 0.01
SQ-7258	10 Jun 65	23°N-09°N	17.7	219	4.20	0.13	0.11	0.02
SQ-7259	10 Jun 65	38°S-55°S	16.2	152	2.16	0.07	0.06	0.01
SQ-7746	10 Jun 65	38°S-55°S	16.2	132	1.83	0.05	0.05	≤ 0.01
SQ-7261	10 Jun 65	38°S-55°S	17.7	156	2.72	0.38	0.07	0.31
SQ-7747	10 Jun 65	38°S-55°S	17.7	158	2.32	(2.40)	0.06	(2.34)
SQ-7178	22 Jun 65	33°N-28°N	19.2	358	6.06	0.21	0.16	0.05
SQ-7179	22 Jun 65	23°N-09°N	19.2	219	4.07	0.14	0.11	0.03
SQ-7262	22 Jun 65	38°S-55°S	18.6	145	2.24	1.46	0.06	1.40
SQ-7183	22 Jun 65	38°S-55°S	19.3	121	1.60	1.89	0.04	1.85
SQ-7748	22 Jun 65	38°S-55°S	19.3	130	1.78	1.75	0.05	1.70
SQ-7177	23 Jun 65	67°N-50°N	18.3	318	5.50	0.20	0.15	0.05
SQ-7263	23 Jun 65	50°N-37°N	18.3	356	6.71	0.19	0.18	0.01
SQ-7264	23 Jun 65	17°S-34°S	16.2	80.6	1.26	(0.24)	0.03	(0.21)
SQ-7566	23 Jun 65	17°S-34°S	16.2	80.9	1.16	0.04	0.03	0.01
SQ-7181	23 Jun 65	17°S-34°S	17.7	108	2.00	0.04	0.05	≤ 0.01

TABLE 9A-1. (continued)

Sample	Collection Date	Latitude Range	Altitude (km)	Nuclide Concentrations (pCi/100 SCM) Total Sr^{90}	Total Pu^{239}	Total Pu^{238}	Weapon Pu^{238}	SNAP-9A Pu^{238}
SQ-7184	24 Jun 65	38°S-55°S	16.2	126	1.88	0.07	0.05	0.02
SQ-7749	24 Jun 65	38°S-55°S	16.2	128	1.97	0.06	0.05	0.01
SQ-7182	24 Jun 65	38°S-55°S	17.7	156	2.46	0.12	0.07	0.05
SQ-7751	24 Jun 65	38°S-55°S	17.7	156	2.48	0.13	0.07	0.06
SQ-7265	25 Jun 65	75°N-67°N	18.6	361	5.22	0.17	0.14	0.03
SQ-7266	25 Jun 65	09°N-10°S	19.2	208	3.16	0.10	0.08	0.02
SQ-7180	25 Jun 65	09°N-10°S	20.0	254	4.31	0.36	0.12	0.24
SX-7239	19 Jul 65	52°N-37°N	18.3	308	7.19	0.23	0.19	0.04
SX-7192	19 Jul 65	52°N-37°N	19.3	426	4.93	(0.87)	0.13	(0.74)
SX-7193	19 Jul 65	36°N-23°N	19.8	439	5.69	0.22	0.15	0.07
SX-7241	19 Jul 65	17°S-34°S	19.0	122	2.43	1.21	0.07	1.14
SX-7194	19 Jul 65	17°S-34°S	19.8	205	2.53	0.63	0.07	0.56
SX-7242	20 Jul 65	38°S-55°S	18.9	122	2.37	1.56	0.06	1.50
SX-7197	20 Jul 65	38°S-55°S	19.5	157	1.81	2.83	0.05	2.78
SQ-7267	21 Jul 65	17°S-36°S	16.2	35	0.41	0.01	0.01	$\leq$ 0.01
SX-7243	21 Jul 65	17°S-36°S	17.7	121	2.37	0.28	0.06	0.22
SX-7244	22 Jul 65	75°N-67°N	18.3	235	5.56	0.20	0.15	0.05
SX-7195	22 Jul 65	38°S-55°S	16.2	160	1.97	0.15	0.05	0.10
SX-7196	22 Jul 65	38°S-55°S	17.7	196	2.07	0.36	0.06	0.30
SX-7245	23 Jul 65	75°N-66°N	15.2	235	5.55	0.16	0.15	0.01
SX-7246	23 Jul 65	75°N-66°N	16.8	331	7.60	0.25	0.21	0.04
SX-7190	24 Jul 65	67°N-52°N	18.3	428	3.93	0.14	0.11	0.03
SX-7191	24 Jul 65	64°N-52°N	19.0	378	4.66	0.20	0.13	0.07
SX-7247	24 Jul 65	09°N-02°S	17.4	99	2.62	0.08	0.07	0.01
SX-7248	25 Jul 65	36°N-23°N	17.7	(92)	2.50	0.08	0.07	0.01
SX-7249	25 Jul 65	23°N-09°N	17.7	(13)	(0.40)	($\leq$0.02)	(0.01)	($\leq$0.01)
SX-7396	28 Jul 65	40°S	12.2	(54)	(0.93)	(0.03)	(0.02)	(0.01)
SQ-7398	10 Aug 65	40°S	12.2	58	1.00	0.14	0.03	0.11
SQ-7198	15 Aug 65	75°N-67°N	18.3	452	4.90	0.15	0.13	0.02
SQ-7199	15 Aug 65	75°N-67°N	19.2	407	4.60	0.24	0.12	0.12
SQ-7200	15 Aug 65	09°N-10°S	19.2	243	4.15	0.13	0.11	0.02
SQ-7201	16 Aug 65	52°N-37°N	18.3	345	5.88	0.19	0.16	0.03
SQ-7202	16 Aug 65	52°N-47°N	19.4	280	5.28	0.20	0.14	0.06

TABLE 9A-1. (continued)

Sample	Collection Date	Latitude Range	Altitude (km)	Total Sr^{90}	Total Pu^{239}	Total Pu^{238}	Weapon Pu^{238}	SNAP-9A Pu^{238}
				Nuclide Concentrations (pCi/100 SCM)				
SQ-7203	17 Aug 65	36°N-23°N	18.9	472	5.82	0.17	0.16	0.01
SQ-7204	17 Aug 65	36°N-23°N	19.6	375	5.88	0.21	0.16	0.05
SQ-7205	17 Aug 65	09°N-10°S	16.2	25	(0.05)	(≤0.16)	(0.00)	(≤0.16)
SQ-7206	17 Aug 65	09°N-10°S	17.7	113	2.08	0.06	0.06	≤0.01
SQ-7207	17 Aug 65	38°S-55°S	18.7	159	2.45	3.02	0.07	2.95
SQ-7208	17 Aug 65	38°S-55°S	19.3	143	2.38	4.98	0.06	4.92
SQ-7209	19 Aug 65	67°N-52°N	18.3	399	8.43	0.27	0.23	0.04
SQ-7567	19 Aug 65	67°N-52°N	19.4	281	4.28	0.17	0.12	0.05
SQ-7211	19 Aug 65	36°N-23°N	17.7	180	3.69	0.12	0.10	0.02
SQ-7212	19 Aug 65	23°N-09°N	17.7	119	2.13	0.06	0.06	≤0.01
SQ-7213	19 Aug 65	23°N-12°N	19.4	254	4.55	0.12	0.12	≤0.01
SQ-7214	19 Aug 65	25°S-36°S	16.2	89	1.44	0.09	0.04	0.05
SQ-7215	19 Aug 65	17°S-36°S	17.7	121	1.70	0.22	0.05	0.17
SQ-7216	19 Aug 65	17°S-36°S	19.7	145	2.75	2.08	0.06	2.02
SQ-7217	21 Aug 65	09°N-10°S	19.7	264	3.54	0.14	0.10	0.04
SQ-7399	9 Sep 65	40°S	12.2	39.8	0.81	≤0.01	0.02	≤0.01
SX-7301	13 Sep 65	75°N-67°N	18.3	329	5.58	0.19	0.15	0.04
SX-7302	13 Sep 65	75°N-67°N	19.3	391	4.67	0.19	0.13	0.06
SX-7303	13 Sep 65	52°N-37°N	18.3	270	4.64	0.17	0.13	0.04
SX-7304	13 Sep 65	52°N-37°N	19.5	382	4.82	0.18	0.13	0.05
SX-7305	13 Sep 65	36°N-23°N	19.8	297	4.32	0.16	0.12	0.04
SX-7306	13 Sep 65	38°S-55°S	19.3	172	2.48	5.10	0.07	5.03
SX-7307	14 Sep 65	67°N-50°N	16.8	248	4.13	0.10	0.12	≤0.01
SX-7308	14 Sep 65	38°S-55°S	16.2	167	2.53	0.50	0.07	0.43
SX-7309	14 Sep 65	38°S-55°S	17.7	172	2.70	3.05	0.07	2.98
SX-7311	15 Sep 65	75°N-67°N	15.2	237	3.58	0.10	0.10	≤0.01
SX-7312	15 Sep 65	75°N-67°N	16.8	391	5.91	0.17	0.16	0.01
SX-7313	15 Sep 65	09°N-10°S	17.7	114	2.23	0.15	0.06	0.09
SX-7314	15 Sep 65	25°S-36°S	16.2	(42.6)	0.95	0.24	0.03	0.21
SX-7315	15 Sep 65	21°S-36°S	17.7	(59.0)	1.68	0.23	0.04	0.19
SX-7316	16 Sep 65	67°N-50°N	15.2	136	2.89	0.09	0.08	0.01
SX-7317	16 Sep 65	67°N-52°N	18.3	396	7.38	0.22	0.20	0.02
SX-7318	16 Sep 65	67°N-52°N	19.8	229	4.13	0.20	0.11	0.09
SX-7319	16 Sep 65	23°N-09°N	20.0	248	5.29	0.14	0.14	≤0.01
SX-7321	17 Sep 65	18°S-36°S	19.2	130	2.43	2.45	0.07	2.38

TABLE 9A-1. (continued)

Sample	Collection Date	Latitude Range	Altitude (km)	Nuclide Concentrations (pCi/100 SCM) Total Sr^{90}	Total Pu^{239}	Total Pu^{238}	Weapon Pu^{238}	SNAP-9A Pu^{238}
SX-7322	18 Sep 65	09°N-10°S	20.1	277	3.04	0.11	0.08	0.03
SX-7464	6 Oct 65	40°S	7.6	2.86	0.06	0.00	0.00	0.00
SQ-7401	6 Oct 65	40°S	12.2	42.6	(2.97)	(0.10)	(0.08)	(0.02)
SQ-7359	10 Oct 65	17°S-36°S	19.8	415	2.72	6.23	0.07	6.16
SQ-7353	11 Oct 65	75°N-67°N	18.3	442	4.82	0.184	0.130	0.05
SQ-7354	11 Oct 65	75°N-67°N	19.1	380	4.32	0.246	0.117	0.13
SQ-7355	11 Oct 65	52°N-37°N	18.3	L	5.15	0.165	0.139	0.03
SQ-7356	11 Oct 65	52°N-37°N	19.7	229	3.23	0.149	0.087	0.06
SQ-7357	11 Oct 65	36°N-23°N	19.9	307	5.04	0.159	0.136	0.02
SQ-7358	11 Oct 65	09°N-10°S	20.1	240	3.72	0.083	0.100	≤0.01
SQ-7361	12 Oct 65	25°S-36°S	16.2	61.7	0.979	0.086	0.026	0.06
SQ-7362	12 Oct 65	19°S-36°S	17.7	102	1.78	0.474	0.048	0.43
SQ-7365	12 Oct 65	38°S-55°S	19.4	194	2.46	4.75	0.066	4.68
SQ-7363	13 Oct 65	67°N-50°N	16.8	342	3.98	0.111	0.107	≤0.01
SQ-7364	13 Oct 65	50°N-37°N	16.8	188	3.59	0.114	0.097	0.02
SQ-7368	13 Oct 65	38°S-55°S	16.2	108	1.70	0.273	0.046	0.227
SQ-7369	13 Oct 65	38°S-55°S	17.7	127	2.30	2.02	0.062	1.96
SQ-7366	14 Oct 65	75°N-67°N	16.8	283	4.96	0.130	0.134	≤0.01
SQ-7367	14 Oct 65	23°N-09°N	20.1	331	6.26	0.157	0.169	≤0.01
SQ-7371	15 Oct 65	67°N-50°N	15.2	246	3.98	0.124	0.107	0.02
SQ-7372	15 Oct 65	67°N-52°N	18.3	289	4.72	0.172	0.127	0.04
SQ-7373	15 Oct 65	67°N-52°N	19.7	267	4.56	0.178	0.123	0.06
SQ-7374	15 Oct 65	09°N-08°S	17.4	76.5	1.43	0.044	0.039	≤0.01
SQ-7531	3 Nov 65	40°S	12.2	69.3	0.803	0.052	0.022	0.03
SQ-7532	4 Nov 65	70°N	12.2	59.9	1.10	0.046	0.030	0.02
SX-7473	7 Nov 65	18°S-36°S	19.9	173	2.80	5.20	0.076	5.12
SX-7467	8 Nov 65	75°N-67°N	18.3	261	4.71	0.191	0.127	0.06
SX-7468	8 Nov 65	75°N-67°N	19.8	164	2.61	0.218	0.070	0.15
SX-7469	8 Nov 65	52°N-37°N	18.3	(471)	(8.90)	(0.281)	(0.240)	(0.04)
SX-7471	8 Nov 65	52°N-37°N	19.5	237	4.32	0.213	0.117	0.10
SX-7472	8 Nov 65	36°N-23°N	19.7	251	4.56	0.134	0.123	0.01
SQ-7489	8 Nov 65	30°S-36°S	16.2	73	1.20	0.127	0.032	0.10
SX-7474	8 Nov 65	18°S-36°S	17.7	122	1.76	0.790	0.048	0.74

TABLE 9A-1. (continued)

Sample	Collection Date	Latitude Range	Altitude (km)	Total Sr^{90}	Total Pu^{239}	Total Pu^{238}	Weapon Pu^{238}	SNAP-9A Pu^{238}
				Nuclide Concentrations (pCi/100 SCM)				
SX-7475	9 Nov 65	75°N-67°N	16.8	2.21	3.54	0.118	0.096	0.02
SX-7476	9 Nov 65	38°S-55°S	19.3	136	2.40	8.01	0.065	7.94
SX-7477	10 Nov 65	67°N-50°N	15.2	173	3.10	0.100	0.084	0.02
SX-7478	10 Nov 65	67°N-50°N	16.8	150	3.74	0.122	0.101	0.02
SX-7479	10 Nov 65	50°N-37°N	16.8	196	(5.79)	(0.211)	(0.156)	(0.06)
SX-7481	10 Nov 65	38°S-54°S	16.2	144	2.35	1.00	0.063	0.94
SX-7482	10 Nov 65	39°S-54°S	17.7	145	2.26	2.64	0.061	2.58
SX-7483	11 Nov 65	67°N-52°N	18.3	218	4.26	0.167	0.115	0.05
SX-7484	11 Nov 65	67°N-52°N	20.1	192	3.64	0.305	0.098	0.21
SX-7485	11 Nov 65	08°N-10°S	19.1	122	2.42	0.060	0.065	≤0.01
SX-7486	11 Nov 65	07°N-10°S	20.4	219	3.82	0.191	0.103	0.09
SX-7487	12 Nov 65	23°N-09°N	19.1	160	3.43	0.111	0.093	0.02
SQ-7491	12 Nov 65	23°N-09°N	20.3	248	4.44	0.156	0.120	0.04
SX-7488	27 Nov 65	64°N-47°N	11.9	74.2	1.65	0.056	0.044	0.01
SQ-7533	6 Dec 65	52°N-37°N	15.2	66.1	1.35	0.094	0.036	0.06
SQ-7534	6 Dec 65	52°N-37°N	16.8	145	2.89	0.089	0.078	0.01
SQ-7752	6 Dec 65	52°N-37°N	16.8	146	2.70	0.09	0.073	0.02
SQ-7535	6 Dec 65	36°N-23°N	17.7	140	2.58	0.089	0.070	0.02
SQ-7536	6 Dec 65	38°S-55°S	15.2	37.5	0.614	0.067	0.016	0.05
SQ-7537	6 Dec 65	38°S-55°S	16.8	96.9	1.62	1.17	0.044	1.13
SQ-7538	7 Dec 65	52°N-37°N	18.3	216	4.34	0.232	0.117	0.12
SQ-7753	7 Dec 65	52°N-37°N	18.3	282	4.36	0.151	0.118	0.03
SQ-7539	7 Dec 65	52°N-37°N	19.2	216	3.93	0.205	0.106	0.10
SQ-7754	7 Dec 65	52°N-37°N	19.2	219	4.18	0.283	0.113	0.17
SQ-7541	7 Dec 65	36°N-23°N	19.2	259	5.02	0.248	0.136	0.11
SQ-7542	7 Dec 65	36°N-23°N	20.0	221	3.91	0.566	0.106	0.46
SQ-7543	7 Dec 65	17°S-36°S	16.2	22.4	0.415	0.043	0.011	0.03
SQ-7544	7 Dec 65	17°S-38°S	17.7	95.2	1.49	0.385	0.040	0.34
SQ-7545	7 Dec 65	38°S-55°S	18.3	122	1.92	3.20	0.052	3.15
SQ-7546	7 Dec 65	38°S-51°S	18.7	127	2.10	3.62	0.057	3.56
SQ-7547	9 Dec 65	17°S-34°S	19.2	95.2	1.54	2.05	0.042	2.01
SQ-7548	9 Dec 65	17°S-36°S	20.2	184	1.88	5.64	0.051	5.59
SQ-7549	14 Dec 65	70°N	12.2	188	3.34	0.095	0.090	≤0.01
SQ-7686	15 Dec 65	45°S	7.6	15	0.251	0.019	0.007	0.01
SQ-7687	16 Dec 65	45°S	12.2	35.4	0.642	0.068	0.017	0.05
SQ-7551	22 Dec 65	55°N-48°N	11.9	175	2.96	0.094	0.08	0.01
SQ-7552	22 Dec 65	55°N-48°N	13.1	114	1.86	0.072	0.05	0.02

TABLE 9A-1. (continued)

Sample	Collection Date	Latitude Range	Altitude (km)	Total Sr^{90}	Total Pu^{239}	Total Pu^{238}	Weapon Pu^{238}	SNAP-9A Pu^{238}
				Nuclide Concentrations (pCi/100 SCM)				
SQ-7568	14 Jan 66	64°N-51°N	18.3	242	3.97	0.830	0.107	0.72
SQ-7569	14 Jan 66	51°N-38°N	18.3	201	3.51	0.293	0.095	0.20
SQ-7571	14 Jan 66	52°N-37°N	18.8	207	3.67	0.388	0.099	0.29
SX-7677	16 Jan 66	70°N	12.2	41.4	0.737	0.034	0.020	0.01
SX-7574	18 Jan 66	47°N-41°N	12.2	79	1.44	0.055	0.039	0.02
SX-7575	18 Jan 66	47°N-41°N	13.1	177	3.19	0.083	0.086	≤0.01
SX-7576	19 Jan 66	64°N-55°N	11.9	98	1.80	0.046	0.049	≤0.01
SX-7577	19 Jan 66	64°N-55°N	13.1	144	2.54	0.096	0.068	0.03
SX-7678	25 Jan 66	35°N	12.2	81	1.38	0.041	0.037	≤0.01
SX-7688	26 Jan 66	40°S	12.2	15.4	0.247	0.010	0.007	≤0.01
SX-7578	30 Jan 66	75°N-62°N	18.3	202	3.60	1.05	0.097	0.95
SX-7579	30 Jan 66	75°N-65°N	18.9	227	4.07	1.26	0.110	1.15
SQ-7755	31 Jan 66	62°N-50°N	18.2	215	4.16	0.938	0.112	0.83
SQ-7572	31 Jan 66	62°N-50°N	18.2	212	3.47	0.994	0.094	0.90
SQ-7573	31 Jan 66	59°N-53°N	19.1	255	4.04	1.05	0.109	0.94
SQ-7756	31 Jan 66	59°N-53°N	19.1	216	3.58	1.10	0.097	1.00
SX-7581	31 Jan 66	36°N-23°N	18.3	171	2.77	0.228	0.075	0.15
SX-7582	31 Jan 66	33°N-23°N	19.3	159	3.01	0.647	0.081	0.57
SX-7584	1 Feb 66	75°N-64°N	16.8	191	2.41	0.057	0.065	≤0.01
SX-7585	1 Feb 66	50°N-37°N	18.3	184	3.25	0.608	0.088	0.52
SX-7586	1 Feb 66	50°N-33°N	19.6	200	3.02	1.01	0.082	0.93
SX-7587	1 Feb 66	23°N-09°N	19.0	126	2.40	0.116	0.065	0.05
SX-7588	1 Feb 66	23°N-09°N	20.0	155	2.81	0.115	0.076	0.04
SX-7589	2 Feb 66	62°N-50°N	18.2	169	2.89	0.899	0.078	0.82
SX-7591	2 Feb 66	65°N-50°N	18.8	190	3.10	1.16	0.084	1.08
SX-7592	3 Feb 66	64°N-49°N	15.2	152	2.25	0.136	0.061	0.08
SX-7593	3 Feb 66	49°N-37°N	15.2	92.2	1.86	0.086	0.050	0.04
SX-7594	5 Feb 66	61°N-52°N	16.8	190	4.22	0.750	0.114	0.64
SX-7595	5 Feb 66	52°N-37°N	16.8	149	2.20	0.204	0.059	0.14
SX-7679	8 Feb 66	70°N	12.2	98	1.76	0.084	0.048	0.04
SX-7627	9 Feb 66	07°N-13°S	18.6	35	0.618	0.103	0.017	0.09
SX-7628	9 Feb 66	13°S-32°S	18.6	61	1.04	1.18	0.028	1.15
SX-7629	15 Feb 66	47°N-41°N	12.7	60	1.37	0.044	0.037	0.01

TABLE 9A-1. (continued)

Sample	Collection Date	Latitude Range	Altitude (km)	Nuclide Concentrations (pCi/100 SCM) Total Sr^{90}	Total Pu^{239}	Total Pu^{238}	Weapon Pu^{238}	SNAP-9A Pu^{238}
SX-7632	16 Feb 66	64°N-55°N	11.9	86	1.93	0.064	0.052	0.01
SQ-7888	24 Feb 66	39°S	12.2	21	0.309	0.179	0.008	0.17
SX-7634	27 Feb 66	75°N-62°N	18.3	224	2.81	2.15	0.076	2.07
SX-7635	27 Feb 66	75°N-63°N	18.6	155	2.79	1.61	0.075	1.54
SX-7636	28 Feb 66	62°N-50°N	18.3	161	2.98	0.887	0.080	0.81
SX-7637	28 Feb 66	65°N-50°N	19.7	157	2.75	1.28	0.074	1.21
SX-7638	28 Feb 66	36°N-23°N	18.3	188	3.07	0.857	0.083	0.77
SX-7639	28 Feb 66	36°N-23°N	19.8	156	2.92	0.783	0.079	0.70
SQ-7659	28 Feb 66	23°N-09°N	18.3	46	0.664	0.043	0.018	0.02
SX-7641	28 Feb 66	23°N-09°N	19.7	161	2.67	0.228	0.072	0.16
SX-7642	1 Mar 66	75°N-64°N	15.2	186	3.29	0.735	0.089	0.65
SX-7643	1 Mar 66	75°N-64°N	16.8	182	3.03	2.40	0.082	2.32
SX-7644	1 Mar 66	14°S-31°S	18.3	46	0.771	0.508	0.021	0.49
SX-7645	1 Mar 66	14°S-33°S	20.1	101	1.66	4.45	0.045	4.40
SX-7646	2 Mar 66	64°N-48°N	15.2	145	2.34	0.300	0.063	0.24
SX-7647	2 Mar 66	48°N-37°N	15.2	135	2.54	0.492	0.068	0.42
SX-7648	2 Mar 66	50°N-37°N	18.3	153	3.35	0.674	0.090	0.58
SX-7649	2 Mar 66	50°N-37°N	19.5	203	3.15	1.41	0.085	1.32
SX-7651	3 Mar 66	35°S-54°S	15.2	50	0.806	0.861	0.022	0.84
SX-7652	3 Mar 66	33°S-54°S	16.8	83	1.35	2.52	0.037	2.48
SX-7661	4 Mar 66	07°N-10°S	18.3	48	0.834	0.099	0.022	0.08
SX-7653	4 Mar 66	09°N-10°S	19.4	64	1.17	0.129	0.032	0.10
SX-7654	4 Mar 66	35°S-55°S	18.3	108	1.60	6.66	0.043	6.62
SX-7655	4 Mar 66	34°S-54°S	19.3	100	1.47	8.35	0.040	8.31
SX-7656	6 Mar 66	64°N-49°N	16.8	146	3.06	1.82	0.083	1.74
SX-7657	6 Mar 66	49°N-37°N	16.8	117	2.49	0.347	0.067	0.28
SX-7658	7 Mar 66	35°N-26°N	16.8	114	2.10	0.157	0.057	0.10
SX-7662	15 Mar 66	64°N-52°N	11.9	106	2.00	0.098	0.054	0.04
SQ-7664	17 Mar 66	46°N-37°N	11.9	107	1.94	0.099	0.052	0.05
SQ-7665	17 Mar 66	46°N-43°N	13.1	243	4.12	0.409	0.111	0.30
SQ-7666	17 Mar 66	43°N-37°N	13.1	40.5	0.733	0.043	0.020	0.02
SQ-7889	23 Mar 66	70°N	12.2	132	2.38	0.122	0.064	0.06
SQ-7689	27 Mar 66	75°N-64°N	15.2	153	2.80	0.861	0.076	0.78
SQ-7691	27 Mar 66	75°N-64°N	16.8	185	3.28	1.18	0.088	1.09

TABLE 9A-1. (continued)

Sample	Collection Date	Latitude Range	Altitude (km)	Nuclide Concentrations (pCi/100 SCM) Total Sr^{90}	Total Pu^{239}	Total Pu^{238}	Weapon Pu^{238}	SNAP-9A Pu^{238}
SQ-7692	28 Mar 66	50°N-37°N	18.3	182	3.22	0.894	0.087	0.81
SQ-7693	28 Mar 66	50°N-37°N	19.8	167	2.98	1.72	0.080	1.64
SQ-7694	28 Mar 66	23°N-09°N	18.3	52.5	0.981	0.081	0.026	0.06
SQ-7695	28 Mar 66	23°N-09°N	19.8	128	2.59	0.208	0.070	0.14
SQ-7696	28 Mar 66	35°S-54°S	15.2	52.9	0.918	1.47	0.025	1.44
SQ-7697	28 Mar 66	33°S-54°S	16.8	46.7	0.782	0.977	0.021	0.96
SQ-7698	29 Mar 66	74°N-63°N	18.3	175	3.52	1.54	0.095	1.44
SQ-7699	29 Mar 66	74°N-67°N	19.2	160	3.15	1.51	0.085	1.42
SQ-7701	29 Mar 66	36°N-23°N	18.3	146	2.73	0.701	0.074	0.63
SQ-7702	29 Mar 66	36°N-23°N	19.2	165	3.21	0.937	0.087	0.85
SQ-7703	30 Mar 66	26°S-33°S	16.8	54.6	0.843	0.611	0.023	0.59
SQ-7704	30 Mar 66	14°S-31°S	18.3	46.0	0.735	0.806	0.020	0.79
SQ-7705	31 Mar 66	62°N-52°N	18.3	167	3.31	1.44	0.089	1.35
SQ-7706	31 Mar 66	64°N-52°N	19.2	166	2.89	1.93	0.078	1.85
SX-7681	12 Apr 66	47°N-41°N	11.9	62.3	1.27	0.062	0.034	0.03
SX-7682	12 Apr 66	47°N-41°N	13.1	108	1.84	0.230	0.050	0.18
SX-7683	13 Apr 66	64°N-55°N	11.9	43.0	0.803	0.108	0.022	0.09
SX-7684	13 Apr 66	64°N-55°N	13.1	26.9	0.496	0.057	0.013	0.04
SX-7685	14 Apr 66	55°N-47°N	13.1	50.6	0.952	0.087	0.026	0.06
SQ-7707	15 Apr 66	41°N-35°N	13.1	47.6	0.842	0.061	0.023	0.04
SX-7885	19 Apr 66	75°N	12.2	88.2	1.41	0.287	0.038	0.25
SP-7890	19 Apr 66	10°N	4.6	1.78	0.041	0.004	0.001	≤0.01
SX-7758	24 Apr 66	64°N-49°N	16.8	133	2.55	0.620	0.069	0.55
SX-7757	24 Apr 66	49°N-37°N	16.8	115	2.06	0.584	0.056	0.53
SX-7759	25 Apr 66	50°N-37°N	18.3	160	3.23	1.04	0.087	0.95
SX-7761	25 Apr 66	50°N-37°N	19.5	175	2.97	1.23	0.080	1.15
SX-7762	25 Apr 66	36°N-23°N	18.3	88.2	1.38	0.197	0.037	0.16
SX-7763	25 Apr 66	36°N-23°N	19.8	160	2.70	0.598	0.073	0.52
SX-7764	26 Apr 66	75°N-64°N	15.2	163	2.89	1.04	0.078	0.96
SX-7765	26 Apr 66	75°N-64°N	16.8	149	2.77	1.10	0.075	1.02
SX-7766	26 Apr 66	36°N-30°N	15.2	121	2.49	0.592	0.067	0.52
SX-7767	27 Apr 66	75°N-62°N	18.3	144	2.88	1.35	0.078	1.27
SX-7768	27 Apr 66	75°N-65°N	19.1	139	2.79	1.73	0.075	1.66
SX-7769	27 Apr 66	07°N-11°S	18.3	20.9	0.348	0.201	0.009	0.19
SX-7771	27 Apr 66	09°N-11°S	19.6	82.8	1.59	0.184	0.043	0.14
SX-7772	27 Apr 66	35°S-54°S	15.2	36.3	0.518	0.714	0.014	0.70
SX-7773	27 Apr 66	33°S-54°S	16.8	72.8	1.08	2.77	0.029	2.74

TABLE 9A-1. (continued)

Sample	Collection Date	Latitude Range	Altitude (km)	Nuclide Concentrations (pCi/100 SCM) Total Sr^{90}	Total Pu^{239}	Total Pu^{238}	Weapon Pu^{238}	SNAP-9A Pu^{238}
SX-7774	28 Apr 66	62°N-55°N	18.3	129	2.14	3.42	0.058	3.36
SX-7775	28 Apr 66	62°N-56°N	19.2	147	2.38	2.03	0.064	1.97
SX-7886	17 May 66	70°N	12.2	91.5	1.98	0.252	0.053	0.20
SQ-7891	19 May 66	40°S	12.2	22.4	0.383	0.523	0.010	0.51
SQ-7797	25 May 66	36°N-23°N	15.2	17.8	0.247	0.038	0.007	0.03
SQ-7798	27 May 66	07°N-09°S	16.8	7.3	0.108	0.007	0.003	≤0.01
SQ-7799	27 May 66	13°S-32°S	18.3	50.9	0.820	1.56	0.022	1.54
SQ-7801	28 May 66	64°N-49°N	16.8	99.1	1.83	0.611	0.049	0.56
SQ-7802	28 May 66	49°N-37°N	16.8	83.7	1.22	0.408	0.033	0.38
SQ-7803	28 May 66	32°N-26°N	17.5	97.0	1.38	0.352	0.037	0.32
SQ-7804	28 May 66	26°N-09°N	18.3	86.1	1.33	0.389	0.036	0.35
SQ-7805	30 May 66	61°N-49°N	18.3	123	1.86	0.926	0.050	0.88
SQ-7806	30 May 66	49°N-37°N	18.2	152	1.97	0.823	0.053	0.77
SX-7887	2 Jun 66	70°N	12.2	99	1.78	0.190	0.048	0.14
SQ-7807	2 Jun 66	64°N-55°N	15.2	109	1.53	0.653	0.041	0.61
SQ-7808	2 Jun 66	55°N-43°N	15.2	112	1.48	0.473	0.040	0.43
SQ-7809	2 Jun 66	43°N-37°N	15.2	54	1.96	0.787	0.053	0.73
SQ-7811	3 Jun 66	35°N-27°N	16.8	19.1	0.275	0.047	0.007	0.04
SQ-7812	3 Jun 66	27°N-20°N	16.8	36.7	0.487	0.082	0.013	0.07
SQ-7813	3 Jun 66	20°N-10°N	16.7	12.8	0.194	0.017	0.005	0.01
SQ-7814	4 Jun 66	35°N-23°N	18.8	149	2.20	0.855	0.059	0.80
SQ-7815	4 Jun 66	23°N-19°N	18.4	89.1	1.31	0.275	0.035	0.24
SQ-7816	4 Jun 66	19°N-12°N	18.2	66.4	1.01	0.182	0.027	0.16
SQ-7817	5 Jun 66	64°N-49°N	15.2	46.9	0.738	0.163	0.020	0.14
SQ-7818	5 Jun 66	49°N-37°N	15.2	71.2	1.08	0.311	0.029	0.28
SQ-7858	10 Jun 66	64°N-49°N	16.8	91.8	1.49	0.602	0.040	0.56
SQ-7859	10 Jun 66	49°N-37°N	16.8	90.0	1.59	0.596	0.043	0.55
SQ-7861	10 Jun 66	36°N-23°N	16.8	34.9	0.477	0.085	0.013	0.07
SQ-7862	10 Jun 66	33°N-23°N	18.3	103	1.66	0.644	0.045	0.60
SQ-7863	10 Jun 66	23°N-10°N	16.8	25.1	0.407	0.075	0.011	0.06
SQ-7864	10 Jun 66	23°N-10°N	18.3	71.0	1.17	0.254	0.032	0.22
SQ-7865	14 Jun 66	34°N-23°N	19.8	120	2.23	1.09	0.060	1.03
SX-7836	14 Jun 66	23°N-12°N	19.2	144	2.05	0.420	0.055	0.36
SQ-7866	14 Jun 66	07°N-09°S	16.8	4.8	0.070	0.011	0.002	0.01
SX-7837	14 Jun 66	13°S-32°S	18.3	70.3	0.947	2.84	0.026	2.81
SQ-7867	15 Jun 66	64°N-49°N	15.2	110	1.62	0.697	0.044	0.65
SQ-7868	15 Jun 66	49°N-37°N	15.2	41.2	0.616	0.158	0.017	0.14

TABLE 9A-1. (continued)

Sample	Collection Date	Latitude Range	Altitude (km)	Total Sr^{90}	Total Pu^{239}	Total Pu^{238}	Weapon Pu^{238}	SNAP-9A Pu^{238}
				Nuclide Concentrations (pCi/100 SCM)				
SX-7838	17 Jun 66	08°N-09°S	18.3	61.2	0.692	0.131	0.019	0.11
SQ-7869	17 Jun 66	17°S-30°S	16.9	18.0	0.303	0.427	0.008	0.42
SQ-7871	18 Jun 66	36°N-19°N	15.2	18.1	0.319	0.048	0.009	0.04
SQ-7872	18 Jun 66	19°N-10°N	15.2	6.5	0.116	0.005	0.003	≤0.01
SX-7839	21 Jun 66	50°N-37°N	18.3	152	2.29	1.16	0.062	1.10
SX-7841	21 Jun 66	50°N-37°N	19.2	160	2.35	1.29	0.063	1.23
SX-7842	22 Jun 66	64°N-49°N	16.8	200	3.68	1.59	0.099	1.49
SX-7843	22 Jun 66	49°N-37°N	16.8	231	3.87	1.52	0.104	1.42
SX-7844	22 Jun 66	36°N-23°N	18.3	160	2.19	0.883	0.059	0.82
SX-7845	22 Jun 66	36°N-23°N	19.6	183	2.94	1.32	0.079	1.24
SX-7846	24 Jun 66	64°N-46°N	15.2	110	1.90	0.632	0.051	0.58
SX-7847	24 Jun 66	36°N-16°N	16.8	65.5	0.969	0.220	0.026	0.19
SX-7848	25 Jun 66	64°N-49°N	15.2	96.7	1.48	0.467	0.040	0.42
SX-7849	25 Jun 66	49°N-37°N	15.2	83.2	1.21	0.677	0.033	0.64
SX-7851	25 Jun 66	36°N-23°N	15.2	20.9	0.298	0.047	0.008	0.04
SX-7852	25 Jun 66	23°N-09°N	15.2	18.0	0.335	0.023	0.009	0.01
SX-7853	26 Jun 66	36°N-23°N	16.8	80.9	1.23	0.336	0.033	0.30
SX-7854	26 Jun 66	23°N-09°N	16.8	36.5	0.586	0.108	0.016	0.09
SX-7855	26 Jun 66	07°N-09°S	16.8	4.54	0.061	0.017	0.002	0.02
SX-7856	30 Jun 66	35°N-23°N	18.3	142	2.31	0.892	0.062	0.83
SX-7857	30 Jun 66	23°N-10°N	18.3	93.7	1.52	0.368	0.041	0.33
SQ-7908	8 Jul 66	64°N-47°N	13.1	55.0	1.03	0.198	0.028	0.17
SX-8199	12 Jul 66	75°N-70°N	12.2	44.6	0.93	0.14	0.02	0.12
SQ-7909	17 Jul 66	64°N-50°N	19.3	129	2.42	1.61	0.065	1.54
SQ-7916	18 Jul 66	50°N-37°N	19.5	183	2.71	1.79	0.073	1.72
SQ-7917	18 Jul 66	23°N-09°N	19.4	130	2.27	0.392	0.061	0.33
SQ-7911	18 Jul 66	35°S-54°S	15.2	59.9	1.03	3.65	0.028	3.62
SQ-7912	18 Jul 66	35°S-54°S	16.8	88.4	1.50	5.21	0.040	5.17
SQ-7913	19 Jul 66	14°S-33°S	19.7	94.2	1.69	2.14	0.046	2.09
SQ-7914	20 Jul 66	64°N-49°N	16.8	123	2.23	0.862	0.060	0.80
SQ-7918	20 Jul 66	36°N-23°N	19.3	151	2.53	1.16	0.068	1.09
SQ-7915	21 Jul 66	07°N-06°S	19.5	134	2.46	0.413	0.066	0.35
SQ-8232	25 Jul 66	40°S-44°S	12.2	14.8	0.315	0.523	0.008	0.52

TABLE 9A-1. (continued)

Sample	Collection Date	Latitude Range	Altitude (km)	Total Sr^{90}	Total Pu^{239}	Total Pu^{238}	Weapon Pu^{238}	SNAP-9A Pu^{238}
				Nuclide Concentrations (pCi/100 SCM)				
SX-7969	1 Aug 66	08°N-13°S	16.8	13	0.224	0.111	0.006	0.10
SX-7957	1 Aug 66	13°S-30°S	16.8	29	0.460	1.00	0.012	0.99
SX-7971	2 Aug 66	64°N-50°N	13.1	52	1.10	0.251	0.030	0.22
SX-7958	4 Aug 66	64°N-44°N	11.9	34.9	0.494	0.105	0.013	0.09
SX-7959	14 Aug 66	64°N-37°N	16.8	106	1.96	0.660	0.053	0.61
SX-7961	14 Aug 66	62°N-50°N	18.3	165	2.73	1.51	0.074	1.44
SX-7972	14 Aug 66	64°N-50°N	19.4	105	2.24	1.79	0.060	1.73
SX-7973	15 Aug 66	36°N-16°N	15.2	14	0.268	0.055	0.007	0.05
SX-7974	15 Aug 66	36°N-23°N	18.3	122	2.22	0.729	0.060	0.67
SX-7975	15 Aug 66	36°N-23°N	19.6	137	2.50	1.06	0.068	0.99
SX-7962	15 Aug 66	43°S-54°S	15.2	73	1.19	3.98	0.032	3.95
SX-7963	15 Aug 66	33°S-53°S	16.8	80	1.32	4.11	0.036	4.07
SX-7976	16 Aug 66	75°N-62°N	18.3	149	2.52	1.56	0.068	1.49
SX-7964	16 Aug 66	75°N-65°N	19.2	133	2.90	8.00	0.078	7.92
SQ-8143	16 Aug 66	75°N-65°N	19.2	118	3.89	1.78	0.105	1.68
SX-7977	16 Aug 66	50°N-37°N	18.3	145	2.47	1.07	0.067	1.00
SX-7978	16 Aug 66	50°N-37°N	19.6	147	2.64	1.60	0.071	1.53
SX-7979	17 Aug 66	75°N-64°N	15.2	96	1.76	0.600	0.048	0.55
SX-7981	17 Aug 66	75°N-64°N	16.8	135	2.54	1.09	0.068	1.02
SX-7965	17 Aug 66	14°S-30°S	18.3	83	1.14	0.953	0.031	0.92
SX-7982	17 Aug 66	14°S-33°S	19.9	108	1.94	4.46	0.052	4.41
SX-7966	18 Aug 66	64°N-40°N	15.2	46	0.983	0.270	0.026	0.24
SX-7983	18 Aug 66	23°N-09°N	18.3	87	1.57	0.356	0.042	0.31
SX-7984	18 Aug 66	23°N-09°N	19.2	115	2.00	0.544	0.054	0.49
SX-7985	18 Aug 66	36°S-52°S	18.3	89	1.40	4.82	0.038	4.78
SX-7967	18 Aug 66	33°S-52°S	19.7	80	1.34	3.37	0.036	3.33
SX-7968	19 Aug 66	07°N-11°S	18.3	69	1.36	0.410	0.037	0.37
SX-7986	19 Aug 66	09°N-11°S	19.3	126	2.26	0.549	0.061	0.49
SX-8201	23 Aug 66	75°N-70°N	12.2	29.7	0.537	0.096	0.014	0.08
SX-7987	31 Aug 66	33°N-26°N	16.8	52	0.834	0.183	0.022	0.16
SX-7988	31 Aug 66	26°N-10°N	16.8	19	0.323	0.054	0.009	0.04
SQ-8126	9 Oct 66	35°S-54°S	15.2	59	0.972	2.32	0.026	2.29
SQ-8127	9 Oct 66	33°S-54°S	16.8	77	1.37	3.39	0.037	3.35
SQ-8128	9 Oct 66	36°S-51°S	18.3	73	1.27	3.42	0.034	3.39
SQ-8129	9 Oct 66	33°S-51°S	19.3	96	2.11	4.53	0.057	4.47

ISOTOPES
A Teledyne Company

TABLE 9A-1. (continued)

Sample	Collection Date	Latitude Range	Altitude (km)	Total Sr^{90}	Total Pu^{239}	Total Pu^{238}	Weapon Pu^{238}	SNAP-9A Pu^{238}
				Nuclide Concentrations (pCi/100 SCM)				
SQ-8102	10 Oct 66	35°N-23°N	18.3	111	1.82	0.629	0.049	0.58
SQ-8103	10 Oct 66	35°N-23°N	19.8	142	2.05	1.17	0.055	1.12
SQ-8098	10 Oct 66	09°N-10°S	20.1	127	2.11	0.944	0.057	0.89
SQ-8131	10 Oct 66	14°S-32°S	19.5	88	1.59	4.32	0.043	4.28
SQ-8104	11 Oct 66	50°N-37°N	18.3	149	2.22	1.19	0.060	1.13
SQ-8105	11 Oct 66	50°N-37°N	19.6	146	2.18	1.77	0.059	1.71
SQ-8101	11 Oct 66	9°N-11°S	18.3	67	0.943	0.658	0.025	0.63
SQ-8099	11 Oct 66	11°S-27°S	18.3	65	0.960	1.98	0.026	1.95
SQ-8106	12 Oct 66	50°N-37°N	15.2	45	0.639	0.157	0.017	0.14
SQ-8107	12 Oct 66	50°N-37°N	16.8	85	1.33	0.412	0.036	0.38
SQ-8108	13 Oct 66	30°N-09°N	15.2	1.08	0.037	0.024	0.001	0.02
SQ-8109	13 Oct 66	36°N-25°N	16.8	20	0.337	0.105	0.011	0.09
SQ-8111	13 Oct 66	25°N-09°N	16.8	10	0.169	0.046	0.004	0.04
SQ-8112	13 Oct 66	36°N-23°N	18.3	94	1.56	0.520	0.042	0.48
SQ-8113	13 Oct 66	23°N-09°N	18.3	95	1.69	0.631	0.046	0.58
SQ-8114	13 Oct 66	36°N-09°N	19.6	104	1.68	0.764	0.045	0.72
SQ-8144	26 Oct 66	64°N-55°N	13.1	26	0.762	0.225	0.020	0.20
SQ-8115	27 Oct 66	09°N-07°S	16.8	11	0.215	0.144	0.006	0.14
SQ-8116	27 Oct 66	15°S-31°S	16.8	50	0.802	1.76	0.022	1.74
SQ-8145	28 Oct 66	64°N-55°N	11.9	18	0.346	0.078	0.009	0.07
SQ-8146	10 Nov 66	75°N-61°N	18.2	96	2.07	1.75	0.056	1.69
SQ-8147	10 Nov 66	75°N-64°N	19.3	90	2.02	2.12	0.054	2.07
SQ-8148	10 Nov 66	13°S-32°S	19.3	63	1.43	2.10	0.039	2.06
SQ-8149	11 Nov 66	75°N-64°N	15.2	100	2.07	0.817	0.056	0.76
SQ-8151	11 Nov 66	75°N-64°N	16.8	127	2.51	1.58	0.068	1.51
SQ-8152	11 Nov 66	35°S-54°S	15.2	54	0.799	2.12	0.022	2.10
SQ-8153	11 Nov 66	33°S-54°S	16.8	37	0.758	1.49	0.020	1.47
SQ-8156	12 Nov 66	34°S-54°S	7.6	0.61	0.026	0.027	0.001	0.03
SQ-8157	12 Nov 66	33°S-50°S	9.1	1.2	0.044	0.036	0.001	0.04
SQ-8154	12 Nov 66	36°S-54°S	18.3	65	1.12	3.22	0.030	3.19
SQ-8155	12 Nov 66	33°S-54°S	19.8	58	0.915	2.82	0.025	2.80
SQ-8158	13 Nov 66	35°N-22°N	19.6	125	2.25	1.27	0.061	1.21
SQ-8159	13 Nov 66	08°N-10°S	19.2	69	1.36	0.624	0.037	0.59
SQ-8161	15 Nov 66	36°N-10°N	9.4	0.14	0.008	0.001	-	≤0.01

TABLE 9A-1. (continued)

Sample	Collection Date	Latitude Range	Altitude (km)	Total Sr^{90}	Total Pu^{239}	Total Pu^{238}	Weapon Pu^{238}	SNAP-9A Pu^{238}
				Nuclide Concentrations (pCi/100 SCM)				
SQ-8229	22 Nov 66	64°N-55°N	11.9	12	0.212	0.052	0.006	0.05
SQ-8231	22 Nov 66	64°N-55°N	13.1	34	0.664	0.184	0.018	0.17
SX-8202	4 Dec 66	35°N-10°N	7.5	0.18	0.006	0.003	0.000	≤0.01
SX-8203	4 Dec 66	35°N-09°N	16.8	11.4	0.262	0.084	0.007	0.08
SX-8221	4 Dec 66	34°N-22°N	18.3	82.	1.38	0.560	0.037	0.52
SX-8222	4 Dec 66	22°N-10°N	19.9	112	2.02	1.06	0.054	1.01
SX-8204	5 Dec 66	64°N-37°N	16.8	63	1.64	0.928	0.044	0.88
SX-8223	5 Dec 66	64°N-37°N	18.2	97	1.86	1.24	0.050	1.19
SX-8205	5 Dec 66	35°N-09°N	15.2	6.5	0.159	0.051	0.004	0.05
SX-8206	6 Dec 66	07°N-12°S	16.8	9.2	0.174	0.250	0.005	0.24
SX-8207	6 Dec 66	14°S-32°S	19.4	55.	1.17	2.67	0.032	2.64
SX-8208	7 Dec 66	75°N-64°N	15.2	112	2.38	1.41	0.064	1.35
SX-8224	7 Dec 66	75°N-64°N	16.8	86	1.22	1.27	0.033	1.24
SX-8225	7 Dec 66	75°N-62°N	18.3	100	1.68	1.69	0.045	1.64
SX-8226	7 Dec 66	75°N-65°N	19.2	69	1.24	1.59	0.033	1.56
SX-8209	7 Dec 66	34°S-54°S	7.6	1.0	0.028	0.034	0.001	0.03
SX-8211	7 Dec 66	35°S-51°S	15.2	33	0.866	1.45	0.023	1.43
SX-8212	7 Dec 66	34°S-51°S	16.8	40	0.730	1.82	0.020	1.80
SX-8213	8 Dec 66	64°N-36°N	15.2	76	1.36	0.719	0.037	0.68
SX-8214	8 Dec 66	36°S-51°S	18.3	68	1.19	3.46	0.032	3.43
SX-8215	8 Dec 66	34°S-51°S	19.4	58	1.15	4.10	0.031	4.07
SX-8228	9 Dec 66	35°N-22°N	19.4	105	2.00	1.21	0.054	1.16
SX-8227	9 Dec 66	22°N-09°N	18.3	-	0.926	0.325	0.025	0.30
SX-8218	9 Dec 66	08°N-10°S	18.3	35	0.857	0.511	0.023	0.49
SX-8219	9 Dec 66	08°N-09°S	19.4	70	1.50	0.734	0.040	0.69
SX-8216	9 Dec 66	11°S-31°S	15.2	2.9	0.086	0.092	0.002	0.09
SX-8217	9 Dec 66	11°S-30°S	16.8	12.1	0.311	0.364	0.008	0.36
SX-8253	19 Dec 66	64°N-55°N	11.9	12.8	0.322	0.112	0.009	0.10
SX-8254	19 Dec 66	64°N-55°N	13.1	14.1	0.355	0.143	0.010	0.13

TABLE 9A-1. (continued)

Sample	Collection Date	Latitude Range	Altitude (km)	Total Sr90	Total Pu239	Total Pu238	Weapon Pu238	SNAP-9A Pu238
				Nuclide Concentrations (pCi/100 SCM)				
SQ-8255	2 Jan 67	64°N-37°N	16.8	61.4	1.60	1.03	0.04	0.99
SQ-8256	3 Jan 67	61°N-37°N	15.2	43.8	0.938	0.870	0.02	0.85
SQ-8261	4 Jan 67	75°N-64°N	19.4	89.9	1.63	1.60	0.04	1.54
SQ-8257	4 Jan 67	08°N-10°S	19.7	72.3	2.42	1.49	0.06	1.43
SQ-8262	4 Jan 67	35°S-53°S	15.2	36.2	1.04	1.80	0.03	1.77
SQ-8263	4 Jan 67	34°S-53°S	16.8	55.0	0.890	2.84	0.02	2.82
SQ-8264	5 Jan 67	62°N-51°N	18.3	93.7	1.70	1.38	0.04	1.34
SQ-8265	5 Jan 67	64°N-51°N	19.4	78.2	1.85	1.65	0.05	1.60
SQ-8326	5 Jan 67	35°N-22°N	19.9	81.4	1.64	1.37	0.04	1.33
SQ-8266	5 Jan 67	22°N-09°N	20.3	103	1.59	0.548	0.04	0.51
SQ-8258	5 Jan 67	35°S-50°S	18.3	52.0	1.18	4.03	0.03	4.00
SQ-8267	5 Jan 67	34°S-50°S	19.5	67.4	1.24	4.14	0.03	4.11
SQ-8259	6 Jan 67	14°S-33°S	18.3	25.3	0.624	1.41	0.02	1.39
SQ-8312	20 Jan 67	64°N-44°N	11.9	27.4	0.950	0.396	0.02	0.38
SQ-8313	20 Jan 67	64°N-40°N	13.1	47.9	1.47	0.747	0.04	0.71
SQ-8314	29 Jan 67	14°S-31°S	18.3	28.3	0.649	(0.348)	0.02	(0.33)
SQ-8315	29 Jan 67	14°S-32°S	19.9	36.9	1.20	3.90	0.03	3.87
SQ-8431	29 Jan 67	14°S-31°S	18.3	26.6	0.563	1.69	0.02	1.67
SQ-8298	30 Jan 67	64°N-50°N	18.3	56.6	1.60	1.59	0.04	1.55
SQ-8309	30 Jan 67	64°N-52°N	18.9	62.1	1.56	1.65	0.04	1.61
SQ-8301	30 Jan 67	50°N-37°N	15.2	19.4	0.526	0.309	0.01	0.30
SQ-8316	30 Jan 67	35°S-52°S	18.3	37.4	1.02	2.87	0.03	2.84
SQ-8317	30 Jan 67	34°S-52°S	19.5	45.5	1.11	4.00	0.03	3.97
SQ-8301	30 Jan 67	50°N-38°N	16.8	88.5	2.13	1.24	0.06	1.18
SQ-8318	31 Jan 67	35°S-52°S	15.2	28.8	0.582	1.46	0.02	1.44
SQ-8319	31 Jan 67	34°S-52°S	16.8	61.0	0.849	2.56	0.02	2.54
SQ-8302	1 Feb 67	75°N-64°N	15.2	62.0	1.67	1.52	0.04	1.48
SQ-8303	1 Feb 67	75°N-64°N	16.8	47.8	1.29	1.81	0.03	1.78
SQ-8321	1 Feb 67	64°N-55°N	15.2	52.5	1.71	1.01	0.05	.96
SQ-8322	1 Feb 67	50°N-36°N	18.3	84.4	1.94	1.62	0.05	1.57
SQ-8304	1 Feb 67	08°N-09°S	16.8	2.56	0.072	0.080	0.00	0.08
SQ-8305	1 Feb 67	08°N-10°S	19.2	54.7	1.38	1.60	0.04	1.56
SQ-8306	1 Feb 67	11°S-31°S	16.8	6.92	0.191	0.347	0.01	0.34
SQ-8307	2 Feb 67	08°N-09°S	18.3	38.1	1.06	1.07	0.03	1.04
SQ-8308	2 Feb 67	11°S-31°S	15.2	0.857	0.034	0.053	0.00	0.05

TABLE 9A-1. (continued)

Sample	Collection Date	Latitude Range	Altitude (km)	Total Sr^{90}	Total Pu^{239}	Total Pu^{238}	Weapon Pu^{238}	SNAP-9A Pu^{238}
				Nuclide Concentrations (pCi/100 SCM)				
SQ-8323	3 Feb 67	63°N-50°N	16.8	51.9	1.52	1.01	0.04	0.97
SQ-8327	3 Feb 67	47°N-35°N	19.1	82.0	2.08	1.62	0.06	1.56
SQ-8324	3 Feb 67	35°N-10°N	16.8	9.16	0.524	0.361	0.01	0.35
SQ-8325	3 Feb 67	35°N-10°N	18.3	29.0	0.779	0.417	0.02	0.40
SQ-8432	3 Feb 67	63°N-50°N	16.8	54.3	1.38	0.945	0.04	0.90
SQ-8433	3 Feb 67	47°N-35°N	19.1	71.1	1.37	1.31	0.04	1.27
SX-8354	27 Feb 67	21°N-10°N	19.2	66.7	1.53	0.696	0.04	0.66
SX-8335	28 Feb 67	64°N-37°N	16.8	63.6	1.38	1.05	0.04	1.01
SX-8343	1 Mar 67	19°S-32°S	19.4	63.3	1.19	2.62	0.03	2.59
SX-8338	2 Mar 67	75°N-64°N	18.3	(49.0)	2.23	1.22	0.06	1.16
SX-8339	2 Mar 67	75°N-64°N	19.1	50.6	1.32	1.58	0.04	1.54
SX-8355	2 Mar 67	50°N-37°N	18.3	72.0	1.47	1.21	0.04	1.17
SX-8356	2 Mar 67	50°N-35°N	19.7	73.3	2.12	2.42	0.06	2.36
SX-8344	2 Mar 67	14°S-32°S	18.3	45.2	0.742	1.73	0.02	1.71
SX-8336	3 Mar 67	75°N-64°N	15.2	56.0	1.81	0.769	0.05	0.72
SX-8337	3 Mar 67	75°N-64°N	16.8	45.4	1.12	0.718	0.03	0.69
SX-8341	3 Mar 67	64°N-51°N	18.3	60.4	1.30	1.24	0.04	1.20
SX-8342	3 Mar 67	64°N-51°N	19.5	46.6	1.40	2.05	0.04	2.01
SX-8345	4 Mar 67	62°N-44°N	15.2	34.8	0.845	0.526	0.02	0.51
SX-8346	4 Mar 67	35°S-52°S	15.2	19.8	0.413	0.920	0.01	0.91
SX-8347	4 Mar 67	34°S-52°S	16.8	31.1	0.514	1.28	0.01	1.27
SX-8348	4 Mar 67	35°S-52°S	18.3	51.3	0.826	2.46	0.02	2.44
SX-8349	4 Mar 67	34°S-52°S	19.2	72.0	1.74	5.30	0.05	5.25
SX-8357	6 Mar 67	35°N-23°N	19.0	73.2	1.32	1.02	0.04	0.98
SX-8353	6 Mar 67	08°N-09°S	19.1	56.6	1.22	0.966	0.03	0.94
SX-8351	6 Mar 67	19°S-31°S	15.2	15.3	0.423	0.494	0.01	0.48
SX-8352	6 Mar 67	11°S-31°S	16.8	5.32	0.153	0.240	0.00	0.24
SX-8358	8 Mar 67	34°N-10°N	18.3	49.1	0.920	0.606	0.02	0.59
SX-8374	16 Mar 67	64°N-55°N	13.1	24.3	0.607	0.435	0.02	0.42
SX-8375	17 Mar 67	64°N-55°N	11.9	31.5	0.654	0.345	0.02	0.32
SQ-8385	26 Mar 67	35°N-26°N	15.2	12.4	0.272	0.186	0.01	0.18
SQ-8386	26 Mar 67	35°N-26°N	16.8	41.2	0.812	0.504	0.02	0.48
SQ-8376	27 Mar 67	64°N-37°N	16.8	46.0	1.06	0.810	0.03	0.78
SQ-8378	27 Mar 67	64°N-50°N	18.8	64.3	1.08	1.01	0.03	0.98
SQ-8407	28 Mar 67	13°S-32°S	19.5	41.7	0.884	2.00	0.02	1.98

TABLE 9A-1. (continued)

Sample	Collection Date	Latitude Range	Altitude (km)	Total Sr^{90}	Total Pu^{239}	Total Pu^{238}	Weapon Pu^{238}	SNAP-9 Pu^{238}
				Nuclide Concentrations (pCi/100 SCM)				
SQ-8387	29 Mar 67	75°N-64°N	15.2	57.6	1.20	1.22	0.03	1.19
SQ-8536	29 Mar 67	75°N-64°N	15.2	66.2	1.34	1.21	0.04	1.17
SQ-8388	29 Mar 67	75°N-64°N	16.8	40.9	0.809	1.94	0.02	1.92
SQ-8537	29 Mar 67	75°N-64°N	16.8	44.5	1.71	2.25	0.05	2.20
SQ-8538	29 Mar 67	75°N-64°N	18.3	25.7	0.619	1.86	0.02	1.84
SQ-8381	29 Mar 67	75°N-64°N	19.7	(12.0)	0.384	1.95	0.01	1.94
SQ-8539	29 Mar 67	75°N-64°N	19.7	18.0	0.383	2.22	0.01	2.21
SQ-8389	29 Mar 67	35°N-22°N	18.3	60.8	1.17	0.865	0.03	0.84
SQ-8379	29 Mar 67	22°N-09°N	20.0	70.3	1.23	0.921	0.03	0.89
SQ-8408	29 Mar 67	35°S-52°S	15.2	34.0	0.527	1.29	0.01	1.28
SQ-8409	29 Mar 67	35°S-52°S	16.8	41.6	0.751	2.26	0.02	2.24
SQ-8377	30 Mar 67	64°N-35°N	15.2	43.8	1.07	0.765	0.03	0.74
SQ-8382	30 Mar 67	64°N-47°N	17.9	(2.24)	1.36	1.06	0.04	1.02
SQ-8383	30 Mar 67	47°N-35°N	19.2	67.5	1.34	1.56	0.04	1.52
SQ-8411	30 Mar 67	35°S-52°S	18.3	50.8	0.965	3.50	0.03	3.47
SQ-8412	30 Mar 67	34°S-52°S	19.5	47.1	0.812	3.02	0.02	3.00
SQ-8391	31 Mar 67	08°N-09°S	18.3	29.5	0.580	0.513	0.02	0.49
SQ-8384	1 Apr 67	35°N-22°N	19.8	66.4	1.37	0.930	0.04	0.89
SQ-8392	1 Apr 67	22°N-14°N	18.3	56.5	1.04	0.584	0.03	0.55
SQ-8413	11 Apr 67	64°N-55°N	11.9	40.9	0.680	0.454	0.02	0.43
SQ-8414	11 Apr 67	64°N-55°N	13.1	37.9	0.644	0.460	0.02	0.44
SQ-8415	11 Apr 67	47°N-41°N	11.9	(0.568)	0.621	0.361	0.02	0.34
SQ-8416	11 Apr 67	47°N-41°N	13.1	28.8	0.517	0.271	0.01	0.26
SQ-8417	23 Apr 67	22°N-10°N	19.4	60.8	1.33	1.03	0.04	0.99
SQ-8438	24 Apr 67	64°N-37°N	16.8	(30.3)	0.873	0.947	0.02	0.93
SQ-8439	25 Apr 67	62°N-50°N	18.3	33.0	0.754	1.18	0.02	1.16
SQ-8441	25 Apr 67	63°N-50°N	19.3	35.9	0.884	1.66	0.02	1.64
SQ-8444	26 Apr 67	14°S-32°S	19.5	35.6	0.830	2.41	0.02	2.39
SQ-8445	26 Apr 67	35°S-52°S	15.2	2.76	0.134	0.396	0.00	0.40
SQ-8446	26 Apr 67	34°S-52°S	16.8	22.8	0.506	1.29	0.01	1.28
SQ-8434	27 Apr 67	75°N-64°N	19.1	(24.4)	(0.593)	(1.25)	(0.02)	(1.23)
SQ-8435	27 Apr 67	50°N-37°N	19.2	(45.6)	1.18	1.22	0.03	1.19
SQ-8442	27 Apr 67	35°S-52°S	18.3	(26.8)	(0.725)	(2.44)	(0.02)	(2.22)
SQ-8443	27 Apr 67	34°S-52°S	19.4	(22.6)	(0.828)	(3.09)	(0.02)	(3.07)
SQ-8447	28 Apr 67	64°N-35°N	15.2	27.5	0.815	0.740	0.02	0.72
SQ-8436	29 Apr 67	08°N-14°S	19.4	39.1	1.06	1.32	0.03	1.29
SQ-8437	30 Apr 67	35°N-22°N	19.1	59.4	1.01	0.767	0.03	0.74

TABLE 9A-1. (continued)

Sample	Collection Date	Latitude Range	Altitude (km)	Total Sr^{90}	Total Pu^{239}	Total Pu^{238}	Weapon Pu^{238}	SNAP-9A Pu^{238}
				Nuclide Concentrations (pCi/100 SCM)				
SQ-8463	9 May 67	64°N-48°N	11.9	27.9	Lost	Lost	Lost	Lost
SQ-8464	11 May 67	64°N-36°N	13.1	25.2	0.686	0.511	0.02	0.49
SX-8466	25 May 67	64°N-37°N	16.8	45.9	1.00	0.986	0.03	0.96
SX-8467	26 May 67	75°N-64°N	15.2	35.4	0.749	0.832	0.02	0.81
SX-8468	26 May 67	75°N-64°N	16.8	58.9	1.20	0.879	0.03	0.85
SX-8469	26 May 67	61°N-51°N	19.4	57.5	1.63	1.56	0.04	1.52
SX-8471	26 May 67	50°N-37°N	18.3	57.4	1.21	1.16	0.03	1.13
SX-8472	26 May 67	35°N-10°N	18.3	50.5	1.14	1.06	0.03	1.03
SX-8473	27 May 67	75°N-64°N	18.3	(20.8)	1.34	1.97	0.04	1.93
SX-8474	27 May 67	75°N-64°N	19.0	48.6	0.876	1.37	0.02	1.35
SX-8475	27 May 67	64°N-40°N	15.2	40.5	0.720	0.598	0.02	0.58
SX-8476	27 May 67	35°N-22°N	16.8	17.7	0.384	0.276	0.01	0.27
SX-8477	28 May 67	64°N-50°N	18.3	(23.9)	1.21	1.11	0.03	1.08
SX-8478	28 May 67	49°N-36°N	19.8	32.6	0.821	1.36	0.02	1.34
SX-8479	28 May 67	14°S-32°S	16.8	24.3	0.458	1.02	0.01	1.01
SX-8481	28 May 67	03°N-27°S	18.3	(2.37)	(2.41)	(1.43)	(0.06)	(1.37)
SX-8482	29 May 67	14°S-32°S	19.1	31.9	0.453	1.12	0.01	1.11
SX-8484	30 May 67	03°N-15°S	18.8	48.7	1.02	0.890	0.03	0.86
SX-8483	30 May 67	15°N-30°S	15.2	10.6	0.193	0.437	0.00	0.44
SX-8485	30 May 67	35°S-52°S	15.2	23.0	0.614	1.21	0.02	1.19
SX-8486	30 May 67	34°S-52°S	16.8	38.1	0.633	2.12	0.02	2.10
SX-8487	31 May 67	34°S-52°S	18.3	32.6	Lost	Lost	Lost	Lost
SX-8488	31 May 67	34°S-52°S	19.4	33.4	0.610	2.78	0.02	2.76
SX-8489	1 June 67	35°N-10°N	19.0	41.4	0.683	0.644	0.02	0.62
SX-8491	6 June 67	64°N-55°N	11.9	14.9	0.261	0.176	0.01	0.17
SX-8492	6 June 67	64°N-55°N	13.1	21.6	0.502	0.380	0.01	0.37
SX-8493	6 June 67	47°N-41°N	11.9	16.9	0.307	0.208	0.01	0.20
SX-8494	6 June 67	48°N-41°N	13.1	24.1	0.436	0.296	0.01	0.29

CHAPTER 10. STRATOSPHERIC DISTRIBUTION OF COSMIC RAY ACTIVITY

Radionuclides are produced continuously in the atmosphere primarily by secondary cosmic ray neutrons and protons interacting with nitrogen, oxygen and argon nuclei. Although their production rates remain relatively constant with time, the rates vary considerably with altitude and latitude. A list of known cosmogenic radionuclides along with their half-lives is given in Table 112. With the exceptions of the argon isotopes the table was reproduced from Young et al[60]. Argon-39 was first detected in the atmosphere by Loosli and Oeschger[63] and argon-37 by Schell[64].

The stratospheric and tropospheric concentrations and ratios of the short-lived radionuclides can be used to study atmospheric circulation and mixing patterns if the equilibrium concentrations of the radionuclides are known. Absolute production rates of many of the nuclides in Table 112 have been estimated by Lal and Peters[61] and by Bhandari, Lal and Rama[62] and have been used for comparisons with the stratospheric concentrations of four radionuclides measured under Project STARDUST.

During various time intervals from late 1959 through early 1965 STARDUST filter samples were analyzed for a number of radionuclides including four produced by cosmic rays: beryllium-7, phosphorus-32, phosphorus-33, and sodium-22.

Stratospheric Distribution of Beryllium-7, Phosphorus-32 and Phosphorus-33

The phosphorus samples were beta-counted with and without absorbers to determine the relative contributions of 1.71 Mev phosphorus-32 and 0.25 Mev phosphorus-33 beta particles. The measurements of phosphorus-32 were moderately successful, but those of phosphorus-33 were less so. An unsuccessful attempt was made to improve the phosphorus-33 data by eliminating counting through absorbers,

TABLE 112. Half-Lives and Decay Characteristics of Cosmic Ray-Produced Radionuclides

Radionuclide	Half-Life
^{10}Be	2.7×10^6 years
^{36}Cl	3.1×10^5
^{14}C	5.57×10^3
^{32}Si	$\sim 7.0 \times 10^2$
^{39}Ar	2.70×10^2
^{3}H	12.3
^{22}Na	2.6
^{35}S	88 days
^{7}Be	53
^{37}Ar	35
^{33}P	25
^{32}P	14.3
^{28}Mg	21.3 hours
^{24}Na	15.0
^{38}S	2.9
^{31}Si	2.62
^{39}Cl	55 min
^{38}Cl	37
^{34m}Cl	32

and by using instead the resolution of the phosphorus beta decay curve into two components (14.3 day phosphorus-32 and 25 day phosphorus-33) to distinguish between the contributions of the two radioisotopes. Unfortunately, by the time the samples reached the laboratory and were processed only low levels of phosphorus activity remained, and this limited the accuracy of the measurements.

The beryllium-7 analysis utilizes gamma spectrometric measurement of the 0.48 Mev gamma ray, and inspection of the gamma spectrum for each sample assures its radiochemical purity. Nevertheless, it was decided that additional evidence for the purity of the samples should be obtained, since the samples which appeared to contain excess beryllium-7 were those which also contained high activities of short-lived fission products. To provide such evidence the decay of a series of samples collected during late 1962 and early 1963 was monitored. Data for four such samples are shown in Figure 109. Decay curves for the 53 day half life of beryllium-7 are drawn through them. The fit of the curves to the data is adequate even though the accuracy of the measurements was reduced by the delay of several months between the collection of the samples and their analysis. In addition, relatively small aliquots of the samples were used in the analyses because they contained high activities of fission products. The beryllium-7 and phosphorus-32 data are probably the most reliable of all of the activities of cosmic ray products measured. Nevertheless, some of the results for these nuclides appear to be too high or too low compared to the concentration range expected in the stratosphere.

The mean distribution of beryllium-7 in the STARDUST (or HASP) sampling corridor (see p.18 of Final Report on Project STARDUST, Volume 1 for description of the corridor) has been calculated for each of a series of time intervals from October 1959 to March 1963. These distributions are shown in Figures 110, 111 and 112.

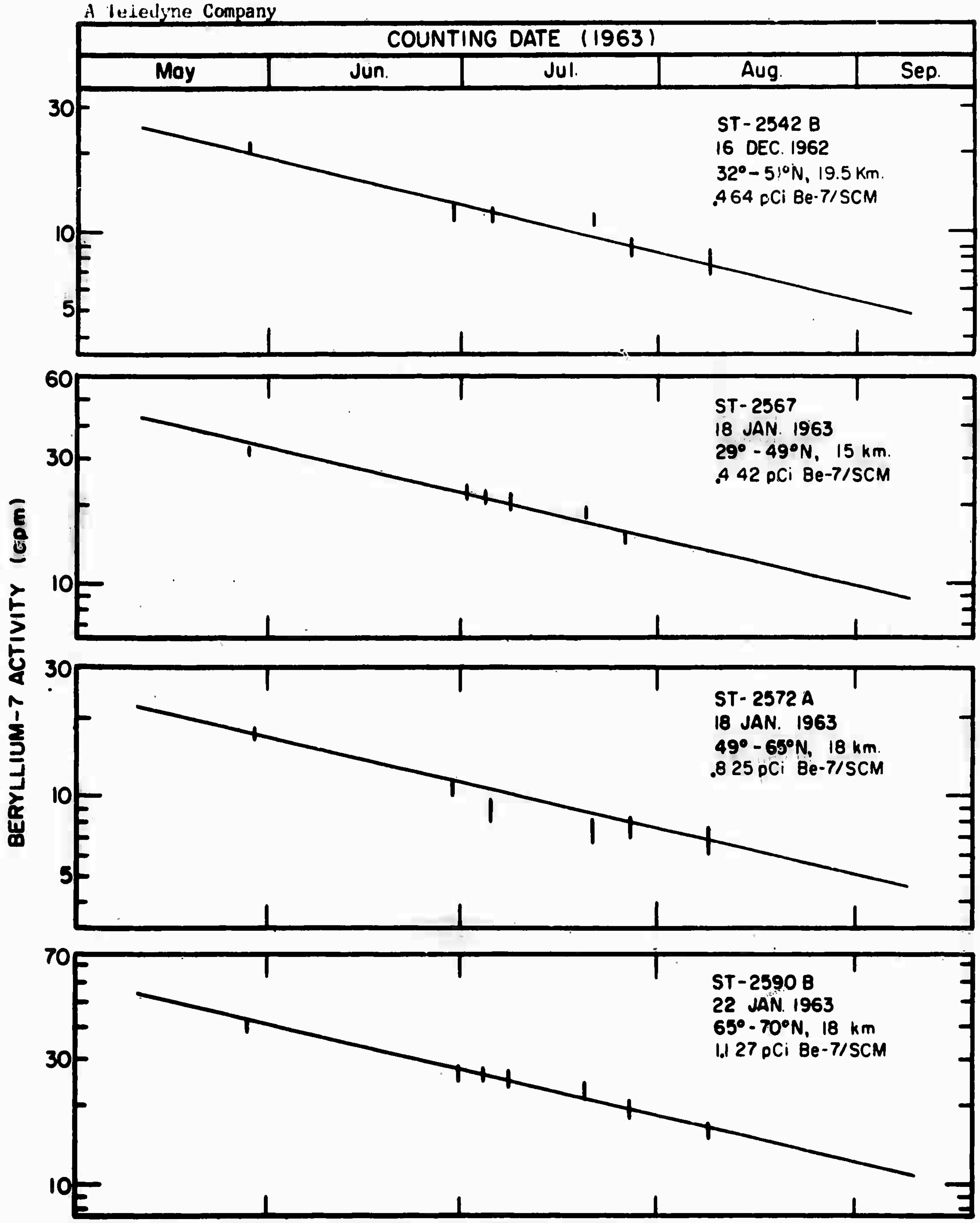

FIGURE 109 · DECAY CURVES OF FOUR HIGH ACTIVITY BERYLLIUM-7 SAMPLES

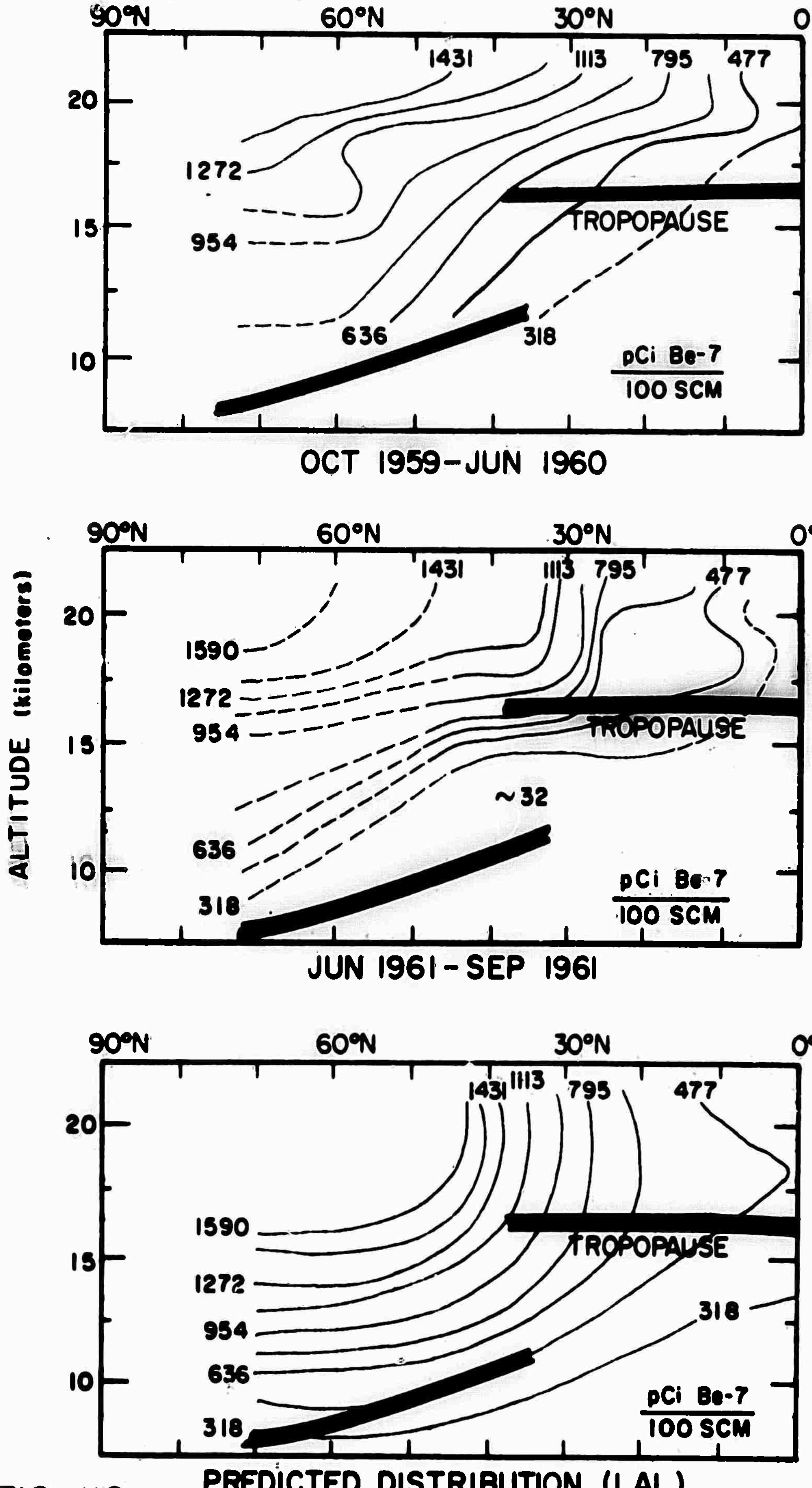

FIG. 110.
STRATOSPHERIC DISTRIBUTION OF BERYLLIUM-7

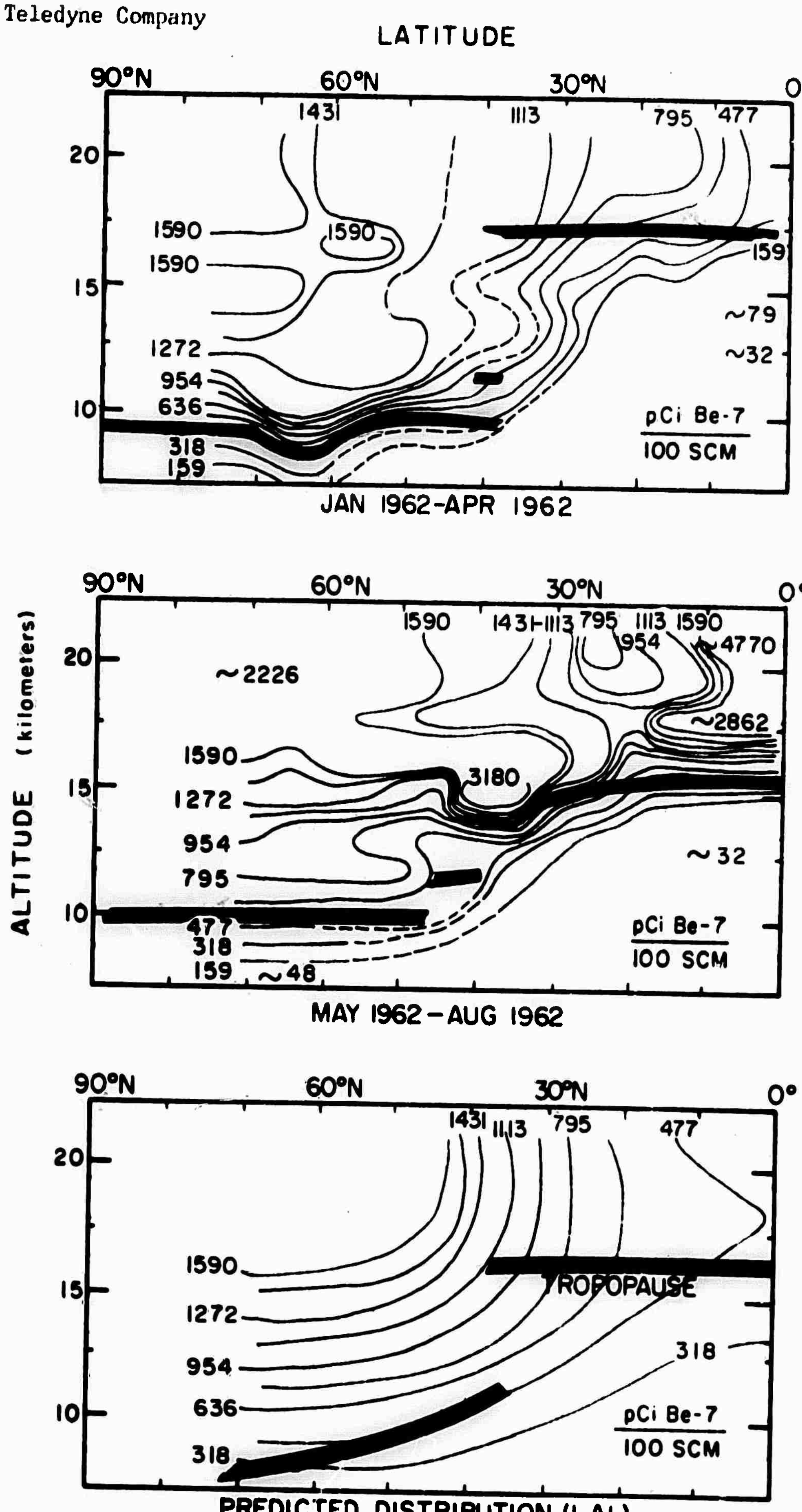

FIG. III.
STRATOSPHERIC DISTRIBUTION OF BERYLLIUM-7

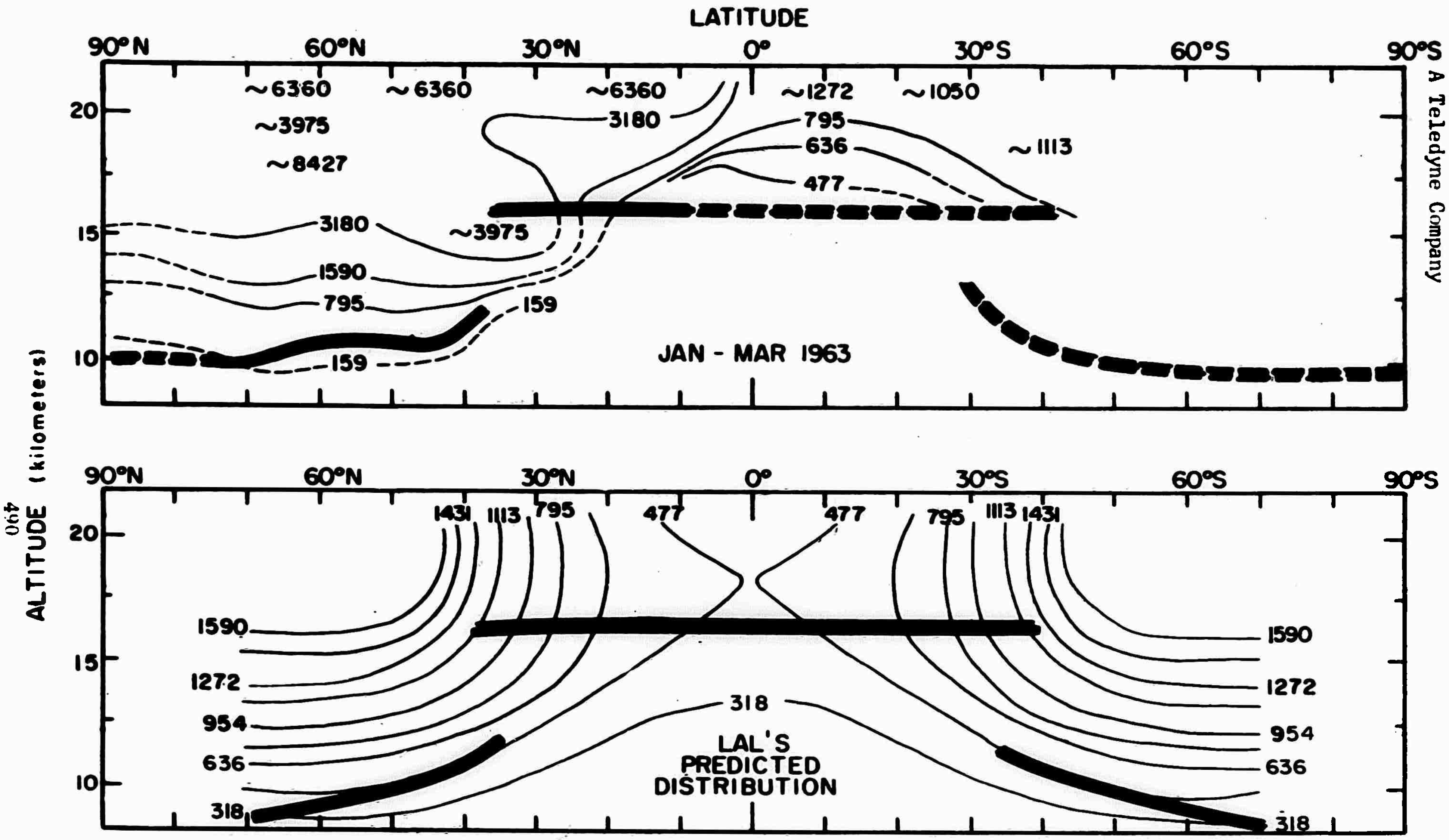

FIGURE 112 STRATOSPHERIC DISTRIBUTION OF BERYLLIUM - 7 (pCi/100 SCM)

A theoretical distribution in a quiescent atmosphere, based on beryllium-7 production rates calculated by Lal and Peters[61] is included in each of these figures for purposes of comparison.

The mean distributions shown in Figure 110 are for October 1959 to June 1960 and June to September 1961 and the data in tabular form are given in Tables 113 and 114. The concentrations found in the vicinity of the tropopause and of the tropopause gap were generally lower than predicted for a quiescent atmosphere. This was expected, of course, for the tropopause acts as a sink for beryllium-7 just as it does for debris from nuclear weapons tests. The concentrations found in the polar stratosphere were lower than the theoretical, but those found in the tropical stratosphere were slightly higher than the theoretical. This situation could results from eddy diffusion in the meridional direction.

In Figure 111 are shown the mean distributions for January to April 1962 and May to August 1962. The data for the same time interval are given in Table 115. During the first of these intervals rather high concentrations of beryllium-7 were found in the northern polar stratosphere. Bleichrodt[65] has described the presence of artificial beryllium-7, produced by the 1961 Soviet test series, at 13 Km in the stratosphere from October to November 1961. The high concentrations of beryllium-7 in the STARDUST sampling corridor during the first third of 1962 are consistent with Bleichrodt's conclusion that beryllium-7 is produced by atmospheric nuclear explosions. Even stronger evidence for such artificial production of this nuclide is found in the very high concentrations of the tropical stratosphere during the interval May to August 1962. These high concentrations of beryllium-7 were associated with fresh debris from the mid-1962 United States weapons tests at Christmas Island.

TABLE 113. Beryllium-7 Activities for Samples Collected from October 1959 through June 1960

Sample No.	Collection Date	Latitude	Altitude (km)	pCi Be^7 / 100 SCM
0-1	27 Oct 59	70°N-50°N	18.3	1160
0-2	27 Oct 59	70°N-50°N	19.8	1370
0-3	28 Oct 59	70°N-66°N	21.3	1160
D1	1 Dec 59	71°N-61°N	16.8	1030
D2	1 Dec 59	71°N-56°N	18.3	1570
D3	1 Dec 59	71°N-61°N	19.8	989
D4	1 Dec 59	09°N-08°S	19.8	507
D5	1 Dec 59	03°N-08°S	19.8	657
D6	3 Dec 59	68°N-50°N	13.7	949
D7	8 Dec 59	48°N-28°N	16.8	1100
D8	10 Dec 59	50°N-28°N	19.8	1510
D9	15 Dec 59	68°N-50°N	13.7	714
D10	17 Dec 59	70°N-50°N	15.2	1220
D11	17 Dec 59	71°N-68°N	18.3	1320
D12	18 Dec 59	48°N-33°N	16.8	731
D13	22 Dec 59	20°N-13°N	21.3	781
D14	23 Dec 59	50°N-39°N	19.8	1160
J1	5 Jan 60	47°N-28°N	19.8	1110
J4	7 Jan 60	66°N-58°N	12.2	928
J3	7 Jan 60	58°N-50°N	12.2	733
J5	7 Jan 60	44°N-31°N	12.2	617
J2	7 Jan 60	48°N-28°N	16.8	510
J9	12 Jan 60	66°N-50°N	16.8	981
J10	12 Jan 60	70°N-60°N	18.3	1200
J11	12 Jan 60	70°N-58°N	19.8	1850
J6	12 Jan 60	15°N-08°S	19.8	485
J7	12 Jan 60	15°N-02°S	21.3	501
J8	12 Jan 60	03°N-08°S	21.3	424
J12	14 Jan 60	15°N-08°S	21.3	447
J13	15 Jan 60	48°N	19.8	1260
J14	19 Jan 60	67°N-50°N	12.2	663
J15	19 Jan 60	59°N-38°N	12.2	808
J16	19 Jan 60	48°N-38°N	15.2	916
J17	19 Jan 60	48°N-28°N	16.8	774
J21	21 Jan 60	49°N-28°N	21.3	2080
J18	22 Jan 60	65°N-58°N	16.8	1140
J19	22 Jan 60	70°N-56°N	18.3	1020
J20	22 Jan 60	70°N-58°N	19.8	1580
J22	26 Jan 60	49°N-39°N	18.3	1220
J23	26 Jan 60	49°N-28°N	19.8	1210
J24	26 Jan 60	20°N-13°N	18.3	434
J25	29 Jan 60	44°N-28°N	12.2	335
J26	29 Jan 60	48°N-28°N	16.8	736
F1	2 Feb 60	48°N-38°N	19.8	862
F2	2 Feb 60	44°N-28°N	19.8	906
F3	2 Feb 60	28°N-17°N	19.8	870
F4	4 Feb 60	50°N-32°N	19.8	870

ISOTOPES
A Teledyne Company
Table 113 (cont'd.)

Sample No.	Collection Date	Latitude	Altitude (km)	pCi Be^7 / 100 SCM
F5	11 Feb 60	50°N-28°N	19.8	1330
F6	11 Feb 60	20°N-13°N	19.8	832
F8	16 Feb 60	65°N-50°N	13.7	970
F9	16 Feb 60	71°N-50°N	19.8	1410
F7	16 Feb 60	15°N-08°S	21.3	432
F11	18 Feb 60	67°N-59°N	12.2	964
F10	18 Feb 60	59°N-50°N	12.2	998
F13	23 Feb 60	48°N	21.3	1570
F15	25 Feb 60	68°N-60°N	13.7	1080
F14	25 Feb 60	60°N-50°N	13.7	1300
F16	25 Feb 60	47°N-28°N	19.8	1310
F17	25 Feb 60	28°N-14°N	19.8	658
M2	1 Mar 60	67°N-59°N	12.2	898
M1	1 Mar 60	59°N-50°N	12.2	1000
M3	3 Mar 60	71°N-61°N	16.8	979
M4	4 Mar 60	50°N-39°N	19.8	995
M5	4 Mar 60	24°N-13°N	19.8	428
M7	10 Mar 60	44°N-36°N	12.2	518
M8	10 Mar 60	48°N-38°N	15.2	816
M9	10 Mar 60	48°N-38°N	16.8	798
M6	10 Mar 60	36°N-28°N	12.2	483
M10	11 Mar 60	67°N-50°N	12.2	838
M11	11 Mar 60	67°N-50°N	15.2	1260
M12	22 Mar 60	67°N-50°N	12.2	660
M13	22 Mar 60	67°N-50°N	15.2	793
M16	22 Mar 60	48°N-28°N	16.8	465
M14	24 Mar 60	65°N-50°N	19.8	1190
M15	24 Mar 60	62°N-50°N	19.8	1240
M17	24 Mar 60	50°N-39°N	19.8	1140
M18	24 Mar 60	44°N-28°N	21.3	1220
M19	29 Mar 60	50°N-39°N	18.3	941
M20	29 Mar 60	50°N-28°N	19.8	672
M21	29 Mar 60	24°N-13°N	19.8	851
M22	31 Mar 60	48°N-30°N	15.2	552
M23	31 Mar 60	48°N-35°N	16.8	563
A1	5 Apr 60	71°N-61°N	16.8	965
A2	5 Apr 60	71°N-50°N	18.3	1260
A3	5 Apr 60	15°N-08°S	19.8	429
A4	5 Apr 60	15°N-08°S	21.3	399
A8	7 Apr 60	68°N-59°N	13.7	466
A7	7 Apr 60	59°N-50°N	13.7	687
A5	7 Apr 60	16°N-05°S	19.8	324
A6	7 Apr 60	15°N-08°S	21.3	442
A10	12 Apr 60	67°N-59°N	12.2	634
A9	12 Apr 60	59°N-50°N	12.2	609
A11	12 Apr 60	50°N-32°N	12.2	307
A12	12 Apr 60	48°N-33°N	16.8	254
A13	14 Apr 60	50°N-28°N	19.8	1100
A14	14 Apr 60	28°N-13°N	19.8	700
A15	19 Apr 60	50°N-28°N	19.8	1040
A16	20 Apr 60	68°N-50°N	13.7	812
A17	20 Apr 60	71°N-62°N	18.3	998
A18	20 Apr 60	71°N-50°N	19.8	1020

ISOTOPES
A Teledyne Company

Table 113 (cont'd.)

Sample No.	Collection Date	Latitude	Altitude (km)	pCi Be^7 100 SCM
A20	21 Apr 60	47°N-38°N	15.2	766
A21	21 Apr 60	48°N-33°N	16.8	523
A19	21 Apr 60	44°N-28°N	12.2	116
A22	26 Apr 60	50°N-28°N	21.3	1100
A23	26 Apr 60	28°N-16°N	21.3	1010
A25	27 Apr 60	71°N-62°N	16.8	1840
A26	27 Apr 60	71°N-50°N	18.3	976
A24	28 Apr 60	28°N-13°N	19.8	1000
A27	30 Apr 60	66°N-50°N	18.3	486
A28	30 Apr 60	66°N-50°N	19.8	1880
A29	3 May 60	64°N-50°N	12.2	630
A30	3 May 60	50°N-32°N	12.2	674
A31	5 May 60	15°N-08°S	21.3	393
A32	6 May 60	48°N	19.8	1360
A33	9 May 60	15°N-07°S	21.3	391
EN-1	10 May 60	70°N-65°N	15.2	812
EN-2	10 May 60	70°N-65°N	18.3	1110
EN-3	10 May 60	71°N-66°N	19.8	1220
EN-4	11 May 60	70°N-67°N	19.8	1500
ES-1	12 May 60	16°N-05°N	19.8	638
ES-2	12 May 60	05°N-06°S	19.8	405
ES-3	12 May 60	08°S-19°S	21.3	393
ES-4	12 May 60	18°S-30°S	21.3	409
EN-5	13 May 60	70°N-66°N	15.2	836
EN-6	13 May 60	70°N-66°N	18.3	1310
EN-7	13 May 60	70°N-66°N	19.8	1610
EN-8	14 May 60	70°N-66°N	18.3	1150
EN-9	17 May 60	70°N-66°N	15.2	618
EN-10	17 May 60	70°N-66°N	18.3	1680
EN-11	17 May 60	70°N-66°N	18.3	1590
ES-7	19 May 60	37°S-40°S	15.2	830
ES-6	19 May 60	36°S-40°S	18.3	983
ES-5	19 May 60	37°S-40°S	19.8	1010
EN-13	20 May 60	70°N-66°N	15.2	754
EN-12	20 May 60	70°N-66°N	18.3	1190
EN-14	20 May 60	70°N-66°N	18.3	1590
3913	23 May 60	40°S	18.3	857
3911	23 May 60	40°S	19.8	1340
EN-15	24 May 60	70°N-66°N	15.2	851
EN-17	24 May 60	70°N-66°N	19.8	1590
3934	31 May 60	40°S	18.3	719
3930	31 May 60	40°S	19.8	1130
ES-12	6 Jun 60	42°S-58°S	21.3	1100
ES-16	8 Jun 60	11°N-01°N	21.3	246
ES-15	8 Jun 60	01°N-11°S	21.3	351
ES-13	8 Jun 60	22°S-31°S	19.8	882
ES-14	8 Jun 60	11°S-22°S	19.8	550
3960	10 Jun 60	29°N-20°N	16.8	439
3962	10 Jun 60	29°N-20°N	18.3	386
3964	10 Jun 60	29°N-20°N	19.8	873

TABLE 114. Beryllium-7 Activities for Samples Collected from June 1961 Through September 1961

Sample No.	Collection Date	Latitude	Altitude (km)	pCi Be^7 100 SCM
ST-701	6 Jun 61	12°N	18.3	690
ST-702	6 Jun 61	12°N	19.8	407
ST-703	8 Jun 61	20°N-12°N	15.2	118
ST-704	8 Jun 61	20°N-12°N	19.8	396
ST-705	13 Jun 61	12°N	15.2	11.5
ST-706	13 Jun 61	20°N-12°N	15.2	572
ST-707	13 Jun 61	12°N-07°N	20.1	364
ST-708	15 Jun 61	12°N	18.3	382
ST-709	15 Jun 61	12°N	19.6	478
ST-710	20 Jun 61	12°N	18.3	471
ST-711	20 Jun 61	12°N	20.0	348
ST-712	6 Jul 61	48°N-29°N	19.7	1740
ST-713	6 Jul 61	48°N-29°N	20.7	1240
ST-714	7 Jul 61	48°N-29°N	18.3	1100
ST-715	11 Jul 61	28°N-15°N	20.2	412
ST-716	11 Jul 61	28°N-15°N	20.7	814
ST-717	14 Jul 61	30°N	16.8	622
ST-718	14 Jul 61	30°N	18.2	734
ST-719	14 Jul 61	30°N	19.8	808
ST-720	14 Jul 61	30°N	20.9	992
ST-721	19 Jul 61	30°N	16.9	(986)
ST-722	19 Jul 61	30°N	18.4	1540
ST-723	19 Jul 61	30°N	20.0	932
ST-724	19 Jul 61	30°N	21.1	812
ST-736	20 Jul 61	48°N-38°N	15.4	653
ST-727	20 Jul 61	48°N-28°N	16.8	876
ST-728	25 Jul 61	48°N-28°N	19.8	1420
ST-729	25 Jul 61	48°N-30°N	20.7	1490
ST-730	28 Jul 61	28°N-15°N	19.9	714
ST-731	28 Jul 61	28°N-15°N	20.7	695
ST-732	2 Aug 61	48°N-28°N	18.5	1170
ST-733	2 Aug 61	48°N-28°N	20.0	448
ST-734	4 Aug 61	30°N	16.8	747
ST-736	4 Aug 61	30°N	19.8	1000
ST-737	4 Aug 61	30°N	21.1	823
ST-738	7 Aug 61	30°N	16.8	677
ST-739	7 Aug 61	30°N	18.4	762
ST-740	7 Aug 61	30°N	20.0	1000
ST-741	7 Aug 61	30°N	21.1	979
ST-742	10 Aug 61	48°N-28°N	15.2	445
ST-743	10 Aug 61	48°N-28°N	16.9	882
ST-744	15 Aug 61	48°N-28°N	19.8	1590
ST-745	15 Aug 61	48°N-28°N	20.6	1360
ST-746	17 Aug 61	28°N-15°N	20.0	714
ST-747	17 Aug 61	28°N-15°N	20.9	688
ST-748	22 Aug 61	48°N-28°N	18.4	1350
ST-749	22 Aug 61	48°N-28°N	20.0	1200
ST-750	24 Aug 61	30°N	16.7	846
ST-751	24 Aug 61	30°N	18.2	603
ST-752	24 Aug 61	30°N	19.8	855
ST-753	24 Aug 61	30°N	21.0	1090

TABLE 114 (cont'd.)

Sample No.	Collection Date	Latitude	Altitude (km)	pCi Be^7 / 100 SCM
ST-754	31 Aug 61	48°N-28°N	15.7	280
ST-755	31 Aug 61	48°N-38°N	17.0	986
ST-756	1 Sep 61	30°N	16.9	576
ST-757	1 Sep 61	30°N	18.4	1050
ST-758	1 Sep 61	30°N	19.9	1070
ST-759	1 Sep 61	30°N	21.2	857
ST-761	6 Sep 61	63°N-51°N	19.5	1540
ST-760	6 Sep 61	51°N-32°N	19.4	1260
ST-762	6 Sep 61	28°N-15°N	18.5	528
ST-763	6 Sep 61	28°N-15°N	19.6	522
ST-777	7 Sep 61	48°N-28°N	20.2	1530
ST-778	7 Sep 61	48°N-28°N	21.0	1320
ST-779	8 Sep 61	48°N-28°N	18.3	1170
ST-780	8 Sep 61	48°N-33°N	19.8	1260
ST-781	9 Sep 61	48°N-28°N	15.3	270
ST-782	9 Sep 61	48°N-28°N	16.9	661
ST-783	10 Sep 61	42°N-29°N	12.2	18.6
ST-784	10 Sep 61	42°N-29°N	13.7	43.1
ST-785	20 Sep 61	30°N	16.7	657
ST-786	20 Sep 61	30°N	18.2	514
ST-787	20 Sep 61	30°N	19.8	380
ST-788	20 Sep 61	30°N	20.8	827
ST-789	26 Sep 61	28°N-15°N	19.7	558
ST-790	26 Sep 61	28°N-15°N	19.7	407
ST-791	28 Sep 61	48°N-28°N	20.3	1500
ST-792	28 Sep 61	48°N-28°N	20.7	1370
ST-793	30 Sep 61	60°N-47°N	19.8	1960
ST-795	30 Sep 61	60°N-36°N	20.1	2100
ST-794	30 Sep 61	47°N-30°N	20.7	1410

TABLE 115. Beryllium-7 Activities for Samples Collected from January 1962 Through August 1962

Sample No.	Collection Date	Latitude	Altitude (km)	pCi Be^7 100 SCM
ST-881	4 Jan 62	48°N-28°N	15.2	803
ST-882	11 Jan 62	30°N	16.8	723
ST-883	11 Jan 62	30°N	18.3	1690
ST-884	11 Jan 62	30°N	19.8	1080
ST-885	11 Jan 62	30°N	21.5	914
ST-886	11 Jan 62	48°N-28°N	20.2	1050
ST-887	11 Jan 62	48°N-28°N	20.8	1240
SZ-2241	15 Jan 62	54°N-31°N	16.8	1460
ST-889	15 Jan 62	54°N-49°N	16.8	1650
ST-888	15 Jan 62	49°N-31°N	16.8	1350
ST-891	15 Jan 62	63°N-48°N	20.7	1150
ST-890	15 Jan 62	48°N-32°N	20.0	1250
ST-893	16 Jan 62	49°N-31°N	12.6	938
ST-892	16 Jan 62	49°N-32°N	18.4	1390
ST-894	17 Jan 62	65°N-64°N	12.3	1050
ST-895	17 Jan 62	65°N-63°N	13.7	2060
ST-896	17 Jan 62	65°N-63°N	15.4	1580
ST-897	17 Jan 62	65°N	16.8	1240
ST-898	17 Jan 62	64°N	16.8	1370
ST-899	17 Jan 62	64°N	18.3	1650
ST-900	17 Jan 62	64°N	19.8	1270
ST-901	17 Jan 62	64°N	20.9	782
ST-902	18 Jan 62	30°N-15°N	16.8	234
ST-904	18 Jan 62	30°N-15°N	18.4	607
ST-903	18 Jan 62	30°N-15°N	19.8	754
ST-905	18 Jan 62	30°N-15°N	20.9	884
ST-906	19 Jan 62	64°N-49°N	13.6	2820
ST-908	19 Jan 62	64°N-52°N	16.8	2570
ST-907	19 Jan 62	64°N-49°N	19.8	1640
ST-909	23 Jan 62	64°N-53°N	12.2	1410
SZ-2242	23 Jan 62	64°N-53°N	12.2	1350
ST-910	23 Jan 62	64°N-49°N	15.2	1140
ST-911	23 Jan 62	64°N-49°N	18.3	1340
ST-912	23 Jan 62	64°N-49°N	20.4	1070
SZ-2243	23 Jan 62	64°N-49°N	20.4	987
ST-913	23 Jan 62	49°N-36°N	13.7	1370
ST-914	23 Jan 62	49°N-36°N	15.5	1600
ST-915	23 Jan 62	49°N-32°N	19.8	1180
ST-916	23 Jan 62	49°N-31°N	19.9	1310
ST-917	25 Jan 62	70°N-65°N	12.1	1870
ST-918	25 Jan 62	70°N-65°N	13.8	3060
ST-919	25 Jan 62	70°N-65°N	15.3	5310
SZ-2244	25 Jan 62	68°N	16.0	3820
ST-920	25 Jan 62	70°N-65°N	16.8	1880
ST-921	25 Jan 62	70°N-65°N	18.3	2960
ST-922	25 Jan 62	70°N-65°N	19.8	4770
ST-923	25 Jan 62	70°N-65°N	20.3	2320
ST-924	25 Jan 62	70°N-65°N	20.7	2660
ST-925	25 Jan 62	30°N	12.5	≤ 2.35
ST-926	25 Jan 62	30°N	13.7	131
ST-927	25 Jan 62	30°N	15.5	285

ISOTOPES, A Teledyne Company

TABLE 115 (cont'd.)

Sample No.	Collection Date	Latitude	Altitude (km)	pCi Be^7 100 SCM
ST-928	25 Jan 62	30°N	16.8	523
ST-929	25 Jan 62	30°N	18.4	1080
ST-930	25 Jan 62	30°N	19.8	1300
ST-931	25 Jan 62	30°N	21.1	700
ST-933	30 Jan 62	64°N-54°N	12.3	1270
ST-934	30 Jan 62	64°N-49°N	15.2	1000
ST-935	30 Jan 62	64°N-49°N	18.3	1060
ST-936	30 Jan 62	64°N-49°N	20.0	936
ST-937	30 Jan 62	49°N-36°N	12.5	90.3
ST-938	30 Jan 62	49°N-31°N	15.6	909
ST-939	30 Jan 62	49°N-31°N	18.4	1780
ST-940	30 Jan 62	49°N-31°N	20.8	1750
ST-941	1 Feb 62	30°N-15°N	16.8	1790
ST-942	1 Feb 62	30°N-18°N	18.4	1120
ST-943	1 Feb 62	30°N-15°N	20.9	817
ST-944	5 Feb 62	30°N-18°N	20.0	987
ST-945	5 Feb 62	30°N-19°N	20.7	720
ST-946	6 Feb 62	63°N	13.7	281
ST-947	6 Feb 62	64°N-49°N	16.8	965
ST-948	6 Feb 62	64°N-49°N	19.8	1020
ST-949	6 Feb 62	49°N-31°N	13.8	539
ST-950	6 Feb 62	49°N-31°N	16.8	1200
ST-951	6 Feb 62	49°N-31°N	19.9	978
ST-952	6 Feb 62	49°N-31°N	20.7	776
ST-957	8 Feb 62	65°N-64°N	12.1	1710
ST-958	8 Feb 62	65°N-63°N	13.6	590
ST-959	8 Feb 62	65°N-63°N	15.2	585
ST-960	8 Feb 62	64°N	16.6	921
ST-961	8 Feb 62	66°N	18.2	3360
ST-962	8 Feb 62	66°N-65°N	19.4	943
ST-963	8 Feb 62	65°N	19.9	992
ST-953	8 Feb 62	30°N	16.8	267
ST-954	8 Feb 62	30°N	18.3	1140
ST-955	8 Feb 62	30°N	19.8	722
ST-956	8 Feb 62	30°N	20.8	2090
ST-969	9 Feb 62	64°N-49°N	13.6	372
ST-970	9 Feb 62	64°N-49°N	19.7	1070
ST-966	9 Feb 62	30°N	13.0	100
ST-967	9 Feb 62	30°N	15.7	176
ST-968	9 Feb 62	30°N	16.9	343
SR-971	13 Feb 62	64°N-50°N	12.1	1940
SZ-2245	13 Feb 62	64°N-50°N	12.1	1790
ST-973	13 Feb 62	64°N-50°N	18.1	1310
ST-972	13 Feb 62	64°N-50°N	15.2	1250
ST-974	13 Feb 62	64°N-50°N	19.4	1130
ST-975	13 Feb 62	44°N-36°N	12.5	382
ST-976	13 Feb 62	49°N-32°N	15.2	483
ST-977	13 Feb 62	49°N-32°N	18.4	200
ST-978	13 Feb 62	49°N-31°N	20.7	1060
SR-979	15 Feb 62	70°N-65°N	12.2	709
ST-980	15 Feb 62	70°N-65°N	13.7	873
SR-981	15 Feb 62	70°N-65°N	15.2	859
ST-982	15 Feb 62	70°N-65°N	16.7	1280

TABLE 115. (cont'd.)

Sample No.	Collection Date	Latitude	Altitude (km)	pCi Be^7 100 SCM
SZ-2246	15 Feb 62	70°N-65°N	16.7	1300
SR-983	15 Feb 62	70°N-65°N	18.3	1100
SR-984	15 Feb 62	70°N-65°N	19.6	1020
SR-985	15 Feb 62	30°N-15°N	16.8	172
SR-986	15 Feb 62	30°N-15°N	18.5	672
ST-987	15 Feb 62	30°N-15°N	19.8	1220
ST-988	15 Feb 62	30°N-15°N	20.9	1210
ST-989	19 Feb 62	49°N-36°N	13.8	866
ST-990	19 Feb 62	49°N-32°N	16.8	1150
ST-991	19 Feb 62	49°N-32°N	20.0	1250
ST-992	19 Feb 62	49°N-32°N	20.6	1040
SF-993	20 Feb 62	64°N-49°N	13.6	1370
ST-994	20 Feb 62	64°N-49°N	16.7	1140
ST-995	20 Feb 62	64°N-49°N	19.8	1200
ST-996	20 Feb 62	64°N-49°N	19.9	1360
ST-1005	21 Feb 62	30°N	12.6	73.1
ST-1006	21 Feb 62	30°N	13.8	111
ST-1007	21 Feb 62	30°N	15.4	455
ST-1008	21 Feb 62	30°N	16.8	555
SF-1009	21 Feb 62	30°N	18.3	1070
ST-1010	21 Feb 62	30°N	19.8	1050
ST-1011	21 Feb 62	30°N	20.8	1030
SF-997	22 Feb 62	64°N	12.0	1220
ST-998	22 Feb 62	64°N-63°N	13.6	1320
SF-999	22 Feb 62	64°N	15.1	1200
SZ-2247	22 Feb 62	64°N	15.6	1510
SF-1000	22 Feb 62	64°N	16.6	2810
SF-1001	22 Feb 62	67°N-64°N	16.8	1110
ST-1002	22 Feb 62	66°N-65°N	18.2	1180
SF-1003	22 Feb 62	66°N-62°N	19.6	1150
ST-1004	22 Feb 62	64°N-63°N	20.3	979
ST-1012	27 Feb 62	64°N-49°N	12.0	1930
SF-1013	27 Feb 62	64°N-49°N	15.1	2280
ST-1014	27 Feb 62	64°N-49°N	18.2	1970
ST-1016	27 Feb 62	49°N-31°N	15.2	1890
ST-1017	27 Feb 62	37°N-31°N	18.3	1160
ST-1018	27 Feb 62	49°N-31°N	20.6	1000
ST-1019	1 Mar 62	70°N-65°N	12.0	636
ST-1020	1 Mar 62	70°N-65°N	13.6	773
ST-1022	1 Mar 62	70°N-65°N	16.7	1170
ST-1023	1 Mar 62	70°N-65°N	18.2	1300
ST-1024	1 Mar 62	70°N-65°N	19.8	1060
ST-1025	1 Mar 62	70°N-65°N	20.6	1120
ST-1026	1 Mar 62	30°N-18°N	16.8	340
ST-1027	1 Mar 62	30°N-15°N	18.3	469
ST-1028	1 Mar 62	26°N-15°N	19.8	1010
ST-1029	1 Mar 62	26°N-15°N	21.0	1050
ST-1031	2 Mar 62	40°N-31°N	12.2	418
ST-1032	2 Mar 62	50°N-31°N	18.3	1360
ST-1033	6 Mar 62	64°N-63°N	6.1	180
ST-1035	6 Mar 62	64°N-63°N	9.1	827
ST-1037	6 Mar 62	64°N-49°N	13.6	803
SF-1038	6 Mar 62	64°N-49°N	16.7	2020

ISOTOPES, A Teledyne Company
TABLE 115 (cont'd.)

Sample No.	Collection Date	Latitude	Altitude (km)	pCi Be^7 100 SCM
ST-1039	6 Mar 62	64°N-49°N	19.9	1210
ST-1040	6 Mar 62	49°N-31°N	13.7	2810
ST-1041	6 Mar 62	49°N-31°N	16.8	808
SF-1042	6 Mar 62	49°N-40°N	20.0	3050
ST-1044	6 Mar 62	49°N-31°N	20.9	1240
SN-1043	6 Mar 62	40°N-31°N	20.0	1360
SF-1045	8 Mar 62	65°N-64°N	12.1	1820
SN-1046	8 Mar 62	65°N-63°N	13.6	889
SNR-1047	8 Mar 62	65°N-63°N	15.1	693
SN-1048	8 Mar 62	64°N	16.7	1170
SNR-1049	8 Mar 62	64°N	18.2	1420
SN-1050	8 Mar 62	66°N-65°N	19.8	1260
SNR-1051	8 Mar 62	65°N	20.5	1170
SN-1052	8 Mar 62	30°N	12.6	56.6
SN-1053	8 Mar 62	30°N	13.7	119
SN-1054	8 Mar 62	30°N	15.2	150
SN-1056	8 Mar 62	30°N	16.8	650
SN-1057	8 Mar 62	30°N	18.3	1810
SN-1058	8 Mar 62	30°N	19.8	1320
SN-1059	8 Mar 62	30°N	21.1	1340
ST-1125	9/10 Mar 62	18°N-00°	19.4	727
ST-1126	9/10 Mar 62	00°-18°S	20.0	509
ST-1127	11/12 Mar 62	20°S-26°S	19.8	552
ST-1128	11/12 Mar 62	26°S-38°S	19.8	1050
ST-1064	13 Mar 62	64°N-63°N	6.1	229
SF-1065	13 Mar 62	64°N-61°N	7.6	623
ST-1066	13 Mar 62	64°N-63°N	9.1	965
SF-1067	13 Mar 63	64°N-63°N	10.7	1780
SN-1068	13 Mar 63	64°N-49°N	12.1	1180
ST-1069	13 Mar 63	64°N-49°N	15.1	1040
SN-1070	13 Mar 63	64°N-49°N	18.3	1230
SF-1072	13 Mar 63	64°N-58°N	19.9	1340
ST-1071	13 Mar 62	64°N-49°N	20.0	1080
SN-1073	13 Mar 62	49°N-31°N	12.4	1260
SF-1075	13 Mar 62	49°N-40°N	15.2	1130
SN-1074	13 Mar 62	40°N-31°N	15.2	717
ST-1076	13 Mar 62	49°N-31°N	18.5	1290
ST-1077	13 Mar 63	49°N-31°N	20.4	1160
SF-1081	14/15 Mar 62	90°N-80°N	11.9	2200
ST-1079	14/15 Mar 62	90°N-80°N	12.0	951
SF-1082	14/15 Mar 62	90°N-80°N	12.2	1150
ST-1078	14/15 Mar 62	80°N-60°N	11.0	992
ST-1080	14/15 Mar 62	80°N-60°N	12.0	976
SF-1083	14/15 Mar 62	80°N-60°N	12.0	1650
ST-1084	15 Mar 62	70°N-65°N	12.0	1280
ST-1085	15 Mar 62	70°N-65°N	13.6	1190
SF-1086	15 Mar 62	70°N-65°N	15.1	2200
ST-1087	15 Mar 62	70°N-65°N	16.6	1220
ST-1088	15 Mar 62	70°N-65°N	18.2	1460
ST-1089	15 Mar 62	70°N-65°N	19.8	1120
ST-1090	15 Mar 62	30°N-15°N	16.9	305
ST-1091	15 Mar 62	30°N-15°N	18.3	639
ST-1092	15 Mar 62	30°N-15°N	19.9	291
ST-1093	15 Mar 62	26°N-15°N	20.7	859

TABLE 115 (cont'd.)

Sample No.	Collection Date	Latitude	Altitude (km)	pCi Be^7 100 SCM
ST-1098	20 Mar 62	65°N-64°N	6.1	35.9
ST-1099	20 Mar 62	64°N	7.6	41.2
ST-1100	20 Mar 62	64°N-63°N	9.1	405
SF-1101	20 Mar 62	64°N-63°N	10.7	1350
ST-1102	20 Mar 62	49°N-31°N	13.7	626
ST-1103	20 Mar 62	49°N-31°N	16.8	1090
ST-1104	20 Mar 62	44°N-31°N	20.5	1240
ST-1105	20 Mar 62	40°S-61°S	19.8	1410
ST-1106	22 Mar 62	30°N	12.5	100
ST-1107	22 Mar 62	30°N	13.7	175
ST-1108	22 Mar 62	30°N	15.2	281
ST-1109	22 Mar 62	30°N	16.8	302
SF-1110	22 Mar 62	30°N	18.4	541
ST-1111	22 Mar 62	30°N	20.0	1210
ST-1112	22 Mar 62	30°N	21.3	1090
SF-1113	23 Mar 62	65°N-64°N	12.0	1310
ST-1114	23 Mar 62	65°N-63°N	13.6	1520
SF-1115	23 Mar 62	65°N-63°N	15.1	1810
ST-1117	23 Mar 62	66°N-64°N	16.6	1380
SF-1118	23 Mar 62	66°N-65°N	18.2	1800
ST-1119	23 Mar 62	66°N-63°N	19.7	1320
SF-1120	23 Mar 62	64°N-63°N	20.5	1600
ST-1121	27 Mar 62	65°N	6.1	25.4
ST-1122	27 Mar 62	64°N	7.6	60.4
SF-1123	27 Mar 62	65°N	9.1	604
SF-1124	27 Mar 62	65°N-64°N	10.7	1030
ST-1129	27 Mar 62	64°N-49°N	12.1	902
ST-1130	27 Mar 62	64°N-49°N	15.1	809
ST-1131	27 Mar 62	64°N-49°N	18.3	1300
ST-1132	27 Mar 62	49°N-44°N	12.2	1150
ST-1133	27 Mar 62	44°N-31°N	12.2	283
ST-1134	27 Mar 62	37°N-31°N	15.4	213
ST-1135	27 Mar 62	49°N-31°N	18.3	723
SF-1136	29 Mar 62	70°N-65°N	12.2	1280
ST-1137	29 Mar 62	70°N-65°N	13.7	1620
SF-1138	29 Mar 62	70°N-65°N	15.1	1910
ST-1139	29 Mar 62	70°N-65°N	16.7	1680
ST-1140	29 Mar 62	70°N-65°N	18.3	1970
ST-1141	29 Mar 62	70°N-65°N	18.3	1390
ST-1142	29 Mar 62	70°N-65°N	19.8	994
ST-1143	29 Mar 62	30°N	12.2	183
SF-1144	29 Mar 62	30°N	13.8	606
ST-1145	29 Mar 62	30°N	14.9	646
SF-1146	29 Mar 62	30°N	17.0	1260
ST-1147	29 Mar 62	30°N	18.5	653
ST-1148	29 Mar 62	30°N	19.7	928
ST-1149	30 Mar 62	49°N-31°N	15.3	779
ST-1150	30 Mar 62	49°N-31°N	20.5	1330
ST-1151	31 Mar 62	63°N-51°N	19.6	1020
ST-1152	31 Mar 62	51°N-32°N	20.0	1170
ST-1153	2 Apr 62	73°N-65°N	19.8	898
ST-1308	3 Apr 62	70°N	4.6	296
ST-1309	3 Apr 62	70°N	4.6	27.0
ST-1310	3 Apr 62	70°N	7.6	63.4

TABLE 115 (cont'd.)

Sample No.	Collection Date	Latitude	Altitude (km)	pCi Be^7 100 SCM
ST-1311	3 Apr 62	70°N	12.2	1130
ST-1312	3 Apr 62	73°N-70°N	15.2	1660
ST-1154	3 Apr 62	67°N-66°N	15.2	1490
ST-1313	3 Apr 62	73°N-70°N	18.3	1360
ST-1314	3 Apr 62	73°N-70°N	19.8	1250
ST-1315	3 Apr 62	36°N	4.6	49.4
ST-1316	3 Apr 62	36°N-35°N	7.6	24.8
ST-1317	3 Apr 62	36°N-35°N	12.2	211
ST-1318	3 Apr 62	32°N	15.2	644
ST-1319	3 Apr 62	32°N	18.3	1660
ST-1320	3 Apr 62	32°N	19.8	1410
ST-1155	4 Apr 62	64°N	6.1	6.2
ST-1157	4 Apr 62	65°N-64°N	9.1	42.0
ST-1158	4 Apr 62	64°N	10.7	545
ST-1159	4 Apr 62	09°N-08°S	12.5	22.6
ST-1160	4 Apr 62	09°N-00°	15.7	81.4
ST-1161	4 Apr 62	09°N-08°S	19.0	394
ST-1162	4 Apr 62	09°N-01°N	19.9	348
ST-1163	5 Apr 62	66°N	15.2	1590
ST-1164	9 Apr 62	15°N-09°N	12.3	18.6
ST-1166	9 Apr 62	15°N-09°N	15.2	83.5
ST-1167	9 Apr 62	15°N-09°N	16.8	183
ST-1168	9 Apr 62	15°N-09°N	18.3	366
ST-1169	9 Apr 62	15°N-09°N	19.8	475
ST-1170	9 Apr 62	15°N-09°N	21.3	636
ST-1180	9/10 Apr 62	40°S-50°S	19.8	1480
ST-1181	9/10 Apr 62	50°S-60°S	19.8	1520
ST-1171	10 Apr 62	69°N-66°N	19.6	1670
ST-1172	11 Apr 62	65°N-64°N	6.1	36.4
ST-1173	11 Apr 62	65°N	7.6	37.0
ST-1174	11 Apr 62	65°N-64°N	9.1	95.4
ST-1175	11 Apr 62	66°N-65°N	10.7	851
ST-1182	12 Apr 62	73°N-67°N	18.3	3290
ST-1183	13 Apr 62	09°N-10°S	13.7	50.1
ST-1184	13 Apr 62	09°N-10°S	17.0	111
ST-1185	13 Apr 62	09°N-10°S	20.0	367
ST-1195	14 Apr 62	19°S-35°S	19.8	1030
ST-1196	16 Apr 62	02°N-16°S	19.8	243
ST-1186	17 Apr 62	72°N-70°N	15.2	1910
ST-1187	18 Apr 62	65°N-60°N	6.1	47.2
ST-1188	18 Apr 62	65°N	7.6	131
ST-1189	18 Apr 62	65°N	9.1	353
ST-1190	18 Apr 62	65°N-64°N	10.7	728
ST-1197	18 Apr 62	09°N	12.2	21.8
ST-1199	18 Apr 62	07°N	15.2	59.6
ST-1200	18 Apr 62	09°N-07°N	16.8	159
ST-1205	19/20 Apr 62	90°N-80°N	12.1	672
ST-1207	19/20 Apr 62	90°N-80°N	12.1	690
ST-1204	19/20 Apr 62	80°N-60°N	11.2	744
ST-1208	19/20 Apr 62	80°N-60°N	12.5	1070
ST-1206	19/20 Apr 62	80°N-60°N	12.6	814
ST-1209	19 Apr 62	73°N-65°N	19.8	1400
ST-1210	19 Apr 62	63°N-50°N	19.7	951
ST-1211	19 Apr 62	50°N-32°N	20.7	1130

ISOTOPES, A Teledyne Company

TABLE 115 (cont'd.)

Sample No.	Collection Date	Latitude	Altitude (km)	pCi Be^7 100 SCM
ST-1212	24 Apr 62	65°N	6.1	45.0
ST-1214	24 Apr 62	65°N	9.1	520
ST-1217	24 Apr 62	09°N-04°S	16.8	78.9
ST-1218	24 Apr 62	09°N-04°S	21.3	297
ST-1215	25 Apr 62	65°N	10.7	1010
ST-1219	25 Apr 62	49°N-31°N	12.5	390
ST-1220	25 Apr 62	43°N-31°N	15.5	482
ST-1221	25 Apr 62	49°N-31°N	18.2	1080
ST-1222	26 Apr 62	49°N-31°N	15.5	741
ST-1223	26 Apr 62	49°N-31°N	19.8	1140
ST-1235	26 Apr 62	15°N-09°N	14.9	63.8
ST-1236	26 Apr 62	15°N-09°N	16.4	125
ST-1237	26 Apr 62	15°N-09°N	18.2	898
ST-1238	26 Apr 62	15°N-09°N	19.7	935
ST-1239	26 Apr 62	15°N-09°N	20.5	1040
ST-1240	26 Apr 62	15°N-09°N	20.9	809
ST-1241	26 Apr 62	09°N-02°N	16.9	235
ST-1244	26 Apr 62	09°N-03°N	21.0	488
ST-1242	26 Apr 62	02°N-10°S	16.9	151
ST-1243	26 Apr 62	02°N-10°S	20.6	444
ST-1224	27 Apr 62	64°N-60°N	12.2	1060
ST-1225	27 Apr 62	64°N-49°N	15.3	1190
ST-1226	27 Apr 62	64°N-49°N	19.9	1330
ST-1227	27 Apr 62	31°N	12.4	510
ST-1228	27 Apr 62	31°N	13.6	830
ST-1229	27 Apr 62	31°N	15.2	461
ST-1230	27 Apr 62	30°N	16.8	442
ST-1231	27 Apr 62	31°N	18.6	1210
ST-1232	27 Apr 62	31°N	19.8	1220
ST-1233	27 Apr 62	31°N	20.9	914
ST-1234	27 Apr 62	28°N-11°N	19.8	1110
ST-1245	1/2 May 62	65°N	6.1	20.2
ST-1246	1/2 May 62	65°N	7.6	42.6
ST-1247	1/2 May 62	65°N	9.1	509
ST-1248	1/2 May 62	65°N	10.7	881
ST-1253	1 May 62	49°N-31°N	13.7	738
ST-1254	1 May 62	49°N-31°N	17.0	1480
ST-1255	1 May 62	48°N-32°N	19.6	1180
ST-1256	1 May 62	48°N-37°N	20.3	1330
ST-1257	3 May 62	70°N-65°N	12.2	1200
ST-1258	3 May 62	70°N-65°N	13.7	1160
ST-1259	3 May 62	70°N-65°N	15.3	1280
ST-1260	3 May 62	70°N-65°N	16.8	1620
ST-1262	3 May 62	70°N-65°N	18.3	2040
ST-1261	3 May 62	70°N-65°N	18.5	2400
ST-1263	3 May 62	70°N-65°N	19.8	1410
ST-1264	3 May 62	70°N-65°N	20.3	1680
ST-1265	3 May 62	30°N-19°N	16.8	840
ST-1267	3 May 62	30°N-19°N	18.2	762
ST-1269	3 May 62	30°N-15°N	19.8	1100
ST-1270	3 May 62	30°N-15°N	20.4	1140
ST-1266	3 May 62	19°N-15°N	16.8	285
ST-1268	3 May 62	19°N-15°N	18.3	405

ISOTOPES, A Teledyne Company

TABLE 115 (cont'd.)

Sample No.	Collection Date	Latitude	Altitude (km)	pCi Be^7 100 SCM
ST-1271	4 May 62	64°N	12.2	851
ST-1272	4 May 62	64°N	13.7	661
ST-1273	4 May 62	64°N	15.2	917
ST-1274	4 May 62	64°N	16.8	1110
ST-1275	4 May 62	64°N	18.4	1850
ST-1276	4 May 62	64°N	19.9	733
ST-1277	4 May 62	64°N	20.5	784
ST-1278	5 May 62	64°N-49°N	12.3	1130
ST-1279	5 May 62	64°N-49°N	18.5	1350
ST-1280	8 May 62	68°N-65°N	6.1	8.87
ST-1281	8 May 62	66°N-65°N	7.6	62.8
ST-1282	8 May 62	67°N-65°N	9.1	52.6
ST-1283	8 May 62	66°N-65°N	10.7	477
ST-1284	8 May 62	64°N-49°N	12.3	957
ST-1285	8 May 62	64°N-49°N	15.2	1110
ST-1286	8 May 62	64°N-49°N	18.3	1750
ST-1287	8 May 62	64°N-49°N	20.3	1560
ST-1288	8 May 62	49°N-31°N	12.5	416
ST-1289	8 May 62	49°N-43°N	15.2	687
SF-645	8 May 62	43°N-38°N	15.2	19800
SF-644	8 May 62	37°N-31°N	15.5	9820
ST-1291	8 May 62	49°N-43°N	18.2	1020
ST-1290	8 May 62	43°N-37°N	18.2	1140
SF-646	8 May 62	37°N-31°N	18.2	1400
ST-1292	8 May 62	49°N-31°N	20.8	1440
ST-1293	10 May 62	64°N-62°N	12.2	1140
ST-1294	10 May 62	65°N-62°N	13.7	832
ST-1295	10 May 62	66°N-65°N	15.2	1080
ST-1296	10 May 62	64°N	16.8	1150
ST-1297	10 May 62	67°N-64°N	18.5	1440
ST-1298	10 May 62	64°N	19.9	1260
ST-1299	10 May 62	64°N	20.4	1590
ST-1300	10 May 62	30°N	12.2	186
ST-1301	10 May 62	30°N	13.6	320
SF-647	10 May 62	30°N	15.1	16000
SF-648	10 May 62	30°N	16.6	3440
SF-649	10 May 62	30°N	17.0	2680
SF-650	10 May 62	30°N	18.3	2180
ST-1302	10 May 62	30°N	19.8	1400
ST-1303	10 May 62	30°N	21.0	1460
ST-1321	15 May 62	65°N	6.1	40.9
ST-1322	15 May 62	66°N-65°N	7.6	47.8
ST-1323	15 May 62	66°N-65°N	9.1	110
ST-1324	15 May 62	65°N	10.7	1250
ST-1325	15 May 62	64°N-58°N	13.8	354
ST-1326	15 May 62	58°N-49°N	13.8	938
ST-1328	15 May 62	49°N-31°N	19.6	1500
ST-1331	16 May 62	61°N-58°N	20.5	1770
ST-1330	16 May 62	58°N-49°N	20.4	1480
ST-1332	16 May 62	64°N-61°N	20.6	854
ST-1333	16 May 62	64°N-58°N	20.6	1700
ST-1329	16 May 62	49°N-32°N	20.1	835

TABLE 115 (cont'd.)

Sample No.	Collection Date	Latitude	Altitude (km)	pCi Be^7 / 100 SCM
SN-1334	17 May 62	70°N-65°N	13.6	1110
SN-1335	17 May 62	70°N-65°N	15.2	1330
SN-1336	17 May 62	70°N-65°N	16.7	1420
SN-1337	17 May 62	70°N-65°N	18.3	1400
SN-1338	17 May 62	70°N-65°N	19.9	1530
SF-651	17 May 62	29°N-24°N	16.8	2370
ST-1340	17 May 62	23°N-15°N	16.8	658
ST-1341	17 May 62	30°N-19°N	18.2	3280
ST-1342	17 May 62	30°N-16°N	19.8	1520
ST-1343	17 May 62	30°N-15°N	20.3	1370
ST-1339	18 May 62	64°N-57°N	16.8	1310
SF-658	18 May 62	40°N-31°N	16.8	3260
SF-657	18 May 62	35°N-31°N	16.8	3300
ST-1347	21 May 62	90°N-80°N	11.6	790
ST-1348	21 May 62	90°N-80°N	11.6	855
ST-1345	21 May 62	88°N	11.6	909
ST-1344	21 May 62	85°N-60°N	11.2	584
ST-1346	21 May 62	85°N-60°N	12.2	499
ST-1349	21 May 62	80°N-60°N	12.2	832
ST-1350	22 May 62	64°N	6.1	84.1
ST-1351	22 May 62	65°N-63°N	7.6	84.9
ST-1352	22 May 62	64°N	9.1	272
ST-1353	22 May 62	64°N-63°N	10.7	404
ST-1354	22 May 62	64°N-49°N	12.2	913
ST-1355	22 May 62	64°N-49°N	18.3	1250
ST-1356	22 May 62	64°N-49°N	20.6	1700
SN-1358	22 May 62	49°N-37°N	12.2	925
SN-1357	22 May 62	37°N-31°N	12.2	256
SN-1359	22 May 62	49°N-43°N	18.2	1110
ST-1360	24 May 62	64°N	12.2	734
ST-1362	24 May 62	64°N	16.7	658
ST-1363	24 May 62	64°N	18.2	1510
ST-1364	24 May 62	64°N	19.7	1680
ST-1365	24 May 62	64°N	20.5	4190
ST-1366	24 May 62	30°N	11.9	61.5
ST-1367	24 May 62	30°N	13.6	243
SF-663	24 May 62	30°N	14.9	1360
SF-664	24 May 62	30°N	16.6	1420
SF-665	24 May 62	30°N	17.1	2440
ST-1368	24 May 62	30°N	18.6	1000
ST-1369	24 May 62	30°N	19.8	1740
ST-1370	24 May 62	30°N	20.8	1350
ST-1372	28 May 62	64°N-49°N	20.2	1900
ST-1371	28 May 62	49°N-32°N	19.8	1620
ST-1373	29 May 62	65°N-63°N	6.1	117
ST-1374	29 May 62	66°N-65°N	7.6	48.8
ST-1375	29 May 62	64°N-63°N	9.1	318
ST-1376	29 May 62	66°N-65°N	10.7	742
ST-1377	29 May 62	64°N-49°N	13.7	944
ST-1379	29 May 62	64°N-49°N	19.8	1430
ST-1378	29 May 62	49°N-31°N	14.0	956
ST-1380	29 May 62	49°N-31°N	19.7	1540
SN-1381	30 May 62	63°N-49°N	16.7	2890
SN-1382	30 May 62	49°N-31°N	16.7	1270

TABLE 115 (cont'd.)

Sample No.	Collection Date	Latitude	Altitude (km)	pCi Be^7 100 SCM
ST-1383	31 May 62	70°N-65°N	12.2	824
ST-1384	31 May 62	70°N-65°N	13.7	701
ST-1385	31 May 62	70°N-65°N	15.3	1060
ST-1386	31 May 62	70°N-65°N	16.8	1820
ST-1387	31 May 62	70°N-65°N	18.3	≤ 3240
ST-1388	31 May 62	70°N-65°N	20.0	1490
ST-1389	31 May 62	30°N-15°N	16.8	588
SF-668	31 May 62	19°N-15°N	18.6	5110
ST-1391	31 May 62	24°N-15°N	20.3	638
ST-1392	5 Jun 62	65°N	6.1	56.3
ST-1393	5 Jun 62	65°N	7.6	74.2
ST-1394	5 Jun 62	65°N	9.1	180
ST-1395	5 Jun 62	65°N	10.7	787
ST-1396	5 Jun 62	64°N-49°N	12.2	787
ST-1397	5 Jun 62	64°N-54°N	15.6	≤ 4480
ST-1398	5 Jun 62	53°N-49°N	15.4	746
ST-1400	5 Jun 62	64°N-49°N	20.4	1770
ST-1402	5 Jun 62	40°N-32°N	12.5	180
ST-1403	5 Jun 62	49°N-31°N	15.3	811
ST-1404	5 Jun 62	49°N-31°N	18.4	1110
ST-1405	5 Jun 62	49°N-31°N	20.1	1170
ST-1406	7 Jun 62	64°N	12.2	1060
ST-1407	7 Jun 62	64°N	13.6	744
ST-1408	7 Jun 62	64°N	15.2	1310
ST-1409	7 Jun 62	64°N	16.8	1280
ST-1410	7 Jun 62	66°N-64°N	18.3	2430
ST-1411	7 Jun 62	66°N-64°N	19.9	6060
ST-1412	7 Jun 62	66°N-64°N	20.4	1740
ST-1413	7 Jun 62	30°N	12.2	56.3
ST-1414	7 Jun 62	30°N	13.7	150
ST-1415	7 Jun 62	30°N	15.2	366
ST-1416	7 Jun 62	30°N	16.9	652
SF-669	7 Jun 62	30°N	17.4	8990
ST-1417	7 Jun 62	30°N	20.0	1390
ST-1418	7 Jun 62	30°N	21.1	1300
ST-1419	12 Jun 62	65°N	6.1	21.0
ST-1420	12 Jun 62	65°N	7.6	17.8
ST-1421	12 Jun 62	65°N	9.1	44.7
ST-1422	12 Jun 62	65°N	10.7	98.1
ST-1423	12 Jun 62	64°N-49°N	13.7	849
ST-1424	12 Jun 62	64°N-49°N	16.8	1510
ST-1425	12 Jun 62	64°N-49°N	19.9	2140
ST-1426	12 Jun 62	64°N-49°N	20.4	2330
ST-1427	12 Jun 62	49°N-36°N	13.9	410
ST-1428	12 Jun 62	36°N-31°N	13.9	129
ST-1431	12 Jun 62	49°N-40°N	19.9	2290
ST-1432	12 Jun 62	49°N-40°N	20.2	2000
ST-1433	12 Jun 62	40°N-31°N	20.7	1510
ST-1435	13 Jun 62	90°N-80°N	12.2	626
ST-1434	13 Jun 62	80°N-60°N	11.0	548
ST-1436	13 Jun 62	80°N-60°N	12.5	730
ST-1437	14 Jun 62	70°N-65°N	12.2	866
ST-1438	14 Jun 62	70°N-65°N	13.7	657

TABLE 115 (cont'd.)

Sample No.	Collection Date	Latitude	Altitude (km)	pCi Be^7 / 100 SCM
ST-1439	14 Jun 62	70°N-65°N	15.3	1480
ST-1440	14 Jun 62	70°N-65°N	16.8	1600
ST-1441	14 Jun 62	70°N-65°N	18.3	1770
ST-1442	14 Jun 62	70°N-65°N	19.8	3040
ST-1443	14 Jun 62	70°N-65°N	19.9	2610
ST-1444	14 Jun 62	70°N-65°N	20.1	2480
ST-1445	14 Jun 62	30°N-15°N	16.8	1380
ST-1448	14 Jun 62	30°N-22°N	20.1	812
ST-1449	14 Jun 62	30°N-15°N	20.5	665
ST-1450	15 Jun 62	15°N-09°N	12.3	≤ 42.3
ST-1451	15 Jun 62	15°N-09°N	15.7	≤ 42.6
ST-1452	15 Jun 62	15°N-09°N	15.2	254
ST-1453	15 Jun 62	15°N-09°N	16.8	547
ST-1454	15 Jun 62	15°N-09°N	19.8	1330
ST-1455	18 Jun 62	09°N	13.7	61.4
ST-1456	18 Jun 62	09°N	15.2	264
ST-1457	18 Jun 62	09°N	19.8	1120
ST-1458	19 Jun 62	65°N	6.1	28.8
ST-1459	19 Jun 62	65°N	7.6	35.1
ST-1460	19 Jun 62	65°N	9.1	25.4
ST-1461	19 Jun 62	65°N	9.1	23.7
ST-1463	19 Jun 62	64°N-49°N	12.2	903
ST-1464	19 Jun 62	64°N-49°N	15.3	1370
ST-1465	19 Jun 62	62°N-49°N	18.3	1480
ST-1466	19 Jun 62	64°N-49°N	20.1	2030
ST-1468	19 Jun 62	49°N-44°N	12.2	399
ST-1467	19 Jun 62	44°N-31°N	12.3	≤ 103
ST-1469	19 Jun 62	49°N-44°N	15.2	486
ST-1470	19 Jun 62	49°N-31°N	18.3	1400
ST-1471	19 Jun 62	49°N-44°N	20.3	2190
ST-1472	19 Jun 62	44°N-31°N	21.2	2050
ST-1462	20 Jun 62	65°N	10.7	53.1
ST-1473	21 Jun 62	64°N	12.2	708
ST-1474	21 Jun 62	64°N	13.8	1100
ST-1475	21 Jun 62	64°N	15.3	2120
ST-1476	21 Jun 62	64°N	16.8	1420
ST-1477	21 Jun 62	64°N	18.3	1650
ST-1478	21 Jun 62	64°N	19.8	2030
ST-1479	21 Jun 62	64°N	20.4	3700
ST-1480	21 Jun 62	30°N	20.1	1310
ST-1481	21 Jun 62	30°N	21.0	1700
ST-1482	22 Jun 62	30°N	12.2	162
ST-1489	22 Jun 62	34°N-31°N	20.0	1980
ST-1490	22 Jun 62	31°N-25°N	21.2	312
ST-1491	23 Jun 62	09°N-04°S	12.2	≤ 51.7
ST-1492	23 Jun 62	04°S-10°S	12.2	70.6
ST-1493	23 Jun 62	09°N-04°S	18.3	429
SF-683	23 Jun 62	02°N-02°S	18.3	3000
ST-685	24 Jun 62	28°N-23°N	18.4	2060
SF-1494	24 Jun 62	25°N-23°N	19.9	≤ 19.7
ST-1497	26 Jun 62	73°N-70°N	11.0	472
ST-1495	26 Jun 62	73°N-60°N	11.0	598
ST-1496	26 Jun 62	73°N-60°N	11.9	703

ISOTOPES, A Teledyne Company

TABLE 115 (cont'd.)

Sample No.	Collection Date	Latitude	Altitude (km)	pCi Be^7 100 SCM
ST-1498	26 Jun 62	73°N-60°N	11.9	483
ST-1502	26 Jun 62	65°	10.7	490
ST-1507	26 Jun 62	64°N-49°N	20.3	2030
ST-1508	26 Jun 62	49°N-31°N	13.8	308
ST-1510	26 Jun 62	48°N-31°N	20.0	2000
ST-1511	26 Jun 62	48°N-31°N	20.7	1790
SF-688	27 Jun 62	19°N-14°N	18.3	1800
ST-1512	27 Jun 62	19°N-18°N	20.1	580
ST-1513	28 Jun 62	70°N-65°N	12.2	2350
ST-1514	28 Jun 62	70°N-65°N	13.8	1400
ST-1515	28 Jun 62	70°N-65°N	15.2	1360
ST-1516	28 Jun 62	70°N-65°N	16.8	1530
ST-1517	28 Jun 62	70°N-65°N	18.4	2020
ST-1520	28 Jun 62	30°N-15°N	18.3	1120
ST-1521	28 Jun 62	30°N-15°N	20.1	1110
ST-1526	29 Jun 62	09°N-10°S	15.1	142
SF-692	29 Jun 62	09°N-04°S	19.8	2000
ST-1527	29 Jun 62	04°S-09°S	19.8	1800
ST-1528	29 Jun 62	04°S-09°S	20.3	649
SF-693	29 Jun 62	02°N-04°S	20.7	≤4000
SF-694	29 Jun 62	09°N-03°N	21.0	7080
SF-697	3 Jul 62	09°N-02°N	16.8	≤1270
SF-698	3 Jul 62	02°N-04°S	16.8	≤ 205
SF-699	3 Jul 62	04°S-10°S	17.0	1040
SF-695	3 Jul 62	15°N-09°N	18.3	≤1490
SF-696	3 Jul 62	15°N-09°N	20.2	1250
ST-1529	3 Jul 62	04°S-10°S	20.4	16400
SF-700	3 Jul 62	09°N-04°S	20.8	≤5540
ST-1530	5 Jul 62	65°N-63°N	6.1	46.3
ST-1531	5 Jul 62	65°N-64°N	7.6	42.9
ST-1532	5 Jul 62	64°N-63°N	9.1	1520
ST-1533	5 Jul 62	65°N-64°N	10.7	221
SF-1535	6 Jul 62	65°N-49°N	15.3	2390
SF-1536	6 Jul 62	65°N-49°N	18.3	1540
SF-1537	6 Jul 62	65°N-49°N	20.2	1060
ST-1539	6 Jul 62	49°N-44°N	12.2	≤ 232
ST-1538	6 Jul 62	44°N-31°N	12.2	≤ 49.9
ST-1540	6 Jul 62	49°N-31°N	15.2	550
ST-1541	6 Jul 62	48°N-31°N	18.4	≤ 165
ST-1542	6 Jul 62	49°N-31°N	20.7	1110
ST-1543	10 Jul 62	70°N-65°N	12.2	533
ST-1545	10 Jul 62	70°N-65°N	15.2	1330
ST-1547	10 Jul 62	70°N-65°N	18.3	1400
ST-1551	10 Jul 62	30°N-15°N	20.0	957
ST-1554	11 Jul 62	90°N-80°N	12.2	801
ST-1559	11 Jul 62	28°N-19°N	19.1	1100
ST-1558	11 Jul 62	19°N-12°N	18.8	2610
ST-1560	12 Jul 62	65°N	6.1	50.9
ST-1570	13 Jul 62	49°N-31°N	16.8	3020
ST-1571	13 Jul 62	49°N-31°N	20.0	1460
ST-1574	13 Jul 62	29°N-22°N	19.9	1160
ST-1575	13 Jul 62	26°N-21°N	19.7	1210
ST-1573	13 Jul 62	22°N-11°N	19.8	1250
ST-1576	13 Jul 62	21°N-10°N	20.3	593

TABLE 115 (cont'd.)

Sample No.	Collection Date	Latitude	Altitude (km)	pCi Be^{7} 100 SCM
ST-1583	19 Jul 62	28°N-17°N	19.6	773
ST-1587	20 Jul 62	65°N-49°N	15.3	1340
ST-1588	20 Jul 62	65°N-49°N	18.3	2000
ST-1589	20 Jul 62	58°N-49°N	20.4	2070
ST-1590	20 Jul 62	65°N-58°N	20.5	2020
ST-1594	20 Jul 62	49°N-36°N	15.2	2250
ST-1595	20 Jul 62	49°N-40°N	18.6	1480
ST-1596	20 Jul 62	40°N-31°N	18.6	1400
ST-1597	20 Jul 62	49°N-31°N	20.5	1430
ST-1601	24 Jul 62	70°N-65°N	12.2	617
ST-1603	24 Jul 62	70°N-65°N	15.3	2030
ST-1605	24 Jul 62	70°N-65°N	18.4	2000
ST-1608	24 Jul 62	31°N-15°N	18.3	≤ 130
ST-1609	24 Jul 62	31°N-15°N	20.7	≤ 959
ST-1610	24 Jul 62	22°N-12°N	16.8	≤ 305
ST-1618	26 Jul 62	65°N-49°N	13.7	292
ST-1620	26 Jul 62	65°N-49°N	19.9	2110
ST-1630	27 Jul 62	62°N-49°N	16.8	1380
ST-1628	27 Jul 62	48°N-31°N	19.8	1480
SF-1637	3 Aug 62	65°N-49°N	18.4	1940
SF-1638	3 Aug 62	65°N-49°N	20.6	2170
SF-1644	3 Aug 62	49°N-31°N	18.4	1510
SF-1645	3 Aug 62	49°N-36°N	20.6	1440
ST-1652	7 Aug 62	31°N-17°N	20.1	727
SF-1660	17 Aug 62	49°N-40°N	15.2	218
SF-1661	17 Aug 62	49°N-31°N	18.3	1670
SF-1664	21 Aug 62	31°N-20°N	18.3	1090
SF-1665	21 Aug 62	20°N-15°N	18.3	854
SF-1667	21 Aug 62	31°N-20°N	20.2	746
SF-1666	21 Aug 62	20°N-15°N	20.0	660
ST-1681	24 Aug 62	51°N-47°N	5.5	≤ 66.0
ST-2515	26 Aug 62	74°N-54°N	18.3	1600
ST-2516	26 Aug 62	74°N-53°N	19.8	2020
ST-1700	27 Aug 62	63°N-55°N	5.5	≤ 57.1
ST-1698	27 Aug 62	39°N-35°N	5.5	≤ 358
ST-1708	29 Aug 62	65°N-48°N	5.5	≤ 56.0
ST-1712	30 Aug 62	51°N-48°N	5.8	≤ 39.8

The mean distribution of beryllium-7 in the sampling corridor during January to March 1963, which is shown in Figure 112, shows anomalously high concentrations in the northern polar stratosphere. In Table 116 the data are listed for the same time period. These, no doubt, resulted from the artificial production of beryllium-7 by the 1962 Soviet test series. It would appear from Figure 112 that the artificial beryllium-7 had reached at least 10°S at high altitudes where concentrations more than twice as high as the theoretical value were found. This might, in part at least, represent a remnant of artificially produced beryllium-7 from the 1962 United States tests. South of 20°S the concentrations found approximated the theoretical values.

Beryllium-7 and phosphorus-32 data for samples collected at three altitudes, 15, 18 and 19 km, at 65° to 70°N are shown in Figure 113 and are listed in Table 117. The data suggest a possible seasonal trend, with high concentrations in the polar stratosphere during the summer months being replaced by low concentrations during the winter months. Beryllium-7 and phosphorus-32 data for equivalent altitudes in the tropical stratosphere and in the southern polar stratosphere do not show similar trends.

A correlation was sought between the appearance of low beryllium-7 and phosphorus-32 concentrations at 65°N during the winter and the shift in the stratospheric circulation which is characterized by the eastward movement onto the North American continent of a high pressure system which persists over the northern Pacific during the first half of the winter. The eastward migration of this high pressure system, associated with the disruption of the typical pole-centered low pressure system of the winter circulation, occurs at the time of the "explosive warmings" which usually affect the upper atmosphere over North America

TABLE 116. Beryllium-7 Activities for Samples Collected from January 1963 Through March 1963

Sample No.	Collection Date	Latitude	Altitude (km)	pCi Be^7 100 SCM
ST-2554	11 Jan 63	20°N-09°N	18.6	1740
ST-2555	11 Jan 63	20°N-09°N	20.7	6960
ST-2707	13 Jan 63	10°N	12.2	≤ 35.4
ST-2708	14 Jan 63	10°N	4.6	≤ 16.5
ST-2709	14 Jan 63	10°N	7.8	≤ 24.2
ST-2710	14 Jan 63	40°S	4.6	≤ 69.8
ST-2711	14 Jan 63	40°S	7.6	51.8
ST-2712	14 Jan 63	40°S	12.2	277
ST-2713	14 Jan 63	40°S	15.2	960
ST-2714	14 Jan 63	40°S	18.3	1670
ST-2715	14 Jan 63	41°S-42°S	20.0	806
ST-2558	17 Jan 63	09°N-10°S	18.0	428
ST-2675	17 Jan 63	15°S-37°S	18.3	604
ST-2676	17 Jan 63	15°S-38°S	20.6	1060
ST-2566	18 Jan 63	65°N-49°N	15.2	1920
ST-2572	18 Jan 63	65°N-49°N	18.4	8140
ST-2577	18 Jan 63	65°N-49°N	20.4	≤ 4340
ST-2567	18 Jan 63	49°N-29°N	15.2	4830
ST-2578	18 Jan 63	49°N-30°N	20.7	≤12300
ST-2722	21 Jan 63	10°N	12.5	≤ 29.2
ST-2580	22 Jan 63	70°N-65°N	12.2	1160
ST-2585	22 Jan 63	70°N-65°N	15.2	1930
ST-2590	22 Jan 63	70°N-65°N	18.3	11600
ST-2597	22 Jan 63	32°N-19°N	18.6	3210
ST-2599	22 Jan 63	32°N-19°N	20.8	4070
ST-4486	24 Jan 63	49°N-37°N	20.7	4450
ST-4487	26 Jan 63	65°N-49°N	20.5	8900
ST-2645	29 Jan 63	40°S	4.6	26.7
ST-2646	29 Jan 63	40°S	7.6	104
ST-2647	29 Jan 63	40°S	12.2	475
ST-2648	30 Jan 63	72°N-70°N	4.6	63.3
ST-2649	30 Jan 63	70°N	7.6	105
ST-2650	30 Jan 63	35°N	4.9	4.90
ST-2651	30 Jan 63	35°N-33°N	7.6	168
ST-2652	30 Jan 63	35°N	12.2	162
ST-2926	4 Feb 63	10°N	13.1	≤ 56.8
ST-2928	4 Feb 63	40°S-44°S	14.0	250
ST-2929	10 Feb 63	10°N-09°N	4.6	≤ 27.7
ST-2930	10 Feb 63	10°N-08°N	7.6	≤ 26.1
ST-2931	10 Feb 63	10°N	12.2	≤ 48.6
ST-2901	12 Feb 63	90°N-60°N	12.3	≤ 280
ST-2902	14 Feb 63	64°N-49°N	12.2	1360
ST-2903	14 Feb 63	64°N-49°N	15.2	2560
ST-2904	14 Feb 63	64°N-58°N	18.3	59800
ST-2905	14 Feb 63	64°N-55°N	20.9	1140
ST-2906	14 Feb 63	49°N-31°N	12.2	723
ST-2907	14 Feb 63	49°N-31°N	15.1	4160
ST-2908	14 Feb 63	49°N-31°N	18.4	10100
ST-2910	14 Feb 63	09°N-06°S	18.6	385
ST-2911	14 Feb 63	09°N-10°S	19.8	766

TABLE 116 (cont'd.)

Sample No.	Collection Date	Latitude	Altitude (km)	pCi Be^7 100 SCM
ST-2912	14 Feb 63	16°S-37°S	18.3	959
ST-2913	14 Feb 63	16°S-37°S	19.8	≤ 3240
ST-2914	19 Feb 63	70°N-64°N	12.2	1940
ST-2915	19 Feb 63	70°N-64°N	15.2	4500
ST-2916	19 Feb 63	70°N-64°N	18.3	6770
ST-2917	19 Feb 63	70°N-64°N	19.8	3780
ST-2918	19 Feb 63	25°N-19°N	18.4	1810
ST-2919	19 Feb 63	25°N-19°N	19.8	2450
ST-2920	19 Feb 63	20°N-09°N	18.5	684
ST-2921	19 Feb 63	20°N-09°N	19.8	2560
ST-2922	21 Feb 63	65°N	6.1	≤ 85.9
ST-2923	21 Feb 63	65°N	7.6	47.1
ST-2924	21 Feb 63	65°N	9.1	≤ 59.0
ST-2925	21 Feb 63	65°N	10.7	1360
ST-3221	10 Mar 63	10°N-08°N	4.6	≤ 90.0
ST-3222	10 Mar 63	10°N	7.6	≤ 188
ST-3223	10 Mar 63	10°N	12.2	450
ST-3224	11 Mar 63	40°S	4.6	≤ 76.5
ST-3225	11 Mar 63	40°S	7.6	≤ 77.1
ST-3226	11 Mar 63	40°S	12.2	≤ 202
ST-3227	11 Mar 63	40°S-41°S	15.2	≤ 1080
ST-3228	11 Mar 63	40°S-41°S	18.3	≤ 3280
ST-3229	11 Mar 63	42°S-43°S	20.3	≤ 5440
ST-3230	19 Mar 63	70°N-64°N	12.2	1680
ST-3231	19 Mar 63	70°N-64°N	15.2	3260
ST-3232	19 Mar 63	70°N-64°N	18.3	6710
ST-3233	19 Mar 63	15°N-09°N	18.0	≤ 3560
ST-3235	26 Mar 63	70°N	4.6	≤ 138
ST-3236	26 Mar 63	73°N-71°N	7.6	≤ 474
ST-3238	26 Mar 63	34°N-33°N	4.9	≤ 103
ST-3239	26 Mar 63	33°N	7.6	≤ 210
ST-3237	26 Mar 63	10°N-05°N	15.2	≤ 571
ST-3240	26 Mar 63	40°S-43°S	4.6	≤ 72.0
ST-3241	26 Mar 63	40°S	7.6	≤ 175
ST-3242	26 Mar 63	40°S	12.2	354
ST-3243	26 Mar 63	40°S-42°S	14.3	606
ST-3244	28 Mar 63	49°N-40°N	15.3	2810
ST-3245	28 Mar 63	49°N-33°N	19.8	2910
ST-3246	28 Mar 63	02°N-10°S	18.6	787
ST-3247	28 Mar 63	03°N-10°S	21.1	1340
ST-3249	29 Mar 63	42°S-45°S	19.5	≤ 5180

TABLE 117 Be^7 and P^{32} Activities and Be^7/P^{32} and P^{32}/P^{33} Ratios for Samples Collected from October 1963 through March 1964

Sample No.	Collection Date	Latitude	Altitude (km)	pCi Be^7 100 SCM	pCi P^{32} 100 SCM	Be^7/P^{32}	P^{32}/P^{33}
ST-4795	3 Oct 63	55°N-47°N	11.9	577	9.32	61.9	1.35
ST-4798	10 Oct 63	65°N-58°N	15.2	1210	-	-	-
ST-4800	10 Oct 63	65°N-49°N	17.1	1830	20.0	91.3	(0.575)
ST-4799	10 Oct 63	65°N-49°N	18.4	1470	18.0	81.7	1.27
ST-4801	10 Oct 63	48°N-32°N	15.5	480	7.54	63.7	(2.29)
ST-4804	10 Oct 63	09°N-10°S	18.2	340	-	-	-
ST-4811	10 Oct 63	09°N-10°S	20.0	-	4.71	-	0.757
ST-4808	15 Oct 63	70°N-65°N	15.4	795	12.3	64.6	1.64
ST-4809	15 Oct 63	70°N-65°N	18.5	1840	21.9	84.0	1.83
ST-4810	15 Oct 63	70°N-65°N	20.2	-	21.3	-	1.78
ST-4806	15 Oct 63	32°N-20°N	18.7	(2320)	6.47	(359)	1.49
ST-4812	15 Oct 63	32°N-20°N	20.1	-	12.7	-	1.46
ST-4813	15 Oct 63	20°N-09°N	18.2	-	≤ 15.6	-	≤ 1.9
ST-4814	15 Oct 63	20°N-09°N	20.3	626	14.2	44.0	1.66
ST-4815	16 Oct 63	70°N-65°N	11.9	-	3.93	-	1.20
ST-5192	22 Oct 63	40°S	12.2	273	-	-	-
ST-4825	23 Oct 63	15°S-37°S	18.3	-	12.6	-	1.83
ST-4826	23 Oct 63	21°S-37°S	20.6	-	12.5	-	1.29
ST-4827	24 Oct 63	48°N-32°N	18.6	1700	20.2	84.2	0.722
ST-4828	24 Oct 63	48°N-32°N	20.8	1860	15.8	117	1.42
ST-4829	28 Oct 63	38°S-47°S	18.3	1120	20.8	54.0	1.99
ST-4830	28 Oct 63	38°S-47°S	19.5	1240	22.7	54.5	(2.44)
ST-5010	26 Nov 63	70°N-65°N	11.9	852	12.5	68.3	1.28
ST-4998	26 Nov 63	70°N-65°N	18.4	1780	19.7	83.6	1.31
ST-4999	26 Nov 63	70°N-65°N	20.6	1990	27.3	72.7	2.04
ST-5000	26 Nov 63	32°N-20°N	18.7	758	8.03	95.4	1.02
ST-5001	26 Nov 63	32°N-20°N	20.8	731	6.84	107	1.06
ST-5002	26 Nov 63	20°N-09°N	18.2	606	6.76	89.6	(0.40)
ST-5003	26 Nov 63	20°N-09°N	20.5	440	6.06	72.7	1.30
ST-5004	26 Nov 63	38°N-50°S	16.9	1210	22.6	53.8	1.60
ST-5005	26 Nov 63	38°S-50°S	18.3	1230	19.2	64.1	1.86
ST-5006	26 Nov 63	38°S-50°S	20.0	3770	34.3	110	1.32
ST-5014	27 Nov 63	66°N	9.1	296	5.56	53.1	1.88
ST-5017	28 Nov 63	15°S-37°S	18.3	(3240)	55.3	(58.6)	-

TABLE 117 (cont'd.)

Sample No.	Collection Date	Latitude	Altitude (km)	pCi Be^7 100 SCM	pCi P^{32} 100 SCM	Be^7/P^{32}	P^{32}/P^{33}
ST-5018	28 Nov 63	15°S-37°S	20.6	1020	-	-	-
ST-5008	29 Nov 63	65°N-49°N	18.4	1250	14.5	86.1	1.43
ST-5009	29 Nov 63	65°N-49°N	20.6	1410	18.0	78.5	1.13
ST-5011	29 Nov 63	48°N-38°N	15.2	1050	15.9	66.0	1.32
ST-5012	29 Nov 63	48°N-32°N	18.3	(299)	(3.48)	(85.8)	(2.20)
ST-5013	29 Nov 63	48°N-32°N	20.8	964	13.0	73.9	1.44
ST-5015	30 Nov 63	09°N-10°S	18.4	475	3.42	139	(≥8.27)
ST-5016	30 Nov 63	09°N-10°S	21.0	394	5.71	69.1	1.10
ST-5193	11 Dec 63	90°N-60°N	12.2	630	7.66	82.2	1.13
ST-5194	17 Dec 63	70°N-65°N	11.9	(240)	9.54	25.2	1.53
ST-5195	17 Dec 63	40°S-44°S	15.2	940	12.0	78.0	1.44
ST-5196	17 Dec 63	40°S	18.3	1330	18.1	73.4	1.56
ST-5216	19 Dec 63	56°N-47°N	11.9	533	(12.1)	(40.0)	(0.974)
ST-5217	20 Dec 63	42°N-35°N	11.9	353	6.41	55.1	1.72
ST-5197	23 Dec 63	70°N-65°N	15.2	1090	14.1	76.9	1.74
ST-5198	23 Dec 63	70°N-65°N	18.3	1400	18.3	76.7	1.43
ST-5199	23 Dec 63	70°N-65°N	20.5	1730	18.9	91.0	1.09
ST-5200	23 Dec 63	32°N-20°N	18.3	1110	10.0	111	1.16
ST-5201	23 Dec 63	32°N-20°N	20.4	944	-	-	-
ST-5202	23 Dec 63	20°N-09°N	18.3	221	2.30	95.9	1.01
ST-5203	23 Dec 63	20°N-09°N	20.6	518	3.56	146	1.76
ST-5204	23 Dec 63	38°S-50°S	18.3	1260	13.4	94.1	1.05
ST-5205	23 Dec 63	38°S-50°S	19.8	1730	19.9	87.0	1.37
ST-5206	26 Dec 63	09°N-10°S	18.3	407	4.93	82.6	1.39
ST-5207	26 Dec 63	09°N-10°S	20.7	≤ 498	3.56	≤140	1.51
ST-5208	27 Dec 63	65°N-49°N	15.2	992	12.5	79.6	1.11
ST-5209	27 Dec 63	65°N-49°N	18.3	1480	19.1	77.5	1.41
ST-5210	27 Dec 63	65°N-49°N	21.0	1150	17.8	64.6	1.43
ST-5211	27 Dec 63	48°N-38°N	15.2	564	8.41	67.1	1.20
ST-5212	27 Dec 63	48°N-32°N	18.3	1110	7.60	147	0.660
ST-5213	27 Dec 63	48°N-32°N	20.6	(1140)	(≤7.79)	(≥147)	(≤2.65)
ST-5214	27 Dec 63	15°S-37°S	18.3	928	8.94	104	1.02
ST-5215	27 Dec 63	15°S-37°S	20.6	1220	8.89	138	-
ST-5371	15 Jan 64	90°N-60°N	12.0	755	(22.6)	(33.4)	(1.01)
ST-5372	21 Jan 64	70°N-65°N	11.9	911	12.2	74.4	-
ST-5373	21 Jan 64	32°N-22°N	18.3	900	10.0	89.7	1.16
ST-5374	21 Jan 64	22°N-10°N	20.4	506	4.88	104	1.02
ST-5375	21 Jan 64	38°S-47°S	18.3	1480	20.0	73.8	1.31
ST-5376	21 Jan 64	38°S-47°S	20.0	1650	(28.1)	(58.8)	(3.76)

TABLE 117 (cont'd.)

Sample No.	Collection Date	Latitude	Altitude (km)	pCi Be^7 100 SCM	pCi P^{32} 100 SCM	Be^7/P^{32}	P^{32}/P^{33}
ST-5377	22 Jan 64	65°N	9.1	307	5.69	53.9	1.27
ST-5378	22 Jan 64	70°N-65°N	15.2	1340	(4.15)	(322)	(4.38)
ST-5379	22 Jan 64	70°N-65°N	18.3	1390	21.5	64.7	1.22
ST-5380	22 Jan 64	70°N-65°N	19.7	1240	20.0	62.0	1.28
ST-5381	23 Jan 64	65°N-49°N	15.2	671	10.3	65.3	1.22
ST-5382	23 Jan 64	65°N-49°N	18.3	1310	19.7	66.4	1.61
ST-5383	23 Jan 64	65°N-49°N	19.7	1050	17.5	59.8	1.24
ST-5384	23 Jan 64	48°N-32°N	15.2	1000	15.7	64.1	1.18
ST-5385	23 Jan 64	48°N-32°N	18.3	1140	19.2	59.2	1.52
ST-5386	23 Jan 64	48°N-32°N	19.9	1010	13.4	75.4	1.21
ST-5387	23 Jan 64	32°N-22°N	20.5	758	-	-	-
ST-5388	23 Jan 64	22°N-09°N	18.3	410	5.60	73.3	(1.82)
ST-5389	23 Jan 64	15°S-37°S	18.3	1010	10.5	97.0	1.07
ST-5390	23 Jan 64	15°S-37°S	20.5	666	6.92	96.3	1.38
ST-5391	24 Jan 64	09°N-10°S	18.3	520	5.20	100	1.68
ST-5392	24 Jan 64	09°N-10°S	20.6	437	7.62	57.4	(≥6.51)
ST-5393	18 Feb 64	70°N-65°N	11.9	1250	16.5	75.7	1.15
ST-5394	18 Feb 64	70°N-65°N	15.2	641	13.4	47.8	1.32
ST-5395	18 Feb 64	70°N-65°N	18.3	874	14.2	61.6	1.72
ST-5396	18 Feb 64	70°N-65°N	19.6	1090	14.9	73.2	1.28
ST-5397	18 Feb 64	32°N-20°N	18.3	843	9.51	88.6	0.838
ST-5398	18 Feb 64	32°N-20°N	20.1	(3290)	12.4	(265)	1.20
ST-5399	18 Feb 64	20°N-09°N	18.3	591	6.71	88.2	1.10
ST-5400	18 Feb 64	20°N-09°N	19.8	518	5.72	90.6	1.01
ST-5401	18 Feb 64	38°S-47°S	18.3	1730	24.6	70.3	1.52
ST-5402	18 Feb 64	38°S-47°S	19.8	1260	16.2	77.6	1.36
ST-5403	19 Feb 64	38°S-39°S	12.2	377	6.96	54.1	1.63
ST-5404	20 Feb 64	65°N-64°N	9.1	89.4	5.15	17.3	1.23
ST-5405	20 Feb 64	65°N-49°N	15.2	1030	(2.96)	(348)	1.24
ST-5406	20 Feb 64	65°N-49°N	18.3	1060	14.3	74.0	0.638
ST-5407	20 Feb 64	65°N-49°N	19.8	955	13.1	70.6	0.98
ST-5408	20 Feb 64	48°N-32°N	15.2	725	11.9	60.9	1.28
ST-5409	20 Feb 64	48°N-32°N	18.3	1090	11.5	94.9	1.18
ST-5410	20 Feb 64	48°N-32°N	20.3	1140	15.1	75.8	1.46
ST-5411	20 Feb 64	15°S-37°S	18.1	1090	10.2	107	1.04
ST-5412	20 Feb 64	15°S-37°S	20.2	894	9.83	90.9	(2.73)
ST-5674	17 Mar 64	70°N-65°N	11.9	895	11.9	75.1	(2.06)
ST-5671	17 Mar 64	70°N-65°N	15.2	1460	18.4	79.0	1.45
ST-5672	17 Mar 64	70°N-65°N	18.3	757	8.57	88.3	1.02

TABLE 117 (cont'd).

Sample No.	Collection Date	Latitude	Altitude (km)	pCi Be^7 100 SCM	pCi P^{32} 100 SCM	Be^7/P^{32}	P^{32}/P^{33}
ST-5673	17 Mar 64	70°N-65°N	19.2	1070	15.2	70.7	1.30
ST-5675	17 Mar 64	20°N-09°N	18.3	827	10.0	82.4	1.33
ST-5676	17 Mar 64	20°N-09°N	21.0	639	≤ 4.77	≥130	≤ 0.93
ST-5677	17 Mar 64	38°S-47°S	18.3	1140	16.4	69.9	1.13
ST-5678	17 Mar 64	38°S-47°S	20.2	1360	19.7	69.0	-
ST-5679	18 Mar 64	90°N-60°N	12.2	1030	13.1	78.6	0.959
ST-5680	18 Mar 64	65°N	9.1	356	5.58	63.8	1.28
ST-5681	18 Mar 64	47°N-41°N	11.9	595	7.22	8.24	1.12
ST-5682	18 Mar 64	32°N-20°N	18.3	770	6.85	112	0.877
ST-5683	18 Mar 64	32°N-20°N	20.7	610	5.17	118	(1.70)
ST-5687	19 Mar 64	65°N-47°N	11.9	887	9.22	96.2	1.09
ST-5684	19 Mar 64	65°N-49°N	15.2	1080	13.3	81.2	0.990
ST-5685	19 Mar 64	65°N-49°N	18.3	1180	-	-	-
ST-5686	19 Mar 64	65°N-49°N	19.8	1300	18.8	69.3	1.51
ST-5688	19 Mar 64	48°N-32°N	15.2	(377)	8.84	(42.6)	(2.57)
ST-5689	19 Mar 64	48°N-32°N	18.3	1370	17.8	77.0	2.08
ST-5690	19 Mar 64	48°N-32°N	20.1	868	14.9	58.1	1.34
ST-5691	19 Mar 64	09°N-10°S	18.3	348	3.90	89.4	1.38
ST-5692	19 Mar 64	09°N-10°S	20.7	329	5.44	60.5	(≥3.21)
ST-5693	19 Mar 64	15°S-37°S	18.3	1070	13.4	79.6	1.53
ST-5694	19 Mar 64	15°S-37°S	20.5	1560	-	-	-

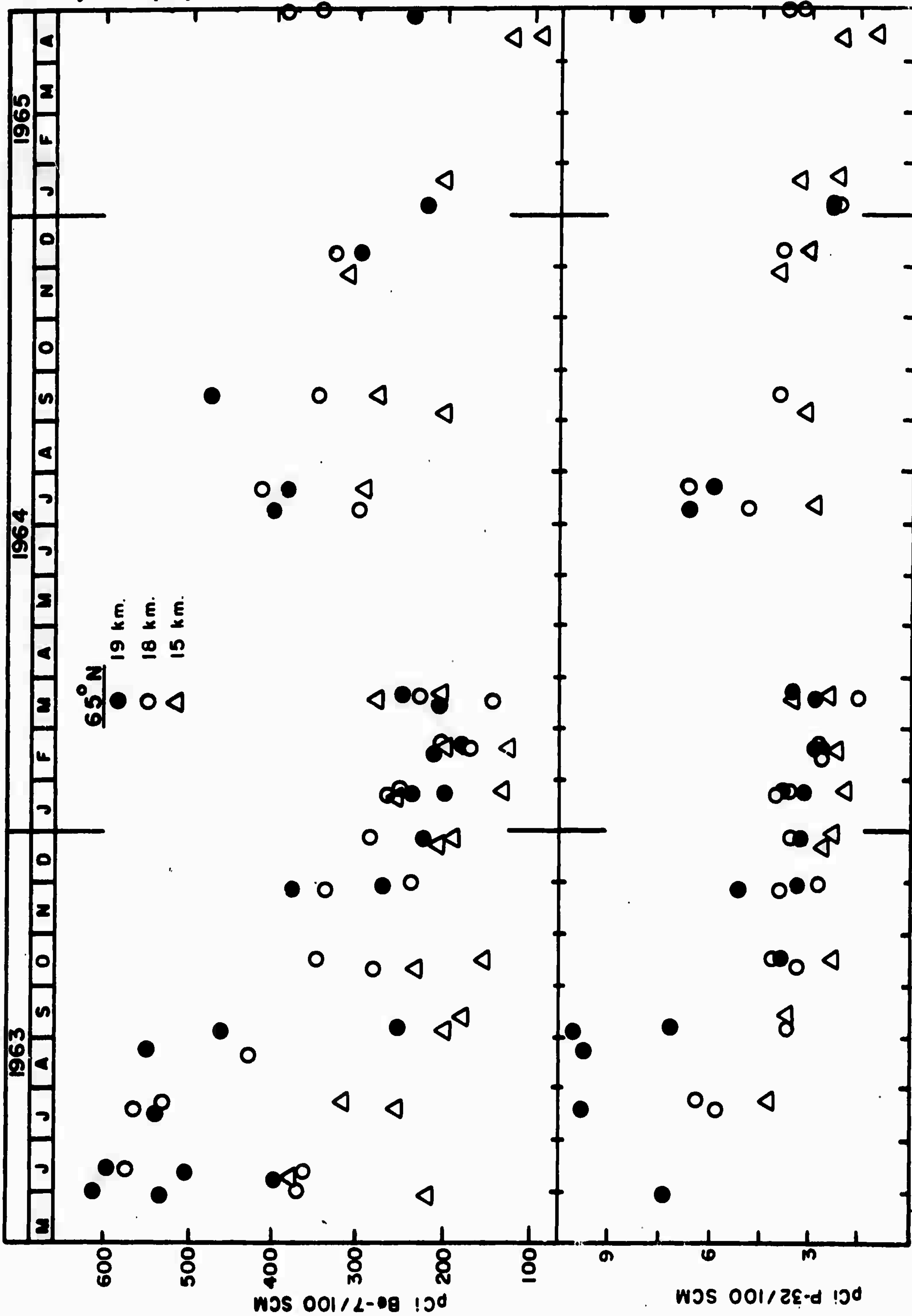

FIGURE 113. CONCENTRATIONS OF Be^7 AND P^{32} AT 65°-70°N

during late winter. During early 1962 and early 1963 the eastward movement of this high pressure system was accompanied by sudden decreases in the total beta activity of STARDUST filter samples collected over Alaska. It was anticipated that such air motions would also produce sudden decreases in concentrations of cosmic ray products in the stratosphere in this region, since they would bring in northward moving air from low latitudes, where the production rates of cosmic ray products are relatively low. The beryllium-7 and phosphorus-32 concentrations and the atmospheric temperatures at 65°N during October 1963 to March 1964 are plotted in Figure 114. The frequency of filter sample collection and the reliability of the radiochemical results were not sufficient to substantiate any possible correlation between changes in temperature and in nuclide concentrations.

The distributions of beryllium-7 and phosphorus-32 in the STARDUST sampling corridor during December 1963 are shown in Figure 115, and those during February 1964 and February 1965 are shown in Figures 116 and 117, respectively. The data are listed in Table 118 for February 1965; the other data are in Table 117. The concentrations are plotted over horizontal lines representing the flight tracks of the sampling missions. The concentration isolines in the figure indicate the concentrations expected in a quiescent atmosphere, and are based on figures from Bhandari, et al[62]. The concentrations at 15 Km and above in the northern polar stratosphere during February 1964 were significantly lower than those in this region during December 1963 indicating the possibility that an influx of air from lower latitudes had recently occurred. This was not true in February 1965, but the data in Figure 111 suggest that a change in the pattern of the stratospheric circulation over Alaska may have occurred earlier, during January 1965.

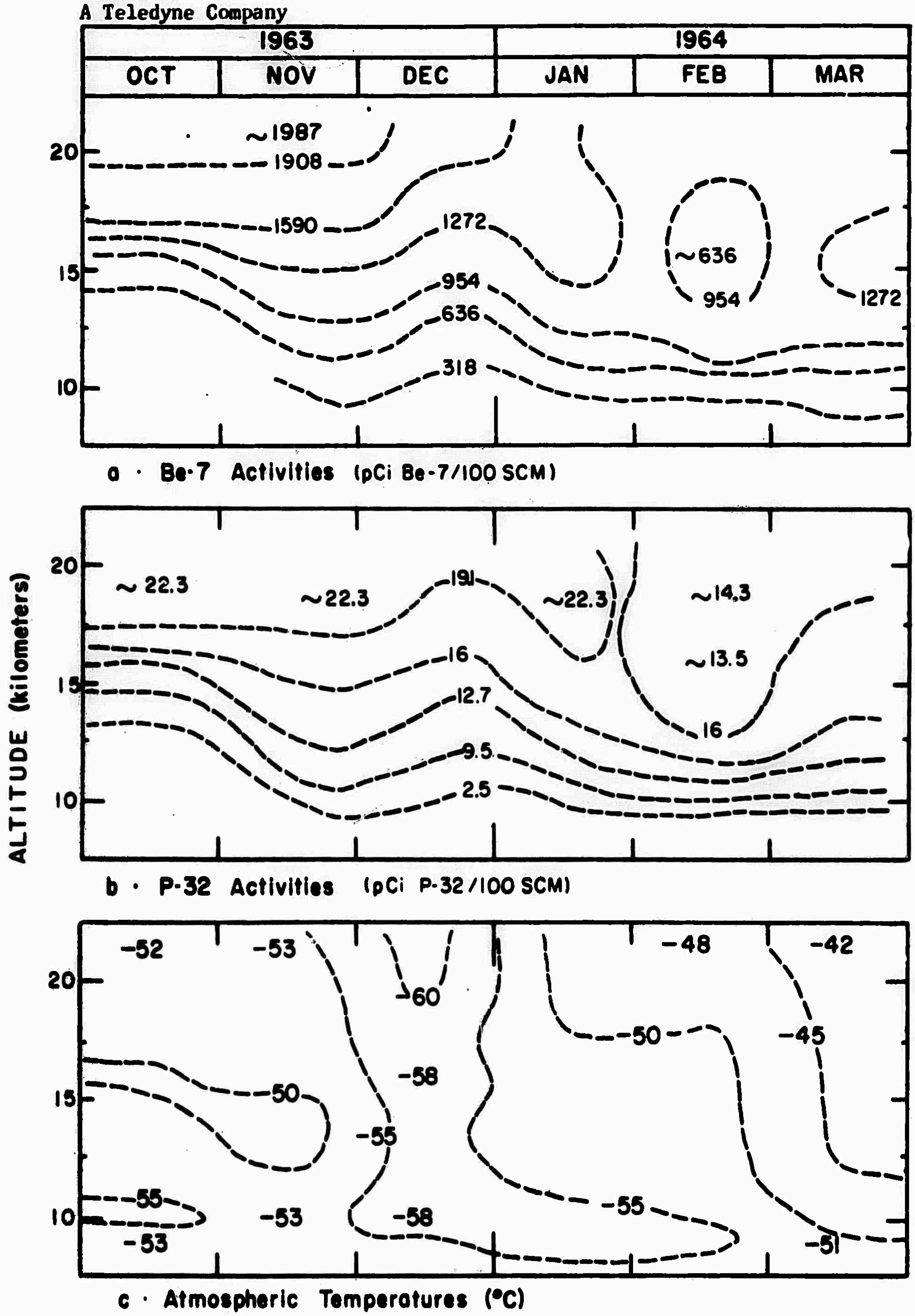

FIGURE 114. ACTIVITIES OF BERYLLIUM-7 AND PHOSPHORUS -32, AND TEMPERATURES AT 65°N DURING OCT. 1963 AND MAR. 1964

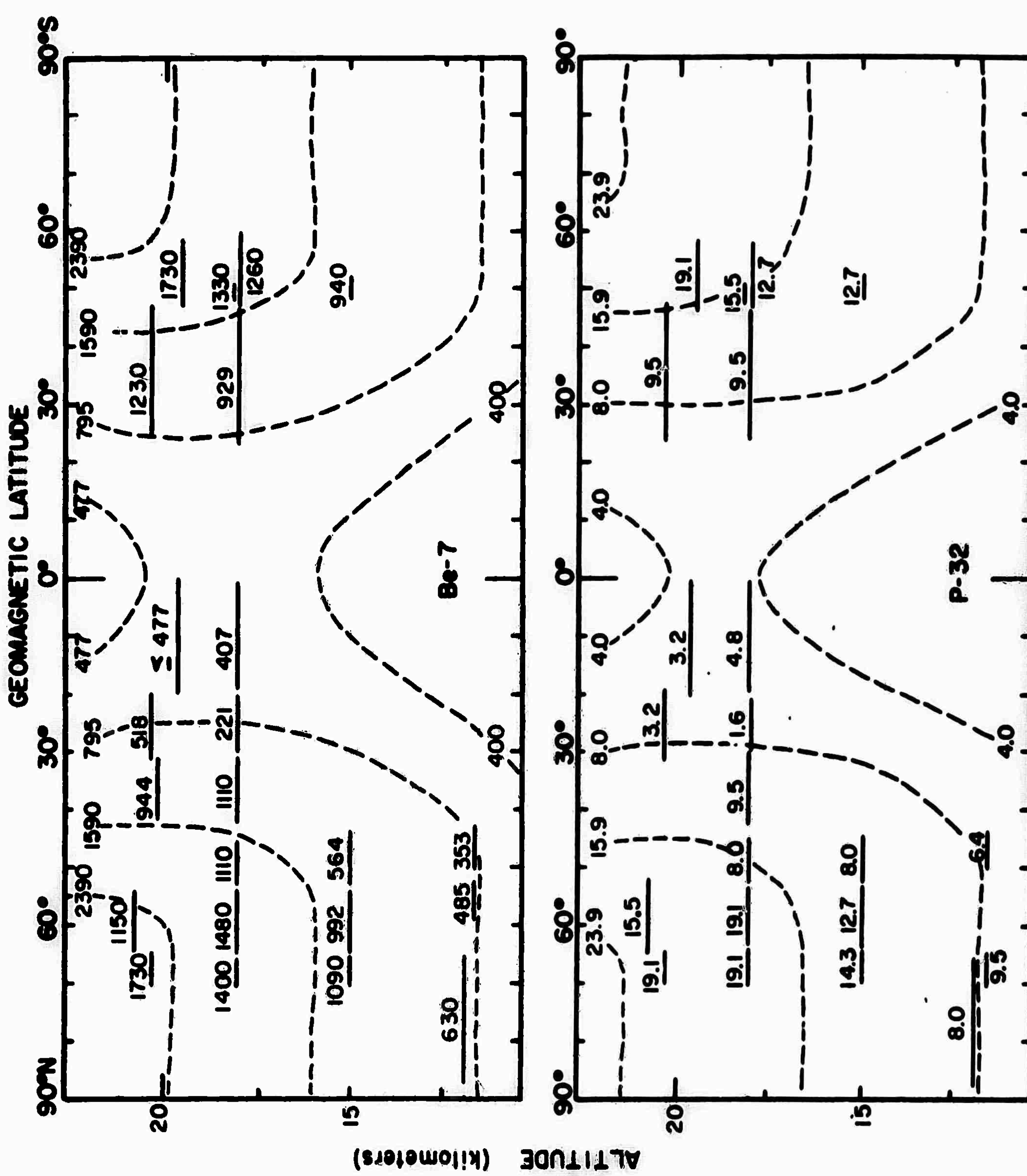

FIGURE 115. MEASUREMENTS OF Be-7 AND P-32 (pCi / 100 SCM) DURING DECEMBER 1963

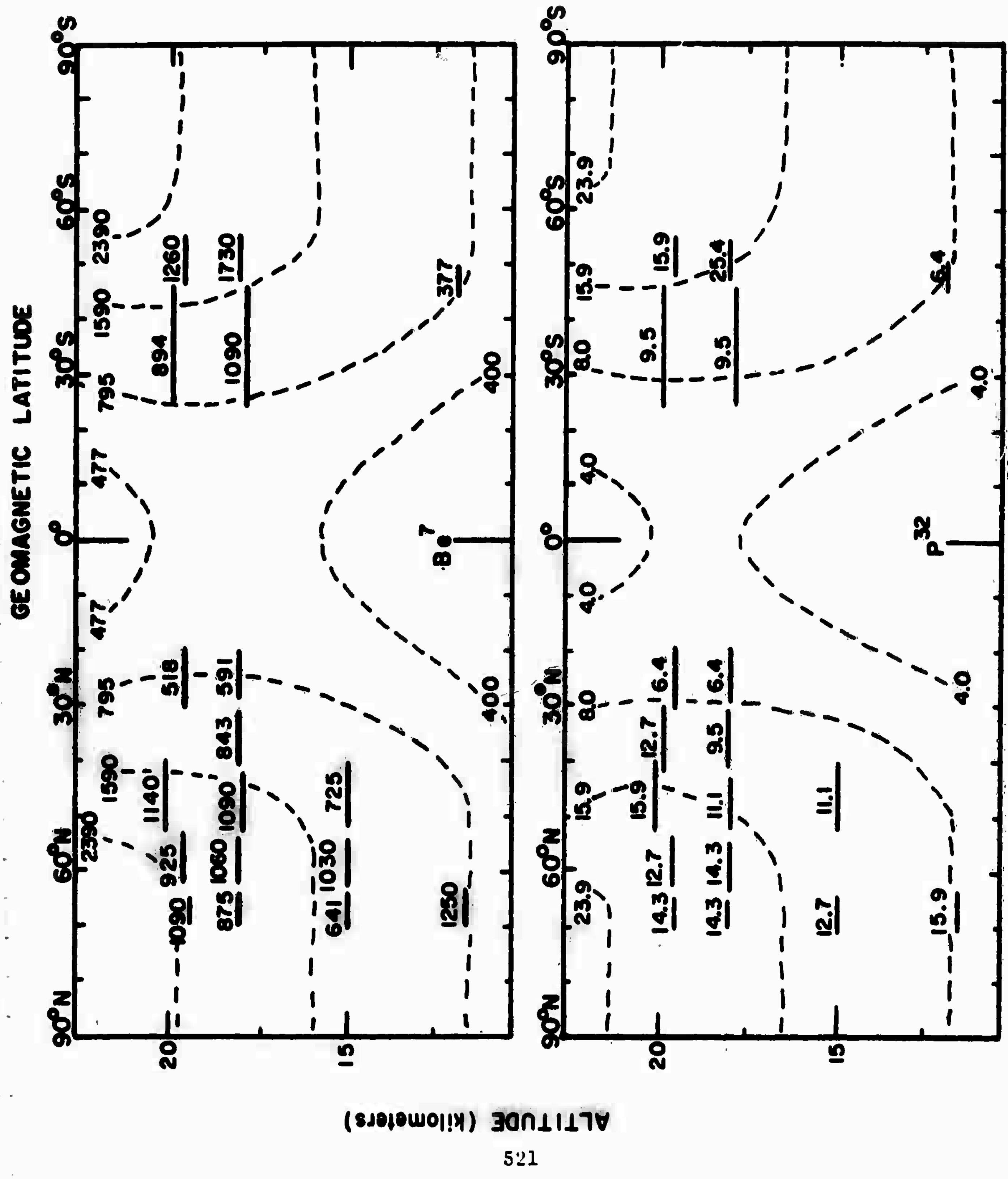

FIGURE 116. MEASUREMENTS OF Be^7 AND P^{32} (pCi/100 SCM) DURING FEB 1964

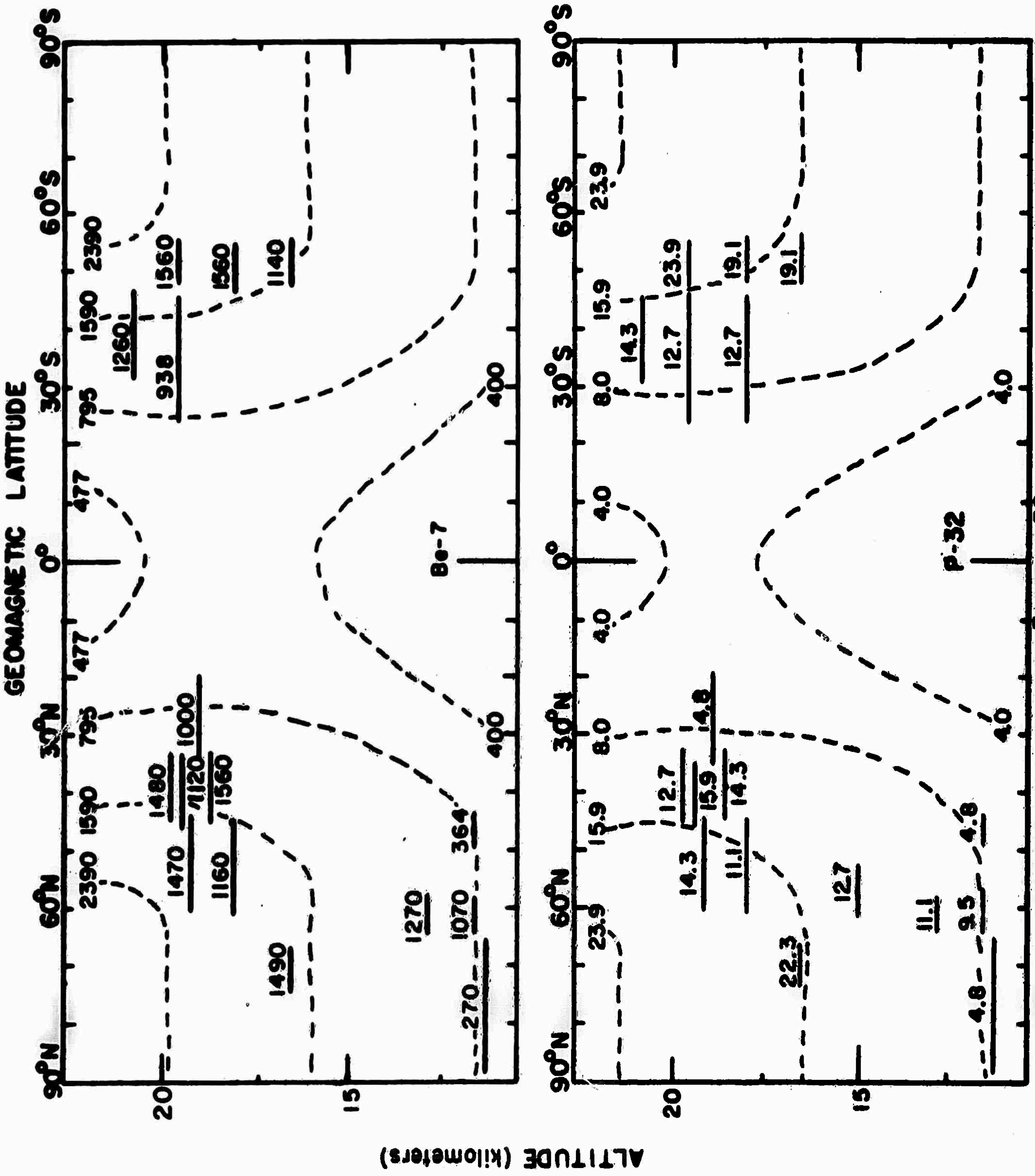

FIGURE 117. MEASUREMENTS OF Be^7 AND P^{32} (pCi 100 SCM) DURING FEB 1965

TABLE 118. Beryllium-7 and Phosphorus-32 Activities for Samples Collected during February 1965

Sample No.	Collection Date	Latitude	Altitude (km)	pCi Be^7 / 100 SCM	pCi P^{32} / 100 SCM
ST-6995	2 Feb 65	52°N-37°N	18.3	1160	11.3
ST-6996	2 Feb 65	52°N-37°N	19.4	1470	14.8
ST-6997	2 Feb 65	36°N-23°N	19.0	1560	24.3
ST-6999	3 Feb 65	64°N-55°N	11.9	1070	10.3
ST-7000	3 Feb 65	64°N-55°N	13.1	1270	11.1
ST-7001	5 Feb 65	41°N-35°N	11.9	364	4.36
ST-7004	5 Feb 65	36°N-24°N	19.6	1120	15.0
ST-7003	5 Feb 65	24°N-09°N	19.3	1000	5.01
ST-7005	11 Feb 65	38°S-47°S	16.8	1140	19.4
ST-7006	11 Feb 65	38°S-47°S	18.3	913	18.1
ST-7007	11 Feb 65	38°S-47°S	19.8	1560	24.6
ST-7008	16 Feb 65	75°N-67°N	15.2	-	(70.1)
ST-7009	16 Feb 65	75°N-67°N	16.8	1490	23.0
ST-7015	16 Feb 65	15°S-37°S	18.3	-	12.5
ST-7016	16 Feb 65	15°S-37°S	19.8	938	12.2
ST-7017	16 Feb 65	22°S-37°S	21.0	1260	14.3
ST-7026	18 Feb 65	90°N-60°N	11.7	270	4.86
ST-7023	20 Feb 65	67°N-58°N	15.2	-	(24.8)
ST-7024	20 Feb 65	58°N-47°N	15.2	-	12.7

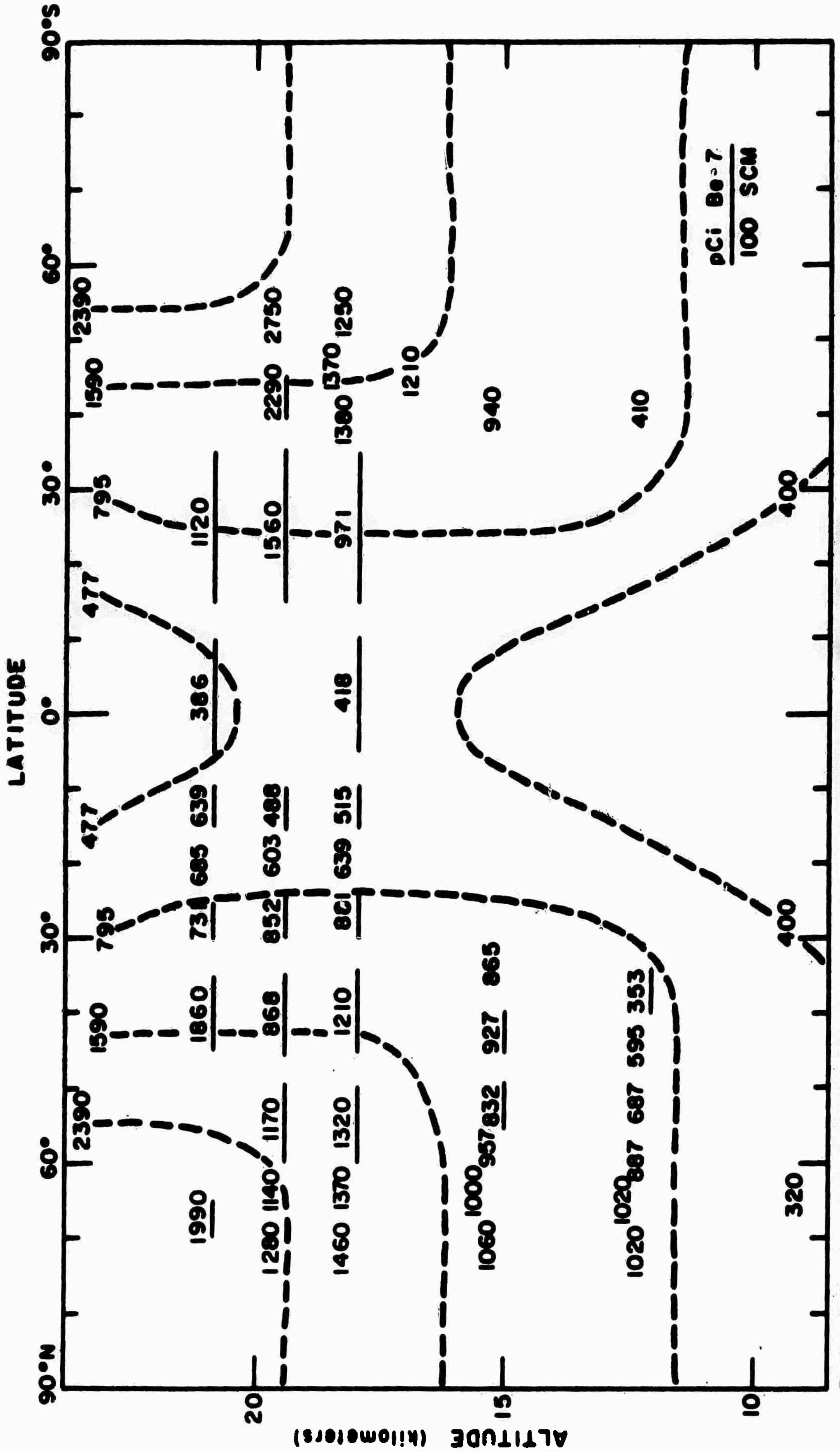

FIGURE 118. STRATOSPHERIC DISTRIBUTION OF BERYLLIUM-7 ACTIVITIES FOR OCTOBER 1963 THROUGH MARCH 1964

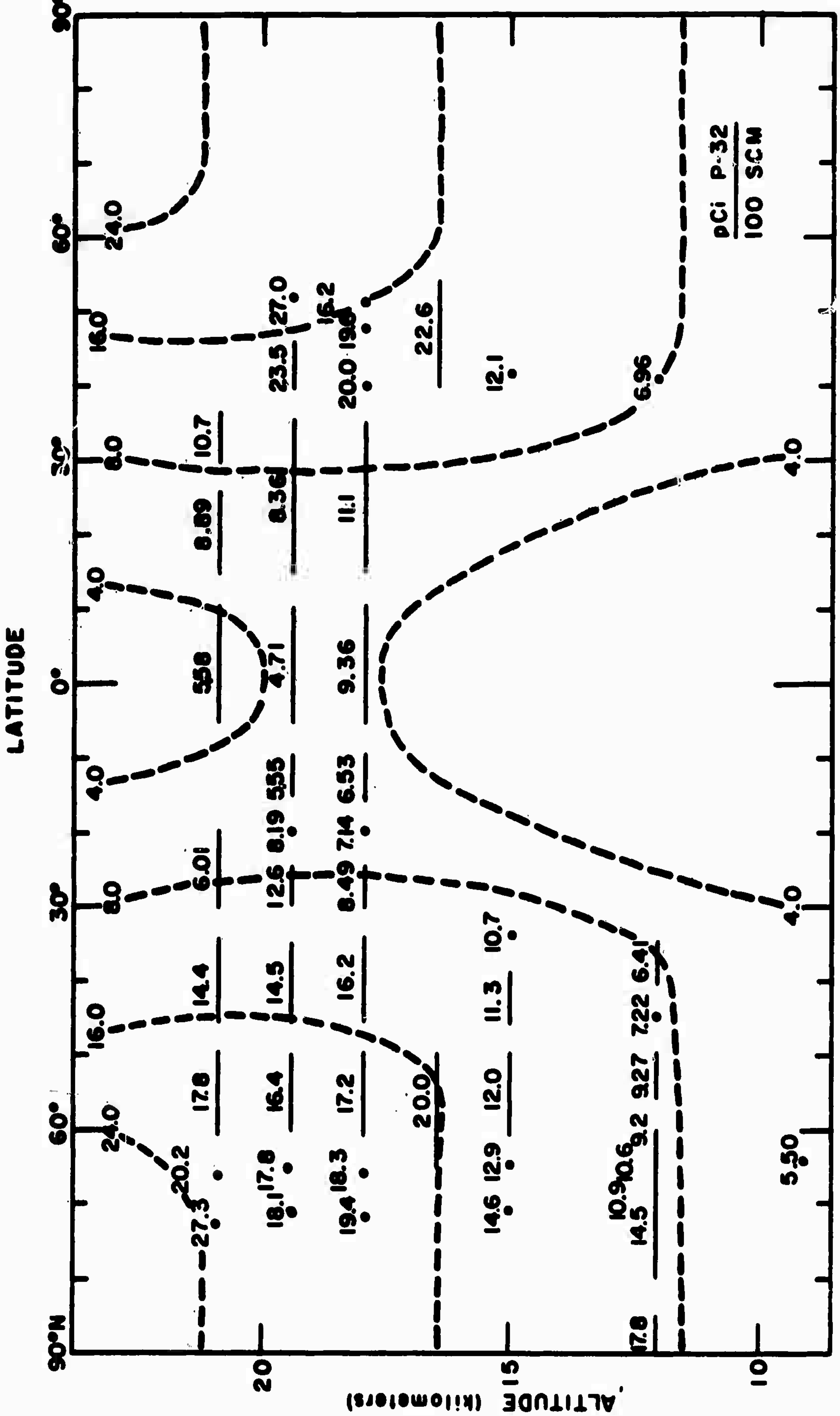

FIGURE 119. STRATOSPHERIC DISTRIBUTION OF PHOSPHORUS-32 ACTIVITIES FOR OCTOBER 1963 THROUGH MARCH 1964

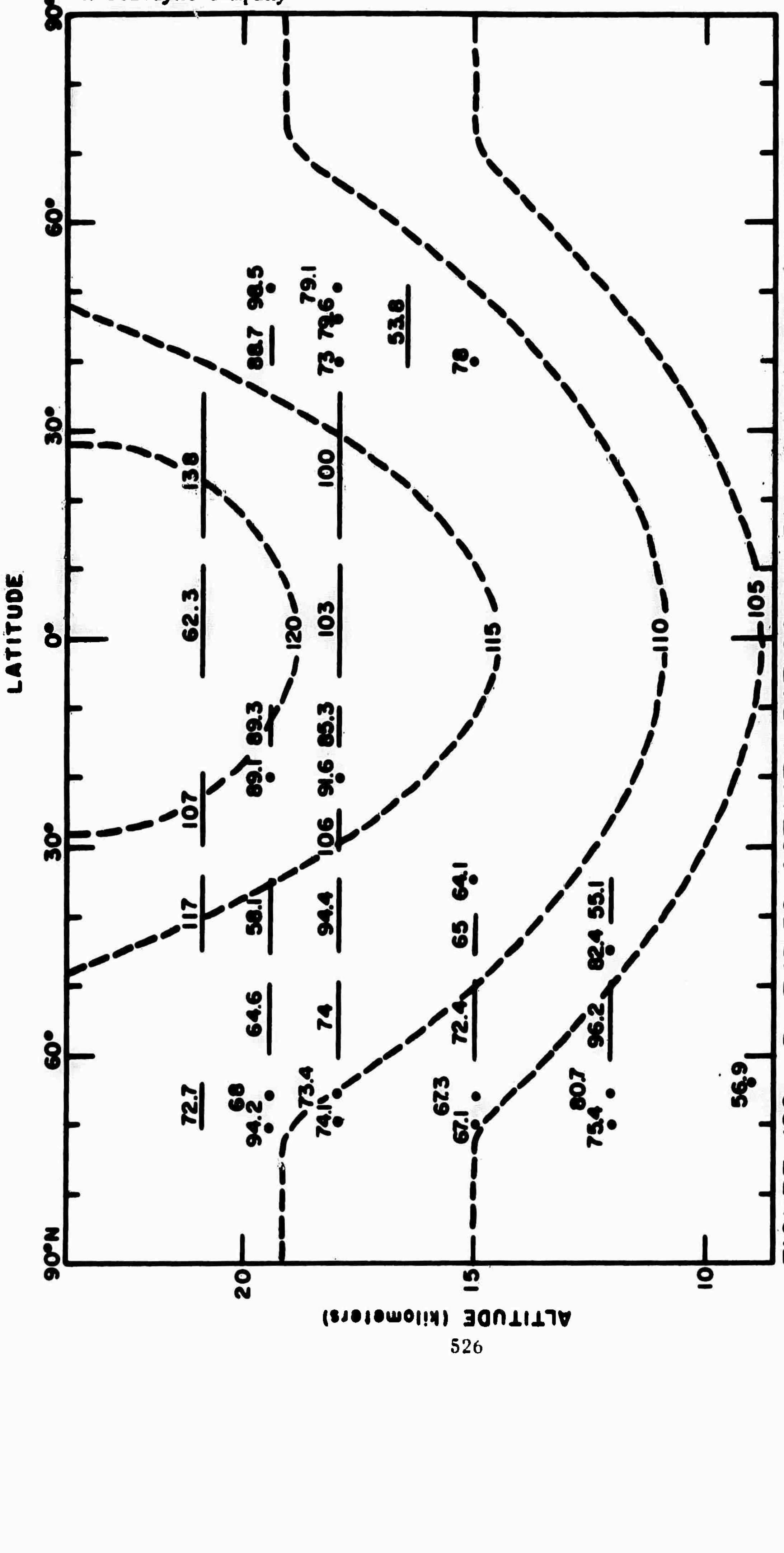

FIGURE 120. Be-7/P-32 ACTIVITY RATIOS IN THE STRATOSPHERE FOR OCTOBER 1963 THROUGH MARCH 1964

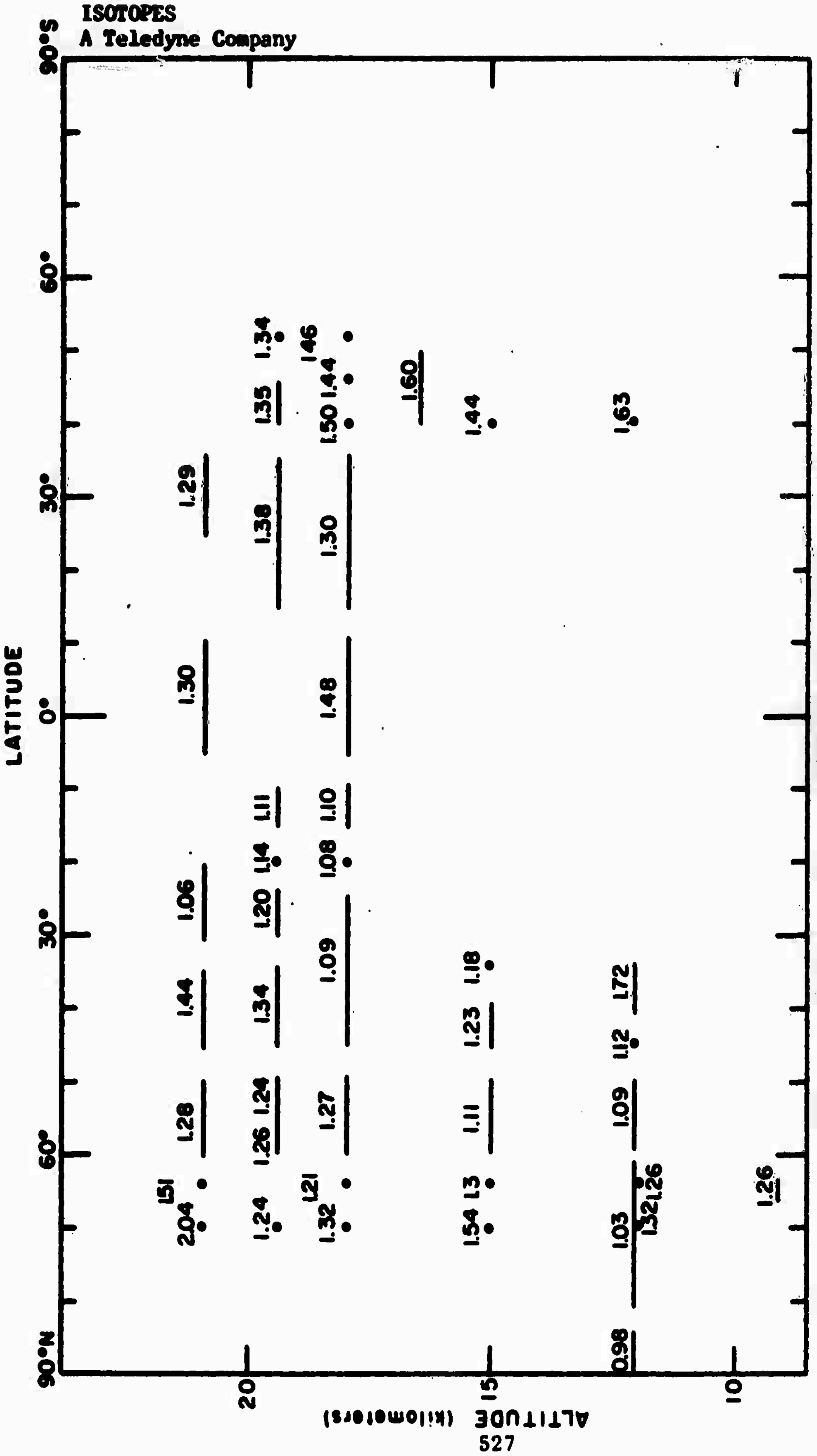

FIGURE 121. P-32/P-33 ACTIVITY RATIOS IN THE STRATOSPHERE FOR OCTOBER 1963 THROUGH MARCH 1964

Comparisons of measured ratios of cosmic ray produced isotopes to the corresponding predicted ratios can provide information on the circulation and mixing patterns of the stratosphere and troposphere [61]. The ratios $^{32}P/^{33}P$ and $^{7}Be/^{32}P$ may be of particular interest since all are of cosmogenic origin and have relatively short half-lives.

The data for phosphorus were not sufficiently plentiful for analysis on a month-to-month basis for all altitudes and latitudes in the sampling corridor. Averages of the data during the period from October 1963 to March 1964 for beryllium-7 and phosphorus-32 are shown in Figures 118 and 119 respectively, and the ratios $^{7}Be/^{32}P$ and $^{32}P/^{33}P$ for the same period of time are shown in Figures 120 and 121. The data in tabular form for the ratios are given in Table 117. From the predicted beryllium-7 and phosphorus concentrations of Bhandari et al.[62], shown by the isolines in Figure 115, the predicted ratio $^{7}Be/^{32}P$ should range between 100 and 120. The measured ratios (with some exceptions) in the altitude range 18 to 20 km and latitude range 30°N to 30°S agree better with the predicted ratios than do those of lower altitude or higher latitude.

The beryllium-7 concentrations show the same variances from the predicted values as do the $^{7}Be/^{32}P$ ratios. The phosphorus-32 concentrations agree quite well with the corresponding predicted values over most of the ranges of latitudes and altitudes. The predicted ratio $^{32}P/^{33}P$ of Lal and Peters [61] for a quiescent atmosphere is 1.22 irrespective of latitude or altitude. The measured ratios as shown in Figure 121 agree quite well with the predicted ratio.

Stratospheric Distribution of Sodium-22

According to Bhandari et al.[62] the only data available considered to represent natural cosmic ray levels of sodium-22 were reported by Bhandari and Rama[66] and Bhandari[67]. The data were accumulated between November 1960 to August 1961 and the observed sodium-22 concentrations are shown in Figure 122. Subsequently the stratospheric sodium-22 concentrations increased rapidly by two orders of magnitude by late 1962, undoubtedly due to major atmospheric nuclear test-series in 1961-1962.

The sodium-22 data accumulated during October 1963 to March 1964 for Project STARDUST are shown in Figure 123 and are listed on Table 119. In the range of 15°S - 45°S and 18 km - 21 km the sodium-22 concentrations are considerably lower than in the same ranges in the northern latitudes - by factors of approximately 4-6. The sodium-22 concentrations for the period October 1963 to March 1964 are considerably higher than the predicted values for cosmogenic-produced concentrations in a quiescent stratosphere but agree quite well with the observations of Bhandari et al.[62] (Figure 8 of that reference). Bhandari et al. reported finding a well defined peak in the sodium-22 concentrations during October to November 1963 in filter samples collected at 20 km in the stratosphere of the Northern Hemisphere. They reported further that during succeeding months well defined peaks occurred successively at lower levels in the 60° - 70°N latitude band. STARDUST data, discussed in DASA 1821, the Eleventh Progress Report on Project STARDUST, neither confirmed nor contradicted the observations of Bhandari et al.

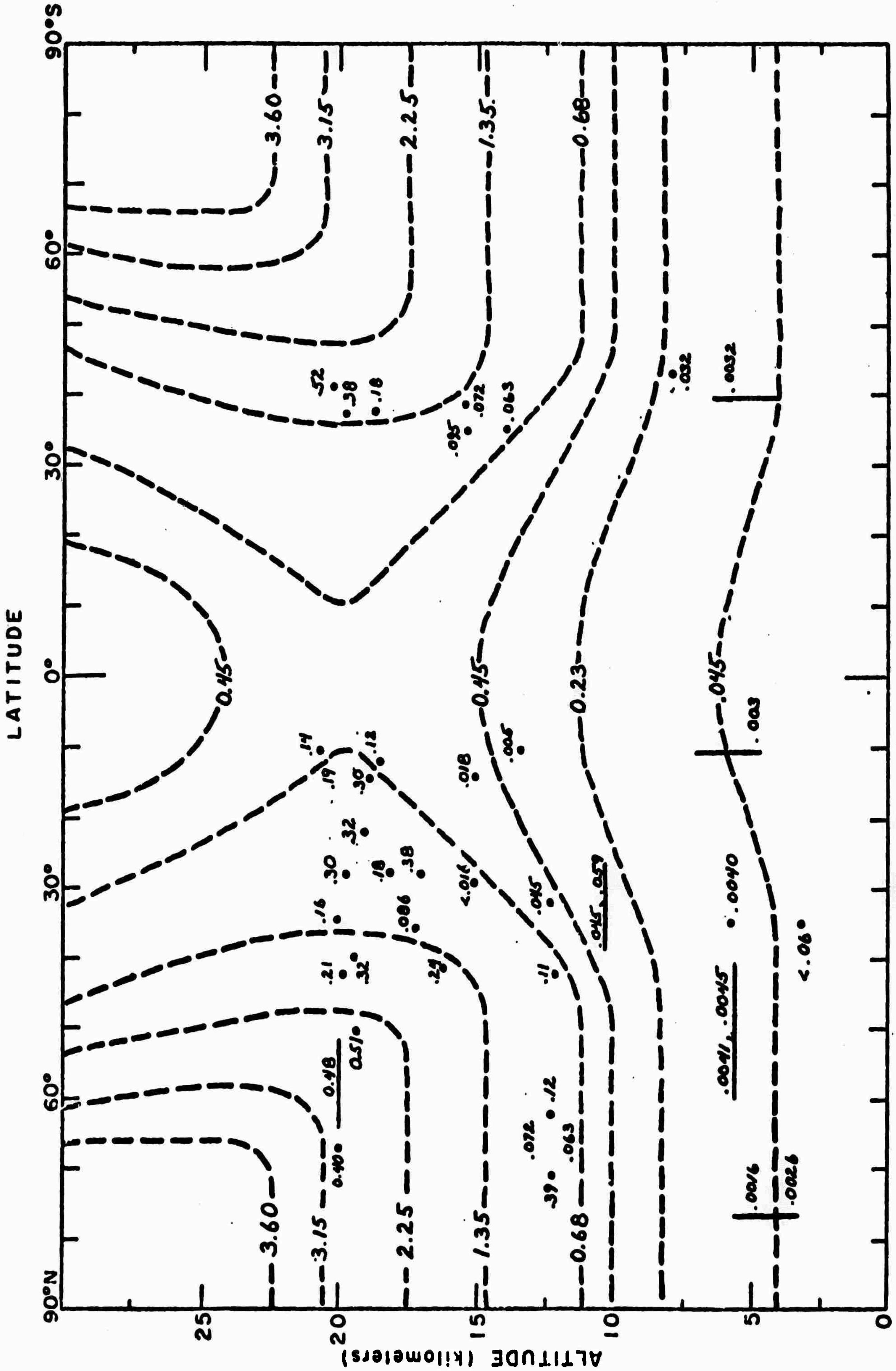

FIGURE 122. OBSERVED Na^{22} CONCENTRATIONS (From Reference 3) FROM NOVEMBER 1960 THROUGH AUGUST 1961 (pCi/100 SCM)

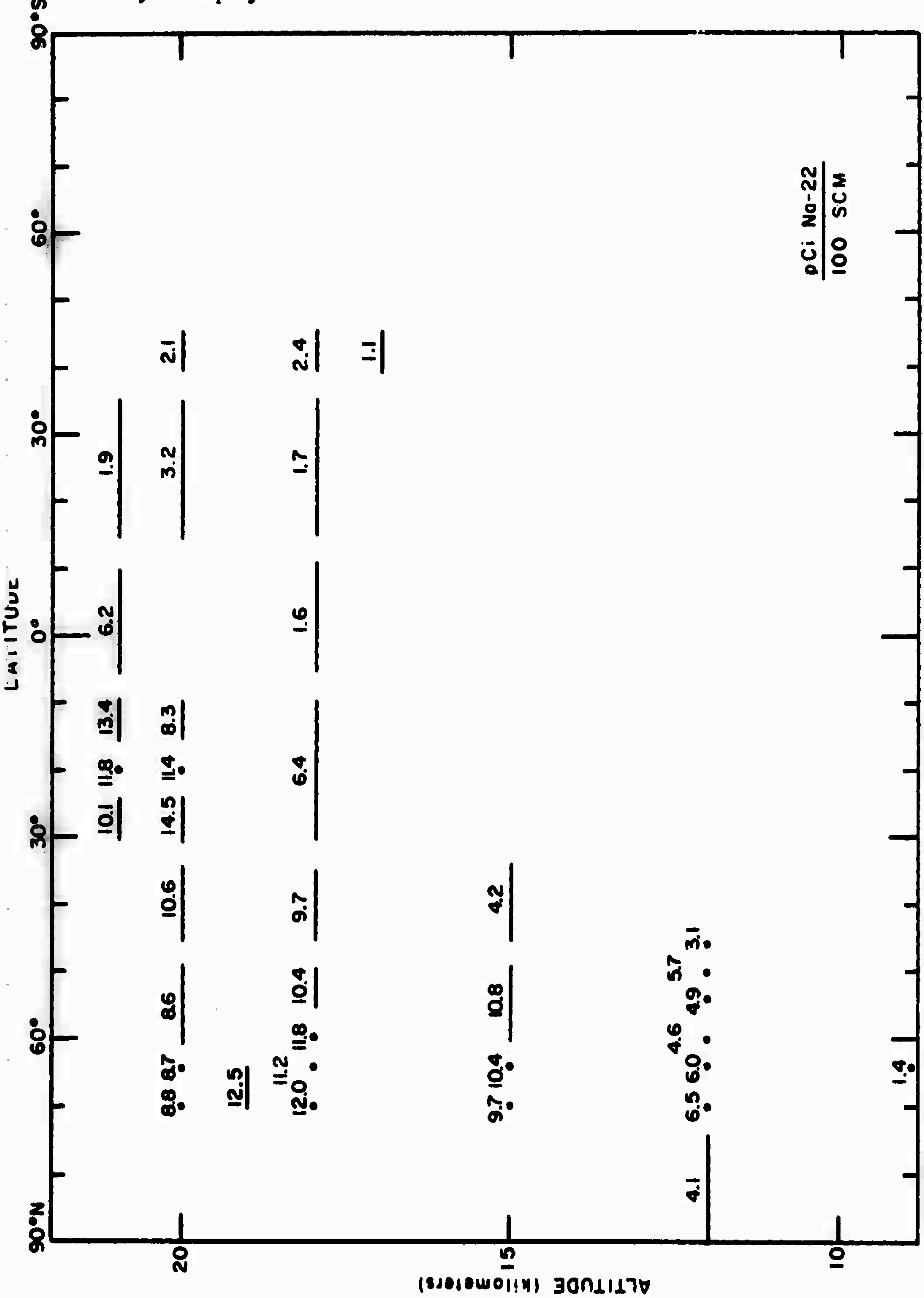

FIGURE 123. STRATOSPHERIC DISTRIBUTION OF SODIUM-22 ACTIVITIES FOR OCTOBER 1963 THROUGH MARCH 1964

TABLE 119. Sodium-22 Activities for Samples Collected from October 1963 through March 1964

Sample No.	Collection Date	Latitude	Altitude (km)	pCi Na^{22} / 100 SCM
ST-8073	10 Oct 63	65°N-49°N	20.2	7.8
ST-8074	24 Oct 63	65°N-49°N	18.4	9.6
ST-8075	24 Oct 63	65°N-49°N	19.9	12.3
ST-8076	31 Oct 63	65°N-49°N	20.0	8.3
ST-8077	12 Nov 63	70°N-65°N	19.8	8.5
ST-8078	14 Nov 63	65°N-49°N	18.4	9.1
ST-8079	14 Nov 63	65°N-49°N	20.1	9.5
ST-6490	14 Nov 63	15°S-37°S	18.3	2.4
ST-6491	14 Nov 63	15°S-37°S	20.7	1.9
ST-8081	19 Dec 63	65°N-49°N	18.3	11.8
ST-8082	19 Dec 63	65°N-49°N	19.8	8.10
ST-6495	7 Jan 64	70°N-65°N	18.3	21.
ST-6499	7 Jan 64	20°N-09°N	18.3	0.6
ST-6494	9 Jan 64	65°N-49°N	15.2	19.1
ST-6496	9 Jan 64	65°N-49°N	18.3	11.8
ST-6497	9 Jan 64	48°N-32°N	15.2	6.7
ST-6498	9 Jan 64	48°N-32°N	18.3	6.8
ST-5695	30 Jan 64	65°N-49°N	19.8	7.6
ST-5696	30 Jan 64	47°N-32°N	19.8	14.2
ST-6492	4 Feb 64	70°N-65°N	11.9	5.6
ST-6493	5 Feb 64	65°N-55°N	11.9	4.1
ST-5697	13 Feb 64	65°N-49°N	18.3	10.7
ST-5698	13 Feb 64	48°N-32°N	18.3	9.7
ST-5393	18 Feb 64	70°N-65°N	11.9	11.9
ST-5394	18 Feb 64	70°N-65°N	15.2	7.4
ST-5395	18 Feb 64	70°N-65°N	18.3	6.7
ST-5396	18 Feb 64	70°N-65°N	19.5	9.2
ST-5397	18 Feb 64	32°N-20°N	18.3	8.0
ST-5399	18 Feb 64	20°N-09°N	18.3	11.2
ST-5400	18 Feb 64	20°N-09°N	19.8	8.3
ST-5401	18 Feb 64	38°S-47°S	18.3	3.1
ST-5402	18 Feb 64	38°S-47°S	19.8	2.1
ST-5403	19 Feb 64	38°S-39°S	12.2	0.2
ST-5404	20 Feb 64	65°N-49°N	9.1	0.7
ST-5405	20 Feb 64	65°N-49°N	15.2	6.7
ST-5406	20 Feb 64	65°N-49°N	18.3	15.1
ST-5407	20 Feb 64	65°N-49°N	19.8	8.8
ST-5408	20 Feb 64	48°N-32°N	15.2	(29)
ST-8083	20 Feb 64	48°N-32°N	15.2	2.99
ST-5409	20 Feb 64	48°N-32°N	18.3	12.2
ST-5410	20 Feb 64	48°N-32°N	20.4	7.1
ST-5411	20 Feb 64	15°S-37°S	18.0	2.0
ST-5412	20 Feb 64	15°S-37°S	20.1	2.8
ST-6503	5 Mar 64	15°S-37°S	20.4	3.5
ST-5674	17 Mar 64	70°N-65°N	11.9	4.3
SF-5671	17 Mar 64	70°N-65°N	15.2	12.0
ST-5672	17 Mar 64	70°N-65°N	18.3	8.4
ST-5673	17 Mar 64	70°N-65°N	19.2	12.5
ST-5675	17 Mar 64	20°N-09°N	18.3	7.5
ST-5676	17 Mar 64	20°N-09°N	21.0	13.4

ISOTOPES, A Teledyne Company

TABLE 119 (continued)

Sample No.	Collection Date	Latitude	Altitude (km)	pCi Na^{22} / 100 SCM
ST-6504	17 Mar 64	38°S-47°S	16.8	1.1
ST-5677	17 Mar 64	38°S-47°S	18.3	1.7
ST-5679	18 Mar 64	90°N-60°N	12.2	4.1
ST-5680	18 Mar 64	65°N	9.1	2.0
ST-5681	18 Mar 64	47°N-41°N	11.9	3.1
ST-5682	18 Mar 64	32°N-20°N	18.3	4.9
ST-5683	18 Mar 64	32°N-20°N	20.7	10.1
ST-5687	19 Mar 64	65°N-47°N	11.9	5.7
ST-5684	19 Mar 64	65°N-49°N	15.2	6.6
ST-5685	19 Mar 64	65°N-49°N	18.3	8.2
ST-5686	19 Mar 64	65°N-49°N	19.8	6.8
ST-5688	19 Mar 64	48°N-32°N	15.2	2.8
ST-5689	19 Mar 64	48°N-32°N	18.3	10.2
ST-5691	19 Mar 64	09°N-10°S	18.3	1.6
ST-5692	19 Mar 64	09°N-10°S	20.7	6.2
ST-5693	19 Mar 64	15°S-37°S	18.3	0.8
ST-6500	31 Mar 64	32°N-20°N	20.4	14.5

CHAPTER 11. THE DISTRIBUTION OF LEAD-210 AND POLONIUM-210 IN THE STRATOSPHERE

11.1 Source of Lead-210

Uranium is a fairly common trace constituent of rocks, soils and natural waters. The main isotope of uranium, uranium-238 (99.27% abundance) is radioactive, decaying through a series of intermediate radioactive daughter products ultimately to stable lead-206. The predominant decay series of uranium-238, which is summarized in Table 120 includes radon, which chemically behaves as a rare gas. When the uranium, or at least the immediate parent of radon, radium-226, is situated in rocks, soil or water close to the surface of the earth, some of the radon atoms produced by its decay may escape into the atmosphere during the few days which pass between their formation and their decay. When they do decay in the free atmosphere their daughter products will be ionized and will tend to undergo chemical reactions and to become attached to dust particles in the atmosphere. For the most part, the radon atoms which enter the atmosphere will remain in the lower troposphere, and their decay products will rapidly be washed out and returned to the surface of the earth. Some, however, will be carried into the upper troposphere or, perhaps, even into the lower stratosphere before they decay, and their daughter products may form within, or may be carried into, the stratosphere. As a result low concentrations of lead-210 (radium-D), bismuth-210 (radium-E), and polonium-210 (radium-F) are found in filter samples of stratospheric air.

11.2 Distribution of Lead-210 and Polonium-210 Reported by Other Workers

Burton and Stewart [68] measured lead-210 and polonium-210 in stratospheric and tropospheric air and concluded that their results substantiated the validity of the concept of the organized circulation of stratospheric air which had been

TABLE 120. The Predominant Decay Series of Uranium-238

Nuclide	Name	Half Life	Mode of Decay
U^{238}	Uranium I	4.51×10^{9} years	α
Th^{234}	Uranium X_1	24.10 days	β^-
Pa^{234}	Uranium X_2	1.18 minutes	β^- (99.4%)
U^{234}	Uranium II	2.48×10^{5} years	α
Th^{230}	Ionium	7.6×10^{4} years	α
Ra^{226}	Radium	1.62×10^{3} years	α
Rn^{222}	Radon	3.823 days	α
Po^{218}	Radium A	3.05 minutes	α (99.97%)
Pb^{214}	Radium B	26.8 minutes	β^-
Bi^{214}	Radium C	19.7 minutes	β^-(99.96%)
Po^{214}	Radium C	1.64×10^{-4} seconds	α
Pb^{210}	Radium D	22 years	β^-
Bi^{210}	Radium E	5.0 days	β^-(~100%)
Po^{210}	Radium F	138.4 days	α
Pb^{206}	Radium G	stable	-

proposed by Brewer[79], and that approximately 200 days were required for air which entered the stratosphere at low latitudes to leave it at mid-latitudes. Measurements by Rama and Honda[69] led them to the conclusion that the high concentrations found by Burton and Stewart "appear to be due to some local causes." Based on their own data Rama and Honda concluded that the residence time of lead-210 in the stratosphere "is long enough to permit the processes of mixing to make the concentration more or less independent of altitude and latitude."

Bhandari et al.[62], on the basis of published values of stratospheric lead-210 concentrations, concluded that the lead-210 content of stratospheric air between 55° and 75° latitude is lower than the lead-210 content of other atmospheric regions, and that the highest lead-210 concentrations occur in the equatorial stratosphere. They attributed the low values in the polar stratosphere to removal of aerosols from that region by gravitational settling, with a mean time of settling of 36 months. They suggested intrusions of tropospheric air into the tropical stratosphere, perhaps by highly turbulent vertical mixing associated with thunderstorms, as the cause of the high lead-210 concentrations in the tropical stratosphere.

Martell[15] suggested that the distribution of lead-210 concentrations in the stratosphere which was noted by Bhandari et al. could have resulted from gravitational settling of particles of the stratospheric aerosol, to which the lead-210 had become attached, as these particles were carried to higher stratospheric levels by quasi-horizontal motions along mixing surfaces which slope upward from the poles toward the equator.

Karol[71] used published results of Project STARDUST measurements of lead-210 and polonium-210 in filter samples of stratospheric air to calculate mean values of quasi-vertical velocity and turbulent diffusion coefficients in the lower stratosphere.

Peirson et al.[72] measured the vertical gradient of lead-210 in the atmosphere over the United Kingdom and found that it conformed to the diffusion models of Jacobi and Andre[70] (for the case of short washout times) and of Machta[73]. Measurements of lead-210 in the stratosphere made as part of another program[75,33] using filter samples collected during 1960 and 1961, show that within the polar stratosphere, at least, concentrations of lead-210 decrease with increasing altitude, and that at altitudes above the level of the tropical tropopause the highest lead-210 concentrations are found in the tropical stratosphere. Lead-210 was measured in samples collected in the vicinity of the jet stream in 1960 as reported by Telgadas[76] and Peterson[77]. The results of these measurements also indicate that lead-210 concentrations tend to decrease with increasing altitude above the level of the tropopause.

11.3 Distribution of Lead-210 - STARDUST Measurements 1957-1959

In another attempt to describe the distribution of lead-210 in the stratosphere, a series of samples collected during 1957 and 1958 on Project HASP were analyzed during Project STARDUST and the results were reported in the Eleventh Progress Report[74]. These data, which are summarized in Table 121 suggest that a layer of relatively high concentrations of lead-210 exists in the lower stratosphere, two to three kilometers above the tropopause, and that concentrations decrease with increasing altitude above this layer. This distribution is shown in Figure 124. The sampling locations at given latitudes and altitudes along various flight paths are identified by symbols corresponding to the number of samples analyzed. The lines of constant radioactivity

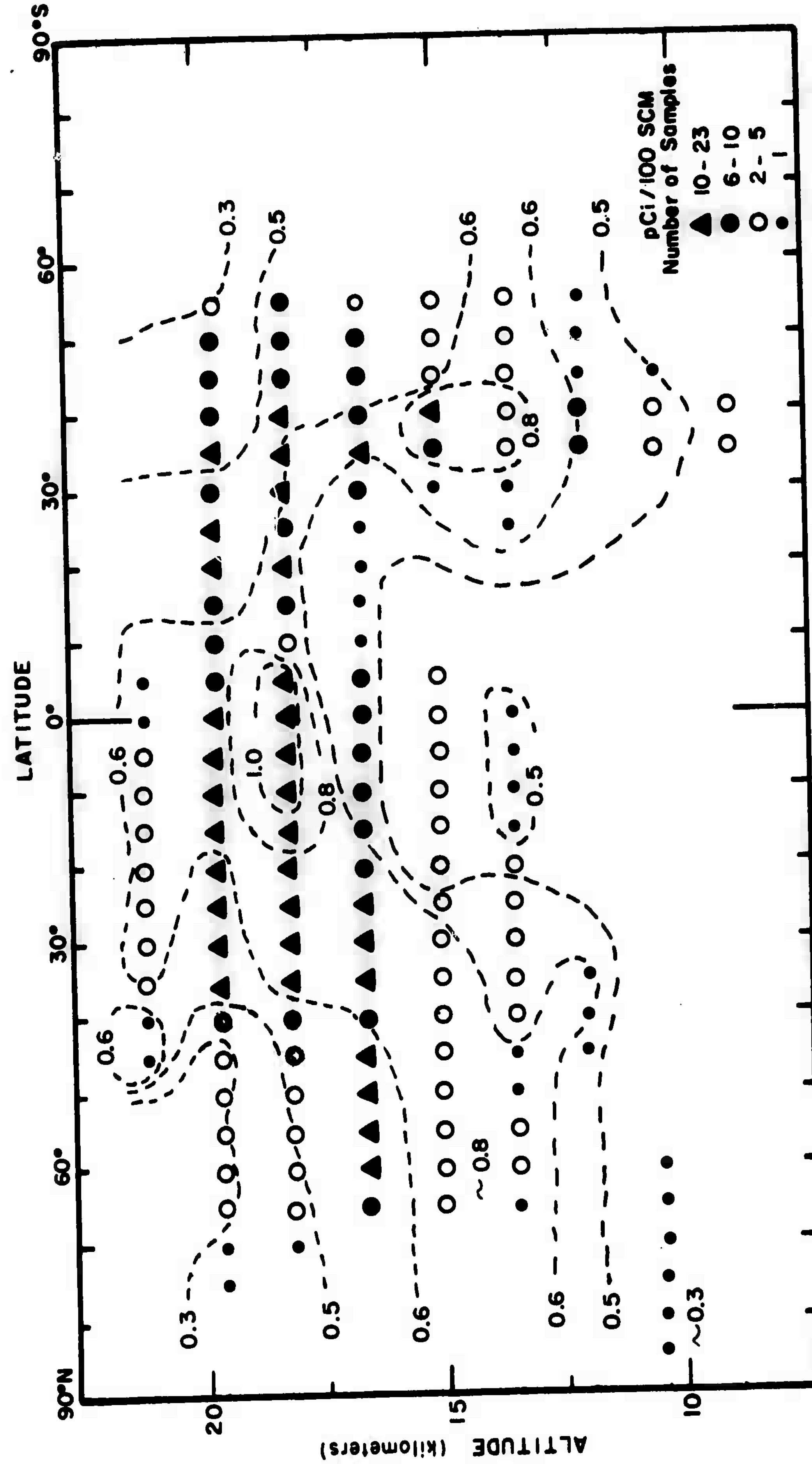

FIGURE 124. THE ATMOSPHERIC DISTRIBUTION OF LEAD-210, OCT 1957-JUL 1959

TABLE 121. The Atmospheric Concentrations of Lead-210 (pCi/100 SCM), During October 1957 - July 1959 (The Number of Samples Which Each Value Represents Follows it in Parentheses)

Latitude	Altitude Kilometers 9.1	10.7	12.2	13.7	15.2	16.8	18.3	19.8	21.3
90°N		0.32 (1)							
85°N		0.32 (1)							
80°N		0.32 (1)							
75°N		0.32 (1)						0.44 (1)	
70°N		0.32 (1)			0.73 (1)		0.41 (1)	0.44 (1)	
65°N		0.32 (1)		0.67 (1)	0.67 (3)	0.60 (9)	0.46 (3)	0.30 (3)	
60°N		0.32 (1)		0.76 (2)	0.67 (3)	0.59 (11)	0.46 (3)	0.32 (4)	
55°N				0.76 (2)	0.67 (3)	0.62 (13)	0.51 (4)	0.32 (4)	
50°N				0.67 (1)	0.67 (3)	0.62 (13)	0.51 (4)	0.32 (4)	
45°N			0.49 (1)	0.64 (1)	0.67 (3)	0.62 (13)	0.51 (4)	0.29 (3)	0.76 (1)
40°N			0.64 (1)	0.59 (3)	0.75 (4)	0.64 (10)	0.49 (6)	0.43 (3)	0.76 (1)
35°N			0.64 (1)	0.59 (3)	0.76 (5)	0.68 (14)	0.73 (16)	0.56 (16)	0.65 (2)
30°N				0.57 (2)	0.76 (5)	0.67 (14)	0.73 (16)	0.62 (21)	0.65 (3)
25°N				0.57 (2)	0.48 (3)	0.68 (12)	0.73 (16)	0.59 (21)	0.65 (4)
20°N				0.44 (2)	0.35 (3)	0.70 (9)	0.78 (17)	0.57 (23)	0.62 (3)
15°N				0.64 (1)	0.35 (2)	0.64 (9)	0.95 (13)	0.70 (12)	0.65 (2)
10°N				0.64 (1)	0.35 (2)	0.57 (7)	0.95 (13)	0.73 (13)	0.65 (2)
5°N				0.64 (1)	0.35 (2)	0.57 (7)	1.0 (11)	0.68 (11)	0.65 (2)
0°N				0.64 (1)	0.35 (2)	0.54 (6)	1.0 (11)	0.75 (11)	0.67 (1)
5°S					0.35 (2)	0.54 (7)	1.0 (11)	0.76 (9)	0.67 (1)
10°S						0.57 (1)	0.67 (5)	0.64 (7)	
15°S						0.57 (1)	0.67 (7)	0.64 (7)	
20°S						0.57 (1)	0.67 (10)	0.52 (11)	
25°S				0.72 (1)		0.57 (1)	0.65 (9)	0.52 (11)	
30°S				0.72 (1)	0.67 (1)	0.59 (3)	0.60 (10)	0.54 (9)	
35°S	0.48 (2)	0.48 (4)	0.62 (6)	0.86 (5)	0.91 (9)	0.64 (10)	0.64 (13)	0.44 (16)	
40°S	0.48 (2)	0.48 (4)	0.64 (8)	0.84 (4)	0.83 (11)	0.64 (8)	0.52 (11)	0.40 (10)	
45°S		0.32 (1)	0.59 (1)	0.67 (2)	0.57 (5)	0.56 (8)	0.51 (9)	0.35 (6)	
50°S			0.59 (1)	0.67 (2)	0.60 (5)	0.56 (8)	0.51 (9)	0.35 (6)	
55°S			0.59 (1)	0.67 (2)	0.60 (5)	0.56 (5)	0.51 (9)	0.32 (3)	

in pCi per 100 SCM were derived from the mean values at each sampling point. Some details of the ditribution are uncertain due to the scarcity of samples in some regions.

The accuracy of some of the Pb^{210} measurements made by counting the Bi^{210} daughter grown in after purification of the lead-210 was checked by also measuring the polonium-210 formed after lead purification. This was done some three to six years after sampling so that equilibrium between the lead-210 and polonium 210 was assured. Some discrepancies between the two sets of results were found as shown in Table 122. The polonium-210 derived data were considered the more reliable since they showed less scatter. However for most samples the "preferred" value is the mean of the two derived values. Where it seemed possible and important to eliminate erroneous data, polonium-210 or bismuth-210 values which appeared too high or too low were rejected, perhaps in some cases arbitrarily. The rejection amounted to about three percent of the analyses.

Table 123 compares the lead-210 concentrations with those of fission products. During the measurements of bismuth-210, traces of beta emitters remaining with the purified lead-210 from high concentrations of fission products in the air particulates could result in erroneously high values for the lead-210 concentration. There is, however, no apparent correlation between concentrations of beta emitters and lead-210. This lack of correlation also suggests the absence of bomb produced lead-210. General agreement with the distribution of lead-210 determined from samples taken during the period October 1957 to July 1959 and that reported by Telegadas [76] and Peterson [77] for the periods in 1960 and 1961 were found

TABLE 122. Lead-210 Concentrations Derived from Bismuth or Polonium-210 Ingrowth Following Lead Purification - Air Particulates Sampled from 1957 to 1959

Sample Number	Collection Date	$\frac{\text{pCi Pb}^{210}}{\text{100 SCM}}$ from Bi^{210}	$\frac{\text{pCi Pb}^{210}}{\text{100 SCM}}$ from Po^{210}	Po^{210}/Bi^{210}	$\frac{\text{pCi Pb}^{210}}{\text{100 SCM}}$ "preferred" value
ST-83	29 Aug 57	1.1A	0.81A	0.76	0.94
ST-84	4 Oct 57	1.4A	(≤0.06)	(≤0.04)	1.41
ST-1	16 Oct 57	0.94B	-	-	0.94
ST-85	8 Nov 57	(2.1)B	0.51C	(0.24)	0.51
ST-86	12 Nov 57	1.1A	0.52A	0.46	0.83
ST-87	12 Nov 57	1.1B	0.41B	0.39	0.73
ST-88	20 Nov 57	0.81B	0.70B	0.87	0.76
ST-4	22 Nov 57	(2.3)A	-	-	-
ST-5	22 Nov 57	0.80C	-	-	0.80
ST-89	22 Nov 57	1.6A	1.0B	0.62	1.3
ST-90	26 Nov 57	-	0.87A	-	0.87
ST-6	26 Nov 57	0.24C	-	-	0.24
ST-91	26 Nov 57	1.1A	0.80A	0.73	0.94
ST-92	3 Dec 57	0.80B	0.33B	0.42	0.57
ST-93	3 Dec 57	1.1B	0.81B	0.71	0.98
ST-94	3 Dec 57	1.1B	0.54B	0.47	0.84
ST-95	14 Dec 57	0.51B	0.56B	1.09	0.54
ST-96	14 Dec 57	(0.14)D	0.78A	(5.44)	0.78
ST-97	14 Dec 57	0.59B	0.70A	1.18	0.64
ST-98	17 Dec 57	0.44B	0.73A	1.62	0.59
ST-99	10 Jan 58	0.87B	0.78A	0.89	0.83
ST-8	10 Jan 58	0.68A	-	-	0.68
ST-100	10 Jan 58	0.35B	0.24B	0.65	0.29
ST-10	24 Jan 58	0.51B	-	-	0.51
ST-11	24 Jan 58	0.41B	-	-	0.41
ST-12	31 Jan 58	0.67A	-	-	0.67
ST-13	31 Jan 58	0.56C	-	-	0.56
ST-102	31 Jan 58	0.80B	0.49A	0.62	0.64
ST-103	4 Feb 58	0.65B	0.67A	1.01	0.67
ST-104	7 Feb 58	1.2 B	0.56A	0.45	0.89
ST-14	7 Feb 58	0.51C	-	-	0.51
ST-15	7 Feb 58	0.35C	-	-	0.35
ST-105	21 Feb 58	0.62A	0.59B	0.95	0.60
ST-17	21 Feb 58	0.54A	-	-	0.54
ST-106	26 Feb 58	0.65A	0.60B	0.93	0.64
ST-107	26 Feb 58	1.4B	0.41B	0.29	0.91
ST-108	1 Mar 58	0.86A	0.73A	0.86	0.80
ST-109	1 Mar 58	0.35C	0.44B	1.23	0.40
ST-18	1 Mar 58	0.41A	-	-	0.41
ST-110	5 Mar 58	-	0.94A	-	0.94
ST-111	5 Mar 58	1.0C	0.64D	0.61	0.83
ST-112	11 Mar 58	0.91A	0.49A	0.54	0.70
ST-19	28 Mar 58	0.48A	-	-	0.48
ST-20	28 Mar 58	0.49A	-	-	0.49

Data rejected as being incorrect are placed in parentheses.

Error % Code: A <5, B = 5-10, C = 10-20, D = 20-50.

ISOTOPES
A Teledyne Company
TABLE 122. (continued)

Sample Number	Collection Date	pCi Pb^{210} / 100 SCM from Bi ^{210}	pCi Pb^{210} / 100 SCM from Po^{210}	Po^{210}/Bi^{210}	pCi Pb^{210} / 100 SCM "preferred" value
ST-21	28 Mar 58	0.49B	-	-	0.49
ST-22	28 Mar 58	0.56A	-	-	0.56
ST-23	1 Apr 58	0.24A	-	-	0.24
ST-24	1 Apr 58	0.41A	-	-	0.41
ST-25	1 Apr 58	1.2 A	-	-	1.2
ST-26	4 Apr 58	0.57A	-	-	0.57
ST-27	4 Apr 58	0.56A	-	-	0.56
ST-28	8 Apr 58	0.35A	-	-	0.35
ST-29	8 Apr 58	0.67A	-	-	0.67
ST-113	8 Apr 58	0.78A	0.59A	0.76	0.68
ST-30	8 Apr 58	0.49A	-	-	0.49
ST-31	15 Apr 58	0.59B	-	-	0.59
ST-32	15 Apr 58	0.52A	-	-	0.52
ST-33	15 Apr 58	0.94B	-	-	0.94
ST-34	25 Apr 58	0.38A	-	-	0.38
ST-115	2 May 58	0.48B	0.56A	1.15	0.51
ST-116	2 May 58	0.57A	0.43A	0.75	0.49
ST-35	6 May 58	0.62B	-	-	0.62
ST-36	6 May 58	0.84A	-	-	0.84
ST-37	6 May 58	0.67A	-	-	0.67
ST-38	6 May 58	0.44B	-	-	0.44
ST-40	6 Jun 58	0.27B	-	-	0.27
ST-41	6 Jun 58	0.60A	-	-	0.60
ST-118	20 Jun 58	0.62B	0.41B	0.66	0.51
ST-43	24 Jun 58	1.0A	-	-	1.0
ST-44	24 Jun 58	0.92B	-	-	0.92
ST-45	1 Jul 58	0.33C	-	-	0.33
ST-46	1 Jul 58	0.41C	-	-	0.41
ST-120	4 Jul 58	1.1B	0.75A	0.66	0.95
ST-121	4 Jul 58	0.70B	0.65A	0.94	0.67
ST-47	8 Jul 58	0.98B	-	-	0.98
ST-48	12 Sep 58	0.49A	0.40B	0.79	0.44
ST-49	12 Sep 58	1.2C	0.92A	0.78	1.0
ST-122	19 Sep 58	(3.6)A	0.92C	(0.26)	0.92
ST-50	19 Sep 58	0.95B	-	-	0.95
ST-51	23 Sep 58	0.97B	0.75B	0.77	0.86
ST-52	23 Sep 58	0.92A	-	-	0.92
ST-53	23 Sep 58	-	0.64A	-	0.64
ST-54	27 Sep 58	0.67A	0.80A	1.20	0.73
ST-55	27 Sep 58	0.44A	(1.1)A	(2.46)	0.44
ST-56	30 Sep 58	0.73A	-	-	0.73
ST-57	30 Sep 58	0.67A	-	-	0.67
ST-58	1 Oct 58	0.41B	-	-	0.41
ST-124	2 Oct 58	-	(0.10)C	-	-
ST-125	3 Oct 58	-	1.2A	-	1.2
ST-59	7 Oct 58	1.1B	-	-	1.1
ST-126	7 Oct 58	2.6C	3.1C	0.84	2.8
ST-128	10 Oct 58	0.54C	0.48B	0.88	0.51

Data rejected as being incorrect are placed in parentheses.

Error % Code: A <5, B = 5-10, C = 10-20, D = 20-50.

TABLE 122. (continued)

Sample Number	Collection Date	pCi Pb^{210} / 100 SCM from Bi^{210}	pCi Pb^{210} / 100 SCM from Po^{210}	Po^{210}/Bi^{210}	pCi Pb^{210} / 100 SCM "preferred" value
ST-60	10 Oct 58	0.67B	-	-	0.67
ST-129	14 Oct 58	(2.5)B	1.1 A	(0.44)	1.1
ST-61	14 Oct 58	0.30B	0.33A	1.06	0.32
ST-62	17 Oct 58	1.2A	-	-	1.2
ST-64	19 Oct 58	0.38B	-	-	0.38
ST-131	21 Oct 58	-	0.80A	-	0.80
ST-132	21 Oct 58	(2.0)B	0.64C	(0.32)	0.64
ST-133	22 Oct 58	-	0.49B	-	0.49
ST-135	29 Oct 58	1.7B	1.4A	0.84	1.5
ST-136	29 Oct 58	0.89B	0.91A	1.02	0.89
ST-71	7 Nov 58	0.81A	-	-	0.81
ST-72	7 Nov 58	0.49B	-	-	0.49
ST-137	15 Nov 58	1.1B	1.1A	1.02	1.1
ST-74	15 Nov 58	0.46C	-	-	0.46
ST-75	16 Nov 58	0.36B	-	-	0.36
ST-138	18 Nov 58	1.6B	0.38A	0.24	1.0
ST-140	18 Nov 58	-	0.25C	-	0.25
ST-141	20 Nov 58	-	0.70B	-	0.70
ST-76	21 Nov 58	0.67B	-	-	0.67
ST-143	21 Nov 58	0.54B	0.54B	1.02	0.54
ST-77	22 Nov 58	0.38B	0.89A	2.31	0.64
ST-78	25 Nov 58	1.3B	-	-	1.3
ST-79	25 Nov 58	1.0A	-	-	1.0
ST-80	25 Nov 58	0.41B	0.51A	1.24	0.46
ST-81	28 Nov 58	1.2B	-	-	1.2
ST-82	28 Nov 58	0.25B	0.73A	2.83	0.49
ST-145	3 Dec 58	0.52B	0.51A	0.95	0.51
ST-146	3 Dec 58	0.62B	0.49B	0.79	0.56
ST-147	3 Dec 58	0.73B	0.73B	0.98	0.73
ST-148	3 Dec 58	1.5D	0.73B	0.50	1.1
ST-149	3 Dec 58	0.72B	0.86B	1.21	0.80
ST-150	3 Dec 58	1.4B	0.95B	0.67	1.2
ST-151	9 Dec 58	1.0B	0.75A	0.74	0.87
ST-152	12 Dec 58	0.97A	0.75A	0.76	0.86
ST-153	12 Dec 58	0.73B	1.1 A	1.45	0.89
ST-154	12 Dec 58	0.27C	0.84A	3.04	0.56
ST-155	12 Dec 58	(1.9) C	0.29D	(0.14)	0.29
ST-156	16 Dec 58	0.86B	0.68B	0.80	0.76
ST-157	16 Dec 58	0.87B	0.65A	0.74	0.76
ST-158	16 Dec 58	0.56B	0.59A	1.05	0.57
ST-159	16 Dec 58	0.36B	0.48B	1.30	0.41
ST-160	19 Dec 58	0.51C	0.54B	1.04	0.52
ST-161	19 Dec 58	0.51C	0.52B	1.04	0.51
ST-162	19 Dec 58	0.91B	0.68A	0.76	0.80
ST-163	19 Dec 58	0.57B	0.29B	0.51	0.43
ST-164	23 Dec 58	0.44B	0.44A	1.02	0.44
ST-165	23 Dec 58	0.56B	0.54A	0.98	0.54

Data rejected as being incorrect are placed in parentheses.

Error % Code: A <5, B = 5-10, C = 10-20, D = 20-50.

TABLE 122 (continued)

Sample Number	Collection Date	pCi Pb^{210} / 100 SCM from Bi^{210}	pCi Pb^{210} / 100 SCM from Po^{210}	Po^{210}/Bi^{210}	pCi Pb^{210} / 100 SCM "preferred" value
ST-166	23 Dec 58	1.0B	0.72B	0.68	0.89
ST-167	23 Dec 58	0.41C	0.48A	1.13	0.44
ST-173	6 Jan 59	-	0.67A	-	0.67
ST-174	9 Jan 59	-	0.78A	-	0.78
ST-175	9 Jan 59	-	0.59A	-	0.59
ST-176	13 Jan 59	-	0.65A	-	0.65
ST-177	13 Jan 59	-	0.57A	-	0.57
ST-178	16 Jan 59	-	0.57B	-	0.57
ST-179	19 Jan 59	-	0.46B	-	0.46
ST-180	22 Jan 59	-	0.59A	-	0.59
ST-181	25 Jan 59	-	0.51A	-	0.51
ST-182	28 Jan 59	-	0.48A	-	0.48
ST-183	3 Feb 59	-	0.57B	-	0.57
ST-184	6 Feb 59	-	0.64A	-	0.64
ST-185	6 Feb 59	-	0.64A	-	0.64
ST-186	6 Feb 59	-	0.35B	-	0.35
ST-187	10 Feb 59	-	0.57A	-	0.57
ST-188	14 Feb 59	-	0.70A	-	0.70
ST-189	14 Feb 59	-	0.57A	-	0.57
ST-190	14 Feb 59	-	0.25C	-	0.25
ST-191	20 Feb 59	-	0.54A	-	0.54
ST-192	20 Feb 59	-	0.59B	-	0.59
ST-193	20 Feb 59	-	0.62A	-	0.62
ST-194	24 Feb 59	-	0.72A	-	0.72
ST-195	24 Feb 59	-	0.49B	-	0.49
ST-196	24 Feb 59	-	0.60A	-	0.60
ST-197	6 Mar 59	-	0.60A	-	0.60
ST-198	6 Mar 59	-	0.54B	-	0.54
ST-199	10 Mar 59	-	0.44A	-	0.44
ST-200	10 Mar 59	-	0.64A	-	0.64
ST-201	13 Mar 59	-	0.30B	-	0.30
ST-202	17 Mar 59	-	0.57A	-	0.57
ST-203	17 Mar 59	-	0.72A	-	0.72
ST-204	17 Mar 59	-	0.59A	-	0.59
ST-205	24 Mar 59	-	0.54A	-	0.54
ST-206	27 Mar 59	-	0.30B	-	0.30
ST-207	1 Apr 59	-	0.67A	-	0.67
ST-208	3 Apr 59	-	0.68A	-	0.68
ST-209	3 Apr 59	-	0.67A	-	0.67
ST-210	7 Apr 59	-	0.52A	-	0.52
ST-211	10 Apr 59	-	0.54A	-	0.54
St-212	10 Apr 59	-	0.51B	-	0.51
ST-213	10 Apr 59	-	0.11D	-	0.11
ST-214	14 Apr 59	-	0.32A	-	0.32
ST-215	17 Apr 59	-	0.64B	-	0.64
ST-216	17 Apr 59	-	0.62A	-	0.62

Data rejected as being incorrect are placed in parentheses.

Error % Code: A <5, B = 5-10, C = 10-20, D = 20-50.

TABLE 122. (continued)

Sample Number	Collection Date	pCi Pb^{210} / 100 SCM from Bi^{210}	pCi Pb^{210} / 100 SCM from Po^{210}	Po^{210}/Bi^{210}	pCi Pb^{210} / 100 SCM "preferred" value
ST-217	17 Apr 59	-	0.48A	-	0.48
ST-218	19 Apr 59	-	0.41A	-	0.41
ST-219	21 Apr 59	-	0.48A	-	0.48
ST-220	21 Apr 59	-	0.25B	-	0.25
ST-221	24 Apr 59	-	0.35C	-	0.35
ST-222	5 May 59	-	0.51B	-	0.51
ST-224	8 May 59	-	0.72C	-	0.72
ST-225	12 May 59	-	0.67B	-	0.67
ST-226	12 May 59	-	0.27C	-	0.27
ST-227	15 May 59	-	0.62A	-	0.62
ST-228	15 May 59	-	0.54A	-	0.54
ST-229	20 May 59	-	0.44A	-	0.44
ST-230	20 May 59	-	0.51A	-	0.51
ST-231	20 May 59	-	0.64A	-	0.64
ST-232	24 May 59	-	0.40A	-	0.40
ST-233	24 May 59	-	0.36B	-	0.36
ST-234	26 May 59	-	0.59A	-	0.59
ST-235	26 May 59	-	0.56A	-	0.56
ST-236	29 May 59	-	0.72A	-	0.72
ST-237	2 Jun 59	-	0.32	-	0.32
ST-238	9 Jun 59	-	0.72A	-	0.72
ST-239	12 Jun 59	-	0.60A	-	0.60
ST-240	16 Jun 59	-	0.57A	-	0.57
ST-241	16 Jun 59	-	0.40B	-	0.40
ST-242	16 Jun 59	-	0.73B	-	0.73
ST-244	26 Jun 59	-	0.49B	-	0.49
ST-245	26 Jun 59	-	0.87A	-	0.87
ST-246	1 Jul 59	-	0.38A	-	0.38
ST-247	7 Jul 59	-	0.22B	-	0.22
ST-248	10 Jul 59	-	(1.9)A	-	-
ST-249	14 Jul 59	-	0.64A	-	0.64
ST-250	21 Jul 59	-	(0.10)A	-	-
ST-251	21 Jul 59	-	0.72A	-	0.72
ST-252	24 Jul 59	-	0.52A	-	0.52
ST-253	24 Jul 59	-	0.36A	-	0.36
ST-254	28 Jul 59	-	0.91A	-	0.91
ST-255	28 Jul 59	-	0.86A	-	0.86
ST-256	28 Jul 59	-	0.54A	-	0.54
ST-257	28 Jul 59	-	0.97B	-	0.97

Data rejected as being incorrect are placed in parentheses.

Error % Code: A <5, B = 5-10, C = 10-20, D = 20-50.

TABLE 123. The Atmospheric Concentrations of Lead-210, Strontium-90 and Cerium-144 from October 1957 to July 1959

Sample Number	Collection Date	Latitude	Altitude (km)	Total β	Activities pCi/100 SCM Sr^{90}(est.)	Sr^{90}(meas.)	Ce^{144}	Pb^{210}
ST-83	29 Aug 57	32°N	17	28,000	92	124A	(3900)A	0.94
ST-84	4 Oct 57	32°N	20	68,000	285	299A	3500A	1.4
ST-1	16 Oct 57	28°-14°N	17	48,000	114	-	-	0.94
ST-85	8 Nov 57	65°-44°N	17	105,000	251	283A	4180A	0.51
ST-86	12 Nov 57	34°-22°N	20	300,000	402	353A	7890A	0.83
ST-87	12 Nov 57	22°N-2°S	20	430,000	448	499A	10,100A	0.73
ST-88	20 Nov 57	45°-22°N	21	32,000	210	204A	2230A	0.76
ST-4	22 Nov 57	65°-45°N	14	150,000	207	-	-	-
ST-5	22 Nov 57	44°-22°N	19	330,000	398	-	-	0.80
ST-89	22 Nov 57	16°N-7°S	19	400,000	1830	2020A	60,100A	1.3
ST-90	26 Nov 57	64°-51°N	13	280,000	328	(40)A	8650A	0.87
ST-6	26 Nov 57	44°-16°N	18	210,000	213	-	-	0.24
ST-91	26 Nov 57	16°N-7°S	18	150,000	122	134A	3720A	0.94
ST-92	3 Dec 57	67°-44°N	18	230,000	312	328A	7820A	0.57
ST-93	3 Dec 57	39°-22°N	17	32,000	51	51A	1240A	0.98
ST-94	3 Dec 57	21°-11°N	17	20,000	30	(8.4)A	824A	0.84
ST-95	14 Dec 57	66°-44°N	18	200,000	318	343A	8600A	0.54
ST-96	14 Dec 57	44°-33°N	17	200,000	278	251A	8080A	0.78
ST-97	14 Dec 57	33°-22°N	17	54,000	94	98A	2350A	0.64
ST-98	17 Dec 57	44°-22°N	16	120,000	175	180A	4670A	0.59
ST-99	10 Jan 58	55°-44°N	17	150,000	329	366A	7550A	0.83
ST-8	10 Jan 58	44°-22°N	16	83,000	175	-	-	0.68
ST-100	10 Jan 58	21°N-6°S	16	7,000	8.0	9.5A	-	0.29
ST-10	24 Jan 58	65°-45°N	15	170,000	347	-	-	0.51
ST-11	24 Jan 58	15°N-5°S	15	1,300	2.5	-	-	0.41
ST-12	31 Jan 58	65°-46°N	14	97,000	245	-	-	0.67
ST-13	31 Jan 58	42°-23°N	13	22,000	≤ 60	-	-	0.56
ST-102	31 Jan 58	20°N -4°S	13	1,100	1.6	(178)A	-	0.64

TABLE 123 (continued)

Sample Number	Collection Date	Latitude	Altitude (km)	Activities pCi/100 SCM: Total β	Sr^{90}(est.)	Sr^{90}(meas.)	Ce^{144}	Pb^{210}
ST-103	4 Feb 58	37°-16°N	20	110,000	420	(710A)	9300A	0.67
ST-104	7 Feb 58	67°-44°N	17	51,000	330	210A	6000A	0.89
ST-14	7 Feb 58	44°-26°N	17	21,000	130	-	-	0.51
ST-15	7 Feb 58	16°N-6°S	17	≤ 1300	≤ 5.6	-	-	0.35
ST-105	21 Feb 58	45°-33°N	17	46,000	300	-	5800A	0.69
ST-17	21 Feb 58	38°-16°N	21	25,000	200	-	-	0.54
ST-106	26 Feb 58	45°-33°N	14	32,000	190	210A	4600A	0.64
ST-107	26 Feb 58	38°-16°N	20	27,000	170	210A	3800A	0.91
ST-108	1 Mar 58	55°-33°N	17	16,000	110	140A	2400A	0.80
ST-109	1 Mar 58	33°-22°N	17	460	3.2	4.8A	-	0.40
ST-18	1 Mar 58	16°N-7°S	17	1100	6.8	-	-	0.41
ST-110	5 Mar 58	67°-44°N	17	33,000	280	300A	4700A	0.94
ST-111	5 Mar 58	16°N-6°S	19	84,000	450	640D	11,000A	0.83
ST-112	11 Mar 58	38°-16°N	20	-	270	320A	4700A	0.70
ST-19	28 Mar 58	61°-44°N	17	780,000	540	-	(140A)	0.48
ST-20	28 Mar 58	44°-21°N	17	(4900)	110	-	-	0.49
ST-21	28 Mar 58	38°-16°N	20	44,000	250	-	-	0.49
ST-22	28 Mar 58	16°N-7°S	17	≤ 750	4.0	-	-	0.56
ST-23	1 Apr 58	68°-44°N	20	70,000	180	170A	3100A	0.24
ST-24	1 Apr 58	44°-16°N	20	220,000	305	340A	6900A	0.41
ST-25	1 Apr 58	16°N-6°S	20	32,000	200	210A	4000A	1.2
ST-26	4 Apr 58	44°-22°N	14	110,000	210	-	-	0.57
ST-27	4 Apr 58	44°-16°N	17	360,000	330	400A	8200A	0.56
ST-28	8 Apr 58	66°-44°N	17	320,000	350	-	-	0.35
ST-29	8 Apr 58	44°-22°N	17	54,000	95	120A	2900A	0.67
ST-113	8 Apr 58	38°-16°N	20	33,000	220	310A	4300A	0.66
ST-30	8 Apr 58	16°N-7°S	17	590	32	-	-	0.49
ST-31	15 Apr 58	67°-44°N	17	170,000	330	400A	9000A	0.59
ST-32	15 Apr 58	44°-21°N	16	240,000	300	280A	5900A	0.52
ST-33	15 Apr 58	16°N-6°S	17	1000	3.2	-	-	0.94
ST-34	25 Apr 58	38°-16°N	20	36,000	170	220A	3300A	0.38

TABLE 123 (continued)

Sample Number	Collection Date	Latitude	Altitude (km)	Total β	Activities pCi/100 SCM: Sr^{90}(est.)	Sr^{90}(meas.)	Ce^{144}	Pb^{210}
ST-115	2 May 58	67°-44°N	17	140,000	320	410A	9000A	0.51
ST-116	2 May 58	38°-16°N	20	30,000	200	260A	3800A	0.49
ST-35	6 May 58	67°-44°N	17	200,000	370	-	9200A	0.62
ST-36	6 May 58	44°-22°N	17	54,000	100	-	3000A	0.84
ST-37	6 May 58	38°-16°N	20	54,000	230	290A	4700A	0.67
ST-38	6 May 58	16°N-5°S	17	9,100	13.0	-	-	0.44
ST-40	6 Jun 58	19°N	14	1,900	4.0	-	-	0.27
ST-41	6 Jun 58	19°N	17	160,000	97	80A	1700A	0.60
ST-42	6 Jun 58	19°N	20	120,000	200	250A	5100A	-
ST-118	20 Jun 58	19°-18°N	20	120,000	250	370A	5300A	0.51
ST-43	24 Jun 58	38°-16°N	18	120,000	280	270A	5100A	1.0
ST-44	24 Jun 58	16°N-6°S	18	180,000	130	-	2500A	0.92
ST-45	1 Jul 58	19°N	17	31,000	65	-	-	0.33
ST-46	1 Jul 58	19°N	20	160,000	320	-	-	0.41
ST-120	4 Jul 58	39°-16°N	18	87,000	190	260A	4800A	0.95
ST-121	4 Jul 58	16°-7°N	18	140,000	120	160A	3000A	0.67
ST-47	8 Jul 58	19°N	17	570,000	310	300A	8800A	0.98
ST-48	12 Sep 58	75°-71°N	20	4,300	120	120A	1260A	0.44
ST-49	12 Sep 58	10°N-18°S	20	330,000	670	600A	9400A	1.0
ST-122	19 Sep 58	3°S-16°S	18	150,000	460	270A	4600A	0.92
ST-50	19 Sep 58	16°S-35°S	18	12,000	130	-	-	0.95
ST-51	23 Sep 58	38°-21°N	18	59,000	210	250A	3400A	0.86
ST-52	23 Sep 58	21°N-6°S	18	400,000	390	400A	7500A	0.92
ST-53	23 Sep 58	35°-40°N	12	7,300	17	16A	270A	0.64
ST-54	27 Sep 58	71°N	15	21,000	240	220A	3600A	0.73
ST-55	27 Sep 58	71°N	20	4,400	95	140A	1300A	0.44
ST-56	30 Sep 58	16°S-35°S	18	20,000	120	120A	1600A	0.73
ST-57	30 Sep 58	35°S-57°S	18	21,000	130	140A	1900A	0.67

TABLE 123. (continued)

Sample Number	Collection Date	Latitude	Altitude (km)	Total β	Sr^{90}(est.)	Sr^{90}(meas.)	Ce^{144}	Pb^{210}
				Activities pCi/100 SCM				
ST-58	1 Oct 58	71°N	18	12,000	250	210A	2600A	0.41
ST-124	2 Oct 58	73°-71°N	15	2,200	(19)	49A	630A	-
ST-125	3 Oct 58	21°N-8°S	18	620,000	580	650A	14,000A	1.2
ST-59	7 Oct 58	38°-16°N	18	72,000	230	290A	4100A	1.1
ST-126	7 Oct 58	35°-40°S	15	24,000	(78)	140A	3300A	2.8
ST-127	7 Oct 58	45°-45°S	20	41,000	320	400A	11,000A	-
ST-128	10 Oct 58	38°-16°N	18	46,000	240	190A	3400A	0.51
ST-60	10 Oct 58	35°-57°S	18	17,000	120	140A	2000A	0.67
ST-129	14 Oct 58	16°N-6°S	18	1,200,000	1400	810A	31,000A	1.1
ST-61	14 Oct 58	35°-45°S	10	8,300	35	-	-	0.32
ST-130	17 Oct 58	38°-23°N	18	240,000	500	580A	13,000A	-
ST-62	17 Oct 58	22°N-8°S	18	810,000	1000	760A	20,000A	1.2
ST-64	19 Oct 58	44°-20°N	15	22,000	76	-	-	0.38
ST-131	21 Oct 58	35°-43°S	18	15,000	120	140A	(5,000A)	0.80
ST-132	21 Oct 58	35°-44°S	20	21,000	180	210A	(81A)	0.64
ST-133	22 Oct 58	44°N	12	1,500	(54)	4.4A	490A	0.49
ST-134	22 Oct 58	44°N	21	160,000	300	220A	7500A	-
ST-67	23 Oct 58	56°-44°N	17	150,000	320	260A	4800A	-
ST-135	29 Oct 58	44°-27°N	15	33,000	89	100A	3100A	1.5
ST-69	29 Oct 58	44°-20°N	17	1,100,000	840	590A	1900A	-
ST-136	29 Oct 58	38°-20°N	17	67,000	170	210A	5600A	0.89
ST-71	7 Nov 58	17°N-22°S	18	240,000	490	470A	11,000A	0.81
ST-72	7 Nov 58	29° 57°S	18	15,000	110	130A	1700A	0.49
ST-137	15 Nov 58	38°-17°N	18	640,000	770	780A	23,000A	1.1
ST-74	15 Nov 58	29°-57°S	18	12,000	110	-	-	0.46
ST-75	16 Nov 58	42°-20°N	15	35,000	67	-	-	0.36
ST-138	18 Nov 58	66°-44°N	15	380,000	430	420A	2300A	1.0
ST-139	18 Nov 58	55°-44°N	18	140,000	320	340A	7300A	-
ST-140	18 Nov 58	66°-44°N	20	14,000	120	110A	1600A	0.25
ST-141	20 Nov 58	55°-45°N	18	83,000	290	340A	-	0.70
ST-142	20 Nov 58	55°-45°N	20	36,000	230	250A	4200A	-
ST-76	21 Nov 58	10°-29°S	18	59,000	160	-	-	0.67
ST-143	21 Nov 58	29°-57°S	18	19,000	87	140A	4800A	0.54
ST-77	22 Nov 58	44°-20°N	18	160,000	330	340A	7000A	0.64

TABLE 123. (continued)

Sample Number	Collection Date	Latitude	Altitude (km)	Activities pCi/100 SCM: Total β	Sr^{90}(est.)	Sr^{90}(meas.)	Ce^{144}	Pb^{210}
ST-78	25 Nov 58	38°-22°N	18	150,000	390	350A	8000A	1.3
ST-79	25 Nov 58	22°N-6°S	18	140,000	360	320A	8000A	1.0
ST-80	25 Nov 58	35°-40°S	10	2,700	4.8	-	-	0.46
ST-144	25 Nov 58	35°-40°S	17	64,000	260	310A	4400A	-
ST-81	28 Nov 58	16°N-8°S	18	87,000	230	200A	5600A	1.2
ST-82	28 Nov 58	17°-57°S	18	19,000	100	150A	2000A	0.49
ST-145	3 Dec 58	35°-40°S	9	1,200	≤ 8.0	(110A)	(3000A)	0.51
ST-146	3 Dec 58	35°-40°S	11	1,600	9.5	(57A)	(680A)	0.56
ST-147	3 Dec 58	40°-41°S	12	6,800	41	(52A)	(6400A)	0.73
ST-148	3 Dec 58	35°-40°S	14	14,000	44	62A	3000A	1.1
ST-149	3 Dec 58	42°S	15	19,000	95	(7.6A)	4700A	0.80
ST-150	3 Dec 58	35°-40°S	17	27,000	100	(33A)	2600A	1.2
ST-151	9 Dec 58	38°-28°N	15	32,000	68	68A	2500A	0.87
ST-152	12 Dec 58	38°-17°N	18	120,000	380	320A	8300A	0.86
ST-153	12 Dec 58	16°N-8°S	18	120,000	300	310A	8100A	0.89
ST-154	12 Dec 58	10°-35°S	18	17,000	87	97A	2100A	0.56
ST-155	12 Dec 58	35°-57°S	18	9,800	98	120A	6300A	0.29
ST-156	16 Dec 58	38°-27°N	17	89,000	230	-	5100A	0.76
ST-157	16 Dec 58	25°-5°N	17	8,000	17	21B	700A	0.76
ST-158	16 Dec 58	2°-35°S	17	8,600	(25)	51B	5200A	0.57
ST-159	16 Dec 58	35°-57°S	17	15,000	97	110A	1000A	0.41
ST-160	19 Dec 58	38°-16°N	20	150,000	570	610A	12,000A	0.52
ST-161	19 Dec 58	16°N-8°S	20	210,000	780	800A	18,000A	0.51
ST-162	19 Dec 58	10°-35°S	20	15,000	92	120A	1900A	0.80
ST-163	19 Dec 58	35°-57°S	20	8,700	76	114A	1700A	0.43
ST-164	23 Dec 58	35°-40°S	9	620	4.8	3.2A	89B	0.44
ST-165	23 Dec 58	35°-40°S	11	1700	3.2	3.5A	190A	0.54
ST-166	23 Dec 58	35°-40°S	14	5400	25	35A	830A	0.89
ST-167	23 Dec 58	42°-43°S	15	10,000	32	40A	920A	0.44

TABLE 123. (continued)

Sample Number	Collection Date	Latitude	Altitude (km)	Total β	Activities pCi/100 SCM: Sr^{90}(est.)	Sr^{90}(meas.)	Ce^{144}	Pb^{210}
ST-173	6 Jan 59	29°-57°S	15	12,000	65	76A	1500A	0.67
ST-174	9 Jan 59	16°-8°S	18	68,000	250	250A	6600A	0.78
ST-175	9 Jan 59	10°-57°S	18	13,000	110	100A	1700A	0.59
ST-176	13 Jan 59	40°S	12	3,300	25	30A	550A	0.65
ST-177	13 Jan 59	41°-43°S	15	10,000	57	80A	1300A	0.57
ST-178	16 Jan 59	10°-51°S	20	15,000	130	160A	2200A	0.57
ST-179	19 Jan 59	38°-20°N	20	80,000	440	460A	8000A	0.46
ST-180	22 Jan 59	35°-57°S	15	9,100	49	73A	(36A)	0.59
ST-181	25 Jan 59	44°-20°N	18	83,000	360	400A	7000A	0.51
ST-182	28 Jan 59	35°-51°S	17	9,400	70	91A	1400A	0.48
ST-183	3 Feb 59	41°-57°S	15	8,400	65	76A	1200A	0.57
ST-184	6 Feb 59	38°-10°N	18	59,000	240	240A	5900A	0.64
ST-185	6 Feb 59	10°-29°S	18	9,400	62	81A	1400A	0.64
ST-186	6 Feb 59	49°-57°S	18	8,000	94	100A	1500A	0.35
ST-187	10 Feb 59	41°-57°S	17	9,500	67	98A	1300A	0.57
ST-188	14 Feb 59	32°N-8°S	20	75,000	340	430A	7600A	0.70
ST-189	14 Feb 59	10°-35°S	20	13,000	110	130A	1800A	0.57
ST-190	14 Feb 59	35°-57°S	20	7,500	91	100A	1300A	0.25
ST-191	20 Feb 59	27°N-8°S	20	81,000	340	400A	7100A	0.54
ST-192	20 Feb 59	16°-35°S	20	12,000	92	120A	1900A	0.59
ST-193	20 Feb 59	35°-57°S	15	8,000	40	54A	940A	0.62
ST-194	24 Feb 59	38°N-8°S	20	91,000	430	480A	8300A	0.72
ST-195	24 Feb 59	16°-35°S	20	10,000	86	110A	1600A	0.49
ST-196	24 Feb 59	35°-57°S	17	11,000	(38)	87A	1300A	0.60
ST-197	6 Mar 59	32°N-2°S	20	65,000	300	360A	6100A	0.60
ST-198	6 Mar 59	16°-35°S	20	10,000	92	110A	1600A	0.54
ST-199	10 Mar 59	38°-16°N	18	46,000	220	270A	6000A	0.44
ST-200	10 Mar 59	35°-57°S	17	7,600	75	80A	1800A	0.64
ST-201	13 Mar 59	35°-51°S	20	9,500	110	110A	3000A	0.30
ST-202	17 Mar 59	32°N-8°S	20	51,000	260	260A	6100A	0.57
ST-203	17 Mar 59	2°-28°S	20	22,000	140	160A	4800A	0.72
ST-204	17 Mar 59	35°-55°S	12	1,900	13	14A	550A	0.59
ST-205	24 Mar 59	35°-57°S	17	6,700	60	59A	2300A	0.54
ST-206	27 Mar 59	16°-52°S	20	9,500	100	97A	2100A	0.16

TABLE 123. (continued)

Sample Number	Collection Date	Latitude	Altitude (km)	Total β	Activities pCi/100 SCM: Sr^{90}(est.)	Sr^{90}(meas.)	Ce^{144}	Pb^{210}
ST-207	1 Apr 59	32°N-8°S	21	72,000	390	440A	8300A	0.67
ST-208	3 Apr 59	35°-40°S	12	1,600	13	14A	440B	0.68
ST-209	3 Apr 59	35°-40°S	15	5,600	40	25A	1000A	0.67
ST-210	7 Apr 59	29°-52°S	17	7,000	80	78A	1500A	0.52
ST-211	10 Apr 59	38°-10°N	20	49,000	310	390A	6000A	0.54
ST-212	10 Apr 59	35°-40°S	18	8,100	81	100A	1800A	0.51
ST-213	10 Apr 59	35°-40°S	20	7,500	92	110A	3100A	0.11
ST-214	14 Apr 59	90°-60°N	11	75,000	270	302A	8000A	0.32
ST-215	17 Apr 59	38°-27°N	17	30,000	181	(2000A)	3700A	0.64
ST-216	17 Apr 59	35°-40°S	12	1,300	9.5	-	-	0.62
ST-217	17 Apr 59	35°-40°S	15	4,900	(25)	49A	630A	0.48
ST-218	19 Apr 59	44°-20°N	18	40,000	250	300A	6900A	0.41
ST-219	21 Apr 59	66°-44°N	15	32,000	160	220A	4000A	0.48
ST-220	21 Apr 59	66°-44°N	18	41,000	400	320A	5800A	0.25
ST-221	24 Apr 59	35°-40°S	20	7,000	100	105A	(170B)	0.35
ST-222	5 May 59	16°-35°S	20	12,000	120	140A	2200A	0.51
ST-224	8 May 59	35°-40°S	20	8,000	98	(230B)	(5000A)	0.72
ST-225	12 May 59	29°-35°S	17	5,100	57	64A	990A	0.67
ST-226	12 May 59	35°-57°S	20	6,000	94	100A	2000A	0.27
ST-227	15 May 59	35°-40°S	12	3,200	30	32A	690A	0.62
ST-228	15 May 59	35°-40°S	15	5,700	64	68A	1000A	0.54
ST-229	20 May 59	68°-44°N	17	27,000	220	240A	3100A	0.44
ST-230	20 May 59	10°-35°S	20	15,900	160	160A	2900A	0.51
ST-231	20 May 59	35°-57°S	14	2,900	32	33A	610A	0.64
ST-232	24 May 59	44°-20°N	18	25,000	200	210A	4220A	0.40
ST-233	24 May 59	44°-20°N	20	32,000	370	350A	-	0.36
ST-234	26 May 59	12°-32°S	18	5,600	70	81A	-	0.59
ST-235	26 May 59	46°-57°S	16	4,900	81	78A	2200A	0.56
ST-236	29 May 59	35°-40°S	12	2,500	35	29A	-	0.72

TABLE 123. (continued)

Sample Number	Collection Date	Latitude	Altitude (km)	Total β	Activities (pCi/100 SCM) Sr^{90}(est.)	Sr^{90}(meas.)	Ce^{144}	Pb^{210}
ST-237	2 Jun 59	31°-35°S	20	7,200	94	(27A)	2300A	0.32
ST-238	9 Jun 59	23°-55°S	14	1,600	17	16A	-	0.72
ST-239	12 Jun 59	38°-4°N	20	30,000	300	(190A)	-	0.60
ST-240	16 Jun 59	60°-47°N	17	25,000	260	240A	-	0.57
ST-241	16 Jun 59	68°-47°N	20	33,000	420	390A	-	0.40
ST-242	16 Jun 59	35° 50°S	17	4,300	57	62A	1400A	0.73
ST-244	26 Jun 59	35°-40°S	12	1,700	24	(140A)	(2100A)	0.49
ST-245	26 Jun 59	35°-40°S	15	2,700	33	32A	890A	0.87
ST-246	1 Jul 59	38°N-2°S	20	30,000	330	(11A)	(340A)	0.38
ST-247	7 Jul 59	2°-28°S	20	16,000	200	(370A)	(1700A)	0.22
ST-248	10 Jul 59	35°-40°S	15	2,700	40	(920A)	(11,000A)	-
ST-249	14 Jul 59	27°-4°N	21	38,000	450	430A	4100A	0.64
ST-250	21 Jul 59	67°-44°N	14	12,000	110	(8.0)	(130A)	-
ST-251	21 Jul 59	15°-35°S	18	5,900	72	70A	1600A	0.72
ST-252	24 Jul 59	68°-45°N	17	25,000	260	290A	3600A	0.52
ST-253	24 Jul 59	62°-45°N	20	25,000	350	340A	4300A	0.36
ST-254	28 Jul 59	35°S	13	$\leq$ 700	6.4	8.3A	(430A)	0.91
ST-255	28 Jul 59	35°S	15	1,400	19	19A	620A	0.86
ST-256	28 Jul 59	35°S	16	4,100	80	73A	1000A	0.54
ST-257	28 Jul 59	35°S	18	8,300	120	130A	2000A	0.97

Note: Letters following nuclide concentrations represent counting statistics:

A = 0-5% C = 10-20%
B = 5-10% D = 20-50%

Data which are believed to be incorrect and have been rejected are placed in parentheses.

The chief feature in the distribution derived from STARDUST data is the occurrence of a layer of maximum concentration in the lower stratosphere at a height of about 14 kilometers in the polar stratosphere but sloping upward toward the equator to a height of 18 kilometers in the tropical stratosphere. Above this layer concentrations decrease with height. The highest concentrations were found in the equatorial stratosphere.

11.4 Distribution of Lead-210 and Polonium-210 STARDUST Measurements - 1961-1963

Analyses of lead-210 and polonium-210 were performed on a large number of STARDUST samples collected between June 1961 and March 1963. The frequency of analysis of these nuclides was decreased during 1962 as it became evident that it would be difficult to obtain useful data because of contamination of the samples by high activities of fission products from the atmospheric nuclear weapons tests performed during late 1961 and during 1962. Indeed the levels of activity of natural lead-210 and polonium-210 in the samples are so low that even contamination by laboratory materials or dust may constitute a problem. Nevertheless some useful conclusions may be drawn from them.

Lead-210 which enters the stratosphere from the troposphere or is produced in the stratosphere by decay of radon may experience a long stratospheric residence time. In this event its daughter product bismuth-210 will rapidly grow into equilibrium with it and, eventually, so will polonium-210. The curve shown in Figure 125 represents the increase in the activity ratio Po^{210}/Pb^{210} to be expected in lead-210 following its formation. If the stratospheric residence time of lead-210 is on the order of several years the ratio Po^{210}/Pb^{210} in stratospheric samples should approach 1.0. If the residence time is significantly shorter, much lower ratios should be found.

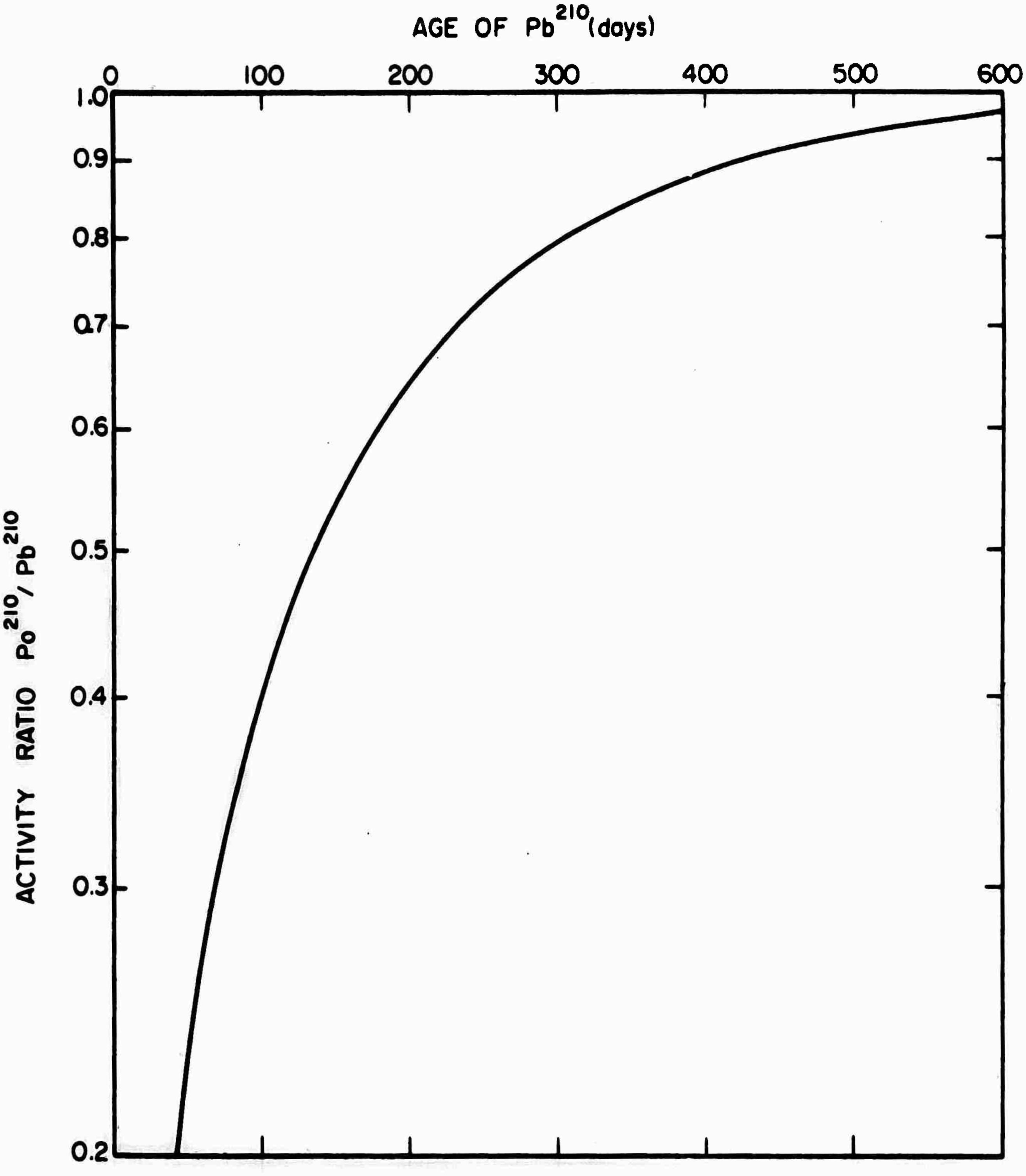

FIGURE 125. VARIATION OF THE ACTIVITY RATIO Po^{210}/Pb^{210} WITH THE AGE OF THE LEAD-210

Data points for a series of samples collected in the Southern Hemisphere during October 1961 - April 1962 are plotted in Figure 126. The straight lines drawn through the data points represent the locus of points for samples in which polonium-210 and lead-210 are approximately in radioactive equilibrium. The data points for samples which are not yet in equilibrium should fall below the lines. Much of the scatter of the points must be attributed to analytical errors. The fact that most points for stratospheric samples fall above the lines suggests that a bias, perhaps due to a calibration error, exists in the data.

In spite of their limitations the data in Figure 126 do permit some conclusions to be drawn. The mean values of the lead-210 concentrations in the tropical stratosphere (0° - 30°S) and the polar stratosphere (30° - 60°S) are virtually the same: 0.5±0.2 pCi/100 SCM. The polonium-210 concentrations also agree within the standard deviation. They are 0.7±0.2 pCi/100 SCM in the tropical and 0.6±0.2 in the polar stratosphere. The Po^{210}/Pb^{210} activity ratio in samples collected in the tropical troposphere and in the tropical tropopause layer is 0.35±0.2. This is much lower than the ratio found in stratospheric samples: 1.4±0.7 in the tropical and 1.2±0.7 in the polar stratosphere.

The mean distributions of lead-210 and polonium-210 in the stratosphere of the Northern Hemisphere during June to September 1961, before debris from the 1961 Soviet tests reached the sampling corridor, are shown in Figure 127 and in Tables 124 and 125. The data suggest that the highest concentrations of these nuclides occur in the tropical stratosphere and in the lower polar stratosphere. Within the polar stratosphere at least, the concentrations appear to be higher in the layer 3 kilometers thick, which is immediately above the tropopause layer, than they are in the higher stratosphere.

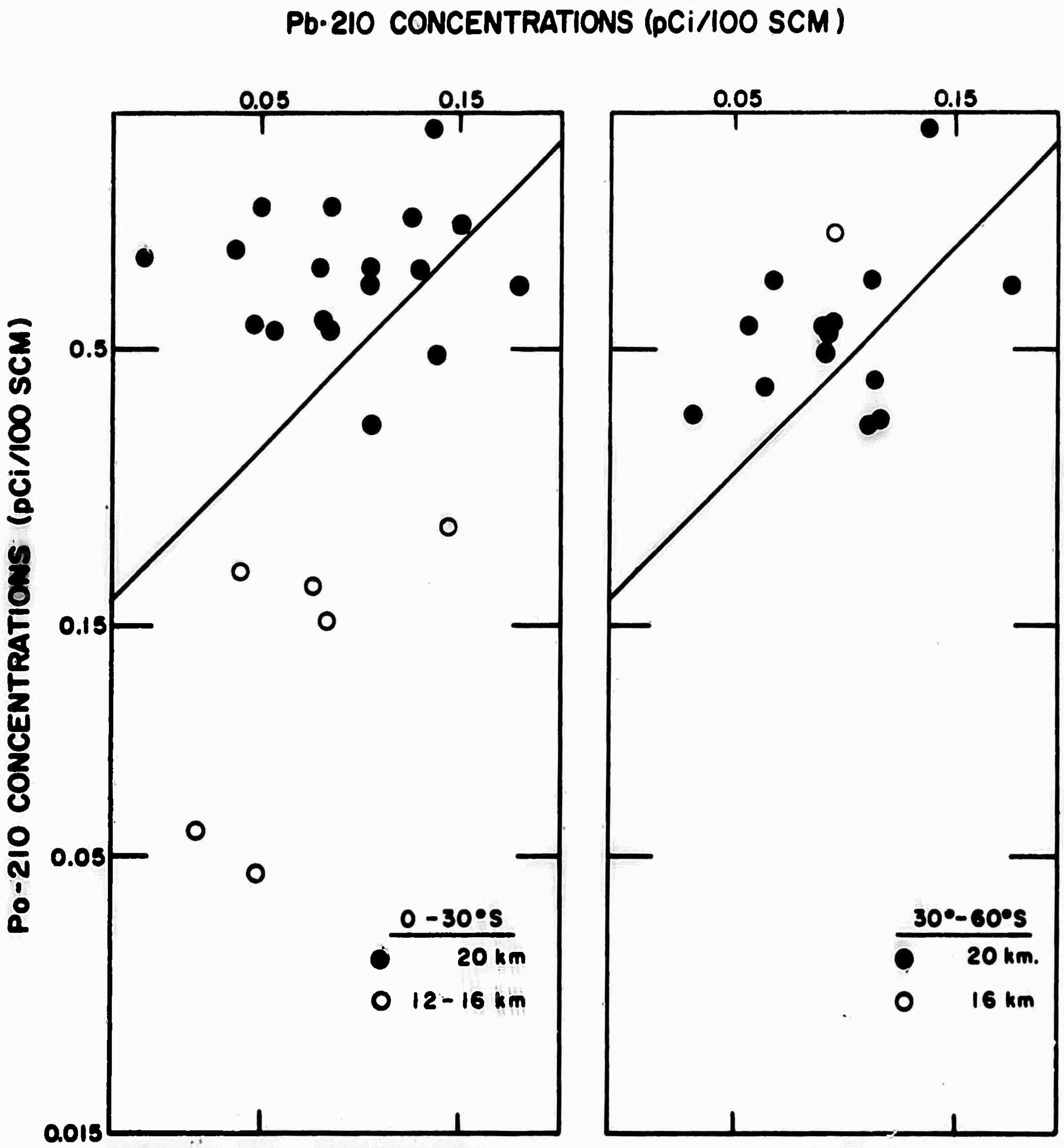

FIGURE 126. CONCENTRATIONS OF Pb-210 AND Po-210 COLLECTED IN THE SOUTHERN HEMISPHERE DURING OCTOBER, 1961 - APRIL, 1962

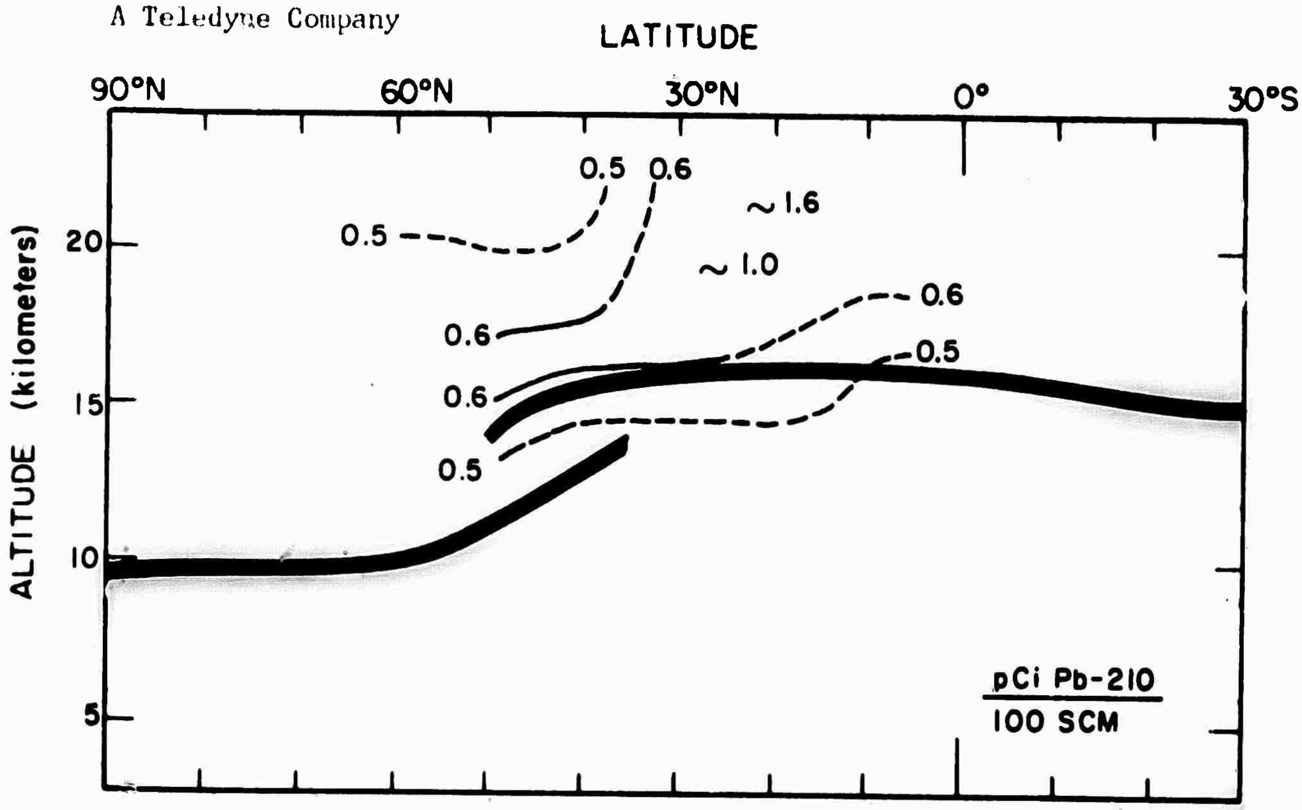

CONCENTRATIONS OF LEAD-210, JUN-SEP 1961

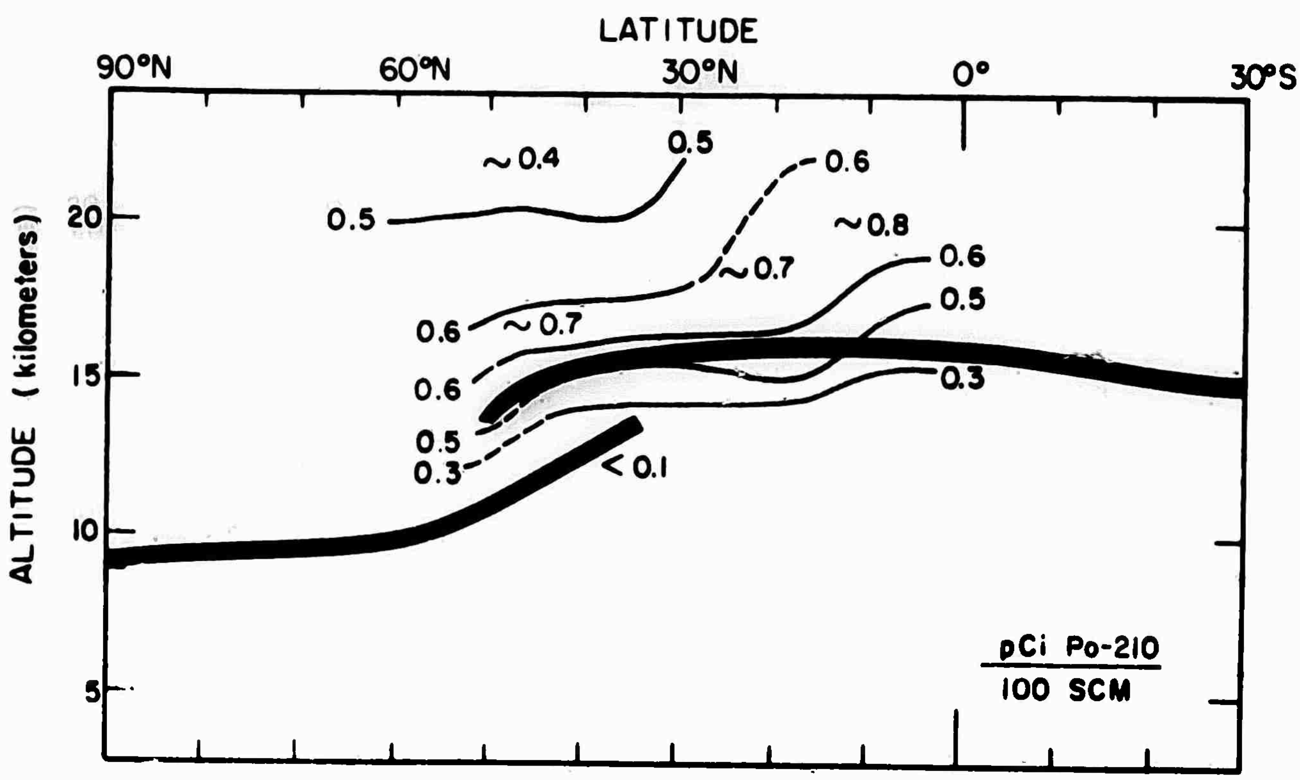

FIGURE 127. CONCENTRATIONS OF POLONIUM-210, JUN-SEP 1961

TABLE 124. The Concentrations of Lead-210 (pCi/100 SCM) in the Stratosphere June - September, 1961

Altitude (km)	Eilson South (~60°N)	Laughlin North (~40°N)	Laughlin Orbit (30°N)	Laughlin South (~20°N)	Hickam South (~10°N)
	Sampled Region				
21.3	-	0.43±0.33 (3)	0.98±0.78 (4)	1.7±1.4 (2)	-
19.8	0.54 (1)	0.65±0.21 (6)	0.54±0.14 (5)	1.0±0.62 (3)	0.64±0.22 (3)
18.3	-	0.46±0.13 (3)	0.62±0.22 (5)	-	0.56±0.11 (3)
16.8	-	0.64±0.10 (2)	1.1±0.27 (5)	-	-
15.2	-	0.57±0.40 (5)	-	-	1.1 ±1.3 (3)

The deviation from the mean, and in parentheses, the number of samples represented by each mean value follow it.

TABLE 125. The Concentrations of Polonium-210 (pCi/100 SCM corrected to plating date) in the Stratosphere, June - September 1961

Altitude (km)	Eielson South (~60°N)	Laughlin North (~40°N)	Laughlin Orbit (30°N)	Laughlin South (~20°N)	Hickam South (~10°N)
	Sampled Region				
21.3	-	0.43±0.06 (5)	0.60±0.14 (7)	0.65±0.05 (3)	-
19.8	0.46(1)	0.48±0.06 (9)	0.57±0.10 (7)	0.59±0.21 (6)	0.80±0.22 (5)
18.3	-	0.62±0.11 (4)	0.57±0.10 (7)	0.72 (1)	0.52±0.05 (3)
16.8	-	0.70±0.13 (4)	0.68±0.19 (7)	-	-
15.2	-	0.43±0.21 (5)	-	-	0.35±0.38 (3)
13.7	-	0.21 (1)	-	-	-
12.2	-	0.05 (1)	-	-	-

The deviation from the mean, and in parentheses, the number of samples represented by each mean value follow it.

Perhaps the data presented in Figures 126 and 127 are too uncentain to support a detailed interpretation. It is interesting, however to compare our results with the predictions of Jacobi and Andre[70] who calculated the vertical distribution of radon-220 and its decay products in the atmosphere by means of a solution of the diffusion equation which permitted them to use any vertical profile of the turbulent diffusion coefficient. For the calculation of vertical distribution of lead-210 and polonium-210, they used a profile of the turbulent diffusion coefficient which they believed to be representative of normal turbulence conditions throughout the troposphere. They have assumed a series of tropospheric residence times for lead-210 varying from 5 days to infinity and have calculated a distribution for each. While none of these actually fits the STARDUST data, the best agreements result from the use of 5- or 20-day residence times. Longer residence times result in predicted tropospheric concentrations of lead-210 which are much too high. The predicted lead-210 concentrations obtained using a 5-day tropospheric residence time are lower than the STARDUST results at all altitudes from 12.2 to 21.3 kilometers, and those obtained using a 20-day tropospheric residence time are higher than the STARDUST results for altitudes below 18 kilometers but agree with the STARDUST results at about 18 kilometers. Above 18 kilometers the predicted concentrations decrease very rapidly with altitude, a situation not confirmed by the STARDUST measurements. The predicted Po^{210}/Pb^{210} ratios increase rapidly with altitude above about 6.1 kilometers, approaching 1.0 at about 15.3 kilometers in the case of the 5-day tropospheric residence time and at about 18.3 kilometers in the case of the 20-day tropospheric residence time.

Although the STARDUST measurements do not confirm the details of the distributions calculated by Jacobi and Andre[70], they do appear to show two features of those distributions: a decrease of lead-210 concentrations with altitude above the tropopause layer, and an increase of the Po^{210}/Pb^{210} activity ratio to an equilibrium value of about 1.0 in the stratosphere.

Results of measurements of tropospheric concentrations of lead-210 and polonium-210 at 65° and 10°N during 1962 are summarized in Figure 128 . At 65°N the concentration of lead-210 increased with altitude, and so did the activity ratio Po^{210}/Pb^{210}. The apparent age of the lead-210, calculated from the Po^{210}/Pb^{210} ratio, increased with altitude from about a month at 7 kilometers to well over a year in the lower polar stratosphere. (The Po^{210}/Pb^{210} ratios are given for the plating date, on which the polonium-210 was separated from its parent lead-210, as well as for collection date since errors in the measurement of the ratio can be increased further by correction for polonium-210 growth between the collection date and plating date.)

Few samples collected in the troposphere at 10°N were available for measurement, so the data for that latitude may not be representative of the normal conditions. There was little variation of lead-210 concentration with altitude found in the tropical troposphere, and the age of the lead-210 appeared to range between about two weeks and ten weeks.

11.5 Distribution of Lead-210 and Polonium-210 STARDUST Measurements - 1964-1966

Lead-210 and polonium-210 measurements were made on a group of samples collected in December, 1964 to check earlier estimates of the stratospheric distribution of the Po^{210}/Pb^{210} activity ratio. To minimize the likelihood that samples would contain interfering beta activity, the samples chosen were those

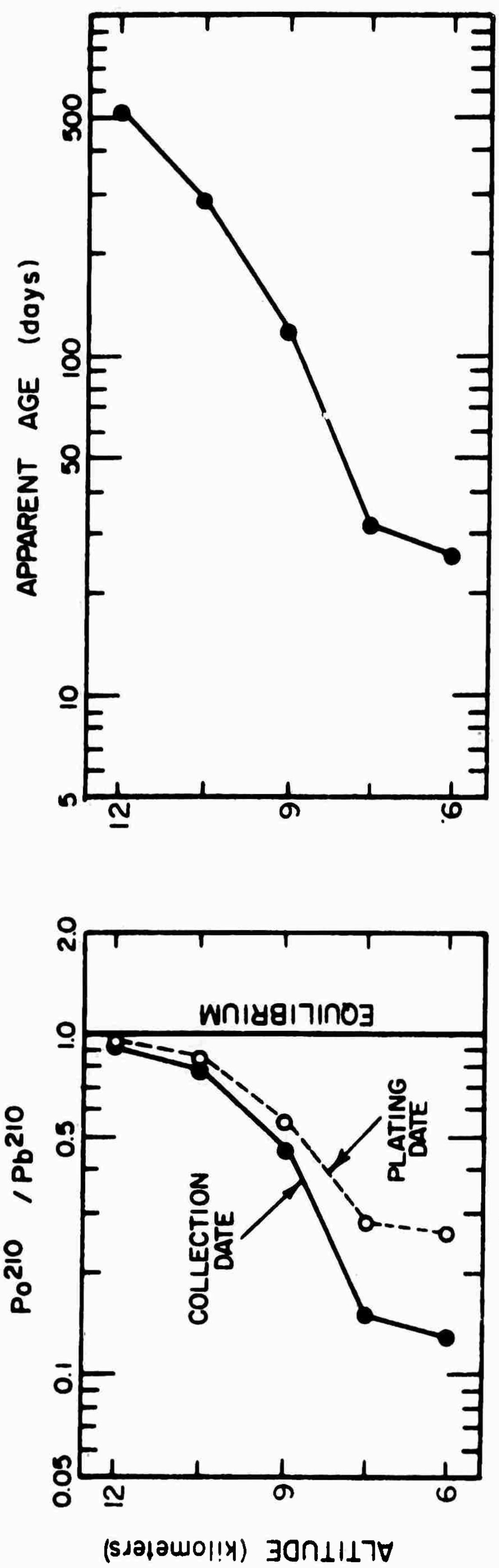

VARIATIONS IN Po^{210}/Pb^{210} AND APPARENT AGE OF Pb^{210} NEAR POLAR TROPOPAUSE (65°N) (1962)

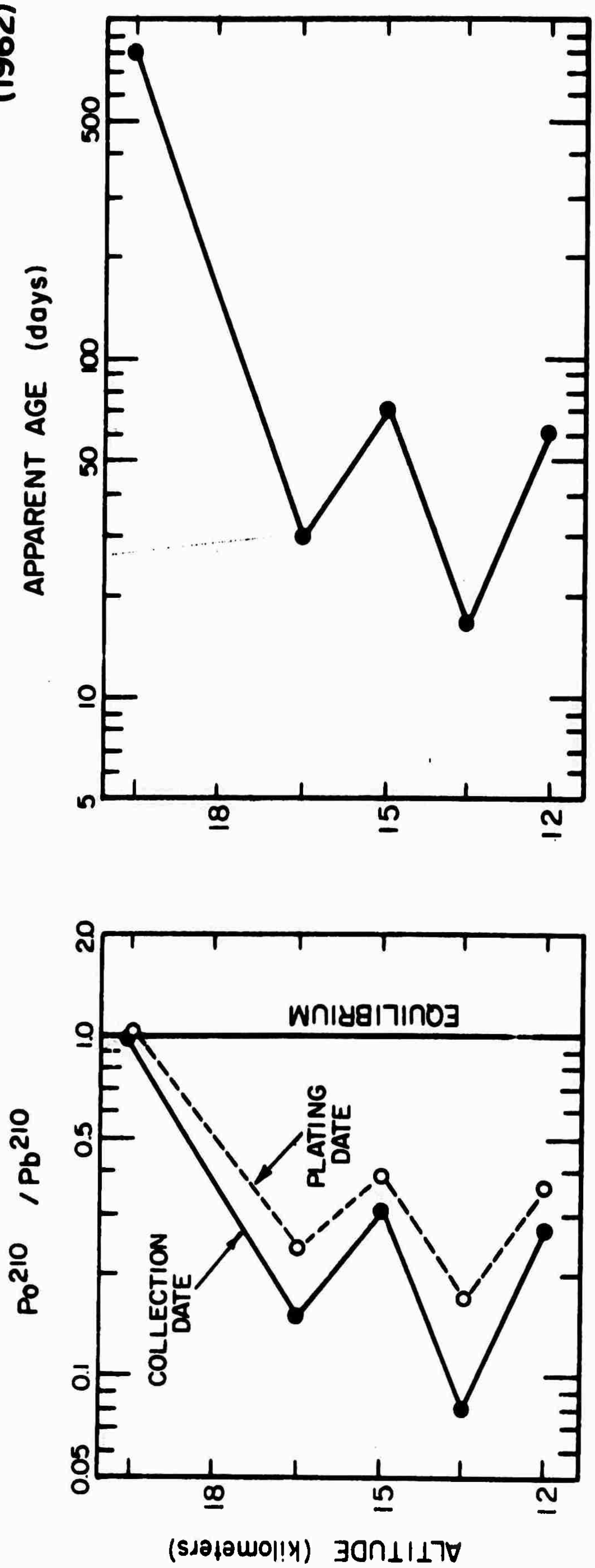

FIG.128 VARIATIONS IN Po^{210}/Pb^{210} AND APPARENT AGE OF Pb^{210} NEAR TROPICAL TROPOPAUSE (10°N) (1962)

collected in the tropical and southern polar stratosphere. The results of the analyses are summarized in Table 126. Lead-210 results given for samples SR-6900, SR-6901 and SR-7734 are based on recent analyses, but polonium-210 results for the first two are based on analyses performed in early 1965.

The flight tracks of the sampling missions which collected these lead-polonium samples and the approximate location of the tropopause are plotted in Figure 129, together with the lead-210 and polonium-210 data.

The available results indicate that the Po^{210}/Pb^{210} activity ratio in the upper troposphere is well below 1.0, but that in the lower stratosphere this ratio equals or even exceeds 1.0. The two samples from 18 and 20 kilometers at 38°-47°S seem to have Po^{210}/Pb^{210} ratios below 1.0, though admittedly the data are of questionable reliability.

Samples collected during the period from December 1965 to April 1966 were again analyzed for lead-210 after plating out the polonium-210 by measuring the bismuth-210 daughter growing in with the purified lead-210. When the ratios of polonium-210 to lead-210 were calculated a number of anomalous results were obtained. Consequently reanalyses of a number of samples for lead-210 were made by allowing the polonium-210 daughter of the bismuth-210 to grow into the sample. Then the 5.3 Mev alpha from polonium-210 was measured with no interference from traces of fission products.

The concentrations of lead-210 calculated from measurment of polonium-210 and bismuth-210 are listed in Table 127 in order of latitude. In all the northern stratospheric samples the numbers derived from the bismuth-210 daughter are higher than those derived from polonium-210. Among the tropical and southern samples the lead-210 concentrations show a higher mean value when derived from bismuth-210. A similar bias is found in Table 122.

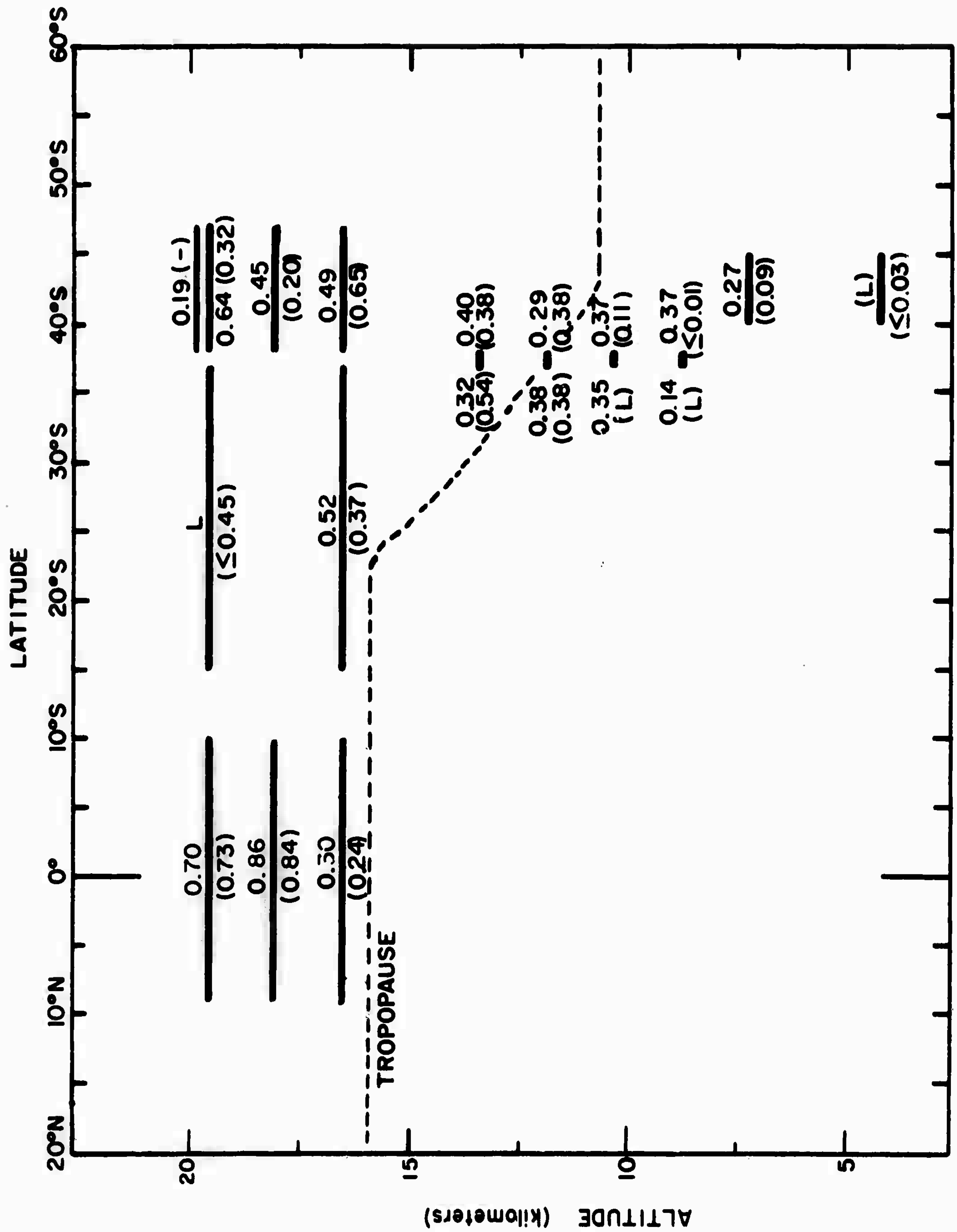

FIGURE 129. CONCENTRATIONS (pCi/100 SCM) OF LEAD-210 AND POLONIUM-210 (IN PARENTHESES) IN DECEMBER 1964 SAMPLES

TABLE 126. Atmospheric concentrations December, 1964 Samples for Lead-210 and Polonium-210 and Strontium-90

Sample Number	Collection Date	Latitude	Altitude (km)	Activities pCi/100 SCM: Total β	Sr^{90}	Pb^{210}	Po^{210}	Po^{210}/Pb^{210}
SR-6893	1 Dec 64	40°-45°S	4.6	62	1.7A	Lost	≤ 0.05	-
SR-6894	1 Dec 64	40°-45°S	7.6	220	6.8A	0.27A	0.10A	0.34
SR-6895	8 Dec 64	37°-38°S	9.2	360	12.A	0.14B	Lost	-
SR-6896	8 Dec 64	37°-38°S	10.7	130	4.6A	0.35A	Lost	-
SR-6897	8 Dec 64	37°S	12.2	1800	62A	0.38C	0.38B	1.00
SR-6898	8 Dec 64	37°-38°S	13.7	3000	67A	0.32D	0.54B	1.71
SR-6899	8 Dec 64	38°-47°S	16.8	7800	240A	0.49C	0.65B	1.32
SR-6900	8 Dec 64	38°-47°S	18.3	6600	230A	0.44C	0.21D	0.46
SR-6901	8 Dec 64	38°-47°S	19.8	8000	190A	0.64C	0.32D	0.50
SR-7734	8 Dec 64	38°-47°S	20.1	6600	170A	0.19B	-	-
SR-6902	21 Dec 64	9°N-10°S	16.8	510	12A	0.30B	0.24A	0.77
SR-6903	21 Dec 64	9°N-10°S	19.8	19,000	430A	0.70B	0.73A	1.03
SR-6904	22 Dec 64	37°-38°S	9.2	140	4.6A	0.36A	≤ 0.02	≤ 0.04
SR-6905	22 Dec 64	37°-38°S	10.7	200	4.6A	0.36A	0.11A	0.30
SR-6906	22 Dec 64	15°-37°S	16.8	2100	59A	0.52A	0.36A	0.68
SR-6907	22 Dec 64	15°-37°S	19.8	9700	180A	Lost	≤ 0.44	-
SR-6908	23 Dec 64	9°N-10°S	18.3	9400	240A	0.86A	0.84A	0.97
SR-6909	23 Dec 64	37°S	12.2	3000	94A	0.29B	0.38A	1.33
SR-6910	23 Dec 64	37°S	13.7	3500	87A	0.40A	0.38A	0.97

Note: Letters following nuclide concentrations represent counting statistics:

A = 0-5% C = 10-20%
B = 5-10% D = 20-50%

TABLE 127. The Atmospheric Concentrations of Lead-210 and Polonium-210 as Determined from Samples Collected During December 1965 - April 1966, and Their Ratios

Sample Number	Collection Date	Latitude	Altitude (km)	Pb^{210} pCi/100 SCM by Bi^{210}	Pb^{210} pCi/100 SCM by Po^{210}	Po^{210} pCi/100 SCM [a]	Po^{210}/Pb^{210} [b]
SR-7507	6 Dec 1965	38°-55°S	15	0.57	0.73	0.65	0.9
SR-7508	6 Dec 1965	38°-55°S	17	0.81	0.59	0.75	1.3
SR-7509	7 Dec 1965	17°-36°S	16	0.61	(0.86)[c]	0.42	(0.5)[c]
SR-7511	7 Dec 1965	17°-38°S	18	0.63	0.72	0.70	1.0
SR-7512	8 Dec 1965	38°-55°S	18	0.60	0.28	0.32	1.1
SR-7735∠	8 Dec 1965	38°-55°S	18	0.30	-	0.26	
SR-7513	8 Dec 1965	38°-51°S	19	0.54	1.26[d]	0.33	
SR-7736∠	8 Dec 1965	38°-51°S	19	0.33	-	0.32	
SR-7514	9 Dec 1965	17°-34°S	19	0.25	0.43	0.33	0.8
SR-7737∠	9 Dec 1965	17°-34°S	19	0.65	-	0.28	
SR-7515	9 Dec 1965	17°-36°S	20	0.39	0.22	0.19	0.9
SR-7738∠	9 Dec 1965	17°-36°S	20	0.40	-	0.19	
SR-7518	21 Dec 1965	64°-55°N	12	0.51	0.71	0.71	1.0
SR-7601	30 Jan 1966	75°-62°N	18	0.53	0.30	0.26	0.9
SR-7602	30 Jan 1966	75°-65°N	19	0.61	0.29	0.32	1.1
SR-7608	2 Feb 1966	65°-50°N	19	0.32	0.28	0.29	1.0
SR-7776	28 Feb 1966	62°-50°N	18	0.43	0.27	0.31	1.1
SR-7777	28 Feb 1966	65°-50°N	20	0.35	0.22	0.19	0.9
SR-7784	25 Apr 1966	36°-23°N	20	0.67	0.62	0.33	0.5
SR-7785	25 Apr 1966	07°N-11°S	15	0.48	0.58	0.18	0.3
SR-7788	26 Apr 1966	30°-10°N	15	0.30	0.44	0.14	0.3
SR-7789	27 Apr 1966	75°-62°N	18	0.42	0.33	0.32	1.0
SR-7791	27 Apr 1966	75°-65°N	19	0.39	0.22	0.22	1.0
SR-7792	27 Apr 1966	07°N-11°S	18	1.40	0.26	0.28	1.1
SR-7793	27 Apr 1966	09°N-11°S	20	0.92	0.66	0.71	1.1
SR-7794	[illegible] Apr 1966	62°-55°N	18	0.41	0.35	0.07	0.2
SR-779[illegible]	[illegible] Apr 1966	62°-50°N	19	0.38	0.22	0.15	0.7

[a] The polonium-210 at the time of plating was used unless the ratio was less than 0.9.

[b] The lead-210 concentration derived from the polonium-210 ingrowth after lead purification was used for the ratio.

[c] This measurement is questionable because of the low chemical yield in the separation.

[d] This measurement was rejected because of the anomalously high value for the number derived from polonium-210 compared to that from the bismuth-210 in both sample and duplicate.

∠ These samples are duplicates of preceding samples.

In determining the ratio of polonium-210 to lead-210 for the 1964 to 1966 samples the lead-210 values derived from the polonium-210 ingrowth were used. In first calculating the ratio, the polonium-210 concentration as measured on the plating date was used. If the ratio was less than 1.0 + 0.1 (within experimental error, a non-equilibrium value), the polonium-210 data were corrected for decay to the collection date and the ratio recalculated.

Accepting the lead-210 concentrations derived from polonium-210 measurements, it may be concluded that the lead-210 concentrations in the 18- to 20-km layer of the polar stratosphere are within the range 0.2 to 0.35 pCi/100 SCM, while concentrations in excess of 0.4 pCi/100 SCM are typical of the 15 to 20 km layer of the tropical stratosphere. These results for samples collected during 1966 are in reasonable agreement with results for samples collected between October 1957 and July 1959 (see Figure 124). Of the ten samples collected in the polar stratosphere, eight have Po^{210}/Pb^{210} ratios between 0.8 and 1.1, indicating a mean stratospheric residence time of one to two years for the lead-210. The two samples collected in the tropical atmosphere at 15 km, near the tropopause level, have ratios of about 0.3, suggesting that the lead-210 encountered there had an atmospheric residence time of about two months. Of the three tropical samples collected between 18 and 20 km, however, two had ratios of 1.1, suggesting a mean stratospheric residence time in excess of a year.

The lead-210 concentrations in the samples taken in the southern stratosphere during early December also agree with the 1957 to 1959 concentrations. A vertical profile at 17° to 38°S showed a decreasing concentration from just above the tropopause to 20 kilometers changing from approximately 0.9 to 0.2 pCi/100 SCM. A similar gradient existed at 38° to 55°S from 15.2 to 18.3 kilometers decreasing in lead-210 concentration from 0.73 to 0.28 pCi/100 SCM.

The polonium-210 to lead-210 ratios for all samples save one indicate that the stratospheric residence time for the lead-210 between latitudes of 17° and 55° S exceeds one year.

Table 127 also shows the four determinations of lead-210 concentrations derived from bismuth-210 measurements done in duplicate. These numbers clearly indicate the poor reproducibility which led to the decision to use lead-210 concentrations derived from polonium-210 measurements. The reproducibility of the polonium-210 measured at the time of plating does, however, show satisfactory precision.

Additional data on measurements of lead-210 and polonium-210 from air particulates sampled during 1965 and 1966 are given in Table 128 . The lead-210 concentrations in the table which are not marked with an asterisk were derived from bismuth-210 measurements. Although these concentration measurements are suspect because of the poor reproducibility,the ratios derived from them appear fairly consistent. The northern tropospheric values show ratios of about 0.3 indicating a residence time at between 4.6 and 7.6 km of about two months. Stratospheric samples at all latitudes show ratios of 0.8 or greater indicating residence times of one year or more. One sample at 12.2 km and 30°N shows a ratio of 0.3 which would appear anomalous.

In a recent report, Feely and Seitz[72] show from experiments with a simplified numerical model of atmospheric transport that the observed distribution of lead-210 in the stratosphere could result from an equilibrium between eddy diffusion and particle settling. They also observed a seasonal effect on lead-210 concentrations in the layer above the tropopause. Concentrations decreased during the winter of 1964-1965 and increased during the summer of 1965.

Finally, remeasurement of air particulates collected during 1963 which had anomalously high concentrations of lead-210 confirmed that the values were in error. The results suggest that little or none of the lead-210 in stratospheric air particulates can be attributed to bomb tests.

TABLE 128. Results of measurements of lead-210 and initial polonium-210 in samples collected during December 1965 - April 1966

Sample Number	Collection Date	Latitude	Altitude (km)	Po^{210} pCi/100SCM Plating Date	Pb^{210} pCi / 100 SCM	Po^{210} / Pb^{210}
SR-7525	1 Dec 65	70°N	4.6	0.21	0.43	0.3
SR-7526	1 Dec 65	70°N	7.6	0.18	0.34	0.4
SR-7507	6 Dec 65	38°-55°S	15.2	0.65	0.73*	0.9
SR-7508	6 Dec 65	38°-55°S	16.8	0.75	0.59*	1.3
SR-7509	7 Dec 65	17°-36°S	16.2	0.47	(0.86)*	0.5
SR-7511	7 Dec 65	17°-38°S	17.7	0.70	0.72*	1.0
SR-7512	8 Dec 65	38°-55°S	18.3	0.32	0.28*	1.1
SR-7735†	8 Dec 65	38°-55°S	18.3	0.26	0.30	0.9
SR-7513	8 Dec 65	38°-51°S	18.6	0.33	1.26*	-
SR-7736	8 Dec 65	38°-51°S	18.6	0.32	0.33	1.0
SR-7514	9 Dec 65	17°-34°S	19.2	0.33	0.43*	0.8
SR-7737†	9 Dec 65	17°-34°S	19.2	0.28	0.65	0.4
SR-7515	9 Dec 65	17°-36°S	20.1	0.19	0.22*	0.9
SR-7738†	9 Dec 65	17°-36°S	20.1	0.19	0.40	0.2
SR-7527	13 Dec 65	30°N	4.6	0.15	0.32	0.3
SR-7528	13 Dec 65	30°N	7.6	0.23	0.47	0.3
SR-7529	13 Dec 65	30°N	12.2	0.24	0.47	0.3
SR-7516	20 Dec 65	47°-41°N	11.9	0.46	0.31	1.5
SR-7518	21 Dec 65	64°-55°N	11.9	0.71	0.71*	1.0
SR-7519	21 Dec 65	64°-55°N	13.1	0.42	0.42	1.0
SR-7521	22 Dec 65	55°-48°N	11.9	0.59	0.66	0.9
SR-7522	22 Dec 65	55°-48°N	13.1	0.71	0.40	1.8
SR-7523	23 Dec 65	41°-35°N	13.1	0.49	0.49	1.0
SR-7524	24 Dec 65	41°-35°N	11.9	0.42	0.51	0.8
SR-7601	1 Jan 66	75°-62°N	18.3	0.26	0.30*	0.9
SR-7602	30 Jan 66	75°-65°N	18.9	0.32	0.29*	1.1
SR-7603	31 Jan 66	33°-23°N	19.3	0.50	0.49	1.0
SR-7604	1 Feb 66	75°-64°N	15.2	0.61	0.44	1.4
SR-7605	1 Feb 66	75°-64°N	16.8	0.48	0.51	0.9
SR-7606	1 Feb 66	50°-33°N	19.6	0.60	0.45	1.3
SR-7607	1 Feb 66	23°-09°N	20.0	0.81	0.85	0.9
SR-7608	2 Feb 66	65°-50°N	18.8	0.29	0.28*	1.0
SR-7776	28 Feb 66	62°-50°N	18.3	0.31	0.27*	1.1
SR-7777	28 Feb 66	65°-50°N	19.7	0.19	0.22*	0.9
SR-7779	24 Apr 66	64°-49°N	16.8	0.48	0.57	0.8
SR-7778	24 Apr 66	49°-37°N	16.8	0.35	0.41	0.8

* Measurement derived from polonium-210 ingrowth after lead purification, other lead-210 concentrations are derived from bismuth-210 ingrowth.

† Duplicate of immediately preceding sample.

TABLE 128 (continued).

Sample Number	Collection Date	Latitude	Altitude (km)	Po^{210} pCi/100SCM Plating Date	Pb^{210} pCi / 100SCM	Po^{210} / Pb^{210}
SR-7781	25 Apr 66	50°-37°N	18.3	0.40	0.49	0.8
SR-7782	25 Apr 66	50°-37°N	19.5	-	0.44	-
SR-7783	25 Apr 66	36°-23°N	18.3	0.45	0.47	1.0
SR-7784	25 Apr 66	36°-23°N	19.8	0.40	0.62*	0.5
SR-7785	25 Apr 66	07°N-11°S	15.2	0.24	0.58*	0.3
SR-7786	26 Apr 66	75°-64°N	15.2	0.34	0.34	1.0
SR-7788	26 Apr 66	30°-09°N	15.2	0.16	0.44*	0.3
SR-7789	27 Apr 66	75°-62°N	18.3	0.32	0.29*	1.1
SR-7791	27 Apr 66	75°-65°N	19.1	0.22	0.22*	1.0
SR-7792	27 Apr 66	07°-11°S	18.3	0.28	0.26*	1.1
SR-7793	27 Apr 66	09°N-11°S	19.6	0.71	0.66*	1.1
SR-7794	28 Apr 66	62°-55°N	18.3	0.13	0.35*	0.2
SR-7795	28 Apr 66	62°-56°N	19.2	0.16	0.22*	0.7

* Measurement derived from polonium-210 ingrowth after lead purification, other lead-210 concentrations derived from bismuth-210 ingrowth.

CHAPTER 12. STRATOSPHERIC METEOROLOGICAL PROCESSES, MODELS AND DATA FROM PROJECT STARDUST

12.1 Introduction

In the early days of fallout studies it was the hope of some workers in the field that observations of tracer distributions in space at various times would permit the proper inference of atmospheric motions, particularly in the stratosphere. It is not surprising that this hope was not largely realized. In few, if any, cases have tracer observations led to unqualified conclusions concerning atmospheric motions on virtually any scale from mesoscale to global. Rather, it has been the direct observation of meteorological variables that have contributed to firm knowledge of atmospheric behavior. Important roles of tracer observations have been generally to verify the conclusions drawn from meteorological observations and to guide the construction of models for estimating the behavior of global scale radioactive fallout.

In some notable cases, particularly as exemplified by the scholarly papers of R. E. Newell of the M.I.T. Planetary Circulations Project there have been fruitful correlations of knowledge of meteorological data and information concerning trace material distributions. In such studies categorical statements of the relative roles of tracers and meteorological data are relatively meaningless. It is the concomitant analysis of both that have lead to increased understanding. Newell's contributions will be further discussed later in the chapter.

No sooner was the quest begun than the community of global fallout investigators fell into two camps - those favoring eddy diffusion and those

favoring mean meridional circulations as the predominant means of transport of trace material in the stratosphere. The findings of Feely and Spar[19] using HASP data for the stratospheric distributions of W^{185} were the first to suggest that transport by eddy diffusion prevailed over transport by mean meridional motions. Since that time numerous investigations (not to be detailed here) led to conclusions that although eddy diffusion is important, the effects of mean meridional circulations could be discerned or at least their existence could not be ruled out. The degree of importance accorded mean-motion transport varied with the investigator. The STARDUST model[80] (see also Chapter 13) and its successor, the STREAK[81] model (with seasonally varying diffusion parameters) used eddy diffusion with no mean motions in the meridional plane to represent the behaviour of tracers injected into the stratosphere. Other models[82,83] added mean circulations to the same basic formalism as the STARDUST and STREAK models. Though details of the model results differ, they all have a general resemblance to observed tracer distributions and fallout behavior. These, however, are model results which may not be realistic because of the nature of the formalism of the models. Thus the question of the relative importance of mean motions in transporting trace materials in the stratosphere has not been answered definitively by the two-dimensional models of eddy diffusion and advection by mean motions. The formalism of these models will be discussed later in the chapter.

One of the most cogent contributions to understanding the relationships between transport by eddy diffusion and transport by mean circulations is that of Manabe and Hunt[84,85] who used a stratospheric general circulation model in three dimensions. In these studies the motions of the atmosphere were simulated by an 18-level (vertical) global network of points, for each of which the time-

dependent equation of motion was solved in finite difference form. The forcing terms of solar radiation and radiation transfer were included in the equations. The eddy and mean motions were presumed to be generated in a "realistic" fashion though some differences in the detailed features of the stratospheric circulations between the computed and observed quantities were noted. These, however, were not thought to have serious implications with regard to the main features of the dynamics generated by the model. Manabe and Hunt's model produced distributions of tracer materials which were the results of complex, interrelated, mean circulations and eddy diffusion. Generally it was found that the relationship between the transport by eddy diffusion and transport by mean motions over a given time period depends upon the initial distribution of tracer, the duration of the time period, and the time since the initial injection. Also, it was pointed out by Manabe and Hunt that significant fluctuations in tracer concentration distributions in their model and in the real atmosphere are caused by synoptic scale features of the general circulation. They state that "it is obviously important to consider the atmosphere in terms of troughs and ridges, as well as eddies and mean meridional circulations, which is the current fashion".

In this chapter, after brief presentation of some concepts in stratospheric general circulations and two-dimensional representations of turbulent diffusion, consideration will be given to the significance of STARDUST data in relation to meteorology. Finally, a discussion will be given of some of the findings of other investigators in the light of the notions and concepts discussed in this chapter.

12.2 Stratospheric Transport and General Circulations

This discussion will be concerned mainly with developing notation and concepts of the motions of stratospheric air so that the relationships of the quantities to similar quantities in the models of eddy diffusion can be readily discerned. It is not intended to treat here the complete details of the stratospheric general circulation. The reader is referred to Newell[86] for a short review of the topic.

12.2.1 General Circulation

The atmospheric motions in the stratosphere are primarily zonal with there being a quasi-biennial oscillation between generally easterly and generally westerly in the tropics. In high latitudes the oscillation between easterlies and westerlies has an annual period with the westerlies generally in the winter hemisphere. Belmont and Dartt[87] have noted and discussed interference effects of annual and biennial waves on the zonal wind patterns in the tropics and subtropics. Newell[86] points out from consideration of energetics that the general circulation in the lower stratosphere is driven by the tropospheric motions.

A suitably time-averaged velocity vector at a given point in the stratosphere will have a primarily zonal direction with generally relatively small components in the meridional and vertical direction. At high latitudes the meridional component of velocity can be considerably larger than in the tropics, though still relatively smaller than the zonal component.

Denoting the three respective velocity components, zonal, meridional and vertical, by u, v and w:

$$\bar{u} > \bar{v}$$

$$\bar{u} \gg \bar{w}$$

where the bar denotes time averages of the quantity. The positive directions are respectively eastward, northward and upward.

The custom in analysis of general circulations is to resolve instantaneous values of quantities of interest, (eg. velocity, temperature, concentration) into average and instantaneous deviation components as in:

velocity: $v = \bar{v} + v'$

temperature: $T = \bar{T} + T'$

concentration: $q = \bar{q} + q'$

The primed quantities represent the instantaneous departures of the quantities from their time averaged values.

12.2.2 Stratospheric Transport

The northward transport of a quantity, q, at a given instant past a fixed point per unit area and unit time (i.e., the instantaneous flux of q), is given by

$$qv = \bar{q}\bar{v} + \bar{q}v' + q'\bar{v} + q'v' \quad .$$

The time average of this transport is

$$\overline{qv} = \bar{q}\bar{v} + \overline{q'v'} \quad . \tag{1}$$

Similar expressions pertain for eastward and upward transports of q with u's and w's instead of v's. In equation (1) the first term on the right is the transport from mean motions in the northward direction, and the second term is the transport due to non-steady or transient eddy processes.

In considering global-scale motions it is frequently of interest to consider transports across entire latitude circles at a given height. Also,

as in the consideration of STARDUST data it is of interest to represent the quantities as zonal averages, i.e., quantities averaged over all longitudes at a given latitude.

Denoting the zonal average of a quantity by square brackets, the zonal average northward transport from equation (1) is:

$$[\overline{qv}] = [\bar{q}\bar{v}] + [\overline{q'v'}] \quad .$$

The time-averaged quantity at a given point may be expressed as the sum of the zonal average for the latitude of the point and a deviation from the zonal average:

$$\bar{q} = [\bar{q}] + \bar{q}^*$$

$$\bar{v} = [\bar{v}] + \bar{v}^*$$

where the quantities denoted by asterisks are the deviations from the zonal averages. Note that all quantities in this decomposition are time averaged.

From the above

$$[\bar{q}\bar{v}] = [\bar{q}]\,[\bar{v}] + [\bar{q}^*\bar{v}^*] \, ,$$

and from equation (1);

$$[\overline{qv}] = [\bar{q}]\,[\bar{v}] + [\bar{q}^* + \bar{v}^*] + [\overline{q'v'}] \quad . \qquad (2)$$

It is thus seen that time-averaged transports further averaged around a latitude circle have three components:

$[\bar{q}]\,[\bar{v}]$; the transport due to mean motions

$[\overline{q'v'}]$; the transport due to transient eddies

$[\bar{q}^*\bar{v}^*]$; the transport due to standing eddies.

The standing eddy terms arise from the presence of some systematic relationship which may exist between q and v in various regions around the latitude circle. It should be noted that the relative values of all three terms may change with changes in the time-averaging interval. The Planetary Circulations Project at M.I.T. has used the zonal average transport formulation of equation (2) to analyze stratospheric motions and transport properties. Observations of wind and temperature by balloon-sondes at more than 200 stations over the globe have provided data for computations of transports of heat, energy and momentum. From these, the energetics[88] and mean motions[89] in the stratosphere have been computed.

Vincent[89] has calculated the velocities associated with mean meridional circulations by applying the zonal averaging procedure simultaneously to the thermodynamic equation, the zonal momentum equation and the equation of continuity. Figure 130 and Tables 129 and 130 are reproduced from Vincent's paper[89] to show the nature of the meridional flow patterns and the magnitudes of the vertical and meridional velocities.

12.2.3 Ozone Transport

In order to apply the techniques of such analyses to tracer transports it is necessary to have simultaneous measurements of the winds and the tracer concentrations. Newell[90,91] has provided some crude hemispheric analyses of ozone transport by assuming that the ozone concentrations in the lower stratosphere were proportional to the total ozone in a vertical column. (The latter is the quantity measured by a Dobson spectrophotometer.) Newell found that generally ozone is transported northward in the lower stratosphere by large-scale standing and transient eddies. More detailed documentation of the

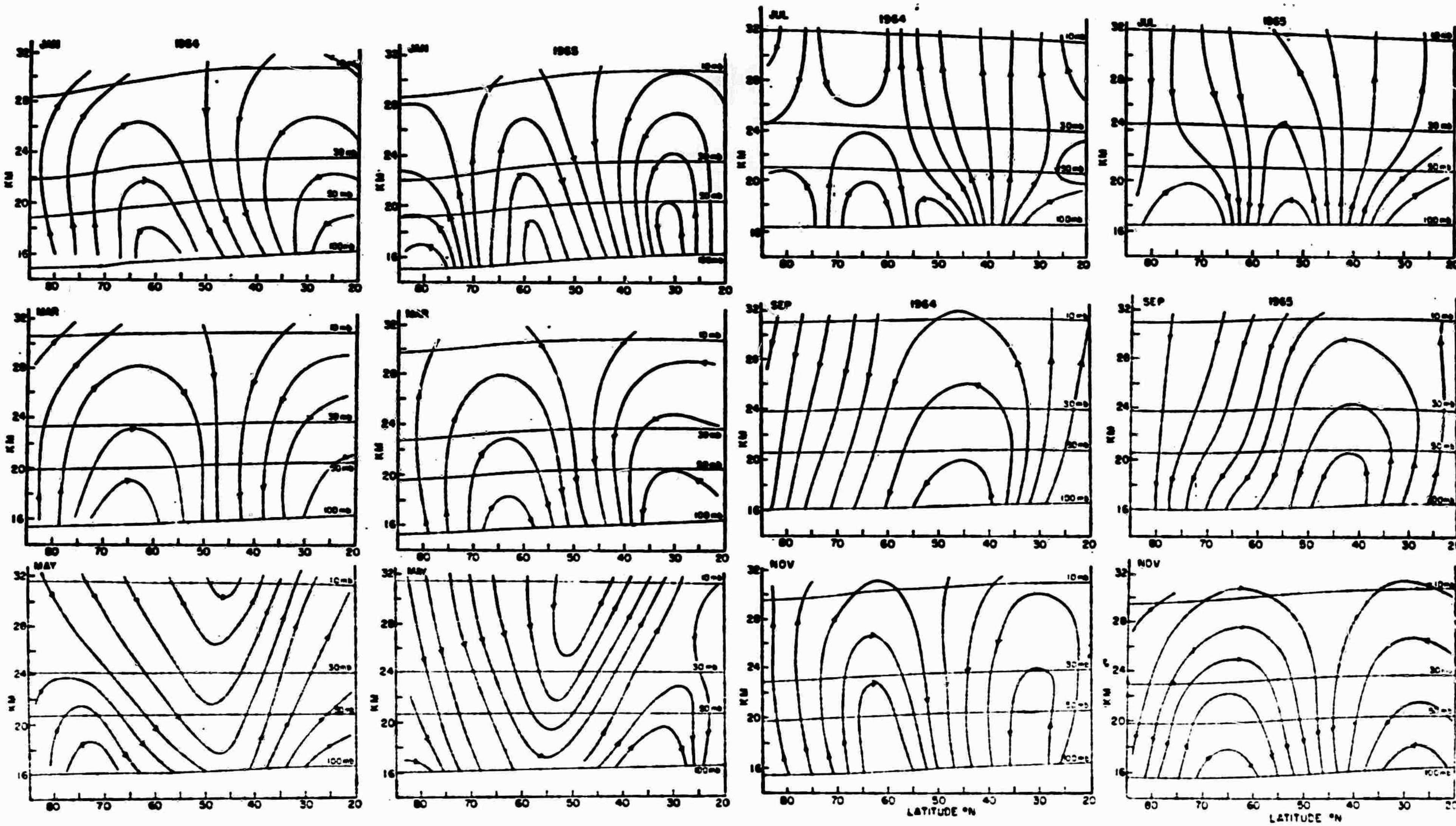

FIGURE 130. Flow patterns for mean meridional circulations

	1964			100-50 mb	1965			
Latitude	Jan.	Apr.	July	Oct.	Jan.	Apr.	July	Oct.
80°N	9·4	− 5·6	− 0·5	− 4·4	54·6	0·9	2·0	− 5·0
75	7·1	− 1·0	− 1·1	− 2·5	24·4	− 0·4	0·7	1·5
70	3·8	1·6	− 1·1	− 0·4	12·9	− 2·6	− 0·3	3·3
65	− 0·4	2·4	− 0·5	− 0·4	5·8	− 4·4	− 1·2	1·6
60	− 5·7	1·3	1·1	− 2·1	− 1·1	− 4·1	− 0·9	− 1·4
55	− 11·6	− 0·1	2·5	− 3·0	− 7·5	− 3·0	0·5	− 3·4
50	− 16·0	− 1·4	2·4	− 2·4	− 15·5	− 2·2	1·0	− 3·4
45	− 14·7	− 3·4	0·6	− 1·3	− 15·4	− 1·8	1·0	− 2·6
40	− 8·1	− 6·0	− 3·0	− 0·6	− 7·8	− 1·4	0·5	− 1·0
35	− 1·7	− 7·2	− 7·5	0·7	− 0·9	− 1·5	− 3·1	2·5
30	4·2	− 5·2	− 10·0	0·6	5·9	− 3·0	− 8·5	5·4
25	19·2	0·5	− 11·3	− 2·8	1·2	− 3·1	− 11·3	5·6

	1964			50-30 mb	1965			
Latitude	Jan.	Apr.	July	Oct.	Jan.	Apr.	July	Oct.
80°N	26·4	− 0·5	0·1	− 1·5	56·0	− 4·2	1·7	− 6·6
75	10·1	0·6	− 0·3	− 1·2	32·0	− 5·7	0·4	− 2·8
70	− 7·2	1·4	− 0·7	− 1·4	6·8	− 8·0	− 0·8	− 0·1
65	− 16·8	1·5	− 0·5	− 1·6	− 6·7	− 9·3	− 1·2	1·0
60	− 18·0	1·0	0·6	− 2·2	− 13·7	− 7·2	− 0·5	0·7
55	− 14·8	0·5	1·4	− 2·1	− 14·9	− 5·2	0·4	− 0·1
50	− 10·4	0·1	1·5	− 0·8	− 11·1	− 0·4	0·5	0·4
45	− 2·7	− 0·4	0·6	0·5	− 5·8	0·8	0·4	1·7
40	5·0	− 0·8	− 0·1	2·3	2·9	2·4	0·6	2·6
35	7·2	− 1·5	− 1·2	4·4	6·4	5·7	0·2	4·6
30	5·1	− 2·9	− 2·9	4·7	7·2	2·0	− 0·4	3·9
25	5·7	− 4·2	− 4·0	0·5	0·0	− 3·3	1·0	3·5

	1964			30-10 mb	1965			
Latitude	Jan.	Apr.	July	Oct.	Jan.	Apr.	July	Oct.
80°N	− 55·8	0·5	0·3	8·0	69·2	− 10·8	1·3	− 11·6
75	− 51·3	1·2	− 0·1	2·2	28·4	− 14·7	0·1	− 10·2
70	− 52·8	1·6	− 0·6	− 4·1	− 16·7	− 17·2	− 0·8	− 6·8
65	− 45·0	1·6	− 0·5	− 7·8	− 44·2	− 15·8	− 0·8	− 2·9
60	− 53·2	1·9	0·4	− 8·6	− 48·1	− 9·8	− 0·0	− 1·2
55	− 19·5	1·9	1·5	− 5·3	− 35·2	− 2·5	0·3	− 0·8
50	− 2·1	1·0	1·4	− 1·3	− 15·6	2·4	0·5	1·0
45	11·4	− 0·2	0·7	2·0	1·7	4·2	0·4	4·3
40	15·9	− 0·8	− 0·2	5·5	14·1	4·6	0·4	6·9
35	14·6	− 1·0	− 0·9	8·7	18·7	5·1	0·4	8·7
30	11·1	− 1·7	− 1·2	10·0	20·5	4·9	0·7	9·8
25	9·3	− 1·2	− 0·5	5·2	12·7	3·6	2·4	11·9

	1964			10 mb	1965			
Latitude	Jan.	Apr.	July	Oct.	Jan.	Apr.	July	Oct.
80°N	− 107·6	0·8	0·1	15·9	70·8	− 14·0	1·2	− 15·2
75	− 116·4	1·4	− 0·1	4·4	17·4	− 20·6	− 0·2	− 15·4
70	− 93·6	1·5	− 0·3	− 6·6	− 41·6	− 23·6	− 1·1	− 11·1
65	− 59·0	1·8	− 0·5	− 15·2	− 77·4	− 20·2	− 0·5	− 3·2
60	− 36·1	2·8	0·3	− 15·3	− 72·9	− 11·5	0·5	− 2·4
55	− 12·8	5·2	1·3	− 7·1	− 40·6	− 1·6	0·9	− 1·4
50	13·2	1·7	1·4	− 0·4	− 11·6	4·7	0·9	1·7
45	26·5	− 0·3	0·8	4·1	11·7	6·9	0·7	6·9
40	25·1	− 1·1	0·1	8·2	26·5	5·9	0·7	10·8
35	19·8	− 1·4	− 0·5	12·3	30·2	5·4	0·6	11·7
30	15·5	− 1·7	0·0	14·0	30·4	6·3	1·1	12·5
25	14·4	2·0	1·1	5·2	18·2	7·6	3·4	17·7

TABLE 129. Mean meridional velocity $(\bar{v})$ in units of cm sec^{-1}

Latitude	1964 Jan.	Apr.	July	Oct.	100-50 mb 1965 Jan.	Apr.	July	Oct.
80°N	1·41	-0·20	0·03	-0·01	-0·22	-0·41	-0·00	-0·04
75	1·73	-0·29	0·03	0·12	1·98	0·44	0·08	-0·21
70	1·27	-0·24	-0·01	0·13	2·32	0·32	0·07	-0·20
65	0·34	-0·13	-0·07	0·11	1·31	-0·02	0·01	-0·08
60	-0·12	-0·04	-0·11	0·00	0·34	-0·35	-0·05	0·01
55	-0·70	0·02	-0·05	-0·18	-0·56	-0·39	-0·04	-0·05
50	-1·05	0·08	0·07	-0·25	-1·03	-0·25	0·02	-0·17
45	-1·03	0·13	0·19	-0·23	-1·15	-0·13	0·06	-0·21
40	-0·72	0·11	0·27	-0·22	-0·89	-0·08	0·14	-0·24
35	-0·32	0·03	0·28	-0·14	-0·31	0·03	0·25	-0·23
30	-0·33	-0·07	0·20	0·17	0·07	0·21	0·20	-0·13
25	-0·49	-0·20	0·13	0·32	0·74	0·37	0·04	0·03

Latitude	1964 Jan.	Apr.	July	Oct.	50-30 mb 1965 Jan.	Apr.	July	Oct.
80°N	2·83	-0·32	-0·03	-0·05	0·29	0·62	-0·02	0·18
75	2·82	-0·33	-0·01	0·31	3·09	0·57	0·06	-0·08
70	1·80	-0·29	-0·02	0·31	3·46	0·33	0·05	-0·27
65	0·47	-0·23	-0·03	0·12	2·12	-0·16	0·00	-0·28
60	-0·72	-0·17	-0·06	-0·13	0·02	-0·59	-0·04	-0·18
55	-1·72	-0·08	-0·02	-0·36	-1·55	-0·62	-0·00	-0·19
50	-2·04	0·02	0·08	-0·41	-2·09	-0·39	0·05	-0·29
45	-1·58	0·04	0·16	-0·34	-1·85	-0·19	0·07	-0·29
40	-0·80	0·03	0·20	-0·29	-1·14	-0·10	0·10	-0·23
35	-0·18	0·06	0·22	-0·19	-0·51	-0·01	0·13	-0·16
30	0·05	0·09	0·18	0·15	0·14	0·16	0·06	-0·11
25	0·03	0·06	0·06	0·70	1·15	0·36	-0·08	-0·17

Latitude	1964 Jan.	Apr.	July	Oct.	30-10 mb 1965 Jan.	Apr.	July	Oct.
80°N	3·83	-0·32	-0·08	-0·18	0·77	0·47	-0·12	0·12
75	3·62	-0·53	-0·09	0·29	3·60	0·45	-0·06	-0·08
70	2·44	-0·50	-0·07	0·28	4·04	0·20	-0·02	-0·34
65	0·62	-0·43	-0·04	0·01	2·48	-0·34	0·01	-0·41
60	-1·15	-0·34	-0·02	-0·29	-0·35	-0·76	0·03	-0·34
55	-2·62	-0·19	0·04	-0·34	-2·47	-0·76	0·08	-0·34
50	-3·00	-0·05	0·14	-0·55	-3·08	-0·48	0·14	-0·38
45	-2·23	0·01	0·24	-0·40	-2·33	-0·21	0·20	-0·34
40	-1·19	-0·01	0·32	-0·26	-1·50	-0·06	0·26	-0·21
35	-0·43	0·03	0·35	-0·14	-0·67	0·01	0·30	-0·11
30	-0·08	0·09	0·30	0·14	0·00	0·10	0·26	-0·07
25	0·08	-0·02	0·20	0·64	0·96	0·23	0·15	-0·16

Latitude	1964 Jan.	Apr.	July	Oct.	10 mb 1965 Jan.	Apr.	July	Oct.
80°N	3·87	-0·79	-0·13	-0·47	1·23	-0·18	-0·24	-0·28
75	4·47	-0·85	-0·21	-0·04	3·37	-0·06	-0·21	-0·22
70	3·86	-0·82	-0·14	-0·08	3·80	-0·09	-0·09	-0·42
65	1·32	-0·71	-0·03	-0·32	2·42	-0·51	0·05	-0·54
60	-1·39	-0·34	0·07	-0·53	-0·76	-0·81	0·12	-0·54
55	-3·37	-0·36	0·14	-0·66	-3·26	-0·75	0·17	-0·51
50	-2·83	-0·19	0·23	-0·61	-3·96	-0·49	0·24	-0·40
45	-2·97	-0·08	0·34	-0·36	-3·03	-0·23	0·34	-0·26
40	-1·84	-0·06	0·47	-0·08	-1·72	-0·04	0·45	-0·10
35	-0·93	0·00	0·33	0·03	-0·77	0·06	0·54	0·01
30	-0·54	0·14	0·33	0·11	-0·21	0·13	0·57	0·10
25	0·16	0·27	0·54	0·24	0·16	0·23	0·50	0·15

TABLE 130. Mean vertical velocity ($\zeta 1$) in units of mm sec^{-1}

northward transport of ozone by transient eddies at mid-latitudes was provided by Hering[22] who analyzed individual ozonesondes over a two year period. Hering also found that almost all of the transport occurred below an altitude of 18 km. Both Newell and Hering found that the maximum transport occurs in the spring season. The reason for the seasonal dependency of ozone transport is given by Newell as being the seasonal variation in the supply of energy from the troposphere into the lower stratosphere. Such variations in energy transport are discernible in the meteorological data analyzed by the M.I.T. group.

So far ozone is the only trace material whose transports have been studied in the stratosphere. With regard to equation (2) it can be said that (with q = ozone mixing ratio) for ozone, the second and third terms contribute significantly to the total transport. The magnitude of the mean circulation transport term, $[\bar{q}][\bar{v}]$, is uncertain because (a) of uncertainties in the determinations of the other terms, and (b) the uncertainty in the computation of $[\bar{q}]$ from the existing data. Presumably the values of $[\bar{v}]$ and $[\bar{w}]$ are now quite reliable,[92] at least in low latitudes in the lower stratosphere. For high latitudes there is still considerable error associated with the means.

12.2.4 <u>Radioactivity and Stratospheric Transport</u>

The observations of radioactive trace substances, natural and man-made, in the stratosphere have not been carried out in a manner to permit the determination of representative zonal averages of the various transports in equation (2). (It should be understood that there is an equation similar to (2) with $\bar{w}$'s instead of $\bar{v}$'s applicable to vertical transports and that what is said here about equation (2) also applies to vertical transports.)

The facts that:

a) no fresh debris from the late October 1958 USSR nuclear test explosions was intercepted in HASP,

b) debris from the December 1962 USSR test explosions was not detected in the STARDUST sampling corridor until March 1963,

certainly seem to bear out the contention that, in general, the concentrations determined in these sampling programs are not necessarily equivalent to zonally averaged concentrations. In the two cases listed above, the existence of the quasi-stationary Aleutian anticyclone in the stratosphere most likely was responsible for maintaining zonal gradients in the radioactive concentrations. The transports associated with such a feature are by those from standing eddies.

The longer debris remains in the stratosphere the less the concentration gradients become and thus the less the transport by eddies. However, stratosphere-troposphere interchange and tropospheric removal processes combine to maintain gradients continually.

The data in Table 37 illustrate that relatively large vertical gradients existed at high latitudes six months after injections in that region. Indeed throughout the STARDUST and HASP programs vertical gradients were always found near the tropopause and horizontal gradients were found in the vicinity of the tropopause gaps. There is thus virtually no possibility of a situation occurring where the sole transport is by mean motions.

12.3 Stratospheric Turbulent Diffusion

This section will present some concepts and formalism related to the theories of turbulence and turbulent diffusion. The relationship between these and the two dimensional models of turbulent diffusion in the stratosphere will

be pointed out. The approach adopted here follows that given by Hinze[93]

The instantaneous rate of change of concentration of a material at any point in an incompressible fluid is:

$$\frac{\partial c}{\partial t} + u_i \frac{\partial c}{\partial X_i} - \frac{\partial}{\partial X_i}\left(D \frac{\partial c}{\partial X_i}\right) + F_c \quad . \tag{3}$$

where:

- c concentration of material (ML^{-3})
- u_i = component of velocity in the i^{th} direction. In this type of notation the index i denotes the following:
  - $i = 1$: X - direction (zonal)
  - $i = 2$: Y - direction (meridional)
  - $i = 3$: Z - direction (vertical)
- X_i = coordinate in the i^{th} direction
- t = time
- F_c = sum of sources and sinks of the material $(ML^{-3}t^{-1})$
- D = molecular transport (diffusion) coefficient (L^2t^{-1}) (taken here to be constant).

(In the above list the units of some of the quantities are shown in general terms where M, L, t stand respectively for mass, length and time.)

In this notation the Einstein summation convention is to be observed. This means that any term in which an index is repeated $\left(\text{e.g., } u_i \frac{\partial c}{\partial X_i} \text{ and } \frac{\partial}{\partial X_i}\left(D \frac{\partial c}{\partial X_i}\right)\right)$ really stands for the summation over all three values of the index.

Equation (3) is Fick's equation which describes the processes of molecular diffusion and advection in a non-turbulent fluid. A similar equation

applies for the diffusion and convection of heat by molecular motions. In this case the molecular transport coefficient becomes:

$$k = \frac{\chi}{\rho c_p}$$

where χ = heat conductivity of the fluid

ρ = density of the fluid

c_p = heat capacity at constant pressure of the fluid

In the presence of turbulence, additional fluctuations in concentrations and velocities will occur.

To deal with this situation it is hypothesized that the velocities and transported quantities fluctuate randomly about respective mean values. This is an hypothetical statistical model. The mean values of the quantities are ensemble averages, i.e., values that would be observed upon averaging the results over all possible realizations of an experiment designed to produce distributions of the observable quantities. The decompositions

$$\begin{aligned} c &= \bar{c} + c' \\ u_i &= \bar{u}_i + u_i' \end{aligned} \tag{4}$$

represent the instantaneous values of concentration and velocity components as means (ensemble averages) plus deviations from the means (primed quantities). In practice, the ensemble averages cannot be obtained, so they are approximated as time averages in the following manner:

$$\bar{c}(t) = \frac{1}{T}\int_0^T c(t + \tau)\, d\tau \tag{5}$$

$$\bar{u}_i(t) = \frac{1}{T}\int_0^T u_i(t + \tau)\, d\tau \tag{6}$$

The interval, T, is supposed to be large compared with the time scale of the turbulent motions. The time variations of the means are supposed to be significant over times large compared to the time scale of the turbulent motions. This last statement is equivalent to assuming that the spectrum of frequencies characterizing all motions has a gap separating the portion characterizing mean motions from that characterizing turbulent motions. In effect, these assumptions permit the time-averaged quantity $\bar{c}$ to have a time derivative. Thus by substituting the relationships (4) for the instantaneous quantities in equation (3) and then averaging over the interval T, the left hand side becomes

$$\frac{\partial \bar{c}}{\partial t} + \bar{u}_i \frac{\partial \bar{c}}{\partial X_i} + \overline{u_i' \frac{\partial c'}{\partial X_i}} = \frac{\partial \bar{c}}{\partial t} + \bar{u}_i \frac{\partial \bar{c}}{\partial X_i} + \frac{\partial}{\partial X_i} \overline{u_i' c'}$$

since

$$c' \frac{\partial u_i'}{\partial X_i} = 0 \quad \text{for an incompressible fluid.}$$

Upon averaging the right hand side and after some rearranging equation (3) now becomes:

$$\frac{\partial \bar{c}}{\partial t} + \bar{u}_i \frac{\partial \bar{c}}{\partial X_i} = \frac{\partial}{\partial X_i} \left(D \frac{\partial \bar{c}}{\partial X_i} - \overline{u_i' c'} \right) + \bar{F}_c \quad . \tag{7}$$

It is at this point that, following Boussinesq, the eddy diffusion coefficient, K_c, is formally introduced by placing

$$- \overline{u_i' c'} = K_c \frac{\partial \bar{c}}{\partial X_i} \quad . \tag{8}$$

Thus the eddy transport term, $\overline{u_i' c'}$, in equation (7) is replaced by a term which is analogous to transport by molecular diffusion.

It can be seen from the form of equation (8) that K_c can be either a scalar or, more generally, a second order tensor. If the latter is considered, then:

$$- \overline{u_i' c'} = K_{ij} \frac{\partial \bar{c}}{\partial X_j} \tag{9}$$

(bearing in mind that the right hand side must be summed over the three values of j).

In the turbulent atmosphere the eddy transport terms are considered to be vastly larger than those of molecular diffusion. Thus

$$K_{ij} \gg \delta ij \; 0, \qquad \delta ij = \begin{matrix} 1 \text{ for } i = j \\ 0 \text{ for } i \neq j \end{matrix}$$

With this knowledge and using the mixing ratio of the material given by

$$q = c/\rho$$

where ρ = density of the fluid (ML^{-3}), equation (7) can be written:

$$\rho \frac{\partial \bar{q}}{\partial t} = \text{div}\,(\rho V q\,) + \frac{\partial}{\partial X_i}\,(\rho K_{ij} \frac{\partial \bar{q}}{\partial X_j}) + \bar{F}_q \tag{10}$$

where

V = velocity vector of the fluid.

This equation coupled with the equation of continuity of the fluid,

$$\text{div}\,(\rho V) = 0 \;, \tag{11}$$

(if the fluid is incompressible) suffices to define the distribution of mixing ratio of any inert substance imbedded in the fluid. Appropriate initial and boundary conditions must be specified. Equations (10) and (11) are essentially the ones solved, in their two-dimensional forms, in the

various models of transport by turbulent diffusion and advection in the stratosphere (see Chapter 13). In principle, the velocity vector can be measured at every point. This leaves only the problem of determining the proper values of K_{ij} to be used. This is the crux of the whole problem of using the so-called K-theory.

Again, in principle, the quantity represented by the left hand side of equation (9) and the gradients of concentration are observable. So the values of K_{ij} could be determined if a proper set of simultaneous observations of concentration and velocity averaged over the appropriate time interval and over a suitably small space increment in the domain of interest were available.

Equations similar to (9) can be written for turbulent transports of momentum components, heat, and kinetic energy, each with their own coefficient of eddy diffusion similar to K_{ij}. The coefficients are theoretically different because of the different manner in which each quantity exchanges its properties with the surrounding medium. There is an extensive body of literature on various types of so-called mixing-length hypotheses which have been made in attempts to gain further insight into eddy-transport processes. In their present application to the atmosphere, these hypotheses result in the introduction of certain time and length scales which serve as parameters in place of the K's. The time scales have relevance in defining the lower limits for the averaging interval, T, in equations (5) and (6). These considerations will not be pursued further here. The interested reader is referred to Hinze[93] or other texts on turbulence. For the purposes of the present discussion it is sufficient to note that:

(a) In the stratosphere there have been no measurements of trace material concentrations in sufficient detail to permit determination of K_{ij}'s by means of equation (9).

(b) Because of (a) the use of equation (10) to represent transport of trace material means that K_{ij} must be treated as a parameter rather than a theoretically or experimentally determined quantity.

It is further to be noted that equation (10) does not contain any terms specifically related to transport by standing eddies in its two-dimensional form. (In this form the quantities V and q are merely replaced by their zonal averages.) This means that any real effects due to standing eddies must be included in V and K_{ij}. And this means that <u>to the extent that V includes effects of standing-eddy transport, it is also a parameter</u>. In effect, if shifts in quasi-stationary features of the stratospheric circulation occur during the modelled season, the quantities V and $K_{ij} \frac{\partial \bar{q}}{\partial X_j}$ in equation (1) may not be equivalent to the (observable) quantities $[\bar{v}]$, $[\bar{w}]$ and $-[v'q']$, $[w'q']$ in equation (2). Also care must be exercised in applying equation (10) to represent concentration distributions at too early times after single injections. This last point arises from the requirement that the interval T be sufficiently large.

12.4 Models and Interpretation of Stratospheric Concentrations of Radionuclides

The general circulation model of the stratosphere of Manabe and Hunt[84,85] can be used to provide understanding of the nature of stratospheric transport processes. It has shown that transport by mean motions and by eddy diffusion are important and that the processes act in a complicated interrelated fashion depending upon time and initial distribution of the material or dynamic property being transported. The two-dimensional models of diffusion and advection have

the processes built into the equations, so that new understanding of the processes does not result from application of the models. The general circulation model requires so much computer time that it is quite impractical at present to use it for simulating the behavior of radioactive nuclides from nuclear explosion injections (or other materials) over time periods of the order of two to five years. It was for the express purpose of doing this that the STARDUST and other models of stratospheric transport were constructed.

Krey[94] has shown that box-models (first order kinetics transfer from one compartment to another) with a sufficient number of compartments can be made to give reasonable accountancy for hemispheric inventories. This is perhaps the simplest type of model. With it there is no attempt to simulate concentration patterns and detailed latitudinal distribution of fallout.

The STARDUST[80], STREAK[81], and other[82,83] stratospheric models of turbulent diffusion and advection have shown that the two-dimensional formalism discussed in 12.3 can simulate reasonably well some of the patterns of stratospheric concentration and latitudinal profiles of fallout over periods of up to three years. The overall differences among models are probably not greater than the overall errors in the observations of the distributions being simulated. Since this is the case, there appears to be no compelling reason to accept any one model in preference to the others. It is suggested that the STARDUST and STREAK models may be preferable in view of the simpler scheme in the values of the parameters.

It was mentioned previously that infrequent sampling and possible improper zonal coverage in the stratospheric radioactivity sampling programs give rise to inabilities to determine a) proper zonally averaged concentrations and b) tracer fluxes. Since these quantities must be known in order to deline-

ate the transport processes, the numerous interpretations of observations as indicating specific mean motions must be viewed as educated guesswork. Telegadas and List[95] ask the question, "Are particulate radioactive tracers indicative of stratospheric motions?" They answer affirmatively and that answer is concurred with herein. However, it is contended here that it cannot generally be determined by present methods precisely what motions are indicated. For the case when knowledge of the general circulation of the stratosphere is available then it can be used to understand the observed distributions of tracer materials. The inverse process of deducing the general circulations from tracer observations is impossible.

A closing note is directed at the interpretations of the behavior of tracers injected at high altitudes given by List et al.[59] and Krey[96]. They have noted that upon their initial appearance in the sampling corridor, Pu^{238} from the 1964 SNAP-9A reentry burn-up, Cd^{109} and Rh^{102} from specific nuclear tests, certain isolines of concentration all descended in the polar stratosphere with a velocity of about 1.5 km/month. While the authors note that interpretations according to simple models is difficult, there is implied that the repeated finding of a vertical velocity of 1.5 km/month may be significant. In view of the foregoing discussion it is suggested here that such analyses of the behavior of single isolines, or "first appearances" of tracer materials, are invalid. To illustrate the point reference is made to Hunt and Manabe's[85] tracer R2 in their general circulation model paper. This was a high altitude tracer meant to resemble ozone. During the simulation period of 180 days tracer concentration isolines descended in the lower polar stratosphere. An isoline line could be found that had a mean descent-rate of 1.5 km/month. Analysis of

the experiment showed that the tracer movements were caused by complex combinations of mean motion and eddy transports during a time when the mean motions in the lower stratosphere were upward and poleward north of 45° latitude.

CHAPTER 13. THE STARDUST NUMERICAL MODEL OF TRANSFER AND RAINOUT OF STRATOSPHERIC RADIOACTIVE MATERIALS

13.1 Introduction

As a consequence of the data analyses conducted under the High Altitude Sampling Program (Project HASP) of atmospheric distributions and surface fallout of radioactive material, it was readily recognized that the introduction of large amounts of artificially produced radioactive nuclides into the stratosphere constitutes a potential health hazard on a global scale and that methods must be devised to evaluate and predict this hazard. Hence, a prime objective of Project STARDUST was to develop a numerical model to predict the transfer, mixing and fallout of such material introduced into the stratosphere.

A basic numerical model in two dimensions (the meridional plane of the earth-atmosphere system) capable of simulating diffusion, transport, particle settling and tropospheric rainout was formulated. The model was progressively developed using guidelines based upon observed atmospheric distributions of radioactive material, particularly tungsten-185, and upon some initial ideas of significant atmospheric transfer processes formulated by Feely and Spar [19].

The model developed as a part of Project STARDUST allowed no variations with season in the properties of the atmosphere and the parameters used to describe them. In this sense it is considered to be a "mean annual" model. In 1966 model studies of Project STARDUST were reassigned to Project STREAK under the sponsorship of the U.S. Atomic Energy Commission. In that study a four-season model was developed. This led to certain improvements and changes, some of which will be referred to near the end of this chapter.

ISOTOPES
A Teledyne Company

In what follows is a summary of the formulation of the mean annual numerical model and of the significant accomplishments resulting from a large number of numerical experiments using tungsten-185 data to simulate a tropical injection and strontium-90 data to simulate a polar injection. This summary was previously presented in a paper presented at the International Symposium on Atmospheric Chemistry, Circulation and Aerosols conducted by the Commission on Atmospheric Chemistry and Radioactivity, August 18-25, 1965, Visby, Sweden[80]. More detailed presentation of the progress of this research effort appeared primarily in three previous reports on Project STARDUST[98,99,100].

The injection of tungsten-185 was associated with a series of weapon tests which took place at a latitude of 11.7°N from May to August 1958. The stratospheric injection of tungsten-185 was estimated by Friend et al.[19] at approximately 54 to 87.5 megacuries (corrected for decay to 15 August 1958). The average center of gravity of the injections is not accurately known, but it is assumed to lie within a three-kilometer layer of the lower tropical stratosphere. The observed tungsten-185 distribution (two-month mean) in the lower stratosphere, one year after the average injection time, is shown in Figure 131a. The heavy line indicates the analyst's impression of the distribution with latitude of the height of maximum concentration. The striking features of the concentration distribution are (a) the poleward declination of the axis of maximum concentration, (b) the maintenance of a center of maximum concentration slightly south of the original injection, (c) the development of a secondary maximum in north and in south polar regions, and (d) the large concentration gradient in the vertical just above the tropical tropopause. Feely and Spar[19], Bolin[102], Hering and Borden[103] and other authors have called attention to these features of the stratospheric distribution and pointed out similarities between the artificially produced radionuclide and ozone distributions in the lower stratosphere.

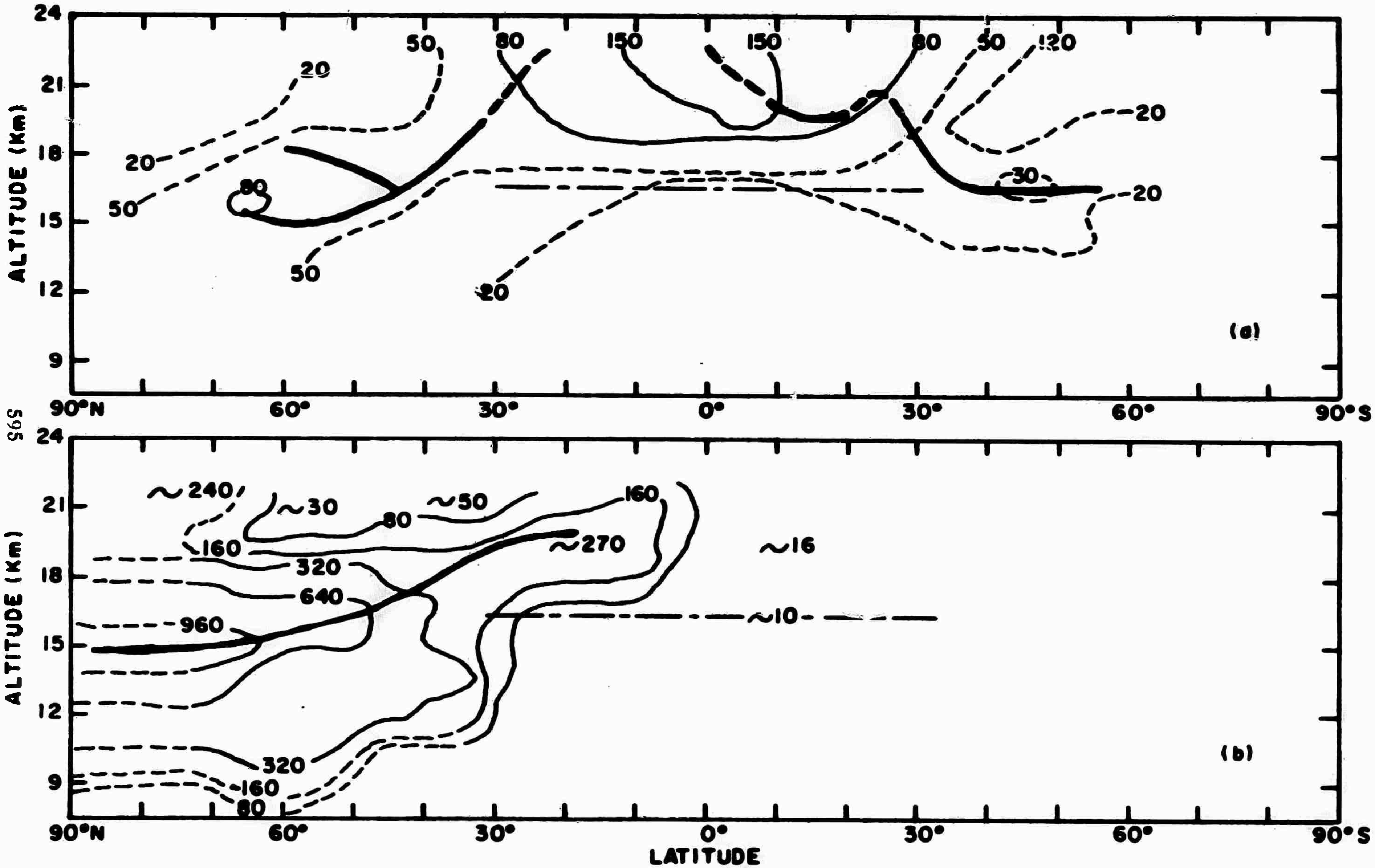

FIGURE 131. (a) MEAN MAY - JUNE, 1959 DISTRIBUTION OF TUNGSTEN-185 (pCi/SCM, corr to 15 Aug 1958).
(b) MEAN JAN - APR, 1962 DISTRIBUTION OF STRONTIUM-90 (pCi/100SCM) FROM SOVIET TESTS.

Experimentation with the numerical diffusion model was designed to investigate systematically the consequences of a general mixing model. The objective is to isolate the simplest model structure which yields reasonable agreement with the observed features of the tungsten experiment. The relevant features are considered to be as follows:

(1) the distribution of concentration isopleths in the stratosphere,

(2) the decrease of central (maximum) concentration with time, and

(3) the observed meridional distribution of the combined rainout and dry fallout of the tungsten-185 for the first year after injection.

To test its general applicability, the model is further required to reproduce the gross features of an injection in the lower polar stratosphere. The 1961 Soviet test series approximates this type of injection. Figure 131b shows the stratospheric distribution of strontium-90 resulting from this test series, six months after a mean injection time[104]. Due to the presence of strontium-90 from previous tests, it was necessary to use isotopic ratio (Sr-89/Sr-90) dating to identify the newly injected strontium-90. This process of identifying Soviet debris was feasible only up to May 1962, at which time the United States introduced fresh debris into the stratosphere. The poleward slope of the axis of maximum concentration indicated in the Soviet data closely approximates that of the tungsten-185 data as shown in Figure 131a.

13.2 Numerical Model

It is our intent to examine the possibilities of reproducing the main features of the observed data by means of eddy diffusion, particle settling, and dry and wet fallout. In the absence of general circulation terms, the two-dimensional anisotropic diffusion equation incorporating the effects of particle fall velocity and variable density is, with good approximation for our domain of interest,

$$\rho \frac{\partial q}{\partial t} = -\frac{\partial}{\partial r}(\rho \Omega q) + \frac{\partial}{\partial r}\left(\rho K_{rr} \frac{\partial q}{\partial r}\right) + \frac{1}{r^2 \cos \phi} \frac{\partial}{\partial \phi}\left(\rho \cos \phi K_{\phi\phi} \frac{\partial q}{\partial \phi}\right)$$

$$+ \frac{1}{r}\frac{\partial}{\partial r}\left(\rho K_{r\phi} \frac{\partial q}{\partial \phi}\right) + \frac{1}{r \cos \phi} \frac{\partial}{\partial \phi}\left(\rho \cos \phi K_{\phi r} \frac{\partial q}{\partial r}\right) , \qquad (1)$$

where:

ρ = air density (gm/cm^3); assumed to be a function of r only,

q = mixing ratio of radioactive material (gm/gm of air or pCi/gm of air),

K = coefficient of eddy diffusion (cm^2/sec),

Ω = particle fall velocity (cm/sec),

ϕ = latitude (deg),

r = radial distance outward from the center of the earth (cm), and

t = time (sec).

It is to be noted that a term, $(2/r)\rho K_{rr}(\partial q/\partial r)$, has been omitted from the right hand side of (1). Since the magnitude of r is of the order of 6×10^8 cm, this term is small with respect to the others and can be neglected.

It is not possible to solve this equation analytically for a complex atmosphere in which the density is a function of altitude and the coefficients of eddy diffusion may be functions of altitude, latitude and time. Furthermore, there is no simple way in which rainout can be incorporated into the equation. The method of finite difference solutions of parabolic differential equations

with complex boundary and initial conditions is particularly appropriate for application to the problem considered in this paper. In what follows, the basis and principal features of the numerical model are presented.

If the tensor defined by the diffusion coefficients in (1) is assumed symmetric, i.e., $K_{\phi r} = K_{r\phi}$, then there exists a set of principal axes along which the off-diagonal or mixed derivative terms vanish. In what follows, we assume:

1. The local principal axis of diffusion is known at each point in the numerical grid.
2. The principal diffusion coefficients, K'_{11} and K'_{22}, are known at each grid point.
3. For the domain of interest, the r, ϕ coordinate system is sufficiently close to being cartesian to warrant the following transformations:

$$K_{\phi\phi} = \cos^2\alpha\, K'_{11} + \sin^2\alpha\, K'_{22}, \tag{2}$$

$$K_{rr} = \sin^2\alpha\, K'_{11} + \cos^2\alpha\, K'_{22}, \tag{3}$$

$$K_{r\phi} = K_{\phi r} = \cos\alpha \sin\alpha\, K'_{11} - \sin\alpha \cos\alpha\, K'_{22}, \tag{4}$$

where α is the angle between the $rd\phi$ direction (positive toward the north pole) and the direction of the principal diffusion of axis. The absolute value of α is reasonably taken to be small; thus K'_{11} and K'_{22} represent quasi-horizontal and quasi-vertical diffusion coefficients respectively.

For numerical computations, it is convenient to express (1) in a μ,z coordinate system, where $\mu = \sin\phi$, $z = r - r_o$ and r_o = the mean equatorial radius of the earth. Thus

$$\rho\frac{\partial q}{\partial t} = -\frac{\partial}{\partial z}(\rho\Omega q) + \frac{\partial}{\partial z}\left(\rho K_{zz}\frac{\partial q}{\partial z}\right) + \frac{\partial}{r_o\partial\mu}\left([1-\mu^2]\rho K_{\phi\phi}\frac{\partial q}{r_o\partial\mu}\right)$$

$$+ \frac{\partial}{\partial z}\left(\rho\cos\phi K_{z\phi}\frac{\partial q}{r_o\partial\mu}\right) + \frac{\partial}{r_o\partial\mu}\left(\rho\cos\phi K_{\phi z}\frac{\partial q}{\partial z}\right) \quad . \tag{5}$$

The numerical method involves considering an earth-atmosphere meridional plane as a grid of discrete points. For the models presented here the grid consists of 840 points; 30 along the μ-axis and 28 along the z-, or height axis. The grid interval in the vertical is a constant 1.5 km while it is variable in the μ-direction so that there are 17 grid points in the Northern Hemisphere and 12 grid points in the Southern Hemisphere.

An implicit, alternating direction scheme is used to integrate (5) numerically because of its inherent stability in producing convergent solutions and for numerical convenience. The finite difference analogue of (5) is expressed by (6) and (7) which are applied alternately with successive time increments.

$$\frac{q^{n+1} - q^n}{\delta t} = -\frac{1}{\rho}\left[\frac{\delta}{\delta z}(\rho\Omega q)\right]^n + \frac{1}{2\rho}\left[\frac{\delta}{\delta z}\left(\rho K_{zz}\frac{\delta q}{\delta z}\right)\right]^n$$

$$+ \frac{1}{2\rho}\left[\frac{\delta}{\delta z}\left(\rho K_{zz}\frac{\delta q}{\delta z}\right)\right]^{n+1} + \left[\frac{\delta}{r_o\delta\mu}\left((1-\mu^2)K_{\phi\phi}\frac{\delta q}{r_o\delta\mu}\right)\right]^n$$

$$+ \frac{1}{\rho}\left[\frac{\delta}{\delta z}\left(\rho\cos\phi K_{z\phi}\frac{\delta q}{r_o\delta\mu}\right)\right]^n + \left[\frac{\delta}{r_o\delta\mu}\left(\cos\phi K_{\phi z}\frac{\delta q}{\delta z}\right)\right]^n \; ; \tag{6}$$

$$\frac{q^{n+1} - q^{*}}{\delta t} = -\left[\frac{1}{\rho}\,\frac{\delta}{\delta z}(\rho \Omega q)\right]^{n} + \frac{1}{\rho}\left[\frac{\delta}{\delta z}\left(\rho K_{zz}\frac{\delta q}{\delta z}\right)\right]^{n} + \frac{1}{2}\left[\frac{\delta}{r_o \delta\mu}\left((1-\mu^2)K_{\phi\phi}\frac{\delta q}{r_o \delta\mu}\right)\right]^{n+1}$$

$$+ \frac{1}{2}\left[\frac{\delta}{r_o \delta\mu}\left((1-\mu^2)K_{\phi\phi}\frac{\delta q}{r_o \delta\mu}\right)\right]^{n} + \frac{1}{\rho}\left(\frac{\delta}{\delta z}\left(\rho \cos \phi K_{z\phi}\frac{\delta q}{r_o \delta\mu}\right)\right]^{n}$$

$$+ \left[\frac{\delta}{r_o \delta\mu}\left(\cos \phi K_{\phi z}\frac{\delta q}{\delta z}\right)\right]^{n} \qquad (7)$$

The superscripts in equations (6) and (7) above indicate values of the quantities at time n and time n + 1. The alternating direction scheme is applied to only the second and third terms on the right in (5). It is apparent that, with respect to these terms, (6) is implicit in the z-direction and explicit in the μ-direction while (7) is implicit in the μ-direction and explicit in the z-direction; hence the term, "alternating direction". All other terms on the right are explicit. Centered differences are used to approximate all derivatives except for the first term which is evaluated as a backward difference since the fall velocity is always negative. The method of solution in two dimensions is described by Douglas[105]. The only modification in our case is to adjust the boundary conditions so that the diffusive flux of material through the vertical and lateral boundaries of the system is always zero.

All models described in this report incorporate a troposphere, tropopause, and stratosphere in a manner which is schematically illustrated in Figure 132. The vertical diffusion coefficient is assumed to be dependent on both stability (lapse rate) and vertical wind shear. Relatively large vertical diffusion coefficient values (K'_{22} = 10^4 to 10^5 cm^2 sec^{-1}) in the principal axis system are associated with the mean annual lapse rate of the troposphere, while, in general,

relatively smaller (at least one order of magnitude) values of K'_{22} are associated with the isothermal layers of the lower polar stratosphere. The line of discontinuity between the large K'_{22} values of the troposphere and the smaller values of the stratosphere constitutes the tropopause.

In the models which are presented in detail, particle fall velocities (Ω) were determined as a function of altitude from calculations by Junge, Chagnon & Manson[3] for spherical particles with 0.1 μ radius and 2 g/cm^3 density. In the simulation of dry fallout, a value of Ω = 0.3 cm/sec was used at the air-ground interface. This value was chosen to represent the effects of absorption, impaction and chemical and electrical affinities at the interface. The necessity in individual cases for a larger deposition velocity than is indicated by the terminal velocities of small particles has been shown from experiments by Chamberlain and Chadwick[108].

In some models, the region between the polar and tropical tropopause is treated as a "gap" region and for these cases K'_{11} and/or K'_{22} are made relatively large as compared to their stratospheric values.

Wet fallout, i.e., removal by precipitation, is simulated in the models by the periodic removal of a fractional amount of q at a fixed grid point. This fractional amount removed (X) is a function of latitude and height and can be expressed:

$$X(\mu,z) = a(z)p(\mu)q(\mu,z) \ , \tag{8}$$

where $p(\mu)$ is a fraction proportional to the mean annual precipitation as given by Moller[109] and $a(z)$ is a height proportionality factor. The total amount

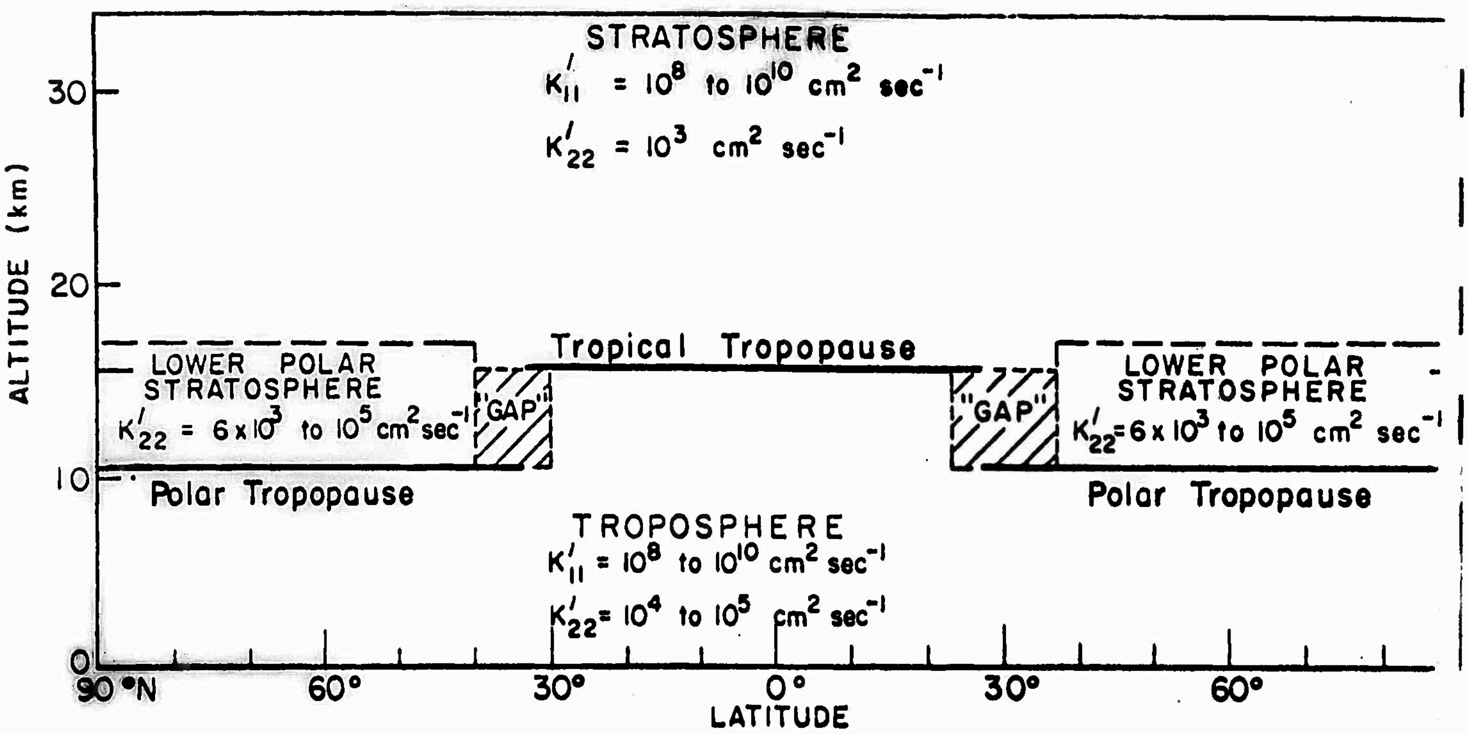

FIGURE 132. SCHEMATIC REPRESENTATIONS OF THE DISTRIBUTION OF DIFFUSION COEFFICIENTS CHARACTERIZING THE REGIONS OF THE ATMOSPHERE IN THE NUMERICAL MODEL.

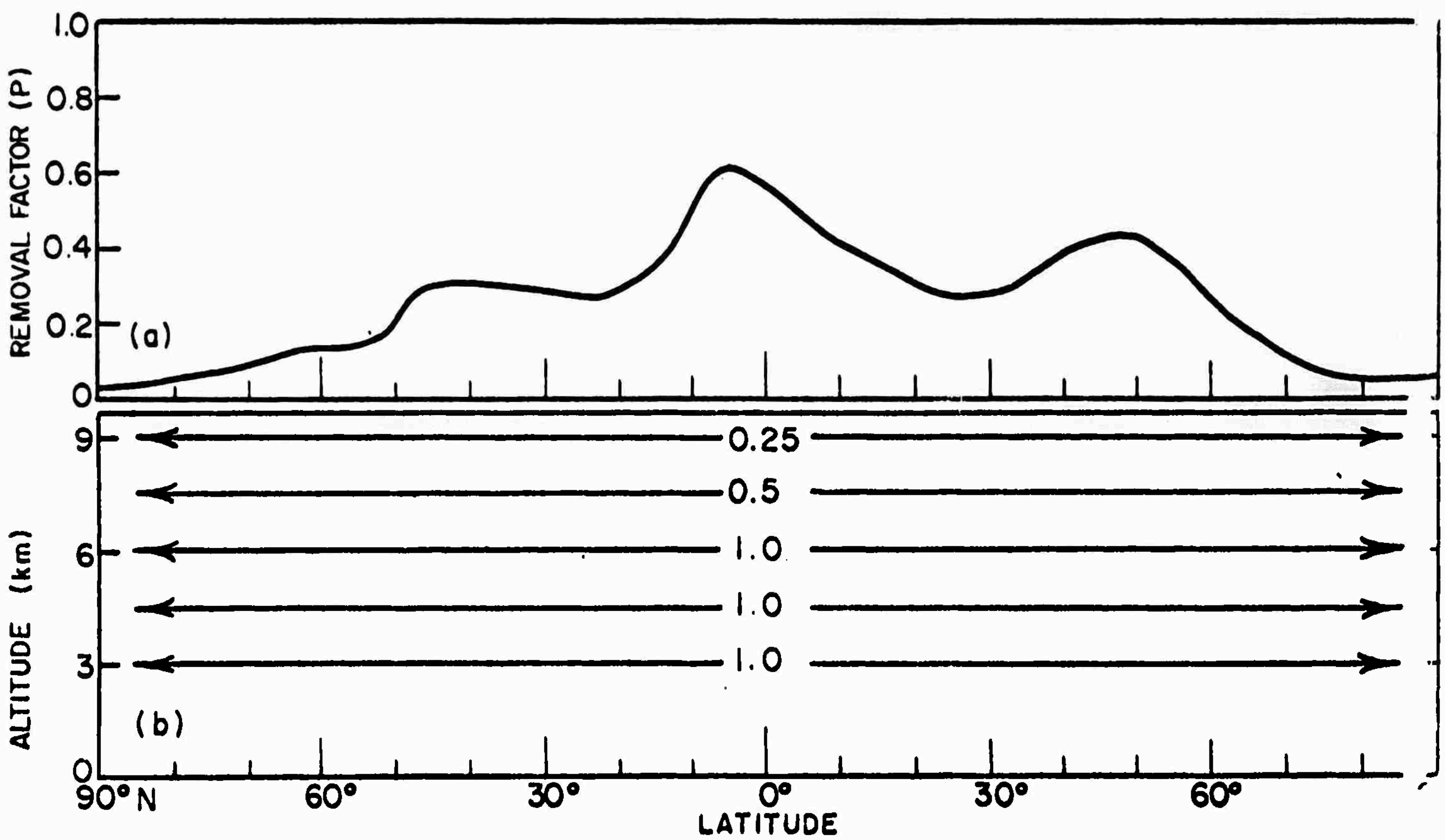

FIGURE 133. VARIATION OF THE REMOVAL FACTOR IN THE NUMERICAL MODEL
(a) P AS A FUNCTION OF LATITUDE
(b) "a" VALUES FOR THE FIVE REMOVAL LEVELS.

removed in a fixed $\Delta\mu$ interval is

$$\Psi(\mu,t) = 2\pi r_0^2 \Delta\mu \quad X(\mu,z) \quad (z)dzdt \; . \qquad (9)$$

The removal levels and values of $p(\mu)$ and $a(z)$ are illustrated in Figure 133. In the models which are presented in detail, the fractional removal was accomplished every 5.0 days. A CDC 1604 computer was used for all computations with a time step of approximately 1.27 days.

In order to test the validity of the transformations (2) to (4), the finite difference approximation to (5), and the effect of the variable grid spacing ($\Delta\,\mu$) in the μ-direction in the Northern and Southern Hemispheres, a test model was run assuming the finite difference equivalent of a point source at μ = 0 (the equator) and z = 21 km. The slope of the surface containing the principal duffusion axis was assumed constant and equal to 9.19×10^{-4}; $K_{11} = 3 \times 10^9$ cm^2/sec and $K_{22} = 10^4$ cm^2/sec were the values of the diffusion coefficients. The transformations (2) to (4) were used to obtain K_{rr}, $K_{r\phi}$ and $K_{\phi\phi}$. A measure of the adequacy of (2) to (5) is the degree to which the meridional slope of the level of maximum concentration, as determined from the computations, conforms to the assumed slope of the surface containing the principal diffusion axis. The extent of the agreement six months after injection is shown in Figure 134. The level of maximum concentration in a vertical section was estimated by parabolic interpolation of the computed concentrations at grid points bracketing the grid point at which a maximum appeared. The agreement is considered to be satisfactory and it is worth noting that the unequal grid intervals in the Northern and Southern Hemispheres do not seriously distort the results.

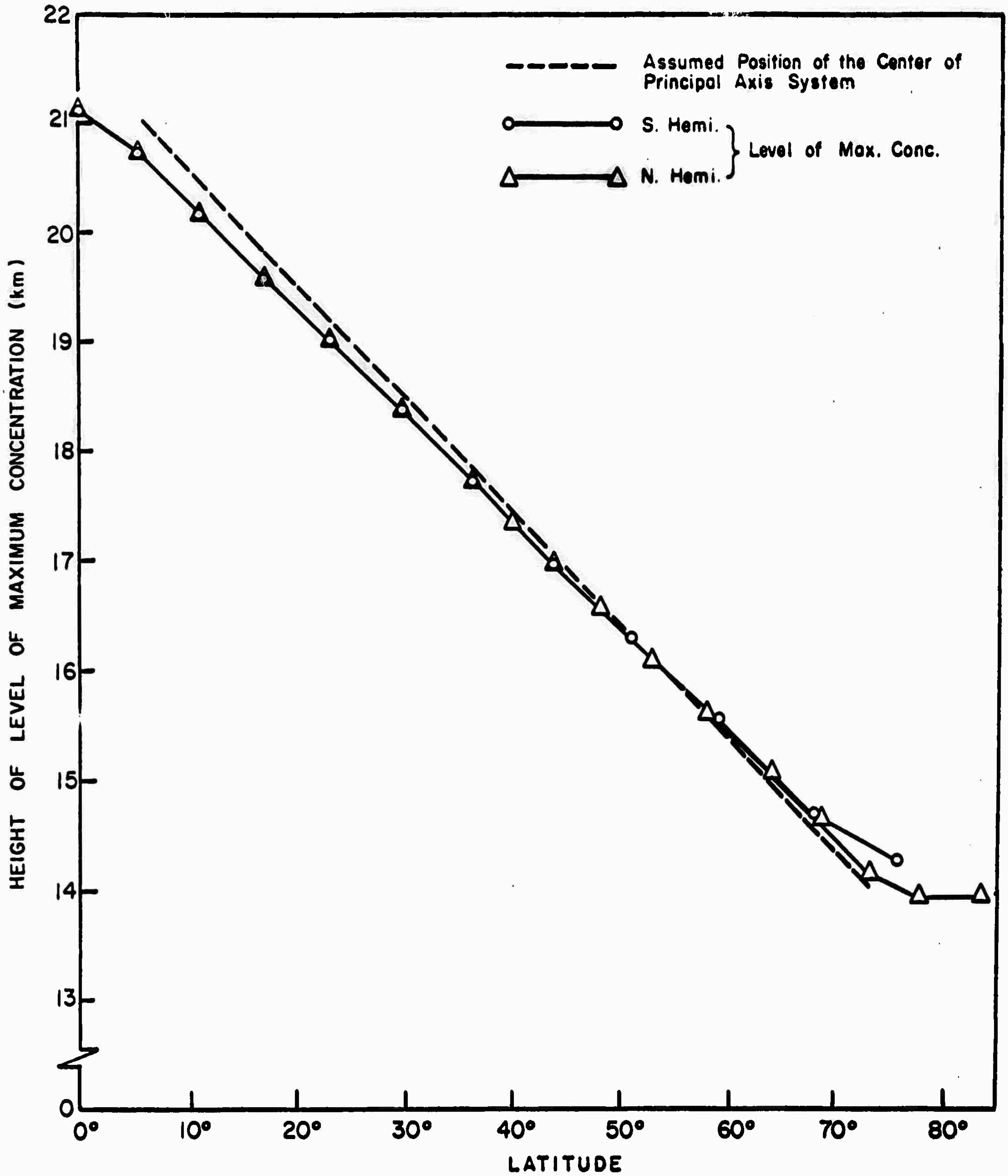

FIGURE 134. SLOPE OF THE LEVEL OF MAXIMUM CONCENTRATION PREDICTED BY THE NUMERICAL MODEL SIX MONTHS AFTER INJECTION COMPARED WITH THE ASSUMED SLOPE OF THE PRINCIPAL DIFFUSION AXIS.

13.3 Tropical Injection

For these experiments a vertical line source representing a tropical injection was assumed at $\mu = 0.2$ (11°32'N) with a center of gravity ranging from 19.5 to 21 km according to the specific experiment. The results are reported for each of the following hypotheses:

1. The principal diffusion axis contained in horizontal planes, ($\alpha = 0$).
2. The principal diffusion axis contained in planes parallel to potential temperature surfaces in the stratosphere.
3. The principal diffusion axis contained in planes parallel to the mean meridional configuration of the tropopause.

For hypothesis 1 the horizontal diffusion coefficient ($K'_{11} = K_{\phi\phi}$) varied from 10^9 to 10^{10} cm^2/sec. The vertical diffusion coefficient ($K'_{22} = K_{zz}$) varied from 10^3 to 10^5 cm^2/sec, i.e. 10^3 cm^2/sec in the tropical stratosphere, 6×10^3 to 5×10^4 cm^2/sec in the polar stratosphere, and 10^4 to 10^5 cm^2/sec in the troposphere and "gap" regions. The horizontal diffusion coefficient was varied strongly with both latitude and height in attempts to obtain the observed meridional variation in the height of the maximum concentration. It was found possible to reproduce the desired stratospheric concentration patterns for only relatively small periods (1 to 4 months) after injection. Beyond these periods the altitude of maximum concentration tended to increase at a rate more rapid in mid and high latitudes than in equatorial regions. After times of 6 to 12 months the maximum concentrations exhibited distributions which were opposite in slope to the observed distribution, i.e., the altitude of maximum concentration had an upward instead of downward pole slope. There are two main factors contributing to this undesirable behavior.

The first is the effect of the vertical variation of air density. From (5) this effect can be isolated as

$$\frac{\partial q}{\partial t} = K_{zz} \frac{\partial q}{\partial z} \cdot \frac{\partial(\ln \rho)}{\partial z} + \ldots \tag{10}$$

The sign of $(\partial/\partial z)$ $(\ln\rho)$ is always negative so that the sign of the contribution of the variable density term to $\partial q/\partial t$ is determined by the sign of $\partial q/\partial z$. For an isolated point source, therefore, the effect of the variable density term is to produce a positive $\partial q/\partial t$ above the source and a negative $\partial q/\partial t$ below. The magnitude of this effect is proportional to the magnitude of the vertical diffusion coefficient, K_{zz}. The second factor comes from the introduction of large vertical diffusion coefficients in the "gap" regions. These large coefficients were needed in order to duplicate the time rate and meridional distribution of surface deposition. This meridional variation of the vertical diffusion coefficients in the lower stratosphere, coupled with the variable density factor and the tropospheric sink, caused the level of maximum concentration to rise more rapidly in mid latitudes than at the equator.

It was, therefore, concluded that, within the range of diffusion coefficients considered to be even remotely reasonable, it was impossible to reproduce correctly the meridional distributions of both the surface deposition and the stratospheric concentration on the basis of diffusion processes alone when the principal diffusion axis is assumed to be everywhere horizontal.

The consequences of hypothesis 2, namely that the principal diffusion axis parallels the isentropes, were examined despite the fact that the observed slope of the isentropes at 20 km is less than one-half the observed slope of the level of maximum concentration of the tungsten-185 distribution. It was con-

sidered that suitable adjustments of K'_{11} and K'_{22} in such an inclined diffusion axis scheme might lead to better agreement than had been obtained with the horizontal axis.

The most elaborate experiment of this type involved varying the slopes of the isentropes seasonally, setting the vertical diffusion coefficient in the "gap" region proportional to the magnitude of the monthly mean jet and fixing the horizontal diffusion coefficients according to the vertical and meridional distribution of the vector standard deviation of the wind (extrapolating values into the stratosphere). Data for these seasonal and spatial variations were obtained from meridional cross-sections published by the U.S. Weather Bureau[111]. For this set of experiments, K'_{11} varied from 10^8 to 10^{10} cm^2/sec and K'_{22} varied from 10^3 to 10^5 cm^2/sec.

The results were not satisfactory. The large diffusion coefficients in the "gap" region and the strong tropospheric rainout mechanism made it impossible to maintain the desired slope of the level of maximum concentration in the stratosphere equatorward of the "gap" region, although more satisfactory results were obtained poleward of the "gap" region. The large spatial variation of the primed diffusion coefficients in the "gap" region tended to obscure the effect of the sloping principal diffusion axis. The one positive conclusion from this set of experiments was that the anisotropic model, with the principal axis of the diffusion tensor oriented along the isentropic surfaces, did significantly slow down the rate of rise of the level of the maximum concentration in the presence of a strong tropospheric sink and relatively large values of K'_{11} and K'_{22} in the "gap" regions.

Finally, hypothesis 3 was investigated by assuming that the quasi-horizontal principal diffusion axis in the stratosphere and upper troposphere

is approximately parallel to the mean annual tropopause configuration at all levels in the meridional plane. The mean slope of the tropopause in the jet stream region was determined each month from meridional cross-sections for 1958[111]. These slopes were then averaged for the year and located at the mean annual latitudinal position of the jet core. The slope thus determined is about 4.1×10^{-3} and in the present model extends approximately from 33.5° to 46.5° N latitude. The principal diffusion axis was assumed parallel to this tropopause configuration from 6 km to 22.5 km; above 22.5 km the slopes were reduced to 2.9×10^{-3} mostly because the slopes of the lines of constant potential vorticity as indicated by Hering and Borden[103] decrease with altitude in the stratosphere. It is recognized that the method of averaging is somewhat arbitrary and must be considered in the interpretation of the results. This, however, is not considered to be a serious drawback in the present development of the model.

It was found for this last scheme that all of the observed features of the tungsten experiment could be reproduced with an extremely simple set of diffusion coefficients. A value of $K'_{11} = 4 \times 10^{9}$ cm^2/sec throughout the system; a value of $K'_{22} = 10^{3}$ cm^2/sec throughout the stratosphere and a value of $K'_{22} = 4 \times 10^{4}$ throughout the troposphere were sufficient to yield satisfactory results. In this series of experiments it was assumed that the injection took place at $\mu = 0.2$ (11°32' N); at z = 18 km, q = 5.1 pCi/g of air and at z = 19.5 km, q = 12.9 pCi/g of air. This source configuration corresponds to a total injection of 70 megacuries, approximately the mid-point of the range of estimates of 54 to 87.5 megacuries.

In Figure 135 the decrease with time of central concentration predicted by the model is compared with the observed decrease. The meridional distributions of total deposition, one year after injection, as predicted by the model and as estimated from observed data by Friend et al.[101] are shown in Figure 136. The predicted peaks occurred at the same latitudes as observed in the Southern Hemisphere and the Tropics while the predicted Northern Hemisphere peak occurred about 5 degrees north of the observed peak. Also, the relative magnitudes of the predicted peaks corresponded well with the observed data. There was, however, some disparity between the totals of global fallout represented by the two curves. The model indicated 45 megacuries deposited while the observed estimate was 61 megacuries. This difference can be attributed to two factors - the magnitude of the injection in the model was not large enough and/or the estimate of surface deposition from the observed data was too large. The experimental uncertainties in both of these factors are sufficient to account for the above mentioned disparity. The injection in the model could justifiably be accepted as 85 instead of 70 megacuries. Also, the estimate of total surface deposition by Friend et al.[101] for 16 months after the tungsten injections is 77.5 megacuries (corrected to August 15, 1958) which exceeds by 10% the total amount initially put into the stratosphere in the model. Indicative of the uncertainty in the estimates of surface deposition is the comparison of Hardy's[112] estimate of 50 megacuries for the 16 month period with the above 77.5 megacuries value.

Another disparity between the observed and model predicted distributions in Figure 136 is the difference in spread of the distributions about the Northern Hemisphere peak. Attempts to improve the spread of the predicted dis-

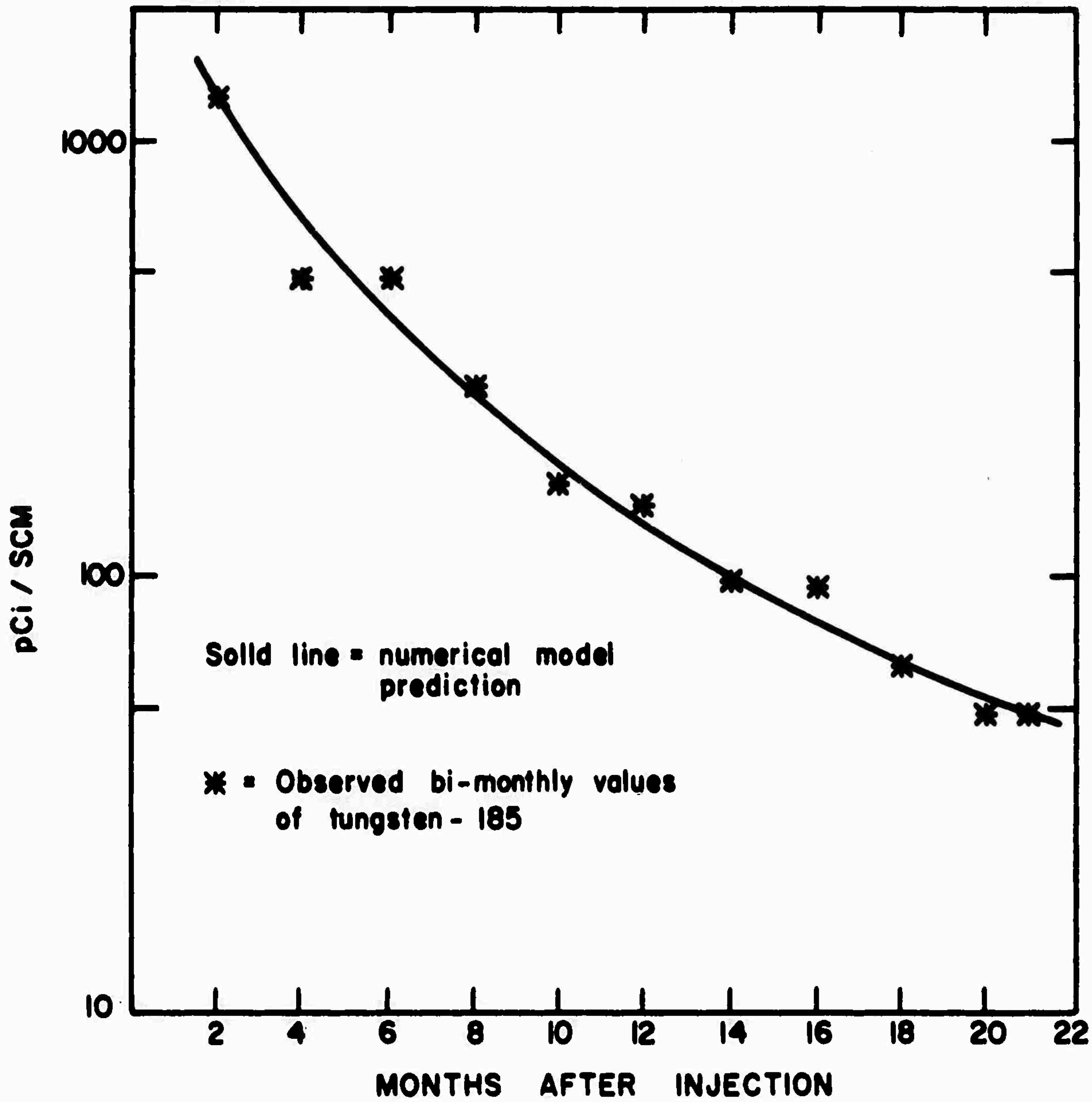

FIGURE 135. DECREASE OF CENTRAL CONCENTRATION WITH TIME.

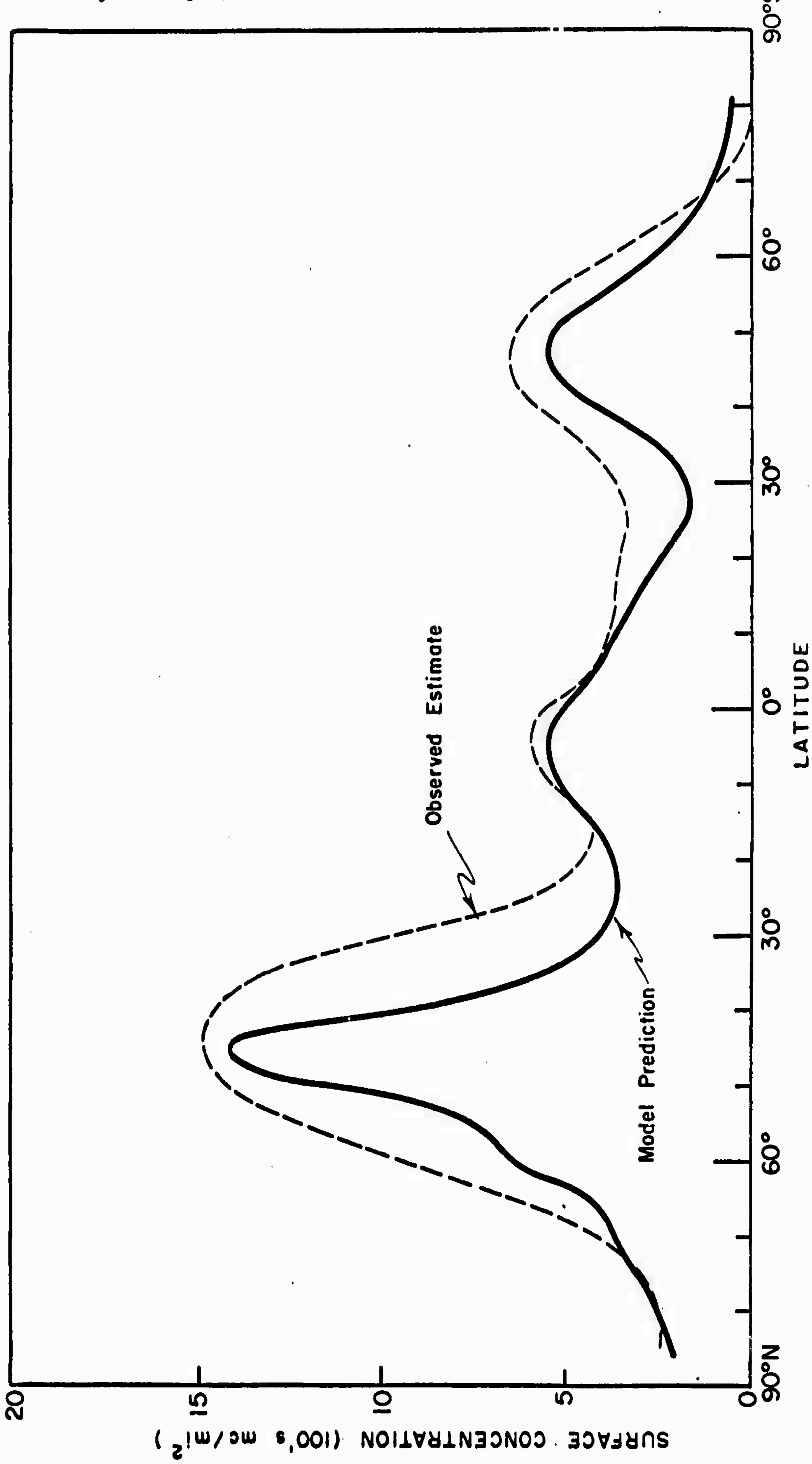

FIGURE 136. DISTRIBUTIONS OF SURFACE DEPOSITION OF TUNGSTEN-185 ONE YEAR AFTER INJECTION.

tribution by variations of the magnitudes of K_{11} and K_{22} in the troposphere were not successful. It is felt, however, that considerable improvement can be realized by a four season model in which there are a seasonal shift meridionally of the tropopause configuration and a seasonal variation in the magnitudes of the wet removal factors.

In view of the uncertainties of the observed surface distribution and magnitude of initial injection and of the simplicity of the model structure these results are considered satisfactory.

Further satisfactory results were achieved by the model with respect to the stratospheric residence half-times for the material. The decrease with time of the stratospheric inventory in the model has been plotted in Figure 137. and compared to rates of decrease corresponding to various theoretical residence half-times. An average residence half-time of 7 months is indicated for the model during the first 16 months after injection. Thereafter, the residence half-time tends to increase to 9 and 10 months. These results are in accord with the 5 to 9 months estimates for stratospheric material made by Friend et al.[101] based on the possible range of magnitudes of injection and stratospheric inventories estimated from observed data.

Figures 138,139,140 compare the observed stratospheric distributions of tungsten with the model prediction 6, 12 and 24 months after injection, respectively. The gross features of the observed tungsten-185 distributions were satisfactorily reproduced by the numerical model at 6 and 12 months after injection but the similarity of features is noticeably less after 24 months. It must be borne in mind, however, that after 24 months, the observed data are much less reliable. The important gross features to be compared between the observed and model results

ISOTOPES
A Teledyne Company

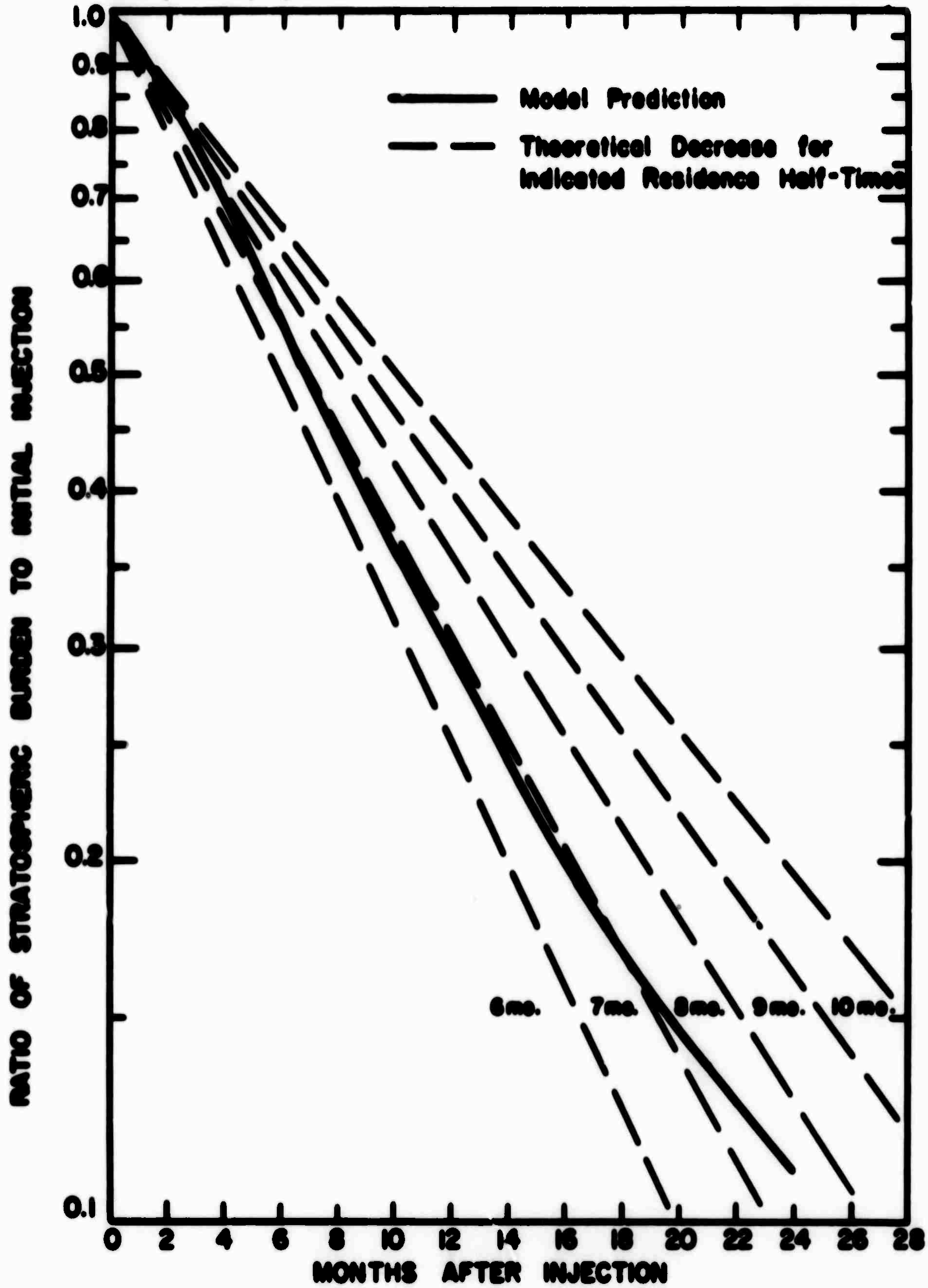

FIG.137 DECREASE OF STRATOSPHERIC BURDEN WITH TIME PREDICTED BY NUMERICAL MODEL FOR TROPICAL INJECTION.

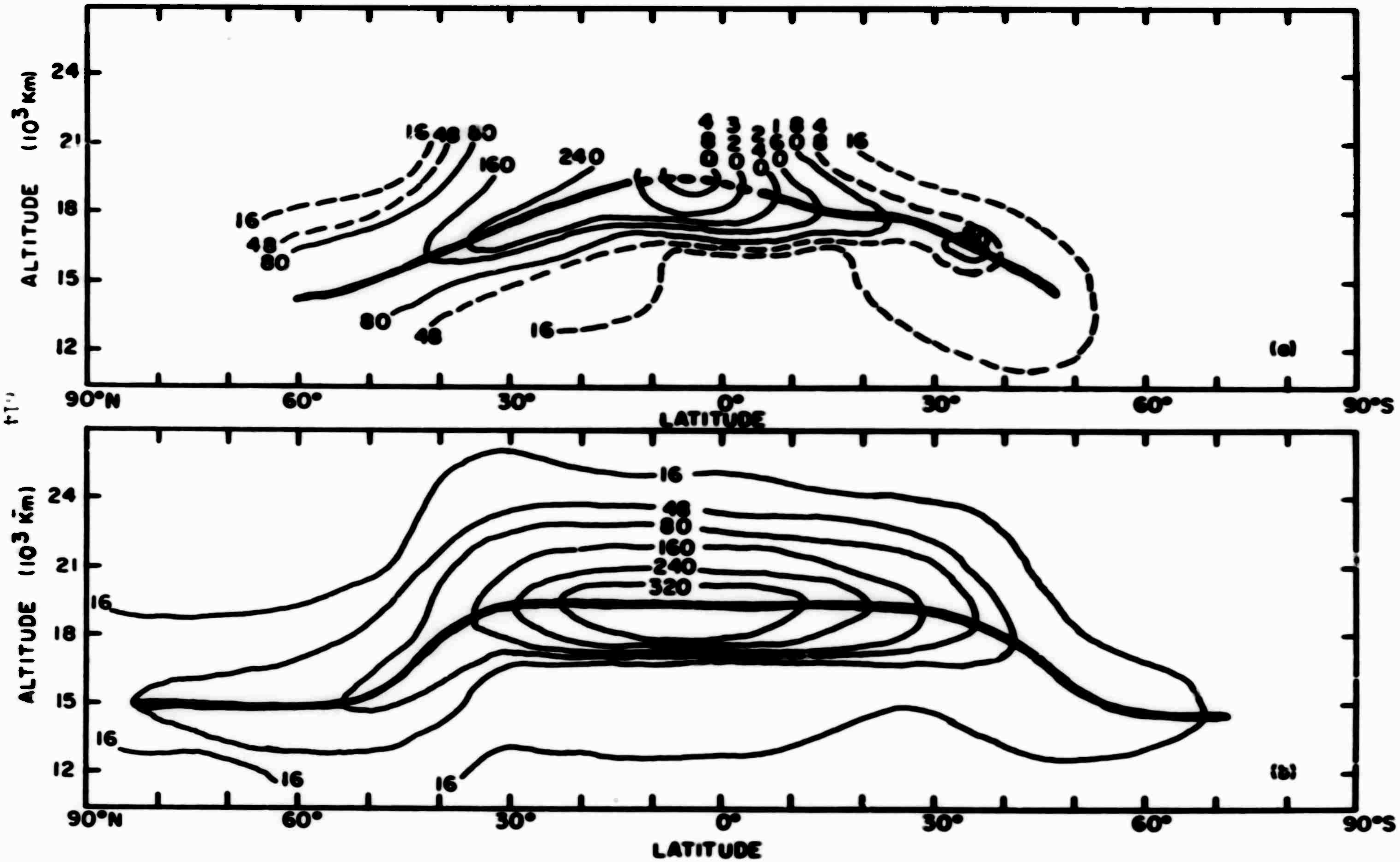

FIGURE 138. DISTRIBUTIONS OF TUNGSTEN-185 SIX MONTHS AFTER INJECTION. (a) OBSERVED MEAN FOR NOV.-DEC., 1958 (pCi/SCM CORRECTED TO 15 AUGUST 1958). (b) PREDICTION BY NUMERICAL MODEL (pCi/SCM).

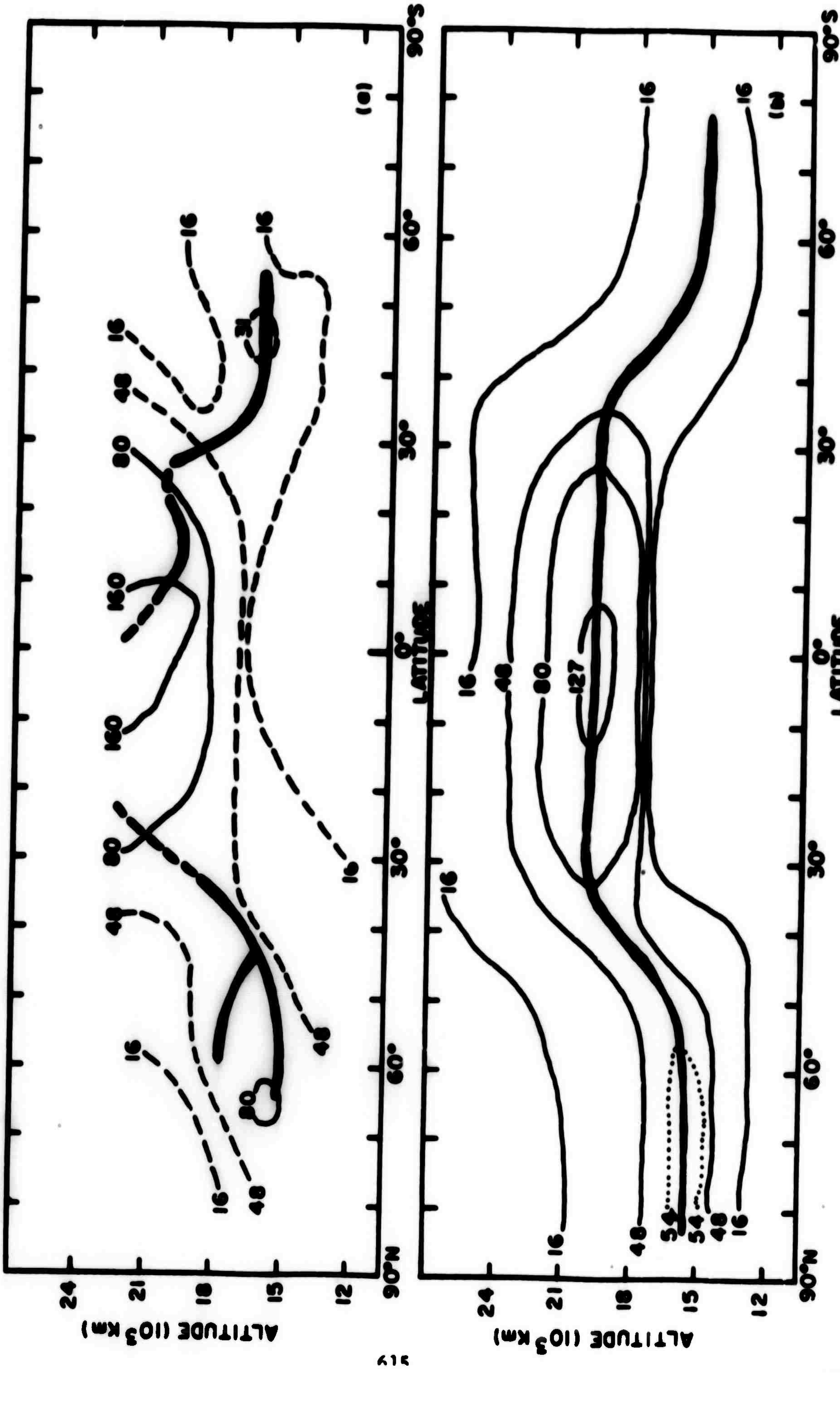

FIGURE 13o. DISTRIBUTIONS OF TUNGSTEN-185 TWELVE MONTHS AFTER INJECTION. (a) OBSERVED MEAN FOR MAY–JUNE, 1959 (pCi/SCM CORRECTED TO 15 AUGUST 1958. (b) PREDICTION BY NUMERICAL MODEL (pCi/SCM).

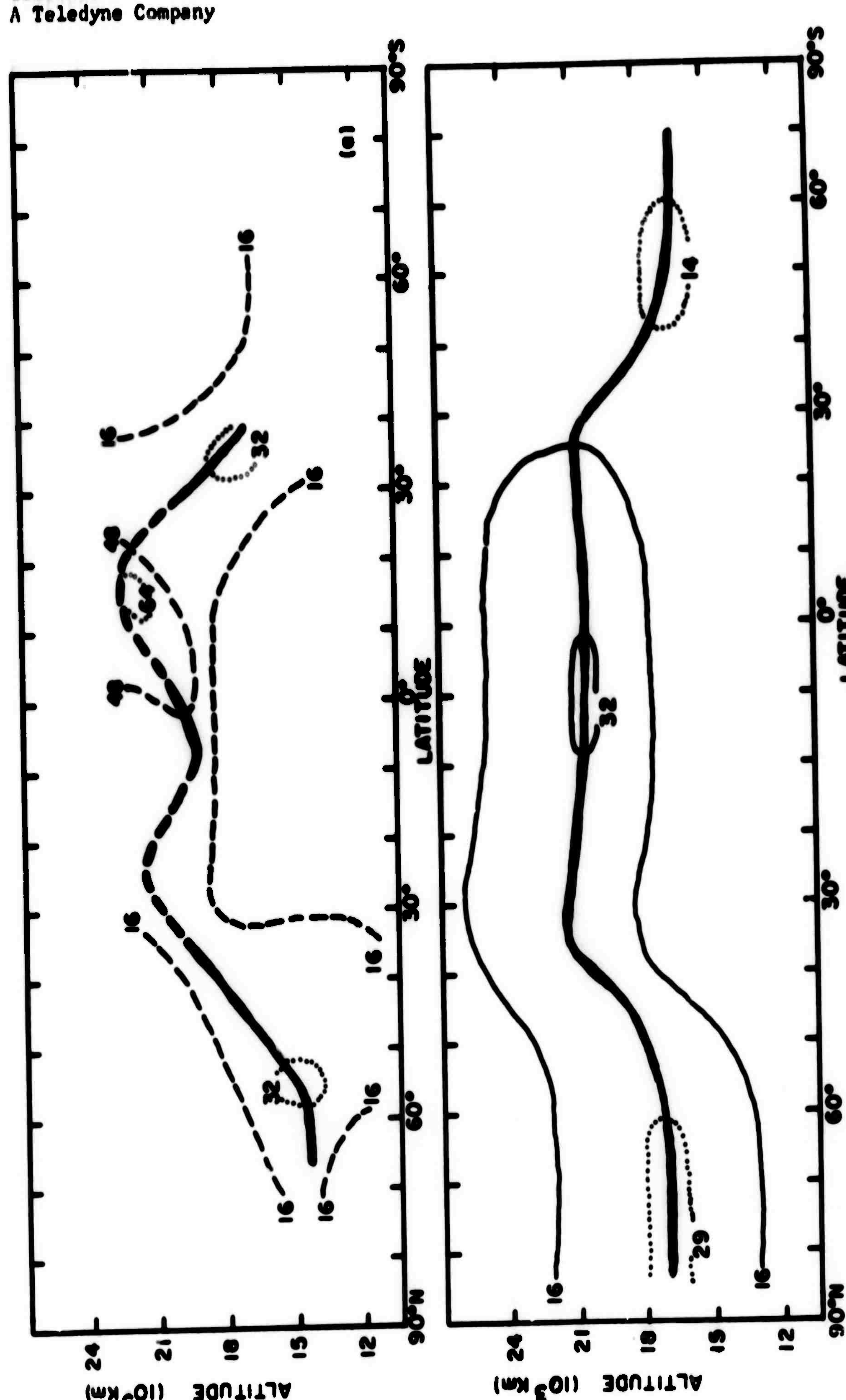

FIGURE 140. DISTRIBUTIONS OF TUNGSTEN-185 TWENTY-FOUR MONTHS AFTER INJECTION. (a) OBSERVED MEAN FOR MAY-JUNE, 1960 (pCi/SCM CORRECTED TO 15 AUGUST 1958). (b) PREDICTION BY NUMERICAL MODEL (pCi/SCM).

are: (1) decrease in height of 3.5 kilometers of the level of maximum concentration from 20° to 60° latitude in both hemispheres; (2) strong vertical concentration gradient in the lower tropical stratosphere just above the tropical tropopause and a considerable decrease in this gradient poleward in the lower polar stratosphere; (3) the tendency for the tropical center of maximum concentration to move equatorward; and (4) development of secondary centers of maximum concentration at higher latitudes.

After 24 months significant difference in concentration distributions appeared, as shown in Figure 140. The observed data indicated a movement of the tropical center of maximum concentration well into the Southern Hemisphere whereas this center remains within the vicinity of the equator in the model. The observed data are considered quite suspect at this time. In the observed concentration distribution 22 months after injection there is no indication of movement of the center of maximum concentration into the Southern Hemisphere. Also, at high latitudes, the height of the level of maximum concentration rose to 57 thousand feet in the model, but remains at approximately 50 thousand feet in the observed data.

13.4 Polar Injection

Since the possibility existed of fortuitous agreement between predicted and observed results for these experiments with tropical injections, it was decided to examine the consequences of the same hypothesis (i.e. the principal axis of diffusion parallels the tropopause configuration) as applied to a lower polar stratospheric injection. For this investigation the [illegible] Soviet test series was selected as representative of such an injection.

The observed strontium-90 data for this test series were determined by isotopic ratio (Sr-89/Sr-90, Ce-144/Sr-90) dating because there was a considerable amount of strontium-90 in the atmosphere due to previous testing. Also, these data are not considered beyond April 1962 because of the injection of new strontium-90 by United States tests after this date. Thus, the observed data are confined essentially to the winter months. The model was adapted for a winter season experiment by assuming the same average slope (4.1×10^{-3}) of the tropopause in the jet core region but the latitudinal position of the jet core was displaced some 15 degrees equatorward.

It was fairly well known that the major testing in this series was conducted at Novaya Zemlya, approximately 75°N latitude, but the altitude, magnitudes and vertical distributions of the individual injections are highly speculative. In the model, therefore, the magnitude of the injection was arbitrary and, using the observed data as guidelines for altitude and vertical distribution, an equally distributed line source was put in between 45 and 50 thousand feet.

Figure 141 shows the results of one of these simplified experiments with polar injections. It can be appreciated that the major features of the stratospheric concentration patterns were reproduced in a qualitative fashion. The most satisfying feature is that the observed upward-equatorward slope of the surface of maximum concentration was reproduced quite well.

In Figure 142 the surface deposition computed from the model is compared with the estimate of distribution from Hardy and Collins[113] and with an estimate determined from data by Telegadas[115] which incorporates a correction for rainfall. The better agreement between the model prediction and

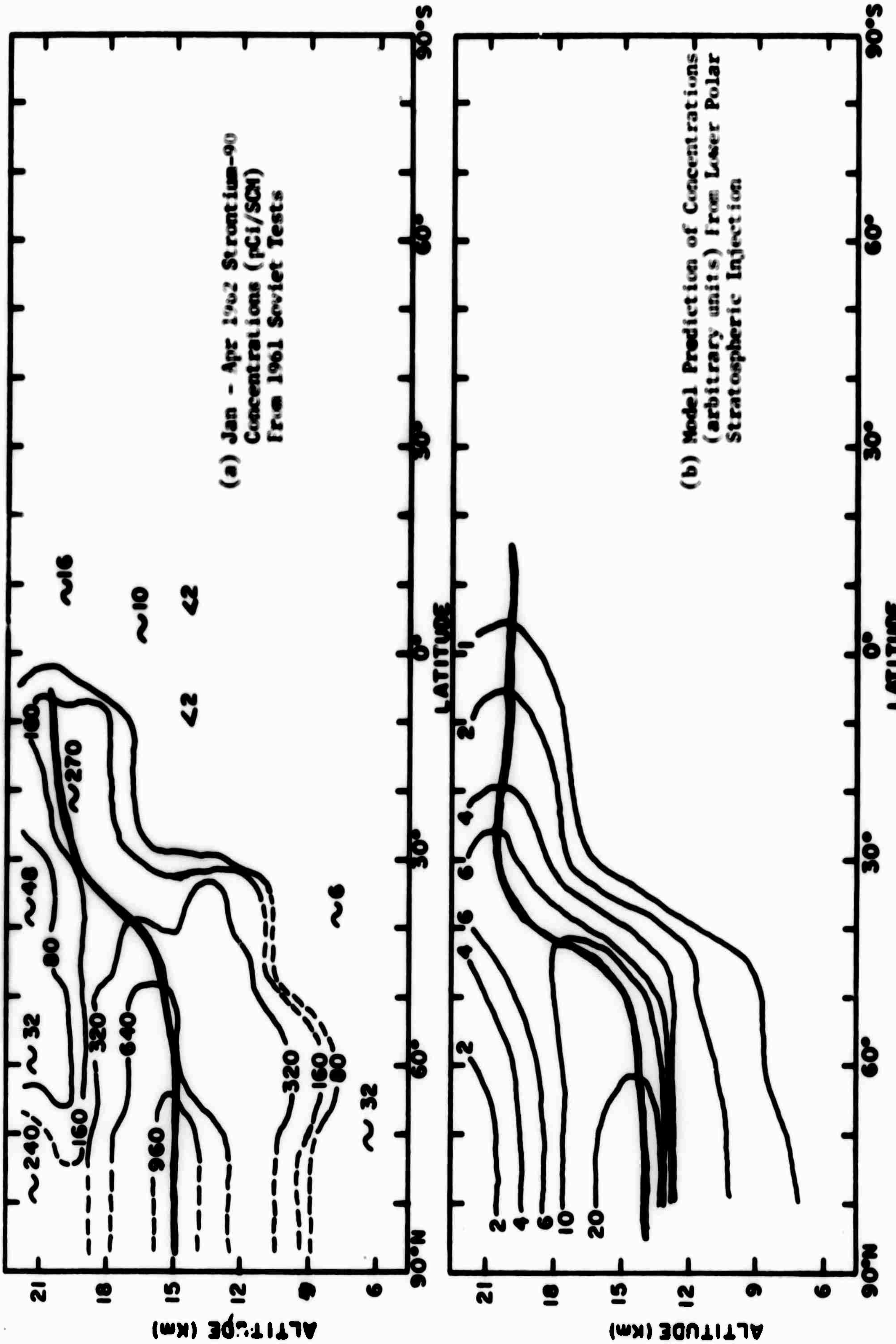

FIGURE 141. MODEL PREDICTIONS (b) AND ACTUAL MEASUREMENTS (a) OF STRONTIUM-90 DISTRIBUTIONS RESULTING FROM LOWER POLAR STRATOSPHERIC INJECTION.

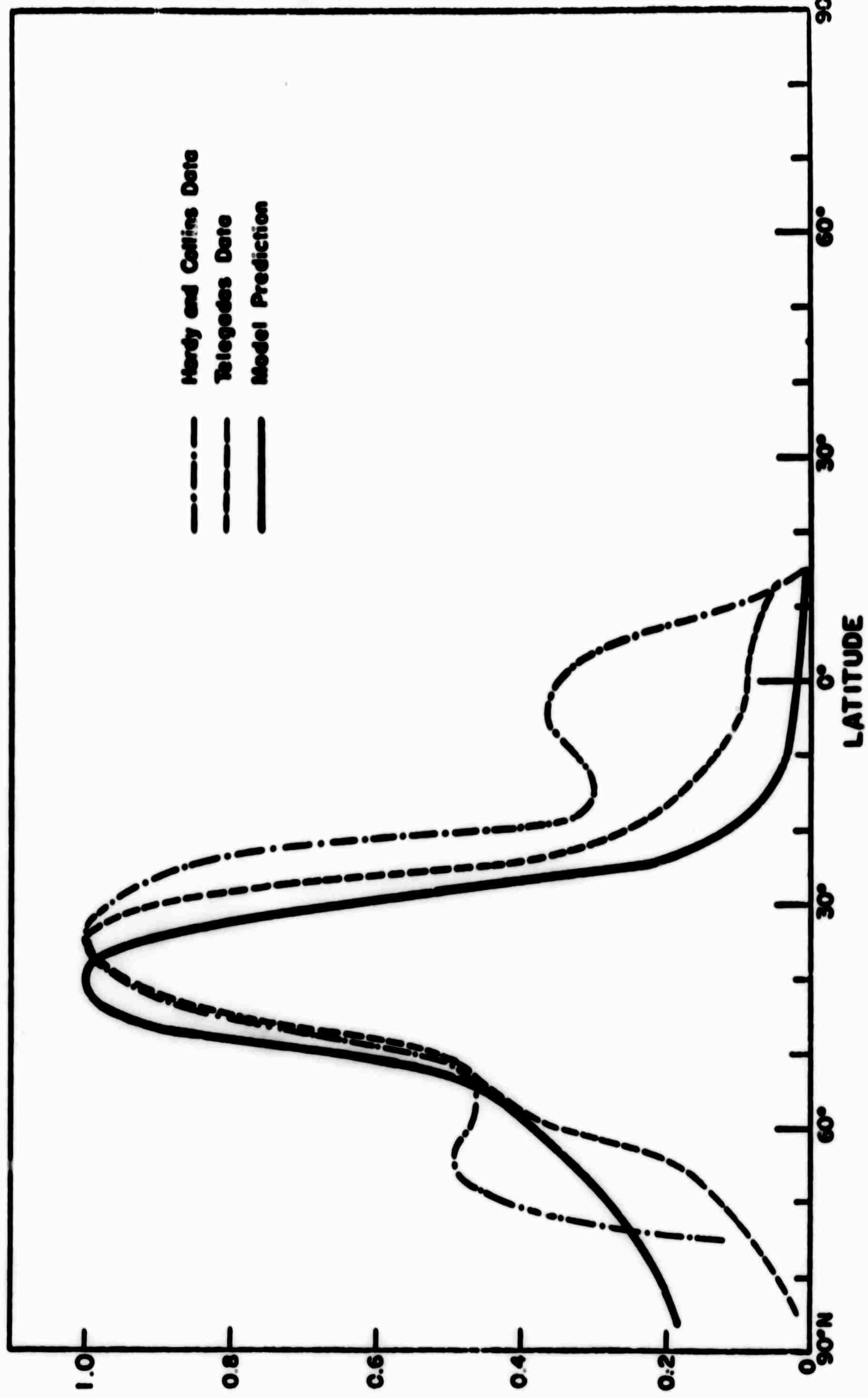

FIGURE 142. DISTRIBUTION OF SURFACE DEPOSITION SIX MONTHS AFTER POLAR STRATOSPHERIC INJECTION.

the Telegadas estimate is noteworthy since the wet-fallout simulation in the model is based on the average meridional distribution of rainfall.

The observed data of the decrease with time of the stratospheric burden of strontium-90 from 1961 Soviet tests are insufficient to provide a worthwhile quantitative estimate of residence half-times of the material. It is generally recognized that the residence time of debris in the atmosphere is dependent upon the height, latitude and season of injection and that it is shorter for higher latitudes and lower altitudes[101,102]. Residence half-times of 3 to 6 months have been considered reasonable for the lower polar stratosphere in computations of burden trends[101]. Figure 143 shows the decrease of stratospheric burden with time as predicted by the numerical model. A residence half-time of 5 to 7 months is indicated for the curve. These values are generally lower than those predicted in the tropical injection and are in reasonable accord with the investigators cited above.

The experimental results of the polar injection presented above required a winter season adaptation of the model as used for the tropical injection. This adaptation was considered to be reasonable, and the later success of the four-season model of Project STREAK tends to substantiate this.

Generally the STREAK model gave results which quite satisfactorily reproduced the strontium-90 behavior for the 1961-1962 U.S.S.R. and U.S.A. atmospheric test series. However it is noteworthy that it did not account for the behavior of the tungsten-185 as well as did the STARDUST mean annual model. Perhaps because of the relative lack of seasonal change in the meteorological properties of the tropical stratosphere the STARDUST model more closely represents the behavior of debris injected in the equatorial regions than does the four-season STREAK model.

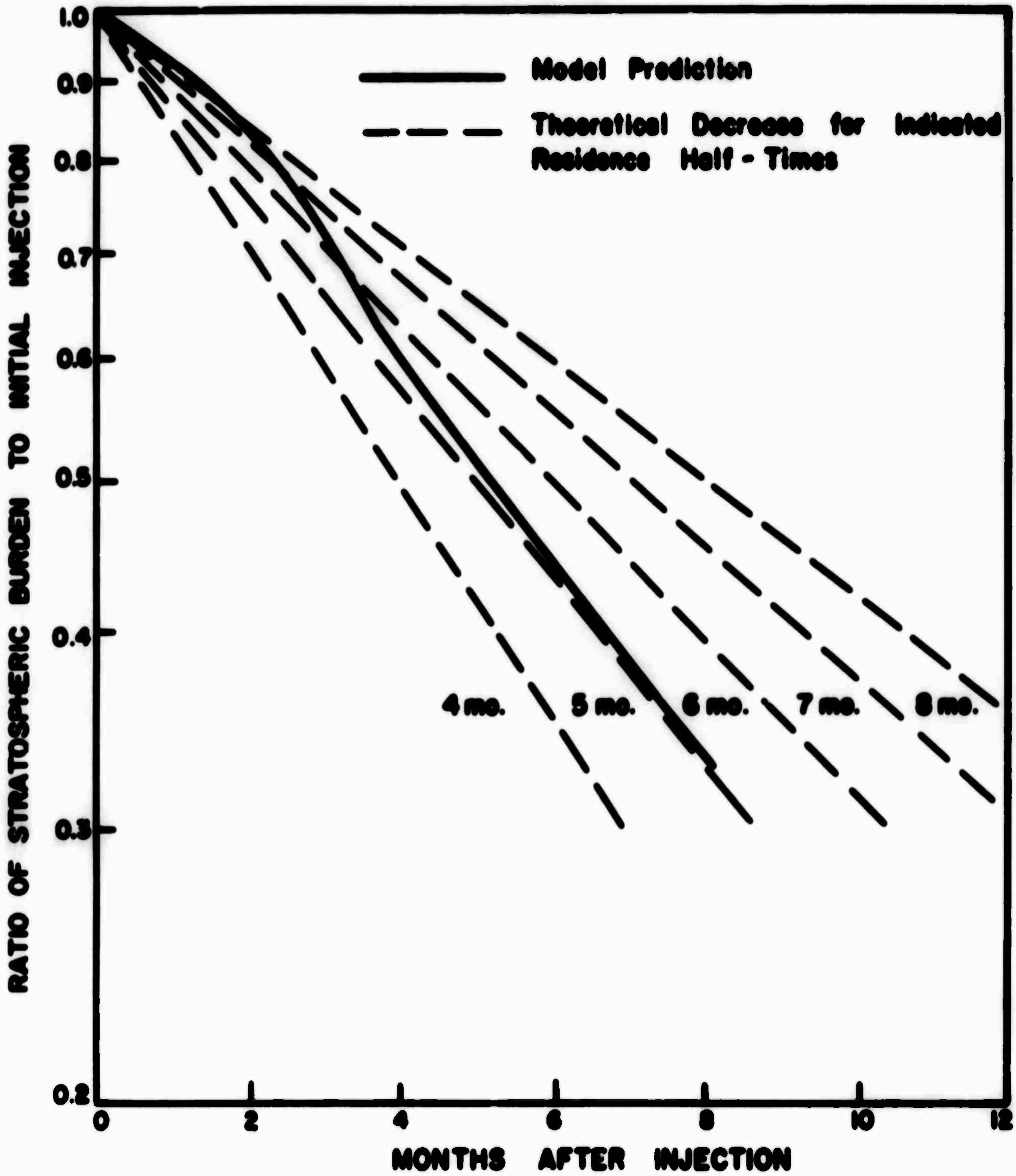

FIG. 143 DECREASE OF STRATOSPHERIC BURDEN WITH TIME PREDICTED BY NUMERICAL MODEL FOR POLAR INJECTION.

13.5 Conclusion

A numerical model of eddy diffusion, particle settling and removal in the stratosphere-troposphere-earth's surface system has been developed which predicts satisfactorily the behavior of injections of material into the lower tropical stratosphere. Applying of this model to lower polar stratospheric injections lead to predictions which, at least, are not in gross error. The model has a relatively simple set of parameters for characterizing the transport-removal system. A prime feature of the model is that the local quasi-horizontal principal axis of the diffusion tensor lies in surfaces parallel to the tropopause. This is an empirical result of the present study.

It has been widely held that large-scale eddy diffusion is basically an isentropic process. The observation was made by Feely and Spar[19], that the tungsten-185 distribution appeared to have been affected by non-isentropic motions. Since basically, the same data considered by them were used in this study, it is perhaps not surprising that a "non-isentropic" model yielded the best results. Hering and Borden[103] in studying ozone transport, computed surfaces of equal potential vorticity in the stratosphere; they concluded that the ozone transport may occur in motions parallel to these surfaces which are more nearly parallel to the tropopause than are the isentropic surfaces. Newell[86] in studying potential energy-kinetic energy relationships in the stratosphere, concluded that non-isentropic processes took place there, especially in mid-latitude regions. These findings, along with the current model study, indicate that the primary large-scale mixing processes in the lower stratosphere may take place along surfaces of constant potential vorticity. This statement must be qualified as conjectural, since there are no reliable climatological stratospheric potential

vorticity data which could be used in proof. The numerical experiment embodied in the present study is, however, sensitive enough to show that some non-isentropic processes are involved in large-scale mixing motions of the lower stratosphere. Furthermore, it appears unnecessary to ascribe a dominant role to meridional circulations in the transport of material in that portion of the atmosphere.

REFERENCES

1. J.P. Friend, H.W. Feely, P.W. Krey, J.Spar and A. Walton, "The High Altitude Sampling Program", U.S. Defense Atomic Support Agency report DASA 1300 (1961).

2. F.T. Hagemann, J.Gray, Jr. and L. Machta, "Carbon-14 Measurements in the Atmosphere - 1953 to 1964", USAEC report HASL - 159, (1965).

3. C.E. Junge, C.W. Chaghon and J.E. Manson, "Stratospheric Aerosols", Jour. of Meteorology, 18, 81-108, (1961).

4. C.E. Junge and J.E. Manson, "Stratospheric Aerosol Studies", Jour. of Geophysical Research, 66, 2163-2182, (1961).

5. S.C. Mossop, "Stratospheric Particles at 20 km Altitude", Geochimica et Cosmochimica Acta, 29, 201-207, (1965).

6. J.P. Friend, "Properties of the Stratospheric Aerosol", Tellus, 18, 465-473, (1966).

7. W.E. Rane and J.B. Wong, "Impaction of Dust and Smoke Particles on Surface and Body Collectors", Industrial and Engineering Chemistry, 44, 1371-1381, (1952).

8. G. Newkirk and J.A. Eddy, "Light Scattering by Particles in the Upper Atmosphere", Jour. of the Atmospheric Sciences, 21, 35-60, (1964).

9. S.C. Mossop, "Volcanic Dust Collected at an Altitude of 20 km", Nature, 203, 824-827, (1964).

10. C.E. Junge, "Vertical Profiles of Condensation Nuclei in the Stratosphere", Jour. of Meteorology, 18, 501-509, (1961).

11. C.E. Junge, "The Formation of the Stratospheric Sulfate Layer", paper presented at the CACR Symposium on Atmospheric Chemistry, Circulation and Aerosols, Visby, Sweden, 18-25 August 1965.

12. R.D. Cadle and J.W. Powers, "Some Aspects of Atmospheric Chemical Reactions of Atomic Oxygen", Tellus, 18, 176-186, (1966).

13. U.S. Weather Bureau, "Announced Nuclear Detonations, 1945-1962", USAEC report HASL - 142, 218-241, (1964).

14. P.J. Dolan, "Calculated Abundances and Activities of the Products of High Energy Neutron Fission of Uranium-238", U.S. Defense Atomic Support Agency report DASA 525 (1959).

15. E.A. Martell, "Tungsten Radioisotope Distribution and Stratospheric Transport Processes", Jour. of Atmospheric Sciences, 25, 113-125, (1968).

16. U.S. Weather Bureau, "Daily Aerological Cross Sections, Pole to Pole along Meridian 75° W for the IGY Period", Washington, D.C., (1963).

17. U.S. Weather Bureau, "Daily 100-Millibar and 50-Millibar and Three Times Monthly 30-Millibar Synoptic Weather Maps of the IGY Period", Washington, D.C., (1963).

18. N. Murayama and L. Machta, "An Analysis of Averaged Balloon-borne Radioactivity Measurements", USAEC report HASL - 105, 141-149, (1961).

19. H.W. Feely and J. Spar, "Tungsten-185 from Nuclear Bomb Tests as a Tracer for Stratospheric Meteorology", Nature, 188, 1062-1064, (1960).

20. H.W. Feely, H. Seitz, R.J. Lagomarsino and P.E. Biscaye, "Transport and Fallout of Stratospheric Radioactive Debris", Tellus, 18, 310-328, (1967).

21. R.E. Newell, "The Transport of Trace Substances in the Atmosphere and their Implications for the General Circulation of the Stratosphere", Geofisica Pura e Applicata, 49, 137-158, (1961).

22. W.S. Hering, "Ozone and Atmospheric Transport Processes", Tellus, 18, 327-336, (1966).

23. U.S. Atomic Energy Commission, "High Altitude Sampling Program (Project ASH CAN)", USAEC report HASL - 115, 70-111, (1961).

24. L. Machta, R.J. List and K. Telegadas, "A Survey of Radioactive Fallout from Nuclear Tests", Jour. of Geophysical Research, 67, 1389-1400, (1962).

25. W.F. Libby and C.E. Palmer, "Stratospheric Mixing from Radioactive Fallout", Jour. of Geophysical Research, 65, 3307-3317, (1960).

26. M.I. Kalkstein, "Rhodium-102 High Altitude Tracer Experiment", Science, 137, 645-652, (1962).

27. A.K. Stebbins, III, "Second Special Report on the High Altitude Sampling Program", U.S. Defense Atomic Support Agency report DASA 539 B, (1961).

28. S. Glasstone, "The Effects of Nuclear Weapons", p. 484, USAEC, (1962).

29. M.I. Kalkstein, "Movement of Material from High Altitude Deduced from Tracer Observations", Jour. of Geophysical Research, 68, 3835-3839, (1963).

30. M.I. Kalkstein, "Rhodium-102 High Altitude Tracer Experiment. I. Stratospheric Results", Air Force Cambridge Research Laboratories publ. No. 62-460 (1), (1962).

31. S. Katcoff, "Fission Products Yields from Neutron-Induced Fission", Nucleonics, 18, No. 11, 200-208, (1960).

32. U.S. Weather Bureau, "Global Atmospheric Radioactivity, May-June 1960 and November 1960", USAEC report HASL - 115, 177-183, (1961).

33. U.S. Government, "Global Atmospheric Radioactivity, May-June 1961", USAEC report HASL - 117, 225-229, (1961).

34. U.S. Government, "Global Atmospheric Radioactivity, November 1961 and April 1962", USAEC report HASL - 142, 272-276, (1964).

35. N. Harley, I Fisenne, L.D.Y. Org and J. Harley, "Fission Yield and Fission Product Decay", USAEC report HASL - 164, 251-260, (1965).

36. K. Telegadas, "The Relationship Between Stratospheric Circulation Patterns and Radioactive Debris in Early 1963", Jour. of Applied Meteorology, 6, 134-141, (1967).

37. K. Labitzke-Behr, Z. Petkovsek and R. Scherhag, "Preliminary Daily Northern Hemisphere 30-Millibar Synoptic Weather Maps of the year 1962", Institut fur Meteorologie und Geophysik der Freien Universitat Berlin, Meteorologische Abhandlungen, Band 25, Heft 1., (1962).

38. I. Bark, B. Kriester, K. Labitzke-Behr, Z. Petkovsek, R. Scherhag, K. Sieland, R. Stuhrmann and G. Warnecke, "Tagliche Hohenkarten der 100-mbar-Flache fur das jahr 1962", Institut fur Meteorologie und Geophysik der freien Universitat Berlin, Meteorolgische Abhandlungen, Band 23, Heft 1, (1962).

39. L.P. Salter, "High Altitude Balloon Sampling Program", USAEC report HASL-140, 166-214, (1963).

40. L. Machta, Personal communication, (1962).

41. Y.P. Rao, Quarterly J. Royal Meteorol Soc., 86, 156, (1960).

42. U.S. Weather Bureau, Technical Paper No. 41, (1961).

43. N.A. Harley, I.M. Fisenne, L.D.Y. Org, and J.H. Harley, USAEC report HASL-117, 194, (1961).

44. S.S. Brar, D.M. Nelson and B.B. Hicks, "Radioactive Debris Measurements from 1965 and 1966 Chinese Nuclear Tests", USAEC report HASL-173, I 18 - I 30, (1966).

45. E.F. Danielsen, "The Laminar Structure of the Atmosphere and Its Relation to the Concept of a Tropopause", Archiv fur Meteorologie, Geophysik und Bioklimatologie, Series A, 11, 293-332, (1959).

46. A.K. Stebbins, III, U.S. Defense Atomic Support Agency report DASA-532B, 147, (1960).

47. U.S. Public Health Service, Radiological Health Data and Reports, 7, 673, (1966).

48. U.S. Public Health Service, Radiological Health Data and Reports, 8, 64, (1967).

49. L.P. Salter, "High Altitude Balloon Sampling Program", in Fallout Program Quarterly Summary Report, USAEC report HASL-149, 54-99, (Oct 1 1964).

50. L.P. Salter, "High Altitude Balloon Sampling Program", in Fallout Program Quarterly Summary Report, USAEC report HASL-158, 214-244, (Apr 1 1965).

51. P.W. Krey, "High Altitude Balloon Sampling Program", in Fallout Program Quarterly Summary Report, USAEC report HASL-171, 223-287 (Apr 1 1966).

52. New York TIMES, May 24 1964.

53. J.H. Harley, "Possible Pu^{238} Distribution from a Satellite Failure", USAEC report HASL-149, 138-142, (Oct 1 1964).

54. L. Machta, "Calculations of Pu^{238} Concentrations from the SNAP-9A Burnup", USAEC report HASL-155, (Jan 1 1965).

55. L.P. Salter, "Stratospheric Distribution of Pu^{238} from the SNAP-9A Abort of April 1964", USAEC report HASL-164, 269-280, (Oct 1 1965).

56. P.W. Krey, USAEC report HASL-172, II - 21 - II - 66, (1966).

57. P.W. Krey, USAEC report HASL-173, II - 21 - II - 78, (1966).

58. K. Telegadas and R.J. List, Jour. of Geophys. Res. 69, 4741-4753, (1964).

59. R.J. List, L.P. Salter and K. Telegadas, "Radioactive Debris as a Tracer for Investigating Stratospheric Motions", Tellus, 18, 345-354, (1966).

60. J.A. Young, N.A. Wogman, C.W. Thomas and R.W. Perkins, "Short Lived Cosmic Ray-produced Radionuclides as Tracers of Atmospheric Processes", Volume 93, Chapter 28, (1970).

61. D. Lal and B. Peters, "Cosmic Ray Produced Isotopes and Their Application to Problems in Geophysics", Progress in Elementary Particle and Cosmic Ray Physics; North Holland Publishing Co., Amsterdam, Chapter 1, (1962).

62. N. Bhandari, D. Lal and Rama, "Stratospheric Circulation Studies Based on Natural and Artificial Radioactive Tracer Elements", Tellus XVIII, 391-405, (1966).

63. H.H. Loosli and H. Oeschger, "Detection of ^{39}Ar in Atmospheric Argon", Earth and Planetary Science Letters 5, 191-198, (1968).

64. W.R. Schell, "An Internal Gas Proportional Counter for Measuring Low Level Environmental Radionuclides", Advances in Chemistry Series: American Chemical Society Publications, Volume 93, Chapter 11, (1970).

65. J.G. Bleichrodt, "Increased Concentration of Beryllium-7 in the Stratosphere after the Nuclear Test Explosions during September-October 1961", Nature 193, 1065-1066, (1962).

66. N. Bhandari and Rama, "Atmospheric Circulation from Observations of Sodium-22 and Other Short Lived Natural Radioactivities", Jour. Geophys. Res. 68, 7, (1963).

67. N. Bhandari, Ph.D. Thesis, University of Bombay, (1965).

68. W.M. Burton and N.G. Stewart, "Use of Long-Lived Natural Radioactivity as an Atmospheric Tracer", Nature 186, 584-589, (1960).

69. Rama and M. Honda, "Natural Radioactivity in the Atmosphere", J. Geophys. Res. 66, 3227-3231, (1961).

70. W. Jacobi and K. Andre, "The Vertical Distribution of Radon-222, Radon-220 and their Decay Products in the Atmosphere", J. Geophys. Res. 68, 3799-3814, (1963).

71. I.L. Karol, "Quantitative Investigation of Stratospheric Mixing Processes by Means of Long-lived Radon Decay Products", Tellus 18, 337-344, (1966).

72. D.H. Peirson, R.S. Cambray and G.S. Spicer, "Lead-210 and Polonium-210 in the Atmosphere", Tellus 18, 425-433, (1966).

73. L. Machta, "A Preliminary Model of Tropospheric Aerosol Removal", a paper presented at Symposium on Air Chemistry and Radioactivity, Helsinki, (1960).

74. H.W. Feely, P.E. Biscaye, B. Davidson and H. Seitz, Eleventh Progress Report on Project STARDUST, Dept. of Defense Report DASA 1821, (1966).

75. U.S. Weather Bureau, "Global Atmospheric Radioactivity, May-June 1960 and November 1960", USAEC report HASL-115, 177-183, (1961).

76. K. Telegadas and R.J. List, "B-57 Air Sampling Program (1960)", USAEC report HASL-105, 150-161, (1961).

77. K.R. Peterson, "B-57 Air Sampling in Southwestern United States - February and March 1961," USAEC report HASL-142, 277-292, (1964).

78. H.W. Feely and H. Seitz, "Use of Lead-210 as a Tracer of Transport Processes in the Stratosphere", J. Geophys. Res. 75, 2885-2894, (1970).

79. A.W. Brewer, Quarterly Journal of the Royal Meteorological Society, London, Volume 75, 351, (1949).

80. B. Davidson, J.P. Friend and H. Seitz, "Numerical Models of Diffusion and Rainout of Stratospheric Radioactive Materials", Tellus 18, 301-315, (1966).

81. H. Seitz, B. Davidson, J.P. Friend and H.W. Feely, "Numerical Models of Transport, Diffusion and Fallout of Stratospheric Radioactive Materials", Final Report on Project STREAK, USAEC report No. NYO-3654-4, (1968).

82. P.H. Gudiksen, A.W. Fairhall and R.J. Reed, "Roles of Mean and Meridional Circulation and Eddy Diffusion in the Transport of Trace Substances in the Lower Stratosphere", J. Geophys. Res. 73, 4461-4473, (1968).

83. T.L. Karol, "Numerical Model of Global Transport of Radioactive Tracers from the Instantaneous Sources in the Lower Stratosphere", J. Geophys. Res. 75, 3589-3603, (1970).

84. S. Manabe and B.G. Hunt, "Experiments with a General Circulation Model: I. Radiative and Dynamic Aspects", Monthly Weather Review 96, 477-502, (1968).

85. B.G. Hunt and S. Manabe, "Experiments with a Stratospheric General Circulation Model: II; Large-Scale Diffusion of Tracers in the Stratosphere", Monthly Weather Review, 96, 503-539, (1968).

86. R.E. Newell, "Stratospheric Energetics and Mass Transport", Pure and Appl. Geophys., 58, 145-156, (1964).

87. A.D. Belmont and D.G. Dartt, "The Non-repeating Variations of the Observed Wind in the Equatorial Stratosphere", Tellus 18, 381-390, (1966).

88. A.H. Oort, "On the Energetics of the Mean and Eddy Circulations in the Lower Stratosphere", Tellus 16, 309-327, (1964).

89. D.G. Vincent, "Mean Meridional Circulations in the Northern Hemisphere Lower Stratosphere during 1964 and 1965", Quart. J. Roy. Meteorol. Soc., 94, 333-349, (1968).

90. R.E. Newell, "Transfer through the Tropopause and within the Stratosphere", Quart. J. Roy. Meteorol. Soc., 89, 167-204, (1963).

91. R.E. Newell, "Further Ozone Transport Calculations and the Spring Maximum in Ozone Amount", Pure and Appl. Geophys. 59, 191-206, (1964).

92. A.H. Oort and E.M. Rasmussen, "On the Annual Variations of the Monthly Mean Meridional Circulation", Monthly Weather Review, 98, 423-442, (1970).

93. J.O. Hinze, "Turbulence, an Introduction to Its Mechanism and Theory", McGraw-Hill, New York (1959).

94. P.W. Krey and B. Krajewski, "Comparison of Atmospheric Transport Model Calculations with Observations of Radioactive Debris", J. Geophys. Res., 75, 2901-2908, (1970).

95. K. Telegadas and R.J. List, "Are Particulate Radioactive Tracers Indicative of Stratospheric Motions?", J. Geophys. Res., 74, 1339-1350, (1969).

96. P.W. Krey, "Atmospheric Burnup of a Plutonium-283 Generator", Science, 158, 769-771, (1967).

97. J.P. Friend, H.W. Feely, P.W. Krey, J. Spar and A. Walton, "Discussion of HASP Results, The High Altitude Sampling Program, Final Report", DASA 1300, 3, Defense Atomic Support Agency, (1961).

98. J.P. Friend and H.W. Feely, Fifth Quarterly Report on Project STARDUST, DASA 1305, Defense Atomic Support Agency, (1962).

99. H.W. Feely, B. Davidson, J.P. Friend, R.J. Lagomarsino and M.W.M. Leo, Ninth Quarterly Report on Project STARDUST, DASA 1309, Defense Atomic Support Agency, (1963).

100. H.W. Feely, P.E. Biscaye, B. Davidson and H. Seitz, Eleventh Progress Report on Project STARDUST, DASA 1821, Defense Atomic Support Agency, (1966).

101. J.P. Friend, H.W. Feely, P.W. Krey, J. Spar and A. Walton, "The Application of HASP Data, The High Altitude Sampling Program, Final Report", DASA 1300, 4, Defense Atomic Support Agency, (1961).

102. B. Bolin, "The General Circulation of the Atmosphere as Deduced with the Aid of Tracers", Agenda Item 3: Discussion of Meteorological Problems with WMO Experts, Thirteenth Session of UNSCEAR, New York, N.Y. (1964).

103. W.S. Hering and T.R. Borden, Jr., "Analysis of the Seasonal and Synoptic-Scale Variations in the Vertical Ozone Distribution," International Atmospheric Ozone Symposium, Albuquerque, N.M., (1964).

104. J.P. Friend, H.W. Feely and M.W.M. Leo, Sixth Quarterly Report on Project STARDUST, DASA 1306, Defense Atomic Support Agency, (1962).

105. J. Douglas, "Numerical Methods for Parabolic Equations", Advances in Computers, 2, Academic Press, New York (1961).

106. A.C. Chamberlain, "Deposition of Iodine-131 in Northern England in October, 1957", Quart. J. Roy. Meteor. Soc., 85, 350, (1959).

107. A.C. Chamberlain, "Aspects of the Deposition of Radioactive and Other Gases and Particles", Int. J. Air Poll., 3, (1961).

108. A.C. Chamberlain and R.C. Chadwick, "Deposition of Airborne Radio-iodine Vapour", Nucleonics, 2, 22, (1953).

109. F. Möller, Vierteljahrskarten des Niederschlags für die ganze Erde, Petermanns Geographische Mitteilungen, 1, (1951).

110. U.S. Weather Bureau, "Meridional Cross-sections, Upper Winds over the Northern Hemisphere", Technical Paper No. 41, U.S. Dept. of Commerce, (1961).

111. U.S. Weather Bureau, "Monthly Mean Aerological Cross-sections, Pole to Pole along Meridian 75° W for the IGY Period", U.S. Dept. of Commerce, (1961).

112. E.P. Hardy, Jr., "Tungsten-185 Deposition on the Earth's Surface", Fallout Program, Quarterly Summary Report, HASL - 95, Health & Safety Laboratory, USAEC, 203-207, (1960).

113. E. Hardy and W. Collins, "Strontium-90 Deposition on the Earth's Surface from 1958 through 1961", Fallout Program, Quarterly Summary Report, HASL - 131, Health & Safety Laboratory, USAEC, 221-229, (1962).

114. Wm. R. Collins, "Strontium-90 Deposition on the Earth's Surface from 1958 through 1962", Fallout Program, Quarterly Summary Report, HASL - 140, Health & Safety Laboratory, USAEC, 240-247, (1963).

115. K. Telegadas, "Global Integrals of Monthly Strontium-90 Fallout, January, 1958 - May, 1962", Fallout Program, Quarterly Summary Report, HASL - 135, USAEC, 215-239, (1963).

116. L.P. Salter, USAEC report HASL - 142, 303-305, (1964).

117. I.J. Russell and R.V. Griffith, USAEC report HASL - 142, 306-322, (1964).

ISOTOPES
A Teledyne Company

ACKNOWLEDGEMENTS

From the initiation of Project STARDUST in 1961 to the publication of the last two volumes of the final report in 1971 many people have made significant contributions to the study. A number of contributors are named as authors in the three volumes of the final report or as authors of published papers describing certain aspects of the work. Others too numerous to mention by name have contributed. In particular, the members of the Gas Analysis, Radiochemistry and Radioassay Sections of Scientific Services at Isotopes who performed the chemical separations and measurements of radionuclides deserve recognition. The extensive calculations, conversions, and tabulations of data were ably accomplished by Mrs. Barbara Maul and Mrs. Edna Cunningham. Dr. Woodland Erlebach and Mr. Milton Trautman reviewed and edited the draft of the report. Mrs. Marie Mandel ably coordinated the work of our capable secretarial and reproduction staff in the typing, printing and assembly of the report.

Acknowledgement is also made for permission given by the Royal Meteorolical Society to publish figures and tables from pages 338 to 341 of volume 94, 1968, of their Quarterly Journal.